Visualisation of Ribosomal Subunits Interaction Reveals 80S Ribosomes in the Nucleus of *Drosophila* Cells

Akilu Sada Abdullahi

Supervised by Dr. Saverio Brogna

A thesis submitted to

The University of Birmingham

For the degree of

DOCTOR OF PHILOSOPHY

School of Biosciences

College of Life and Environmental Sciences

The University of Birmingham

November 2014

Abstract

In eukaryotes, transcription and RNA processing events are spatially separated from translation by the nuclear envelope. Although ribosomal subunits are synthesised and assembled in the nucleus, it is believed that they are kept inactive and cannot bind mRNA and engage in translation whilst in the nucleus. Yet, there were observations from this and other laboratories that suggest translation can occur in the nucleus. To further investigate whether translating ribosomes exist in the nucleus, I employed a technique previously developed in our laboratory that detects 80S assembly in *Drosophila* cells. This technique is based on tagging pairs of ribosomal proteins (RPs) located at the interaction surface of 40S and 60S subunits with mutually complementing halves of a fluorescent protein, termed bimolecular fluorescence complementation (BiFC). The initial characterisation indicated that the assay reports ribosomal subunit interaction, but other explanations could not be excluded. My first aim was to assess whether this technique is genuinely reporting translation-dependent subunits association. My results were consistent with the assay reporting 80S ribosomes formed as a consequence of translation. Following up from this, I developed a similar technique with Venus, which resulted in a more sensitive 80S reporter. While the 80S signal was more apparent in the cytoplasm, in both cell culture and fly tissue cells, a fraction of the cells showed a signal in the nucleus, particularly concentrated in the nucleolus. This signal was enhanced by translation elongation inhibitors in both cytoplasm and nucleus indicating that the detected 80S are engaged in translation. Notably, the nucleolar signal was prevented by RNA Pol II inhibition, suggesting that the 80S might be associated with mRNA in the nucleolus. Additionally, I showed data indicating that level of nuclear 80S increases upon serum starvation and other forms of cellular stress, suggesting a role for nuclear translation in stress response.

Acknowledgements

First of all, I would like to thank the Almighty for giving me the opportunity and ability to overcome all the challenges and obstacles I encountered during the course of my PhD studies.

My sincere gratitude goes to my supervisor Dr. Saverio Brogna for accepting me to work in his laboratory and spending a lot of his time in guiding and supporting me from the start of my PhD program until its end. I will forever remain grateful.

I would also like to express my appreciation to other principal investigators in our floor (6^{th}) for allowing me to use some of their equipment, reagents and guidance particularly Dr. Alicia Hidalgo and Dr. Yun Fan. Equally I would like to thank all past and present members of the Brogna laboratory for their support and providing a happy working environment and the entire 6^{th} floor members at large. Specifically I would like to mention Preethi Ramanathan, Kim Piechocki and Dr. Jikai Wen for their help during the early days of my PhD and some key experiments in my work. I'd also like to extend my deep gratitude to Tina Mcleod who spent her time to edit some chapters of my thesis.

I wish to extend my heartfelt gratitude and special appreciation to my family; my parents for their unending support and prayers, my dearest wife Rukayya for her patience, understanding and support throughout duration of my PhD and my lovely kids Abubakar, Hindatu and Rukayya (jnr) whose presence is always a source of joy and inspiration. I would also like to say a "big thank you'' to all my brothers, sisters, relatives, friends and well-wishers both in Nigeria and here in the UK for their support, kindness and brotherly advice.

Last but not the least, my special gratitude goes to the Islamic Development Bank (IDB) for funding my PhD in one of the best institution in the United Kingdom.

Thank you and God bless.

Akilu Sada Abdullahi.

Dedication

This work is dedicated to my dearest parents Muhammad Sada Abdullahi and Hindatu S. Abdullahi, my lovely wife Rukayya Ibrahim Maiunguwa and our beautiful kids Abubakar, Hindatu and Rukayya (jnr).

Table of Contents

List of Abbreviations

40S	Eukaryotic small ribosomal subunit
60S	Eukaryotic large ribosomal subunit
80S	Eukaryotic ribosomes
4E-BPs	eIFE binding proteins
AF	Assembly factors
AMP	Adult midgut progenitor cells
ATF	Activating transcription factor
ARK	Apaf-1 related killer protein
BiFC	Bimolecular fluorescence complementation
BSA	Bovine serum albumin
CBC	Cap binding complex
CBP	Cap binding protein
Cryo-EM	Cryo-electron microscopy
DAPI	4'-6-Diamidino-2-phenylindole
DBA	Diamond blackfan anemia
DDAB	Dimethyl dioctadecyl ammonium bromide
DFC	Dense fibrillar component
DNA	Deoxyribonucleic acid
DSE	Downstream sequence
EB	Enteroblast
EC	Enterocytes
EDTA	Ethylenediaminetetraacetic acid
EE	Enteroendocrine
eEF (1, 1A)	Eukaryotic translation elongation factors
eIF4 (F, A, E, G)	Eukaryotic translation initiation factors
EJC	Exon-exon junction complex
ER	Endoplasmic reticulum
eRF1/3	Eukaryotic release factor 1 and 3
FBS	Fetal bovine serum
FC	Fibrillar component

GC	Granular component
GCN2	General control non-depressible 2
GFP	Green fluorescent protein
HAT	Histidine affinity tag
HRI	Haem-regulated inhibitor
HRP	Horseradish peroxidase
ISC	Intestinal stem cells
JNK	c-Jun N-terminal kinase
lmRNAs	Leaderless mRNAs
LB	Luria Broth
NMD	Nonsense-mediated mRNA decay
NPC	Nuclear pore complex
NTP	Nucleotide triphosphate
PBS	Phosphate buffered saline
PEG	Polyethylene glycol
PERK	Double-stranded RNA-activated protein kinase-like ER kinase
PKR	Double stranded RNA-activated protein kinase
Pol (I, II, & III)	RNA polymerases (I, II, and III).
PTC	Premature termination codon
RNA	Ribonucleic acid
RP	Ribosomal protein
RpL	Ribosomal protein large subunit
RpS	Ribosomal protein small subunit
SD	Shine-Dalgarno
SDS	Sodium dodecyl sulfate
TBS	Tris buffered saline
Tris	Tris(hydroxymethyl) aminomethane
UAS	Upstream activating sequences
UPF	Up-frameshift
UTR	Untranslated region
VFP	Venus fluorescent protein

VC	C-terminal VFP fragment
VN	N-terminal VFP fragment
WT	Wild type
YC	C-terminal YFP fragment
YFP	Yellow fluorescent protein
YN	N-terminal YFP fragment

CHAPTER 1

1.0 Introduction

1.1 Overview of gene expression and pre-mRNA processing in eukaryotes

The expression of a protein-encoding gene involves transcription of DNA into RNA and the subsequent translation of the RNA into protein. This process is significantly different between prokaryotes and eukaryotes. While RNA translation in prokaryotes is coupled to transcription, with ribosomes engaging with the transcript as it emerges from the RNA polymerase, in eukaryotes the primary transcript, the precursor of the mature mRNA (pre-mRNA), undergoes a series of post-transcriptional processing (details below and Figure 1.0) before it exits the nucleus to the cytoplasm, where translation takes place (Palazzo and Akef, 2012; Moore and Proudfoot, 2009).

Pre-mRNA processing is a co-transcriptional event that begins with 5' end capping whereby the triphosphate (pppN) 5' terminus of nascent transcripts are replaced with a 7-methylguanosine via a 5'-5' triphosphate linkage (7meGppp) (Shuman, 2001; Moore and Proudfoot, 2009). The 3' end of the mRNA is generated by a process that requires cleavage of the pre-mRNA and insertion of a poly(A) tail at the 3' end (Colgan and Manley, 1997). The cleavage and polyadenylation site is located between an evolutionarily conserved AAUAAA sequence, which is recognized by the cleavage and specificity factor (CPSF), and the G/U-rich sequence elements which are identified by cleavage stimulation factor (CstF) (Zorio and Bentley, 2004). The 5' cap and poly (A) tail play important roles in mRNA stability, transport and effective translation (Zorio and Bentley, 2004; Moore, 2005). Most pre-mRNAs in eukaryotes contain introns; non-coding regions within the coding exon sequences that are

spliced out. This splicing reaction is catalysed by a macromolecular complex called the spliceosome (Zhou et al., 2002). In higher eukaryotes, pre-mRNAs are subjected to alternative splicing, producing alternative mature mRNAs from the same precursor that encode different proteins (Stamm et al., 2005). Alternative splicing has been observed in nearly 75% of human pre-mRNAs and this might explain why humans are more complex than organisms that possess a similar number of genes such as worms and flies (Stamm et al., 2005; Johnson et al., 2003). Processed mRNAs are exported through the nuclear pore complex (NPC) to the cytoplasm where the nucleotide sequence of the open reading frame (ORF) is translated into proteins by the ribosome. The export of a fully processed mRNA requires its association with several proteins forming an mRNA protein complex (mRNP), that are required for traversing the NPC (Brodsky and Silver, 2000). The link between transcription, mRNA processing, export, mRNA stability and translation is determined by the composition and structure of the mRNP (Moore and Proudfoot, 2009).

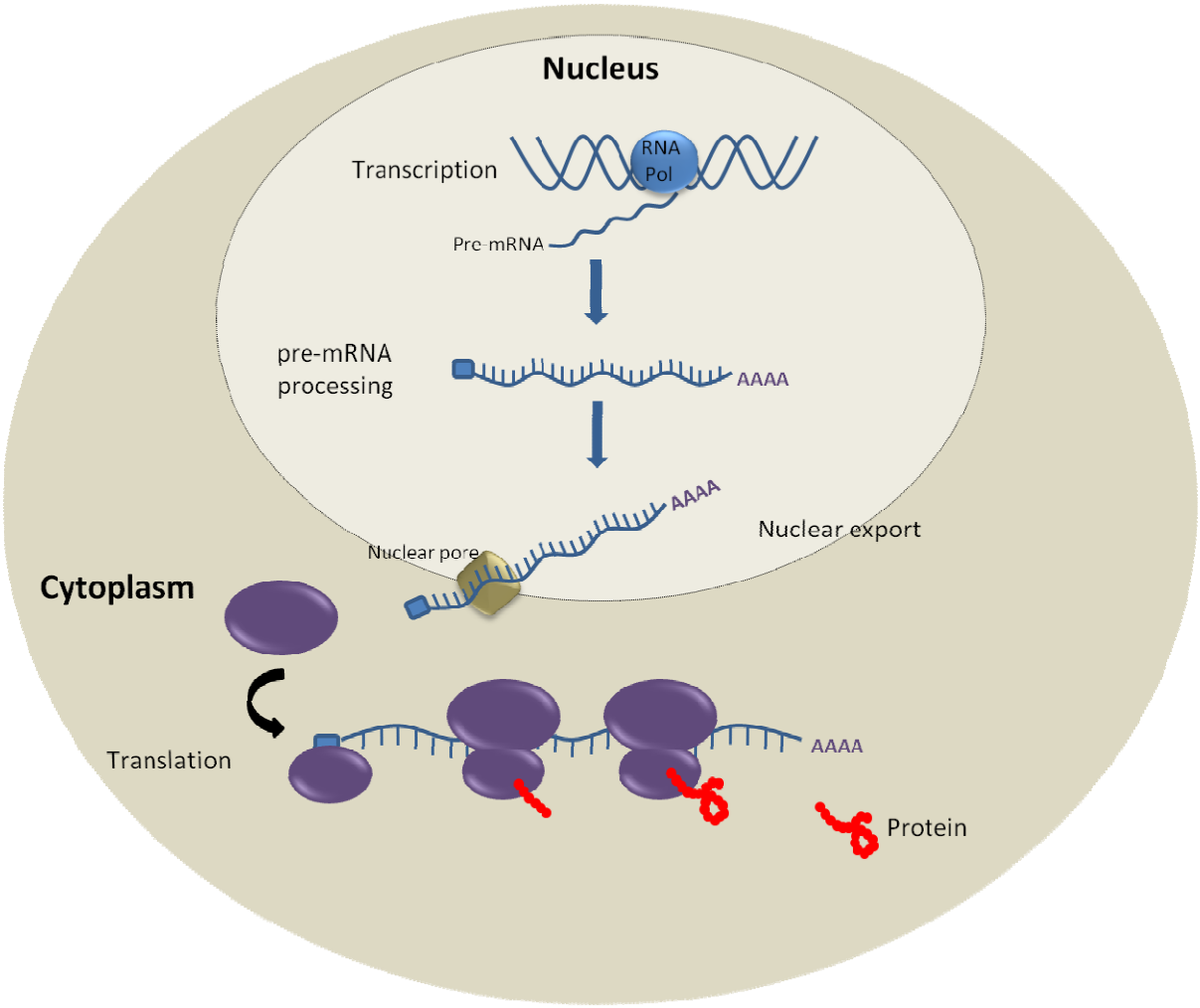

Figure 1.0. Schematic of the compartmentalized eukaryotic gene expression. Transcription and pre-mRNA processing occurs in the nucleus (region illustrated with lighter background colour). Processed mRNAs associates with many other proteins to form export competent mRNPs which are exported from the nucleus via the NPC. The mRNAs are then translated into proteins by the ribosome in the cytoplasm.

1.2 Translation

While it is increasingly understood that some RNAs have important biochemical functions as nucleic acids, it is generally accepted that most RNAs will be translated into the specific proteins and enzymes that make a living organism. Translation is the process whereby proteins are synthesised by the decoding of the genetic message contained within the mRNA open reading frame (ORF). Translation is catalysed by the ribosome (detailed further on), aminoacylated tRNAs and several translation factors. Translation is biochemically divided into four sequential stages: translation initiation, peptide chain elongation, termination and ribosome recycling (Kapp and Lorsch, 2004; Myasnikov et al., 2009). The first step is translation initiation and begins with the recruitment of the cap-binding protein complex; eukaryotic initiation factor 4F (eIF4F), to the cap structure at the 5' end of the mRNA. eIF4F is a trimeric complex comprising eIF4E (cap binding protein), eIF4A (RNA helicase) and eIF4G (scaffolding protein) (Gebauer and Hentze, 2004; Holcik and Sonenberg, 2005). Consequently, the pre-initiation complex, which is composed of the 40S subunit, eIF3 and the ternary initiator tRNA- eIF2-GTP complex, associates with the 5' cap of the mRNA through an interaction between the scaffold protein eIF4G and eIF3 (Spriggs et al., 2008; Gebauer and Hentze, 2004). eIF4E binds the cap and eIF4A elicits mRNA unwinding via its helicase activity. eIF4E availability and ability to associate with eIF4G, and subsequently to the 43S pre-initiation complex, is regulated by a group of eIF4E inhibitory proteins called the eIF4E-binding proteins (4E-BPs) (Lin et al., 1994; Waskiewicz et al., 1999). Once loaded, the 43S complex then slides and scans along the mRNA in the 5'-3' direction until the AUG initiation codon is detected. Scanning by the 43S complex requires the joint action of eIF1 and eIF1A. Upon recognition of the start codon the 60S subunit associates with the 40S to form a fully assembled translation competent 80S ribosome, with the AUG of the mRNA

pairing with the anticodon of the initiator-tRNA at the peptidyl (P) site of the ribosome. Hydrolysis of GTP, which is bound to eIF2 by eIF5B is required in this step, which is followed by the release of initiation factors which signals the commencement of elongation phase (illustrated in Figure 1.1). Translation elongation is the phase in which the peptide chain is synthesised; the mechanism is similar across species, from prokaryotes to eukaryotes (Ramakrishman, 2002), and involves three distinct steps. Step 1 is the binding of an incoming aminoacyl-tRNA in the A-site of the ribosome. Step 2 is peptide bond formation between the incoming amino acid and the amino acid in the P-site and step 3 involves movement of the ribosome to the next mRNA codon and translocation of the peptidyl-tRNA complex from A site to P, site leaving the A site vacant to accept the next amino acid charged-tRNA. This phase requires two conserved proteins, eEF1 and eEF2 (and eEF3 in yeast). Polypeptide synthesis occurs as peptide bonds are formed between the nascent peptide and incoming amino acids in the P-site of the ribosome, in a reaction catalysed by the ribosomal peptidyl transferase centre localised in the RNA core of the large subunit (Doudna and Rath, 2002). Remarkably, there are no proteins in the vicinity of the peptidyl transferase centre, consistent with the view that the ribosome is primarily a ribozyme, evolved to join amino acids together (Polacek and Mankin, 2005). The peptide bond formation is followed by the passage of tRNAs along with the associated mRNAs via the ribosome's A, P and exit E site in a process called translocation (Beringer and Rodnina, 2007; Joseph, 2003). In the translocation step, the ribosome shifts the A-site to the next codon in the mRNA, the peptidyl-tRNA relocates to the P-site and the deacylated tRNA exits the ribosome via the E-site. When the translating ribosome encounters a stop codon, the release factor eRF1 enters the A site instead of a tRNA, and, acting along with eRF3, triggers the release of the nascent peptide and probably the dissociation of the ribosome from the

mRNA (Pisareva et al., 2006). In eukaryotes, an increasing body of evidence suggests that translation takes place on mRNAs that are in a closed-loop conformation, and upon translation termination, the 40S subunit is reutilized to reinitiate translation on the same mRNA (Wells et al., 1998; Jacobson, 1996; Kahvejian et al., 2001). It was proposed that 43S recruitment results in the circularization of the mRNA into the closed-loop conformation, during which the capped 5' end is linked to the poly(A) tail through the association of eIF4G with PABP (Myasnikov et al., 2009). Many viruses, and to a lesser extent, a small fraction of cellular mRNAs use a specialised translation initiation mechanism which does not require a 5' cap, such as structured sequences in the 5' UTR referred to as internal ribosome entry sites (IRESs), to initiate translation by direct recruitment of the ribosome through these sites to their mRNA start codon (Sonenberg and Hinnebusch, 2009).

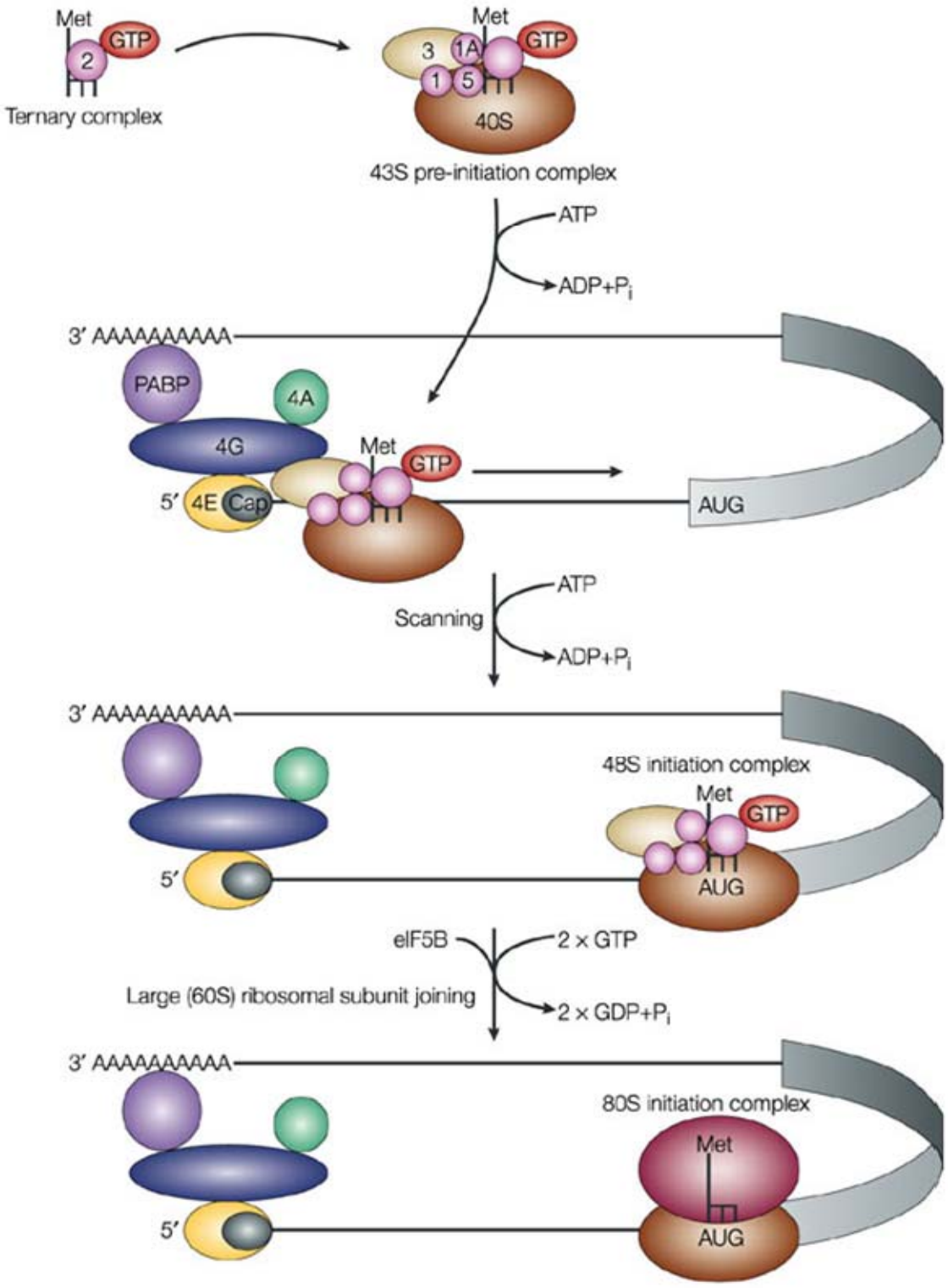
Met
GTP
2
Ternary complex
Met
3
1A
GTP
1
5
40S
43S pre-initiation complex
ATP
ADP+Pi
3′ AAAAAAAAAA
PABP
4A
4G
Met
GTP
5′ 4E Cap
AUG
ATP
Scanning
ADP+Pi
3′ AAAAAAAAAA
48S initiation complex
Met
GTP
5′
AUG
eIF5B
2 × GTP
Large (60S) ribosomal subunit joining
2 × GDP+Pi
3′ AAAAAAAAAA
80S initiation complex
Met
5′
AUG

Figure 1.1. Schematics of cap-dependent translation initiation in eukaryotes.

Translation initiation factors (eIFs) are indicated in various colours and designated with numbered shapes. Met-initiator tRNA (L-shaped) forms a complex with eIF2-GTP which is referred to as the ternary initiator complex. This complex then binds to the 40S subunit bearing eIF3 and other translation initiation factors to yield the 43S pre-initiation complex. The 43S complex binds the cap structure of the mRNA via an interaction between eIF3 and the scaffold protein eIF4G and then scans the mRNA in the 3' direction until it detects the AUG start codon. Binding of the 43S complex to the AUG codon on the mRNA, produce the 48S initiation complex. Subsequently, the 60S subunit joins the complex, forming the 80S translation competent ribosome. This figure was taken from (Gebauer and Hentze, 2004).

1.2.1 Translational Response to Stress

Cells often encounter numerous environmental stresses such as temperature changes, oxygen deprivation, ultraviolet radiations (UV), exposure to lethal chemical agents or toxins and physiological stress such as nutrient starvation to which they respond by repairing the damage or apoptosis. Different forms of stress require different responses that usually result in the reconfiguration of gene expression, such as a global repression of translation, as a means conserving essential cellular materials needed for the cell's survival, or apoptosis induction. How the cells adjust and adapt to such adverse conditions is important for their survival. Cellular response to stress brings about changes that require expression of stress response genes which play an important role in either overcoming the stress or inducing apoptosis (Pearce and Humphrey, 2001; Holcik and Sonenberg, 2005).

A number of studies have revealed that translation rate is globally reduced under nearly all forms of cellular stresses and that this effect is often coupled to the preferential translation of the specific proteins needed to counteract the damage or induce apoptosis (Harding et al., 2000). Most of what is currently known about down-regulation of protein synthesis following cellular stress focuses on down-regulation of translation, mostly at the initiation stage. Regulation of translation initiation involves two translation initiation factors, eIF2, which is a component of the ternary initiation complex, and eIF4E (the cap binding protein). eIF2 translational regulation involves its regeneration to the active GTP-bound form as a component of the ternary initiator complex (Holcik and Sonenberg, 2005). In mammals, the response to stress triggers a family of protein kinases that phosphorylate eIF2. eIF2 is composed of 3 subunits, α, β and ϒ. Four kinases can phosphorylate α-subunit of eIF2; these are the heme-regulated inhibitor kinase (HRI), double stranded RNA–activated protein

kinase (PKR), double stranded RNA-activated protein kinase-like endoplasmic reticulum kinase (PERK), and general control non-depressible-2 (GCN2). These kinases integrate various stress signals and align them into a single pathway. HRI is activated by heme deprivation, heat shock or toxicity from heavy metals. PKR is mainly activated by viral infection, PERK by ER stress and GCN2 by stress associated with nutrient starvation (Sheikh and Fornace, 1999; Holcik and Sonenberg, 2005). Phosphorylation of eIF2α by these kinases at Ser 51 prevents eIF2 activation to the GTP-bound form that is required to initiate another translation cycle. This effect leads to a gradual depletion of the active eIF2-GTP and eventually results in down-regulation of global protein synthesis and a switch to translation of specific mRNAs, for example, those that code for the basic leucine zipper (bZIP) ATF4 (Activating transcription factor 4) and the yeast transcription activation factor GCN4 (Holcik and Sonenberg, 2005; Wek et al., 2006). ATF4 is a transcription factor that regulates transcription of several genes required for cell survival and its translation is up-regulated by the unfolded protein response (UPR) which is activated by ER stress (Holcik and Sonenberg, 2005). UPR down-regulates general protein synthesis and initiates the selective translation of ATF4. The ATF4 mRNA has 2 upstream open reading frames (uORFs 1 and 2) in the 5' UTR. uORF2 is an inhibitory element that overlaps with the ATF4 ORF and prevents ATF expression. Under conditions of eIF2α hypophosphorylation, uORF2 is translated by the ribosome. On the other hand, hyperphosphorylation of eIF2α allows the ribosome to initiate translation at the ATF4 initiation codon by scanning through the inhibitory uORF2. Translation of ATF4 brings about the expression of more regulators of transcription like ATF3 and CCAAT/enhancer binding protein homologous protein (CHOP)/ growth arrest and DNA-damage inducible protein 153 (GADD153), whose actions result in the reconfiguration of gene expression, required by the cells either for survival or apoptosis induction

(summarised in Figure 1.2) (Wek et al., 2006; Sheikh and Fornace, 1999). Similarly in yeast, GCN4 possesses 4 uORFs in the 5' UTR of the mRNAs which regulate its expression in a manner similar to that described above for ATF.

The translation initiation factor eIF4E also plays an important role in the regulation of global translation under stress. eIF4E function is regulated by a family of proteins referred to as 4E-binding proteins (4E-BPs) which are phosphorylated under stress conditions and indirectly inhibit translation initiation by impairing the interaction between eIF4E and eIF4G, and subsequently 43S pre-initiation complex. The pathway for the regulation of eIF4E following stress is illustrated in (Figure 1.3).

Other forms of translational response to stress include utilization of specialized ribosomes which translate a specific sub-set of mRNAs. This heterogeneity of ribosomes could play a significant role in adaptive measures during stress conditions. Ribosome heterogeneity could be as a result of changes in the rRNA sequences or composition of ribosomal proteins (RPs) within the ribosome subunits. This phenomenon was well documented in *E. coli,* where stress adaptation involves the generation of a population of ribosomes with altered rRNA sequences that are used for selective translation of a set of leaderless mRNAs (mRNA's lacking 5' UTR and hence Shine-Dalgarno (SD) sequence) which are also generated during stress (Filipovska and Rackham, 2013). In eukaryotes, these leaderless mRNAs are translated irrespective of whether they are capped or not (Grill et al., 2000). (specialized ribosomes and translation of leaderless mRNAs are discussed in detail below). IRES-mediated translation initiation is also activated during stress, whereby mRNAs are selectively translated by the ribosomes. Key regulators of apoptosis, pro-apoptotic protease activating

factor-1 (Apaf1) and X-chromosome-linked inhibitor of apoptosis (XIAP), are reported to be translated through the IRES-mediated translation machinery (Holcik and Sonenberg, 2005).

In *Drosophila* cells, stress from UV irradiation or transcription inhibitors such as Actinomycin D (act.D), trigger Apaf-1 related killer protein (ARK) which is an apoptosis activator. *Drosophila* ARK is the homologue of Apaf1 in mammals and CED-4 in nematodes (Zimmermann et al., 2002). Similarly, reaper, another *Drosophila* apoptosis inducer, was reported to block translation during stress in a mechanism that does not employ the apoptosis machinery. It directly binds to the 40S ribosome subunit, blocking translation at the late initiation stage by inhibiting the recruitment of the 60S ribosomal subunit on the 48S pre-initiation complex (Colon-Ramos et al., 2006). Inhibition of 80S assembly by reaper blocks cap-dependent translation initiation and allows cap-independent initiation mediated by CrPV IRES, an action that changes the type of proteins that are expressed (Colon-Ramos et al., 2006).

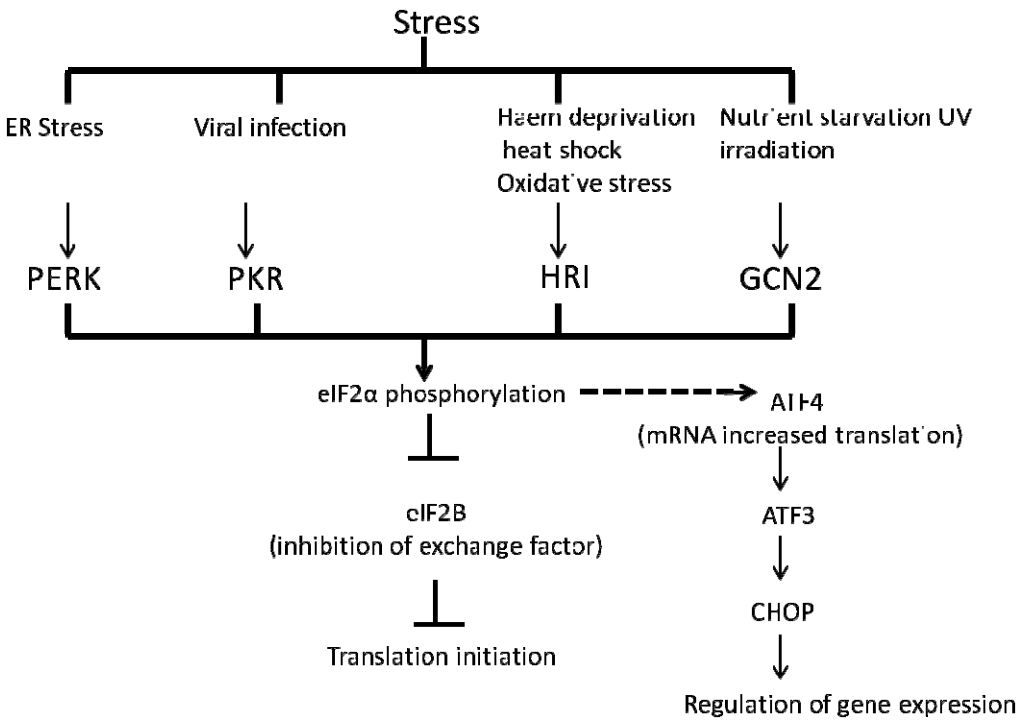

Figure 1.2. Illustration of how stress signalling induces phosphorylation of eIF2α. In mammalian cells, four different kinases phosphorylate the α-subunit of eIF2 (eIF2-α) under stress conditions. This action is accompanied by translational repression that permits the cells to remediate the stress effect and trigger selective translation of important transcripts required for the remediation; for example ATF4 as indicated above. Increased levels of ATF4 induce ATF3, CHOP and GADD34 and other transcription factors regulate gene expression.

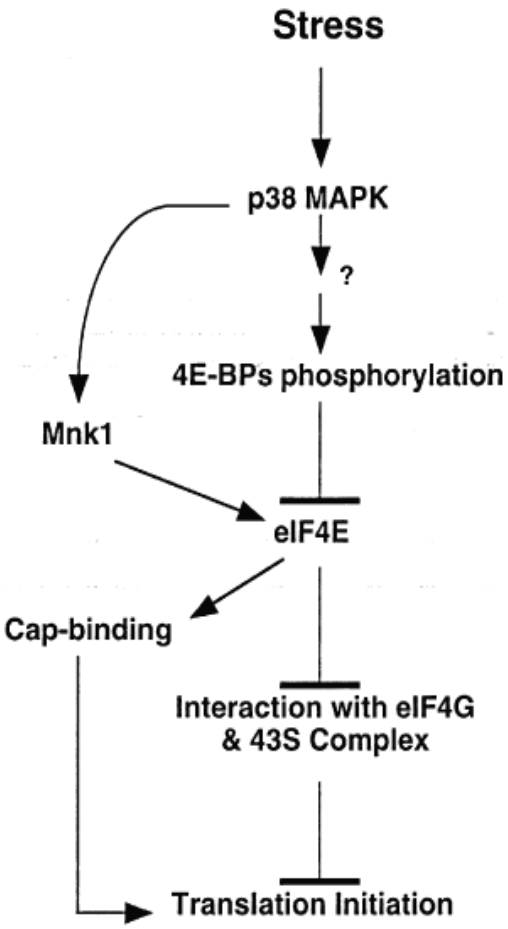

Figure 1.3. Regulation of eIF4E following stress. Stress-induced phosphorylation of 4E-BPs can indirectly affect eIF4E activity to inhibit translation initiation. Stress-induced activation of p38 MAPK promotes eIF4E phosphoryla-tion via Mnk1. Phosphorylation of eIF4E potentiates its interaction with `cap' and promotes translation initiation. p38 MAPK can also phosphorylate 4E-BPs, phosphorylated 4E-BPs prevent interaction between eIF4E and eIF4G and thus inhibit translation initiation. This figure was taken from (Sheikh and Fornace, 1999).

1.2.2 Compartmentalized translation in eukaryotic cells

A unique feature of eukaryotic organisms is the compartmentalization of cells. Eukaryotic cells have a nuclear membrane that separates them into two main compartments, nucleus and cytoplasm. Some key stages of gene expression are restricted to either of these compartments. Transcription and processing of the transcripts are confined to the nucleus, whereas translation is believed to occur solely in the cytoplasm. It is usually assumed that the nuclear membrane emerged to physically separate RNA processing from translation so that the two processes would not impede on one another, ensuring that translation of pre-mRNA would not produce junk proteins (Iborra et al., 2001). The implication of this assumption is that there are no direct links between transcription and post-transcriptional processing of pre pre-mRNAs in the nucleus and downstream events that occur in the cytoplasm, such as translation and mRNA degradation. This notion has been disputed by later observations from the NMD field (discussed below), indicating that the composition of the mRNP in the nucleus may affect cytoplasmic processes including translation and RNA degradation (Wen and Brogna, 2010; Muhlemann et al., 2001; Moore and Proudfoot, 2009).

1.3 Previous evidence of nuclear translation

The isolation of what appeared to be nuclear polysomes (cluster of translating ribosomes on mRNA) and some evidence of nuclear translation, had been reported about 40 years ago and had been extensively reviewed over the years (Goldstein, 1970; Mangiarotti, 1999; Allen, 1978; Goidl et al., 1975; Goidl, 1978). These studies concluded that translation can occur in the nucleus. In more recent years, new evidence for the presence of functional ribosomes in the nucleus was reported by two studies. One of these studies demonstrated that Biotin or BODIPY tagged amino acids were incorporated into nascent peptides in highly

purified nuclei (Iborra et al., 2001). The observed nuclear fluorescence was found to depend on ongoing transcription by RNA polymerase II (RNA Pol II), and conversely was prevented by translation inhibitor drugs. Thus, the interpretation of these findings was that nascent transcripts are translated by nuclear ribosomes as soon as they emerge from Pol II, as occurs in bacteria (Iborra et al., 2001). A later study, again by Iborra et al., provided further support for nuclear protein synthesis by showing that transcription, translation and NMD factors co-purify in biochemical procedures, and again co-localize in electron microscopy (EM) immunostaining assays (Iborra et al., 2004). Evidence for the presence of ribosomal subunits at transcription sites was also reported by Brogna et al. (2002). This study indicated that many ribosomal proteins associate with nascent RNAs at RNA polymerase II transcription sites in the polytene chromosome of *D. melanogaster* salivary glands. In addition, rRNA and some translation factors were reported to be present at these sites and amino acid incorporation could also occur at nuclear and nucleolar sites (Brogna et al., 2002).

Both studies were criticised on technical grounds; it was argued that the seemingly nuclear translation reported by Iborra et al. may come from contamination of the supposedly purified nuclei with Endoplasmic Reticulum (ER). The ER is attached to the nuclear envelope and it is difficult to isolate nuclei without possible contamination (Dahlberg et al., 2003). Another criticism was that the nuclear signal could be an artefact of over-permeabilization of the nuclei leading to the entry of cytoplasmic ribosomes into the nucleus (Nathanson et al., 2003).

Questions as to the reliability of the study by Brogna et al. (2002) came from concerns that the antibodies used were not sufficiently specific for the ribosomal proteins investigated, which may have led to cross reaction. Additionally, it was argued that the immunostaining

procedure could have allowed some cytoplasmic substances to gain entry into the nucleus (Dahlberg et al., 2003).

However, in line with Brogna et. al (2002) findings, a more recent study reached the same conclusion, since many fluorescent tagged ribosomal proteins were visualised at Pol II transcription sites in *Drosophila* polytene chromosomes (Rugjee et al., 2013). Additionally, another recent study reported that RpL12 binds the chromatin regulator Corto at the chromatin (Coleno-Costes et al., 2012). In the same vein, RpL12 and Corto were both detected on polytene chromosomes and the interaction of Corto with RpL12 may involve a network of many ribosomal proteins, mediated by RpL12 (Coleno-Costes et al., 2012). Again, this is in agreement with the earlier findings in *Drosophila* polytene chromosomes (Brogna et al., 2002). Ribosomal proteins have been detected also at transcription sites in both budding and fission yeast (Schroder and Moore, 2005; De et al., 2011). A case has been made that the association of ribosomal proteins with transcription sites might be a common characteristic of all eukaryotic organisms (De et al., 2011). However, at the start of this study, it was not yet clear whether the presence of ribosomal proteins at such sites is due to the presence of complete ribosomes or whether they have some other function as individual ribosomal proteins that are not incorporated into functional ribosomes.

1.4 Nonsense-mediated mRNA decay (NMD)

NMD is a translation-coupled mechanism that functions in eukaryotes as a surveillance pathway for detecting and eliminating aberrant mRNAs that harbour premature translation termination codons (PTCs). Nearly 25% of inherited disorders are PTC related (Culbertson, 1999). In humans, mutations resulting in PTC generation are associated with many diseases such as Cystic fibrosis, Duchenne muscular dystrophy and several others. The initial

discovery of NMD came from the observation that cells frequently have unusually small amounts of transcripts arising from nonsense mutation alleles (Brogna and Wen, 2009). This trend was detected in all the organisms studied, with the bulk understanding of the NMD pathway coming from studies in yeast and mammals (Maquat, 1995). NMD is considered a protective mechanism to avert the translation of transcripts coding for truncated proteins that might be harmful to cells. NMD is suggested to have a proofreading function in the process of gene expression, in which PTC containing transcripts produced from mutations and incorrect splicing due for example to poor splicing signals are identified and eliminated (Sayani et al., 2008; Jaillon, 2008).

NMD relies on mRNA translation for the scanning, detection and degradation of aberrant mRNAs. Agents that inhibit translation and tRNA suppressors also prevents NMD (Maquat, 1995). This active process requires a number of specific trans-acting factors (Amrani et al., 2006; Maquat, 2004). The best known of these are the upstream frame-shift proteins (upf), *upf1, upf2* and *upf3* which were initially identified in *S. cerevisiae* (Culberton et al., 1980). The genes encode highly conserved proteins, and their deletion or silencing has been shown to abolish NMD in all investigated eukaryotes (Conti and Izaurralde, 2005). The UPF proteins are the central NMD machinery and forms the pathway's surveillance complex for mRNA degradation (Brogna and Wen, 2009). In addition to the UPF proteins, other factors are possibly associated with NMD (Conti and Izaurralde, 2005). In multicellular organisms, these additional factors include the well characterized SMG proteins, SMG-1, SMG-5, SMG-6 and SMG-7 (Conti and Izaurralde, 2005). SMG 1 is a protein kinase that acts to phosphorylate upf1 (Grimson et al., 2004) while SMG 5, 6 and 7 are recognised to have a regulatory function in the phosphorylation state of upf1 (Conti and Izaurralde, 2005; Unterholzner and Izaurralde, 2004). In *D. melanogaster*, *upf1* and *upf2* were reported to be

essential for NMD and the NMD pathway plays an important role in the regulation of transcripts required for cell growth and development, whereas upf3 acts as an NMD effector and is dispensable for the degradation of nearly all NMD substrates (Avery et al., 2011). Additionally, *Upf3* is not essential for development or viability but upf1 and 2 deletions prevent cell growth and lead to apoptosis (Avery et al., 2011).

1.4.1 NMD as a nuclear event

Early studies in mammalian cells suggested that PTC containing mRNAs may be recognised and degraded by the NMD machinery within the nucleus (Cheng and Kan, 1979; Iborra et al., 2004). PTC affects nuclear events such as transcription and splicing, for example, it was observed that PTCs can prevent splicing of the immunoglobulin k light chain gene (Aoufouchi et al., 1996). This led to the interpretation that PTCs can have an effect on both nuclear and cytoplasmic mRNAs, suggesting the occurrence of NMD in the nucleus or at least during the course of nuclear export. Furthermore, the presence of an intron downstream of a PTC was shown to be essential to elicit NMD (Zhang et al., 1998; Thermann et al., 1998). Similarly, normal stop codons behave as PTCs by insertion of a downstream intron (Zhang et al., 1998). A number of early nonsense mutation studies pointed out that some mammalian transcripts including those of triosphosphate isomerase TPI, T-cell–receptor β and the enzyme dihydrofolate reductase, were reportedly subjected to NMD in the nucleus (Belgrader et al., 1993; Lozano et al., 1994; Urlaub et al., 1989). In *D. melanogaster*, an Alcohol dehydrogenase (Adh) mutant mRNA harbouring a PTC was found to undergo NMD in both the nuclear and cytoplasmic compartments (Brogna, 1999). These Adh PTC containing pre-mRNAs and mRNAs were observed to possess a longer poly(A) tail relative to the wild type; the nearer the PTC is to the 5’ end of these transcripts, the longer

the poly (A) tail (Brogna, 1999). Other studies in mammalian cells reported that NMD takes place while the transcripts are still bound to nuclear cap complex factor (CBP) (Ishigaki et al., 2001; Matsuda et al., 2007). The CBP is a heterodimer composed of the cap binding proteins (CBP80 and CBP20), which although nuclear, shuttle to cytoplasm. NMD of PTC containing transcripts is reported to occur prior to the substitution of the nuclear cap by eIF4E, the cap-binding protein acquired in the cytoplasm (Ishigaki et al., 2001; Matsuda et al., 2007). It appeared that NMD most likely occurs during the first round of translation referred to as pioneer translation since it occurs while the mRNA is still associated with the nuclear envelope (Lejeune et al., 2002; Ishigaki et al., 2001). CBP80 associates with components of the EJC and appears to facilitate NMD in mammalian cells (Lejeune et al., 2002). In line with this, RNAi depletion of CBP80 stabilizes NMD substrates (Hosoda et al., 2005). Still, this may not rule out the possibility that a fraction of NMD occurs in the nucleus. More recently, live imaging of a PTC containing immunoglobulin-μ reporter gene revealed that nonsense mutations are detected co-transcriptionally (de Turris et al., 2011). The identified PTC containing transcripts are predominantly unspliced and require the NMD factors UPF1 and SMG-6. Chip analysis revealed the association of the PTC containing transcript with these NMD factors and their depletion results in the release of the transcripts (de Turris et al., 2011). However, a recent study in mammalian cells, which utilized single RNA-FISH to measure degradation times and identify NMD sites in individual cells, reported that PTC recognition and NMD do not occur in the nucleus (Trcek et al., 2013). This study put forward that all transcripts (both PTC and non-PTC containing) are engaged with ribosomes and are translated as soon as they exit the NPC, and that NMD occurs at a position close to the nuclear envelope (Trcek et al., 2013). Despite this new observation in mammalian cells, nuclear NMD remains a possibility.

1.5 Ribosome structure

The ribosome, a large ribonucleoprotein particle, is composed of two subunits in all species and comprises nearly two thirds ribosomal RNA (rRNA) and one third ribosomal proteins (RPs) (Alberts et al., 2008). The two subunits are the large ribosomal subunit (50S in prokaryotes and 60S in eukaryotes) and the small ribosomal subunit (30S in prokaryotes and 40S in eukaryotes). The 60S subunit consist of three rRNAs, 28S (25S in yeast, 3392 nt), 5.8S (158 nt) and 5S (121 nt) and 45 ribosomal proteins where as the small subunit is made up of 18S (1798 nt) and 32 ribosomal proteins. The large subunit contains the peptidyl transferase centre, which catalyzes peptide bond formation between amino acids. The small subunit contains the decoding domain, responsible for decoding the mRNA message, contained within the open reading frame (ORF), by scanning its codons with an initiator tRNA anticodon (Maguire and Zimmermann, 2001). The emergence of electron microscopy has set the stage towards the progress in our understanding of the ribosome, with 3D images of the ribosome being generated at a resolution that enables the detection of both nucleic acids and several proteins that are associated with it (Agrawal et al., 1998). Rapid improvements came from crystallization studies that have significantly increased our knowledge of ribosome structure over the last two decades. The possibility of applying x-ray crystallography to reveal the organisation of the ribosome at atomic resolution brings forth a remarkable development in unravelling the structure, function and general translational mechanisms of the ribosome. Over the course of the past years, this has led to the development of high resolution structures of *Haloarcula marismotui* 50S subunits at 2.4 Å (Ban et al., 2000), and *Thermos thermophilus* 30S subunits at two different resolutions, 3.3 Å and 3.0 Å (Wimberly et al., 2000; Schluenzen et al., 2000), within the same year. This is followed by a high resolution complete structure of the *T. thermophilus* 70S ribosome at 5.5

Å, while the 70S structure bound to mRNA and tRNAs positioned in the A, P and E sites was resolved in the subsequent year (Yusupov et al., 2001), providing a detailed outlook of this vast and intricate ribonucleoprotein complex. The large subunit is nearly twice the size of the small subunit, but both share certain common features. First, their interface side is mainly free of proteins and second, most of each subunit's proteins have globular domains that are located on the solvent side, and bear long extensions which interact with ribosomal RNA (rRNA) and stabilize its tertiary structure.

Eukaryotic ribosomes, although more complex, share certain basic structural aspects with those of prokaryotes. Reconstruction of yeast 80S ribosome at 15 Å resolution by cryo-electron microscopy (Spahn et al., 2001a) revealed the similarities and differences between the eukaryotic and prokaryotic ribosomes. The eukaryotic ribosome is approximately 30% larger than that of prokaryotes, with an additional rRNA particle and 20-30 more proteins. The small subunit 18S rRNA in *S. cerevisiae* is arranged into three distinct components head (3' domain), body (5' domain) and platform (central domain) which associate with RPs. Two key morphological features of the 40S in yeast are the helix 16 structure located in the shoulder of the 18S rRNA, and the helix 44 segment being positioned in the lower part of the subunit. The large subunit rRNAs, 25S and 5.8S are 646 nucleotides bigger compared to that of bacteria and 505 nucleotides longer than the rRNA of the archaea *H. marismotui* (Doudna and Rath, 2002). The yeast 80S ribosome is majorly distinguished by its expansion segments (ESs) positioned in the 60S rRNA, found in the domains of both 5.8S and 25S rRNA, and which are densely located on the opposite side of the 60S. The ESs are the none core regions of the rRNA that forms bulk of the difference in length between organisms. Seven bridges that were found in the bacterial 70S and *T. thermophilus* 70S between the subunits

are equally identified in yeast, with four additional bridges at the surface that are recognised to be specific to eukaryotes (see Figure 1.4) for the outline of the features eukaryotic ribosomes compared to the prokaryotes). Cryo-EM analysis of the mammalian 80S ribosome at 8.7 Å resolution was revealed to be a larger complex compared to yeast (Chandramouli et al., 2008), but with a similar number and arrangement of proteins as reported earlier in the yeast 80S (Spahn et al., 2001a).

A recent study has revealed the crystal structure of the 80S ribosome of *S. cerevisiae* at 4.15 Å resolution (Ben-Shem et al., 2010). Generally, the basic structural organisation of the eukaryotic ribosome resembles that of prokaryotes but with a considerably larger complex portraying several common recognizable features. The solvent exposed side at the surface of the subunits contains the rRNA expansion elements. A key expansion element is ES6 of the 40S subunit which significantly expand the ribosome's interaction network. A more accurate outline of the components of the inter-subunit bridges, described earlier by cryo-EM, corresponds to the bridges in the crystal structure of the bacterial ribosome (Ben-Shem et al., 2010). This work describes the ribosomal movement in a ratcheted state, showing counter-clockwise rotation of the 40S subunit by 4^0 to 5^0 relative to the 60S, and rotation of the head of the 40S by 15.5^0 in the direction of the tRNA E-site. This report is followed by yet another crystal structure of the eukaryotic 80S ribosome from *S. cerevisiae* at 3.0 Å resolution, showing almost all of the rRNA bases alongside protein side chains (Ben-Shem et al., 2011). This latter study provided a more detailed account of the complex network of interaction in eukaryotic ribosomes. The core conserved region of the ribosome is surrounded by eukaryotic-specific elements, ESs and additional proteins that are located around the surface of the ribosome. Several key variations in the spatial organisation of

rRNA and ESs were observed. In the 40S, eukaryotic specific rRNAs are mostly located towards the bottom, a position where the largest ESs (ES3S and ES6S) interact, and eukaryotic specific proteins are scattered across its surface. In the 60S, the ES form a circle that surrounds the exit channel in a ring-like manner and this structure associates with the eukaryotic specific proteins. The network of the central protuberance of the 60S is expanded and contains many additional elements that contribute towards its function. This study also revealed that the *S. cerevisiae* protein stm1, previously reported to inhibit translation through its association with the ribosomes (Van Dyke et al., 2006; Van Dyke et al., 2009), binds to the head of the 40S and inserts an α helix in the entry tunnel and prevent mRNA accessibility.

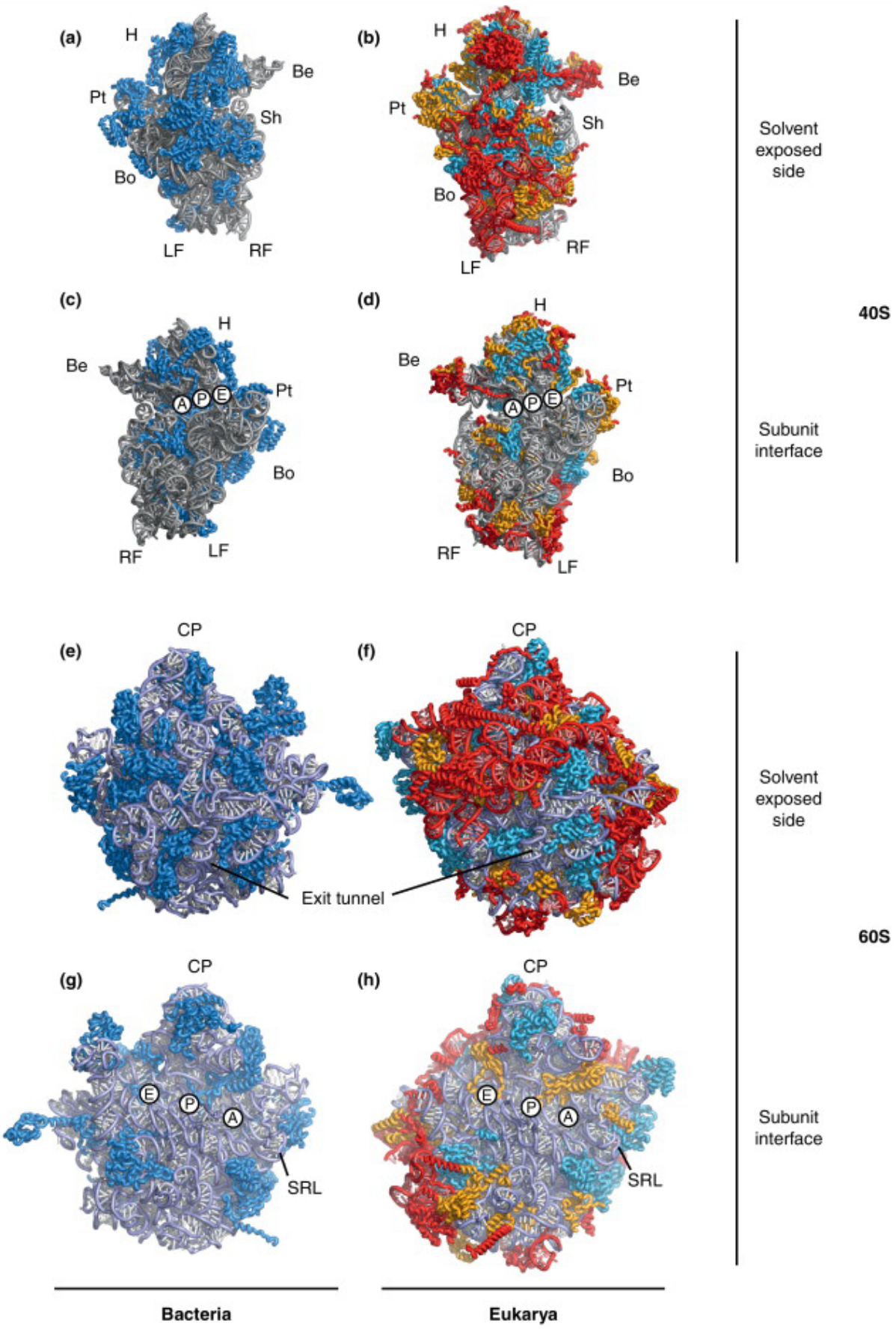
(a)
H
Be
Pt
Sh
Bo
LF
RF
(b)
H
Be
Pt
Sh
Bo
RF
LF
(c)
H
Be
A
P
E
Pt
Bo
RF
LF
(d)
H
Be
Pt
A
P
E
Bo
RF
LF
Solvent exposed side
Subunit interface
40S
(e)
CP
Exit tunnel
(f)
CP
(g)
CP
E
P
A
SRL
(h)
CP
E
P
A
SRL
Solvent exposed side
Subunit interface
60S
Bacteria
Eukarya

Figure 1.4. Specific features of the Eukaryotic ribosome. Structures of bacterial ribosome subunits are indicated in shades of blue and gray while eukaryotic ribosomes are shown in coded colours as follows: Universally conserved RPs are indicated in light blue, common RPs between archaea and eukaryotes in gold, RPs and RNA elements exclusive to eukaryotes in red. (a) and (c), solvent-exposed side and subunit interface of *Thermus thermophilus* 30S subunit respectively (PDB code 2J000). (b) and (d), solvent-exposed side and subunit interface of *Tetrahymena thermophila* subunits respectively (PDB code 2xzm). Key features of the small subunit such as head (H), beak (Be). Platform (Pt), shoulder (Sh), body (Bo), left foot (RF) and the A-, P- and E-sites are all indicated. (e) and (g) indicates the solvent-exposed side and subunit interface of *T. Thermophilus* 50S subunit respectively (PDB code 2j01). Likewise, (f) and (h) indicates the solvent-exposed side and subunit interface of T. thermophila 60S subunit (PDB codes 4A17 and 4A19). Central protuberance region (CP), SRL, peptide exit tunnel and A-, P-, and E-sites are all indicated. This figure was taken from (Klinge et al., 2012).

More recently, high resolution cryo-EM density maps of *Drosophila* and human ribosomes were reported (Anger et al., 2013). This study unravelled the complex structure of the *D. melanogaster* 80S ribosome from embryonic extracts, and human 80S ribosome from human peripheral mononuclear cells in complex with eEF2, E-site transfer RNA and some stm1-like proteins. These structures were determined with an average resolution of 5.4 to 6 Å, with the human 80S ribosome's local resolution ranging from 9 Å on the flexible periphery, to 4.8 Å for the larger regions. Key observations include metazoan-specific rRNA and RPs compared to the yeast 80S. An appreciable increase in protein mass was observed in *Drosophila* ,about 1094 amino acids, representing about an 8% increase, and 7996 amino acids in humans representing about 6% of the increase when compared to yeast (Anger et al., 2013). Some extra RNA layers were observed in metazoan ribosomes; a highly organised inner layer formed as a result of many RNA-RNA tertiary interactions, which is protected by a flexible outer layer resulting from helical insertions and extended rRNA ES (Anger et al., 2013). Human and *Drosophila* have the same number of ESs as yeast and protists, but their ESs were found to be longer and contain extra ES30L and E343L that are metazoan specific. The EF2 of humans was found to contain additional insertions that were not observed in *Drosophila* EF2 thereby increasing its density. Furthermore, two metazoan-specific inter-subunit bridges were observed in addition to all bridges previous reported in yeast as eukaryotic specific (Ben-Shem et al., 2011).

1.5.1 Ribosome biogenesis

Biogenesis of ribosomes is a conserved, essential process in eukaryotic cells. The pathway for ribosome synthesis is a complex and highly coordinated multi-step process which utilises hundreds of genes that are required to produce functional rRNAs and the associated RPs. In

eukaryotic organisms, this process occurs in the nucleolus, a compartment located in the nucleus (Figure 1.4) (Tschochner and Hurt, 2003; Thomson et al., 2013). Within the nucleolus, this coordinated process occurs in the three sub-nucleolar regions, the fibrillar centre (FC), dense fibrillar centres (DFC) and the granular component (GC) (Figure 1.4) (Shaw and Brown, 2012).

Ribosome biogenesis has been well-studied over the past three to four decades, with a good understanding of the pathway coming from a study in the yeast, *S. cerevisiae* (Li et al., 2009). The process requires the action and coordination of all three RNA polymerases (I, II and III) and begins with transcription of the rRNA genes that encode the 18S, 5.8S and 28S (25S in yeast) rRNAs. These rRNA genes are separated within their sequences by internal transcribed spacer (ITS) sequences and their 5' and 3' ends are flanked by external transcribed spacers (ETS) (Tschochner and Hurt, 2003). The 28S, 18S and 5.8S are transcribed from rDNA repeats by Pol I in the nucleolar organiser regions (NORs) as a polycistronic pre-rRNA in the DFC and at the peripheral regions of the FC of the nucleolus (Hozak et al., 1994; Dundr and Raška, 1993). The 5S rRNA is transcribed by Pol III in the GC region (Dundr and Raška, 1993) and the RP genes transcribed by Pol II (Figure 1.5 and 1.6). Ribosomal proteins are synthesised in the cytoplasm and are rapidly imported to the nucleus where they associate with rRNA to form the pre-ribosomal subunits (Lam et al., 2007; Tschochner and Hurt, 2003).

The first detected transcribed intermediate is a 35S precursor, which folds to yield a transient 90S pre-ribosomal particle (Perez-Fernandez et al., 2007; Schneider et al., 2007; Fromont-Racine et al., 2003). The 90S pre-RNA particle undergoes a series of co-transcriptional and post-transcriptional cleavages thereby releasing the pre-40S particle,

which contains an extended 20S pre-rRNA that is trimmed in the cytoplasm (Grandi et al., 2002; Udem and Warner, 1972). Subsequently, the pre-60S complex forms on the remaining transcript. The RPs of the small subunit assemble on the body and platform regions of the pre-40S co-transcriptionally. Other RPs bind the head region of the 40S within the nucleus prior to cytoplasmic export, except for RpS10 and RpS26 which become incorporated into the small subunit in the cytoplasm (Ferreira-Cerca et al., 2005). Conversely, the bulk of the 60S RPs are assembled on the large subunit in the cytoplasm during late maturation. Both the small and large subunits independently undergo additional processing within the nucleus and are then exported separately to the cytoplasm via the NPC. The maturation of both subunits occurs in the cytoplasm, for example, cleavage of the 20S pre-rRNA to 18S rRNA (Udem and Warner, 1973). In mammalian cells, it was initially reported that the 18S rRNA of the 40S subunit is fully processed in the nucleus (Penman et al., 1966), but a later study indicated that the pre-40S is also exported to the cytoplasm with the 20S pre-rRNA still intact (Rouquette et al., 2005). Two very recent studies reported that the last processing step of the pre-40S ribosome, involving trimming of the 20S pre-rRNA to 18S rRNA, requires the association of the pre-40S subunit with the 60S subunit to form a translation-like 80S ribosome, facilitated by eIF5B (Lebaron et al., 2012; Strunk et al., 2012). The 80S, however, is devoid of mRNA and tRNA and hence does not engage in translation. This 80S-like assembly must be dissociated before the mature 40S subunit can bind mRNA and initiate translation (Strunk et al., 2012). Thus, it was believed that the immature subunits are incapable of mRNA binding and translation initiation. Despite this, a previous study in *S. cerevisiae* concluded that the immature pre-40S ribosome is competent enough to initiate translation, but the resultant 80S proves ineffective during translation and is targeted and destroyed by mRNA decay mechanisms (Soudet et al., 2009). The pre-40S and pre-60S

subunits contain some assembly factors (AFs) that prevent them from premature translation initiation, keeping the subunits inactive in the nucleus until they are removed during final steps of maturation in the cytoplasm (Udem and Warner, 1973; Strunk et al., 2011; Panse and Johnson, 2010).

Ribosome biogenesis requires several trans-acting factors which participate at various steps of the pathway (Venema and Tollervey, 1999). These include an array of non-ribosomal proteins, small RNAs (SnoRNPs), endo and exonucleases, chaperones (assembly factors) and other transacting factors, that collectively modify and cleave pre-rRNAs and assemble and export ribosomal particles (Zemp and Kutay, 2007; Kressler and al., 1999). Defects in ribosome biogenesis are associated with certain disease conditions, for example Diamond-Black fan anaemia and 5q- syndrome are associated with a reduced level of actively dividing bloodline cells, both resulting from haploinsufficiency of RPs (Karbstein, 2013).

As reviewed above, although the majority of earlier studies are of the view that pre-40S subunits are inactive, and hence nuclear translation cannot take place, there is some evidence that they can indeed, to some extent, engage in translation.

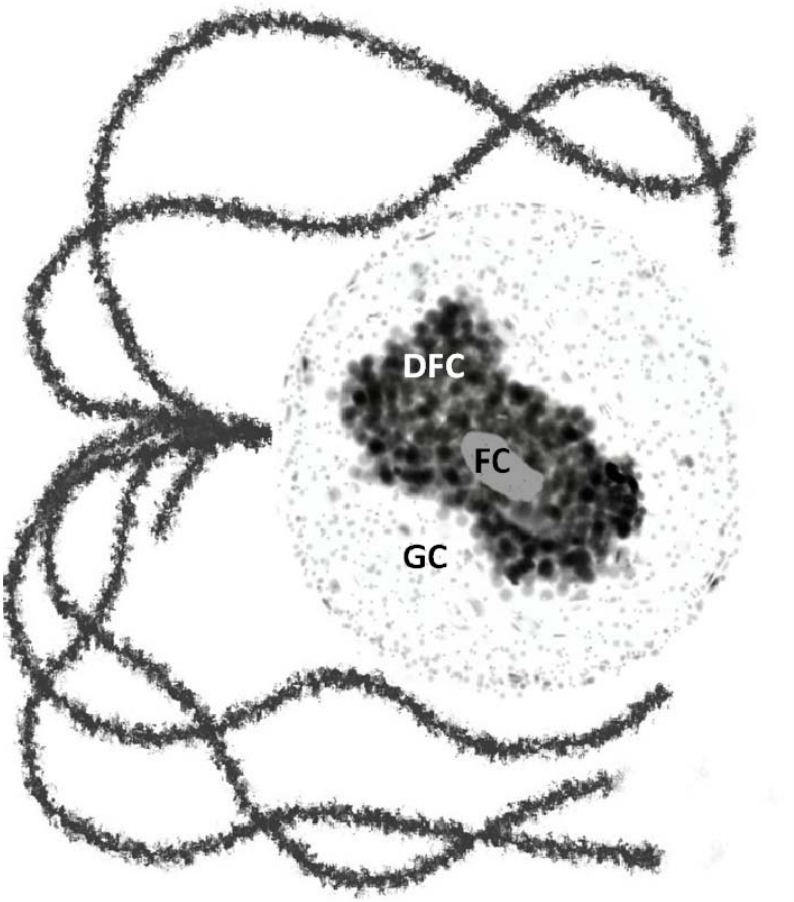

Figure 1.5. Schematic of a typical nucleolus surrounded by the chromosome. Schematic representation of a typical eukaryotic nucleolus showing the regions involved in ribosome biogenesis**;** fibrillar centre (FC) which constitutes about 2 %, dense fibrillar center (DFC) which make up about 17% and the granular component (GC) which constitutes about 75% of the nucleolus. Transcription of rRNA occurs mostly within the DFC and the peripheral regions of the FC whereas pre-ribosomal assembly occurs at the GC region. This figure is taken and modified from (McLeod et al., 2014).

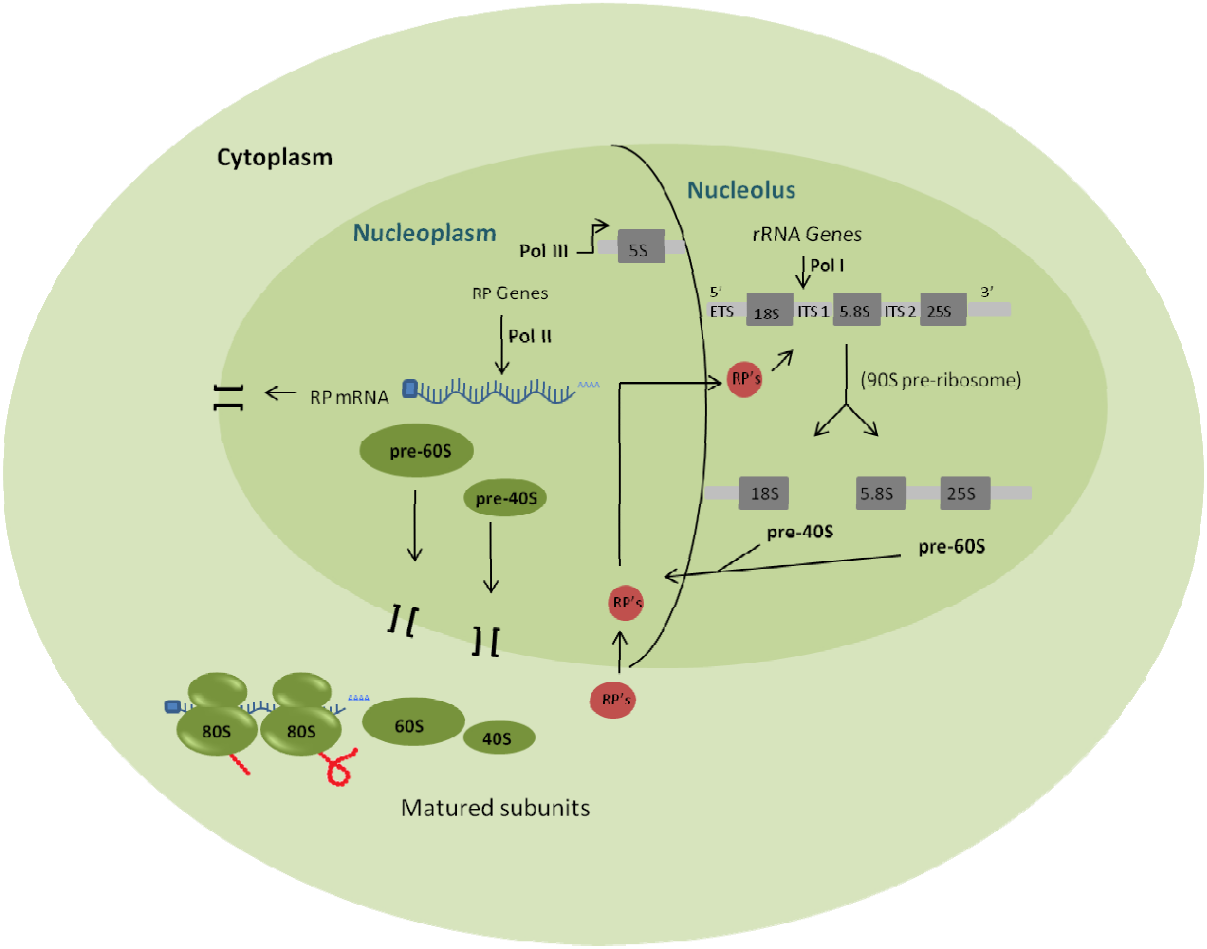

Figure 1.6. Schematic of the eukaryotic ribosome biogenesis. The rRNAs 18S, 5.8S and 28S (25S in yeast) are transcribed by Pol I in the DFC and possibly at the peripheral area of the FC whereas 5S is transcribed separately by Pol III. Further processing and assembly occur in the nucleus. RPs genes are transcribed in the nucleus and translated in the cytoplasm by the ribosome. The RPs are then imported to the nucleolus where they mostly assemble on the pre-RNA co-transcriptionally. Some of the RPs assembles on the ribosome in the cytoplasm during the last maturation steps.

1.5.2 Specialized ribosomes

Although ribosomes were thought to be identical across an organism's cell types, recent studies are increasingly indicating that there are variations in composition between individual ribosomes and that this feature may have a significant role in defining the kind of proteins they produce (Xue and Barna, 2012; Gilbert, 2011; Moll and Engelberg-Kulka, 2012). An early study that demonstrated the existence of specialized ribosomes in translation was reported nearly 30 years ago in *E. coli* (Hui and de Boer, 1987). This study demonstrated that some modified ribosomes, with altered Shine-Delgarno (SD) sequences, were able to translate some mutated mRNAs. More recently, a study in *E. coli* reported the translation of leaderless mRNAs by a group of ribosomes that are modified by the MazF toxin (Vesper et al., 2011; Moll and Engelberg-Kulka, 2012; Filipovska and Rackham, 2013). The MazF toxin is an endoribonuclease produced from the stress-induced toxin-antitoxin (TA) module Maz EF, that acts on both single stranded mRNA and the 16S rRNA of the bacterial 30S ribosome subunit, cutting them at the ACA codon (Vesper et al., 2011). This action generates leaderless mRNAs (lmRNAs) and a unique 30S subunit ribosome with a 16S that is 43 nucleotides shorter at the 3'end. This 30S can form a translation competent ribosome that preferentially translates lmRNAs (Moll and Engelberg-Kulka, 2012; Vesper et al., 2011). Interestingly, lmRNAs are found in all kingdoms of life (Janssen, 1993). Additionally, some observations revealed that many mRNAs possess segments that are complementary to a sequence within either the 18S or 28S, suggesting the possibility of a mechanism that allows direct interaction between mRNAs and ribosomal subunits through base pairing of these complementary sequences (Mauro and Edelman, 2007). Furthermore, eukaryotic ribosomes were reported to differ in rRNA sequences and RPs composition at

different developmental stages and in particular cells or tissues (Ramagopal, 1992). This led to the hypothesis that there exists an array of structurally different ribosomes that can translate a specific set of mRNAs (Mauro and Edelman, 2007).

Previous studies have reported that heterogeneity in RP composition within a ribosome may confer these specialized functions in translation, and may regulate the translation of a subset of mRNAs by controlling access to the binding sites within the rRNA (Mauro and Edelman, 2002; Mauro and Edelman, 2007). Similarly, the degree of expression of several RPs was found to differ in different cell types, growth conditions or developmental stages in *D. discoidium*, *Arabidopsis thaliana*, *D. melanogaster and human cells* (Weijers et al., 2001; Ramagopal, 1990; Filipovska and Rackham, 2013; Kondrashov et al., 2011). For example in *Arabidopsis*, one ribosomal protein of the small subunit, RpS5, has two duplicates, RpS5A and RpS5B, of which RpS5A is the most highly expressed in actively dividing cells, whereas the RpS5B is expressed in differentiating cells (Weijers et al., 2001). In translation, RpS25 was reported to be required for IRES-mediated translation initiation and 40S ribosomal subunits devoid of RpS25 could not initiate translation via an IRES element (Nishiyama et al., 2007; Muhs et al., 2011). Similarly, an RpL38 mutation in mice was found to show a minimal effect in general translation inhibition but selectively inhibits the translation of Homeobox (Hox) mRNAs (Filipovska and Rackham, 2013; Barna, 2013). Recently, a ribosomal protein of the large subunit, RpL40, that on the whole is not required for general cellular mRNA cap-dependent translation initiation, was reported to be essential for initiating translation in a number of *Mononegavirales viruses*, for example vesicular stomatitis virus cap-dependent mRNA translation, and completely dispensable for IRES-mediated translation of other viral mRNAs (Lee et al., 2013; Barna, 2013). This suggested that the RpL40 translation dependent

pathway is involved in stress responses. Further evidence supporting this view came from a survey of protein expression in mice using sub-cellular fractionation coupled with tandem mass spectrometry-base shotgun sequencing (Kislinger et al., 2006). Analysing this data with a web-browser interface revealed that certain RPs were present in all tissues examined whereas others were not always detected (Kislinger et al., 2006). Other RPs were found to be more abundant in particular tissues, or were less abundant or completely absent in other tissues. For example RpS3 and RpS7 were observed in all tissues but RpS6, which was found to be abundant in the brain, kidney and liver has a lower level in the lungs and is completely absent in the heart (Mauro and Edelman, 2007). Similarly, we have observed in our laboratory that endogenously YFP-tagged RpL41, which was found to be abundant in many tissues and cell types, is particularly concentrated in larval *Drosophila* adult midgut progenitor cells (AMPs) but absent in differentiated enterocytes and enteroendocrine cells (unpublished data in our lab). Taken together, these data indicate that the composition of ribosomes is of great importance in determining the sets of mRNAs they translate.

1.6 Ribosomal proteins

Ribosomal proteins (RPs) are essential elements of the ribosome and play a vital role in its biogenesis, functions and structural integrity. Although rRNA is the catalytic core and constitutes the bulk of the ribosome's structure, RPs are required for viability in all cell types. Many RPs are evolutionary conserved from bacteria to humans. The number of RPs, and the extent of their conservation, varies between prokaryotes and eukaryotes. Eubacteria possess 50-54 RPs, archaea 57 -68 and eukaryotes have 79-81 (Nomura, 1999). RPs are mostly located on the surface of the ribosome, characterized by their exposed N-terminal globular domain and a long C-terminal domain that extends inwards to the rRNA (Brodersen et al., 2002). An early investigation of the *Drosophila* genome identified 78 RPs

by two-dimensional gel electrophoresis (Lambertsson, 1975), of which nearly 30 RPs were purified and biochemically analysed. A further comprehensive genetic characterization of RP genes in *Drosophila* has revealed 88 genes encoding 79 different RPs (32 from the 40S subunit and 47 from the 60S subunit) (Marygold et al., 2007). These identified proteins have corresponding orthologs in humans (Marygold et al., 2007). The majority of *Drosophila* RPs are encoded by single genes, however, nine arise from duplicated genes, both of which are functional, with the two distinct genes for each RP being identified by a lower case 'a' or 'b' suffix to the gene symbol, for example RpL34a and RpL34b are different genes that encode the same protein (McConkey et al., 1979; Wool, 1996; Marygold et al., 2007). Of these duplicated genes, 6 are components of the 40S subunit and the remaining 3 belong to the 60S. The possible origin of these duplications is either gene transposition or retrotransposition of a copy of an ancestral gene. The copy of the gene that resembles the human ortholog is steadily expressed and produces the bulk of the RPs in most cells, while the other copy is expressed in some specific tissues and may have additional roles apart from ribosome biogenesis (Marygold et al., 2007). However, the most highly expressed RPs in cells are encoded by single genes (Marygold et al., 2007). Orthology of *D. melanogaster* Rps genes with that of human, *S. cerevisiae* and *E. coli* are presented in (Table 1). RP genes are also given the prefix 'Rp' based on the standard metazoan gene nomenclature (Wool et al., 1991). Ribosomal proteins mutation in *D. melanogaster* causes a minute phenotype characterized by a delay in larval development, thin and short bristles, decrease in body size, poor fertility and overall decreased viability (Lambertson, 1998; Marygold et al., 2007). Such haploinsufficiency is caused by both RP homologs being required in equal proportions; deletion of one copy causes a reduction in the cell's ribosome pool, leading to sub-optimal

protein synthesis (Marygold et al., 2007). In *Drosophila,* 66 of the 88 genes are possibly haploinsufficient and can be linked with a minute phenotype (Marygold et al., 2007).

Table 1: Orthology of *D. melanogaster* RP genes with human, *S. cerevisiae* and *E. coli* RPs

Human RPs	*S. cerevisiae* RP's	*D.melanogaster* RP's	*E. coli* RP's
RPSA	RPS0A RPS0B	**sta**	RPS2
RPS3	RPS3	**RpS3**	RPS3
RPS9	RPS9A RPS9B	**RpS9**	RPS4
RPS2	RPS2	**sop**	RPS5
RPS5	RPS5	**RpS5a** **RpS5b**	RPS7
RPS15A	RPS22A RPS22B	**RpS15Ab** **RpS15Aa**	RPS8
RPS16	RPS16A RPS16B	**RpS16**	RPS9
RPS20	RPS20	**RpS20**	RPS10
RPS14	RPS14A RPS14B	**RpS14a** **RpS14b**	RPS11
RPS23	RPS23A RPS23B	**RpS23**	RPS12
RPS18	RPS18A RPS18B	**RpS18**	RPS13
RPS29	RPS29A RPS29B	**RpS29**	RPS14
RPS13	RPS13	**RpS13**	RPS15
RPS11	RPS11A RPS11B	**RpS11**	RPS17
RPS15	RPS15	**RpS15**	RPS19
RPL10A	RPL1A RPL1B	**RpL10Ab** **RpL10Aa**	RPL1
RPL8	RPL2A RPL2B	**RpL8**	RPL2
RPL3	RPL3	**RpL3**	RPL3
RPL11	RPL11A RPL11B	**RpL11**	RPL5
RPL9	RPL9A RPL9B	**RpL9**	RPL6
-	RPP0	**RpLP0**	RPL10
RPL12	RPL12A RPL12B	**RpL12**	RPL11
RPLP1	RPP1A RPP1B	**RpLP1**	RPL7/L12
RPL13A	RPL16A RPL16B	**RpL13A**	RPL13
RPL23	RPL23A RPL23B	**RpL23**	RPL14
RPL27A	RPL28	**RpL27A**	RPL15
RPL10	RPL10	**Qm**	RPL16
RPL5	RPL5	**RpL5**	RPL18
RPL17	RPL17A RPL17B	**RpL17**	RPL22
RPL23A	RPL25	**RpL23A**	RPL23
RPL26	RPL26A RPL26B	**RpL26**	RPL24
RPL35	RPL35A RPL35B	**RpL35**	RPL29
RPL7	RPL7A RPL7B	**RpL7**	RPL30

Source: Ribosomal Protein Gene Data base/(Marygold et al., 2007).

Apart from their major role in the biogenesis and functions of the ribosomes, various RPs were reported to exhibit extra ribosome-independent functions across all organisms. Extra ribosomal functions of some RPs include certain roles in DNA repair, transcription, apoptosis, mRNA processing, development and tumor genesis (Lindsrom, 2009; Wool, 1996). For example, RpS3, which is conserved from bacteria to humans, is involved in DNA repair via specific enzymatic activity. *Drosophila* RpS3 exhibits N-glycosylase activity, an enzyme involved in oxidative stress associated DNA repair via a base excision repair mechanism (Kim et al., 1995; Graifer et al., 2014). RpS3 is also involved in gene regulation via the NF-kb (nuclear factor-kappa B) signalling pathway. It acts through association with the P65 component of NF-kb and facilitates its binding to DNA, raising the expression of kb-dependent genes (Graifer et al., 2014). Other suggested roles of RpS3 include immune responses, cell proliferation, apoptosis induction and auto-regulation of its own gene (Graifer et al., 2014). RpS27a was recently described as an enhancer of proliferation, cell cycle regulation and apoptosis suppression (Wang et al., 2014). RpL11 was reported to be transcriptionally activated by the oncoprotein c-Myc, and its high expression inhibits the transcriptional activation of target genes by c-Myc by binding and suppressing it (Dai et al., 2007). In mammalian cells, RpS13 is reported to inhibit its own splicing by binding to its own pre-mRNA near the splice site of the first intron, which likely prevents spliceosome assembly (Malygin et al., 2007). Similarly RPs S14, L12 and L30 are reported to inhibit their own splicing, reviewed in (Warner and McIntosh, 2009) and L2 and S28 shorten their own mRNA half-life. In *Drosophila*, RpL22 was found to interact with the linker histone H1 on condensed chromatin; its depletion increases transcription rate while high expression leads to transcriptional repression (Ni et al., 2006). In summary, there are several line of evidence for

RPs that are not assembled into ribosomes, but which play additional important roles, unrelated to their primary function in the ribosome during translation.

1.7 Aim and Objectives

As reviewed above, a number of previous studies have indicated that translation, or a translation-like mechanism, exists in the nucleus. At the start of my PhD, this issue remained controversial, although, evidence from a previous project in the Brogna laboratory had demonstrated the presence of assembled 80S ribosomes in the nucleus of *Drosophila* cells. Whether these corresponded to functional ribosomes was not understood and it remained to be resolved as to whether their occurrence increased under stress conditions.

The major aims of my PhD project were therefore to:

1. Further address the issue of whether ribosomal subunits interact to form 80S ribosomes in the nucleus, and whether this interaction is translation dependent.
2. To investigate whether nuclear ribosomes increase during cellular stress.

To investigate these issues, I further characterised the bimolecular fluorescence complementation (BiFC) technique that was previously developed in our laboratory to study ribosomal subunit interactions in living cells. Additionally, I developed a similar but more sensitive BiFC assay with which we were able to obtain compelling evidence that the assay is in fact reporting translation-dependent joining of 80S ribosomes, in both the nucleus and cytoplasm of *Drosophila* cells and that cells stress increases this event in the nucleus

CHAPTER 2

2.0 Materials and Methods

2.1 Solution and Buffers

All buffers, media and other solutions were made based on the standard protocols described in Molecular Cloning 3rd Edition, (Sambrook et al., 1989) unless otherwise stated. Solutions were prepared with analytical grade reagents made in deionised water and sterilized by either autoclaving or filtration with 0.22 μm Supor filter (Pall Corporation).

2.2 DNA cloning in Escherichia coli (E. coli).

Standard protocols as described in Molecular Cloning 3rd Edition, 1989 (Sambrook et al., 1989).

2.2.1 *E. coli* Strains

Strains *XL1-Cell blue* strains were used as the host for general cloning.

2.2.2 Growth media for Bacteria

Recipes for LB broth liquid media, agar plates and NZY media are given in Appendix I.

2.2.3 DNA fragments ligation and *E. coli* transformation

Ligation of DNA fragments was typically done in a 10 μL reaction containing typically 100 μg/mL of linearised plasmid and a fourfold molar excess of the insert DNA, typically with 10 units of T4 DNA ligase (New England Biolabs, NEB). The ligation reaction was kept at 18^0C overnight. *E. coli* competent cells 100 μL were transformed with 5 μL of ligation mixture as follows: the ligation mixture was mixed with competent cells and kept on ice for 20 min, the

cells were then heat shocked for 45 sec at 42^0C and cooled on ice for 2 min. The competent cells were mixed with 0.5 mL NZY media and incubated at 37^0C for 1 hr with gentle shaking. The cells were briefly centrifuged and then spread on an LB plate containing 100 μg/mL ampicillin.

2.2.4 Small Scale preparation of plasmids (miniprep)

A single colony was inoculated into 2 mL LB broth containing 100 μg/mL ampicillin and grown overnight at 37^0. Plasmid DNA was extracted from 1 mL of the culture using a commercial kit (Bioline) or boiling prep method (see details of the protocol in Appendix II) for plasmid verifications.

2.2.5 Medium scale preparation of plasmid DNA

A single colony was inoculated into 1 mL of LB broth containing 100 μg/mL of ampicillin and grown for 6-7 hrs at 37^0C with shaking; this culture was then inoculated into 50 mL of LB broth containing 100 μg/mL ampicillin and grown overnight at same growth conditions. Plasmid DNA was extracted from the culture using a commercial midi prep kit (HiPure Plasmid Filter, Invitrogen). The extracted DNA plasmid was resuspended in 300 μL TE buffer, and the concentration of the DNA was measured with a spectrophotometer (ND-1000, NanoDrop).

2.3 Restriction enzyme digestion

All restriction enzymes used in this study were purchased from New England Biolabs (NEB). Restriction enzyme digestions were carried out in 20-60 μL reaction volumes. All the

conditions for a single enzyme or double enzyme digestion were applied according to the NEB enzyme instructions.

2.3.1 Dephosphorylation of DNA

Antarctic phosphatase (NEB) was used to remove the 5' terminal phosphate of the DNA. This was done to prevent self ligation of the digested plasmid DNA. Following the restriction enzyme digestion, 1 µL of the enzyme (5 units/µL) was added to the reaction mix and incubated at 37^0C for 1 hr. The DNA sample was then heat inactivated at 65^0C for 15 min and purified by gel electrophoresis and gel extraction using Silica Bead DNA Gel Extraction Kit (Fermentas).

2.4 DNA purification

Two methods were employed for the purification of DNA after restriction enzyme digestion. These are Polyethylene glycol (PEG) purification and Gel extraction method.

2.4.1 PEG purification

An equal volume of PEG solution (13% PEG8000 (w/v), 0.6 M NaAc, and 6 mM $MgCl_2.6H_20$) was added to DNA samples and mixed by vortexing. The samples were then centrifuged at 13000 rpm for 20 min and the supernatant discarded. The pellet was washed with 0.6 mL of 75% ethanol by spinning twice, each for 5 min. The pellet was then air dried and dissolved in 20-30 µL TE buffer.

2.4.2 Gel purification

The DNA fragment was sliced out of the gel and placed into a 1.5 mL eppendorf tube. The DNA was then purified by silica powder as described in the manufacturer's instructions Silica Bead DNA Gel Extraction Kit (Fermentas).

2.5 PCR for colony screening

Fresh bacterial colonies were mixed with 10 µL of PCR solutions which contained 1X PCR buffer (Go Taq, Promega), dNTP's mixture (0.2 mM each), 1.5 mM $MgCl_2$, 2 µM primers and 0.25 Taq Polymerase (Go Taq, Promega), and amplified using standard parameters.

2.5.1 PCR for cloning

High fidelity (HF) Phusion DNA polymerase (NEB) was used to amplify DNA fragments from *Drosophila* cDNA plasmid libraries (available at Drosophila Genomic Resource Center, (DGRC)). Approximately 1 ng of DNA was used as a template and amplified in 25 µL reactions containing 1X Phusion HF buffer, dNTP mixture (0.2 mM of each), primers and 1 U DNA polymerase. The PCR parameters were typically: 98^0C for 30 seconds, 98^0 C for 10 seconds, 50^0 C for 30 seconds, 72^0C for 30 seconds and 72^0C for 10 min run for 30 cycles.

2.5.2 Agarose gel elecrophoresis of DNA

Following PCR or restriction enzyme digestion, the DNA samples are normally run on an agarose gel to separate and verify whether correct bands of the right molecular weight were obtained. The DNA samples were mixed with DNA loading buffer (10X stock, 20% glycerol, 0.1 M EDTA, pH 8.0,, 0.25% bromophenol blue and 0.25% xylene cyanol), and loaded onto

4% agarose gel with 0.5 μg/mL ethidium bromide and run at 90 volts. DNA 1 kb ladder was used as a loading control.

2.6 Protein-protein interaction detection techniques in living cells

Protein–protein interaction and proteins-other macromolecules interactions are essential for cell survival. Identification and classifying various interactions between proteins that participate in the same cellular processes may give us a broad picture of how the network of event occurs within cells. The Bimolecular fluorescence complementation technique (BiFC) is an assay that allows the detection of protein-protein interactions, and localisation of putative interacting protein partners in living cells (Hu et al., 2002b). This technique offers a convenient and more direct alternative to Fluorescence or Foster Resonance Energy Transfer (FRET) that is equally used to study interacting proteins partners in cells. The BiFC method utilise a fluorescent protein which is split into two complementing halves, and then each half is fused to one of the pair of predicted interacting protein partners (Figure 2.0). When the BiFC tagged protein pairs are co-expressed in cells, their interaction brings the non-fluorescent halves into close proximity, permitting the formation of the BiFC complex. This process requires the regeneration of the intact fluorescent protein, thereby facilitating the detection of the interaction sites (Shyu et al., 2008). BiFC assay uses a number of fluorescent proteins which may include yellow fluorescent protein (YFP), enhanced cyan fluorescent protein, cerulean, mCherry, citrine, mRFP1, Venus and many other variants of GFP that were demonstrated to be effective in fluorescent complementation in many different cells and organisms (Shyu et al., 2008). For the purpose of this research, the Yellow fluorescent protein (YFP) and Venus fluorescent protein (VFP) were employed. Initially, I started this project with YFP fragments before shifting to the more sensitive VFP. In YFP, delay in chromophore maturation and sensitivity to high temperatures is a limiting factor

and hence chromophore development requires pre-incubation at a low temperature before visualisation. In addition, fluorescent intensity is generally weak in YFP complementation. The Venus fluorescent protein is an improved mutant of YFP which exhibit several folds higher BiFC efficiency, relatively short incubation, almost twice increase in BiFC-specific signals, and low amount of plasmid was shown to be effective in achieving optimum transfection (Shyu et al., 2006). The major benefit of BiFC assay over previous or similar techniques is that interactions can be directly detected in living cells avoiding the possibility of potential artefacts from either cell lysis or fixation. Furthermore, the putative interacting partner proteins are expressed at a level that is comparable to their corresponding endogenous counterparts (Hu and Kerppola, 2003). However, the irreversible nature of the BiFC fluorescent complex limits the application of this technique for investigating kinetic changes in protein interactions. Also, a fluorescent complementation does not always signify direct association of the fusion proteins, but shows that they are localized within the same compartment in the cell (Hu and Kerppola, 2003). The BiFC assay was first employed by a study in *E. coli* and *Hela* cells (Nagai et al., 2001). The *in vivo* visualisation of interacting protein partners was first validated by Hu *et al*. in a study in mammalian cells, where they explored the associations between transcription factors (Hu et al., 2002b). In this project, the BiFC assay was employed to investigate generation of BiFC complexes *in vivo* between ribosomal subunits to monitor the sub-cellular localisation of the subunits interaction as a consequence of translation initiation in *Drosophila* S2 cells and transgenic flies.

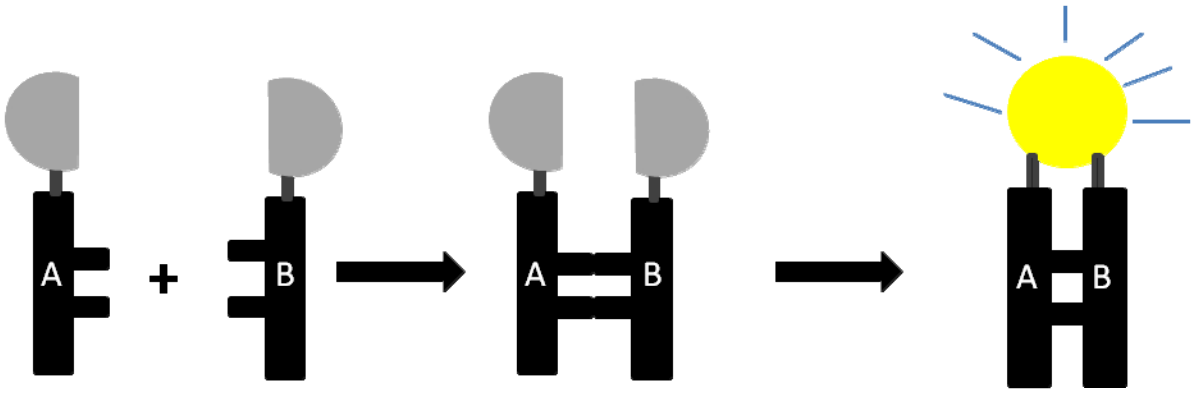

Figure 2.0. Schematic illustration of the BiFC assay. Fragments of Venus fluorescent protein (VFP): N-terminus Venus (VN) and C-terminus Venus (VC) are fused to potential interacting proteins partners A and B. Association of these potential interacting partners brings the split fragments into close proximity which drives the formation of the intact fluorescent protein leading to the generation of bimolecular fluorescence complex. BiFC fluorescence can be observed by a standard fluorescence microscope.

2.6.1 Generation of construct expressing BiFC tagged ribosomal proteins (RPs)

To generate plasmids expressing RPs tagged at carboxy terminus (C –terminus) with either YFP or VFP derived BiFC fragments, I employed the same cloning strategy throughout. The description below gives a detailed protocol on how I constructed tagged Rp18 and RpL11 with Venus fragments (Figure 2.1). First, I PCR amplified the DNA fragments coding for the N-terminal (VN: 1-173) and C –terminal (VC: 155-238) moieties of Venus. In the first cloning step, the VN fragment was PCR amplified with primers A1 and A2 (see Appendix III for the list of primers). The A1 primer corresponds to the beginning of the VFP coding region flanked with an in frame sequence encoding RSIAT, the same linker as between Jun and YN in the previously described pBiFC Jun-YN construct (Hu et al., 2002b). Similarly, the VC fragment was PCR amplified with the A3 and A4 primers. The A3 primer corresponds to the beginning of the VC fragment flanked with an in-frame sequence encoding KQKVMNH, the same linker as between Foss and YC in pBiFC Foss-YN construct (Hu et al., 2002b) and the A4 to the reverse complement of the end of the VC. Both A1 and A3 are 5' tailed with EcoRI recognition site and A2 and A4 with XhoI site. I then inserted both the VC and VN fragments into the EcoR1 and XhoI located at the multiple cloning sites of pUAST vector (see pUAST vector map in Appendix V). This step generates intermediate plasmids pUAST.VN and pUAST.VC. Inserts coding for RpS18 and RpL11 were generated by PCR from cDNA library using specific forward primers (A9 and A11) that corresponds to the beginning of the RPs coding regions, and reverse primers (A10 and A12) that corresponds to the end of the RPs sequences. Both forward and reverse primers are 5' and 3' tailed with EcoRI recognition site. In the final step, I cloned these RPs fragments into EcoRI site of the previously produced intermediates pUAST.VN and pUAST.VC to obtain our complete tagged BiFC

reporter constructs. In some of the BiFC reporter constructs, I introduced a 25 amino acid linker Helical linker 4 (HL4) that was previously reported to effectively divide the domains of a bi-functional fusion protein (Arai et al., 2001) with the following sequence LAEAAAKEAAAKEAAAKEAAAKAAA. This is to enhance the flexibility of the BiFC peptides. Most of the plasmids are sequences verified while some are verified by restriction enzyme digestion. A list of the BiFC reporter constructs gives detail information about all plasmids used in this study and their sources (Appendix IV).

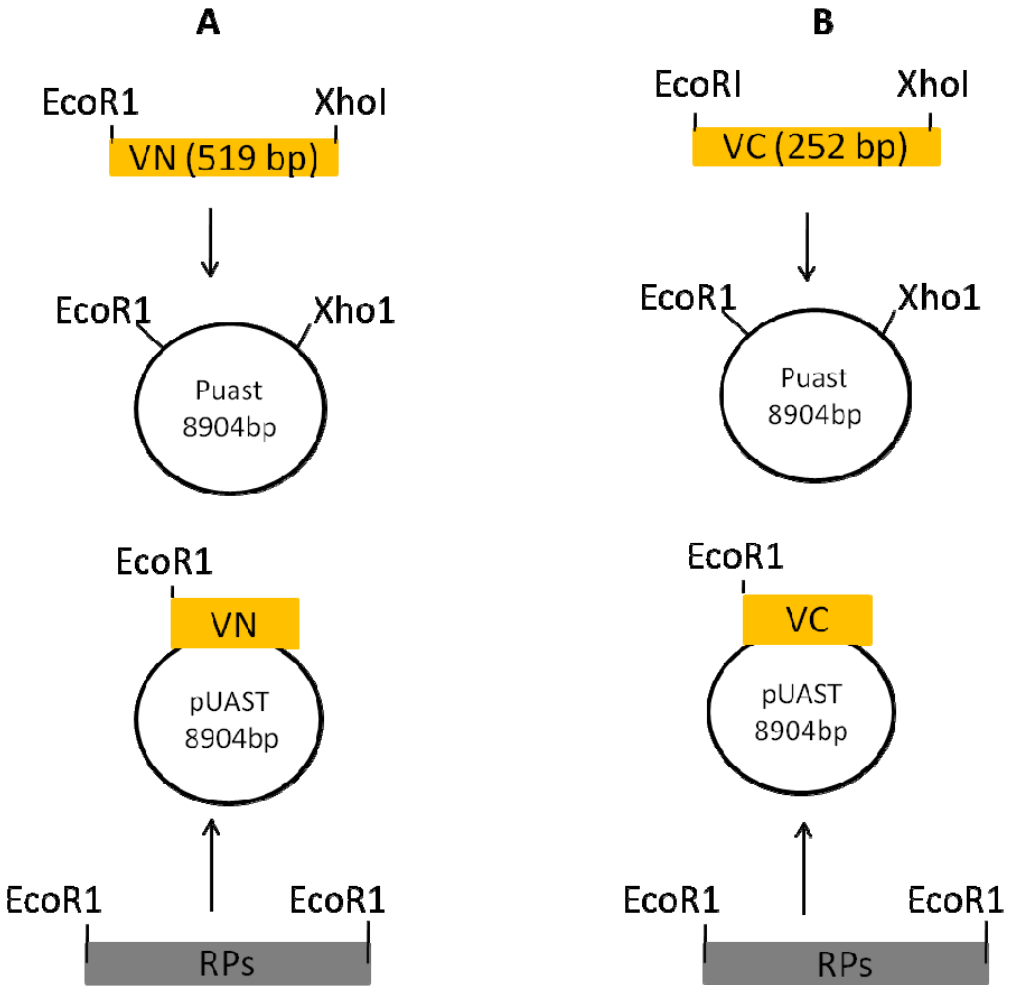

Figure 2.1. Schematic of the cloning strategy for generating constructs expressing BiFC-tagged ribosomal proteins. A and B, Maps of BiFC expression constructs; Ribosomal proteins are C-terminally tagged with VN and VC fragments respectively. The VN and VC coding regions were PCR amplified with specific primers (see the text) tailed with 5' EcoR1 and 3' XhoI sites and cloned into the EcoR1 and XhoI sites of pUAST. The RPs coding regions were PCR amplified with specific primers (see the text) tailed with EcoRI sites and cloned into the intermediates pUAST-VN and pUAST-VC respectively.

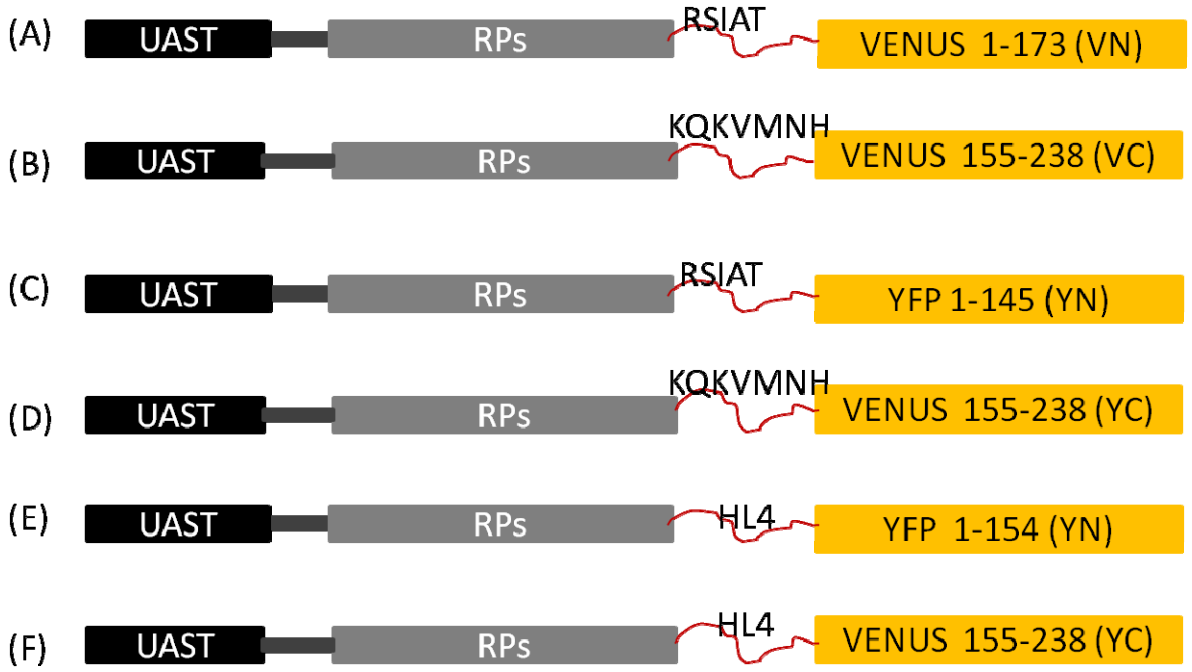

Figure 2.2. Schematic Illustration of the different BiFC-tagged ribosomal proteins. (A-F); Illustration of the BiFC reporter constructs showing the sequence of Venus fluorescent protein based BiFC fragments, C-D; illustrations of BiFC reporter constructs indicating the sequence of yellow fluorescent protein based BiFC fragments and E-F, are illustrations of BiFC reporters indicating sequence of yellow fluorescent protein based BiFC fragments with 25 amino acids helical linker (HL4).

2.7 Polysome analysis

2.7.1 Cell fractionation

Transfected cells (typically after 2 nights) were treated with 100 µg/mL cyclohexamide 15 min before harvest. Cells were chilled on ice and then pelleted at 4^0C. The pellet was washed in cold PBS and then lysed in 1X lysis buffer containing 20 mM HEPES pH 7.4, 2 mM magnesium acetate, 1 mM dithioreitol (DTT), 250 µg/mL heparin, 0.05 mM aurintricarboxylic acid (ATA, Sigma), 0.25% Triton X-100 and 100 µg/mL cyclohexamide. The lysis buffer also contains EDTA free protease inhibitor cocktail (Roche). When required, cells were treated with EDTA for 15 min. In this case, the lysis buffer and the gradient also contained EDTA. The lysates was centrifuged at 13,000 rpm for 20 min at 4^0C and supernatant (cell lysate) was collected in a clean eppendorf and the OD_{260} was determined. The lysates was then centrifuged at 37,000 rpm through a 10%-50% sucrose gradient for 2.5 hrs at 4^0C in a Beckman SW40Ti rotor. All the steps above were done at 4^0C. After centrifugation, the gradients were pumped (from the bottom using a steel capillary through a flow-through UV spectrophotometer (Pharmacia LKB-Optical Unit UV-1) with a peristaltic pump (P-1, Pharmacia) at a speed of 0.8 mL/min. The A_{254} was recorded as the fractions passed through the flow cell.

2.7.2 Fluorimetry

BiFC transfected cells were split into aliquots (0.5–1 × 107 cells) and then pre-incubated at room temperature with or without translation inhibition drugs. Cells were then washed once with ice-cold PBS, centrifuged, and the pellet was resuspended in 200 µL of polysome lysis buffer (as above) supplemented with the corresponding translation inhibitor drug at

the same concentration used for the cell culture treatment. Samples were cleared by centrifugation at maximum speed for 20 min at 4°C. The fluorescence was measured in a 100 µL micro quartz cuvette (Starna Scientific Ltd) using a PTI QuantaMaster 40 fluorimeter (Photon Technology International Inc), then analysed with the instrument FeliX32 software. To measure the YFP/VFP BiFC excitation spectrum, the sample was excited at the fixed wavelength of 488 nm and the excitation measured between 500 to 550 nm with the emission monochromator set at band pass of 3 nm. The BiFC fluorescence of each sample was automatically measured three times. Mean values were normalized by subtracting background readings of a parallel control extract of untransfected cells which was adjusted to have same OD260 as the other samples.

2.7.3 Protein precipitation

Following cell fractionation, the proteins were precipitated using trichlroacetic acid (TCA). To 0.8 mL of each fraction, 80 µL of 100% TCA was added and incubated at 4^0C overnight. The fractions were then centrifuged at maximum for 15 min at 4^0C and the supernatant discarded. 1 mL of acetone was added to the pellet, vortexed, incubated at room temperature for 5 min and then centrifuged for 5 min at 4^0C. This was done twice, and then the pellet was dried at 95^0C. The precipitate was then resuspended in 40 µL of 2X SDS gel loading buffer with 5% β-mercaptoethanol, and the proteins were denatured by 5 min boiling. The protein extract was kept on ice for 1 min and then centrifuged at maximum speed for 2 min at 4^0C. The clear supernatant of the samples were then loaded on SDS gel.

2.8 Cell culture and transfection

D. melanogaster Schneider line-2 cells (S2 cells) were grown on coverslips in a six-well plate in Insect-XPRESS medium (Lonza) supplemented with 10% fetal bovine serum, 1% penicillin/streptomycin/glutamine mix (Invitrogen), and grown at 27^0C incubator without $C0_2$. Transfection was done 24 hrs after seeding with 3 x 10^6 cells/ well and grown over-night to about 70% confluence. Transfection was done using 2.5 µg/mL of plasmids diluted in serum free media (250 µL). Cells were transfected using either TransIT (Mirus) following manufacture instructions or dimethyldioctadecylammoniumbromide (DDAB, Sigma) as previously described (Ramanathan et al., 2008). TransIT 2 µL or 6.5 µL of DDAB (4 mg/mL) per well was added to the DNA mix and incubated for 20 min at room temperature. While the DNA mix was incubating, cells were washed twice with no-serum containing Insect-XPRESS and left in the final wash until the end of incubation. At the end of the incubation, the transfection mix was diluted by adding 800 µL of no-serum media, mixed and gently transferred to the well/cells and incubated for 2 hrs at 27^0C without $C0_2$. After the incubation, the media was removed and replaced with 2 mL of 10% complete media with serum and antibiotics. This was then incubated for 1 or 2 nights at 27^0C without $C0_2$.

2.8.1 Fixation of S2 cells

Cells grown on coverslips for 24-48 hrs were fixed with 4% formaldehyde in PBS, pH 7.4, for 20 min at room temperature, washed 3 times in PBS at 10 min intervals. Permeabilized with cold 0.1% TWEEN 20/PBS on ice and then washed 3 times in PBS at 10 min interval each. DAPI (4-6-diamidino-2-phenyl indole) (Sigma-Aldrich) was added to PBS in 1:10,000 dilutions (0.1 µg/mL) to stain the DNA. Coverslip was mounted with a drop of fluorescence mounting medium (PromoFluor, Promokine). Slides were kept at 4^0C in a slide folder if they were not

to be viewed immediately. The remaining cells in the six well plates were lysed and the cells extracts was used for Western blotting.

2.8.2 Fluorescent immunostaining

Transfected S2 cells were fixed with 4% formaldehyde as described above but all washes were done in PBS/0.1% TWEEN 20. Fixed cells were washed for 10 min with 50 mM NH_4Cl to reduce the background then washed 3 times in PBS/0.1% TWEEN 20 at 10 min intervals each wash. The cells were then blocked with 4% BSA for 30 min, washed 2 times in PBS/0.1% TWEEN 20 at 10 min interval. Incubation with primary antibody (rabbit anti-GFP, Molecular Probes) was done at a dilution of 1: 100 in 4% BSA for 2 or 3 hrs at room temperature in a humid chamber. Diluted antibody 30 µL was placed on a glass plate covered with PARAFILM and the coverslips were put cells facing down slowly onto the primary antibody solution. At the end of the incubation, 1 mL of PBS/ 0.1% TWEEN was used to dislodge the coverslips from the PARAFILM by pipetting it around the edges of the coverslips. This will prevent the cells from detaching as the coverslip would be floating on PBS/TWEEN. The cells were washed 3 times with PBS/0.1 TWEEN 20 and the incubated with secondary antibody Cy-3 conjugated Affinity-pure goat anti rabbit IgG or Cy5-conjugated goat anti-rabbit (Jackson laboratories or Invitrogen) 1:250 dilution in 4% BSA as described above for primary antibody. This was done in a dark humid chamber at room temperature for 1.5-2 hrs. Following the secondary antibody incubation, the cells were washed with PBS /TWEEN twice for 10 min each. DAPI was added during the second wash at final concentration of 0.1 µg/mL in PBS/TWEEN to stain the DNA. Lastly cells were washed 1 time with PBS only and the coverslip was mounted as described above. For apoptosis detection, Anti-active caspase

3 (Ab13847, Abcam) primary antibody was used as described above and subsequently detected by Cy5-conjugate anti-rabbit (Jackson laboratories or Invitrogen).

2.8.3 Fluorouridine (FU) labeling and immunostaining

S2 cells were pulse labelled for 10 min with 2 mM FU (SIGMA, F5130); cells were then fixed with 4% formaldehyde diluted in PBS-Triton (0.1% Triton X-100) 15 min at RT, and then washed 2 times in PBS-Triton for 5 min each. Blocking was done in 10% fetal bovine serum (FBS) diluted in PBS for 30 min at RT. FU was detected with a mouse anti-BrdU primary antibody (1:200 dilution in 0.1% Triton X-100 in PBS with 10% FBS, SIGMA B2531) incubated for 4 hrs at room temperature. The anti-BrdU was subsequently detected with an Alexa Fluor 647 goat anti-Mouse secondary antibody (Invitrogen) diluted in 0.1% Triton X-100 in PBS (1:250) and incubated for 2 hrs at room temperature.

2.9 Cell synchronization and flow cytometric analysis

Exponentially growing transfected S2 cells were incubated with 2 mM hydroxyurea (HU for 18 hrs) 2 days after transfection. Cells were washed twice at the end of the incubation with serum free media and then gently resuspended in fresh complete media. Aliquots containing 0.5-1 million cells were collected at the end of HU incubation time (T_0), and at 2 hrs interval after HU washout for a duration of 24 hrs. Aliquots collected were either fixed with either 90% ethanol for flow cytometry or with 4% formaldehyde in PBS for fluorescence microscopic imaging. For flow cytometry, the fixed cells in ethanol were spun for 5 min at 1000 rpm, the ethanol was discarded and the cells were resuspended in fresh PBS a day before analysis and incubated for 15 min at room temperature to allow the cells to rehydrate. The cells were spun again for 5 min at 1000 rpm, PBS discarded and

resuspended in 1 mL of fresh sterile PBS. RNase A 100 µg/mL and propidium iodide 40 µg/mL were added to the cells and incubated overnight at 4^0C. Cells were incubated for 30 min at room temperature on the day of the analysis and then transferred to 6 mL FACS tube. DNA content was measured with BD FACSCalibur (BD Biocience) and the results analyzed with CellQuestPro software.

2.9.1 Determination of S2 cells doubling time

1.5 x 10^6 S2 cells were diluted in 5 mL of complete media (Insect-XPRESS, Lonza) supplemented with 10% fetal bovine serum, 1% penicillin/streptomycin/glutamine mix (Invitrogen). The diluted cells were then grown at 27^0C incubator without $C0_2$ in a T25 culture flask. Growth rate was monitored by counting live cells with an automated cell counter (Countess, Invitrogen) at time intervals of 6, 12, 24 and 36 hrs. Doubling time and growth rate were calculated from the exponential regression plot with Weisstein, Eric W. "Least Squares Fitting--Exponential" from *MathWorld*--A Wolfram Web Resource.

2.10 Western blot analysis

Protein samples were resolved by SDS-PAGE and transferred to a nitrocellulose membrane (Protran BA-85, Pierce Protein Biology). The membrane was blocked in 5% milk/1X TBST (Tris-buffered Saline - TWEEN 20) and incubated on a rocker at room temperature for 30 min. After the blocking, the membranes were incubated with primary antibody polyclonal goat anti-GFP (AbD Serotec) 1: 2000 of antibody in TBST overnight at 4^0C. At the end of the incubation, the membranes were washed 3 times with TBST at 5 min interval each and then incubated with secondary antibody (polyclonal anti-Goat HRP) 1: 10000 of antibody in TBST for 1 hr at room temperature on a rocker. The membranes were washed again as done at

the end of primary antibody incubation. The blots were then incubated with West Pico Chemiluminescent Substrate (Pierce) and then visualised with Gene Snap Software (SynGene).

2.11 Genetics

D. melanogaster stocks were maintained on standard corn meal medium with little dry yeast added on top of the food. The flies are kept either in 18°C or 25°C incubators with relative humidity and stocks were transferred every 28 or 21 days respectively.

2.11.1 GAL4/UAS Expression System

Gal4/UAS expression system is routinely used in *Drosophila* genetic systems to drive the expression of transgenes in specific tissues/cells at given times during development. Gal4 is a yeast transcriptional activator that consist of 881 amino acids (Keegan et al., 1986) and acts by binding the yeast upstream activating sequences (UAS) and inducing transcription (Duffy, 2002). Gal4 can be expressed with different endogenous promoters that are active in different cells. If the transgenes are flanked by the UAS sequence, it will be expressed only in the cells expressing gal4.

2.11.2 Female virgin flies collection

The fly stocks are maintained at 18°C in plastic vials; stocks are transferred to fresh food vials every 4 weeks or every 2 weeks, if stocks were kept at 25°C. Virgin female flies were collected twice a day, usually at 9:00 am and 5:00 pm. In the evening, cleared vials are kept at 18°C overnight to delay hatching. All collected virgins were kept in glass vials at 18°C incubator before setting up crosses.

2.11.3 Drosophila germline transformation

The BiFC transgenes were generated by germ-line transformation using P-element mediated integration in the *yw* host strain (Bischof et al., 2007). The transformations were done by BestGene Inc. (Chino Hills, U.S.A.).

2.11.4 Generation of double-insert flies carrying both BiFC transgenes

To generate flies homozygous for the BiFC inserts, I crossed the individual strains carrying the inserts p[W+=UAST.Rp18-VN] on 2nd chromosome (line A05) and p[W+=UAST.RpL11-VC] on 3rd chromosome (line A12) with double balancer virgin females. Red eye males from the F1 (A) progeny with *IF* and *TM6B* markers were collected and crossed with red eye virgin females with *CyO* and *MKRS* of the F1 (B) progeny. In the F2 progeny, red eye males with the markers *CyO* and *TM6B* and virgin females of the same genotype were collected and crossed. In the F3 progeny, recombinant flies homozygous for the two inserts were identified by the absence of markers from balancer flies (Figure 2.3). Presence of the two inserts in the established recombinant lines was verified by single fly PCR using primers specific for either VN or VC. Single bands of the right size corresponding to the sizes of VN and VC were obtained (Figure 2.4B).

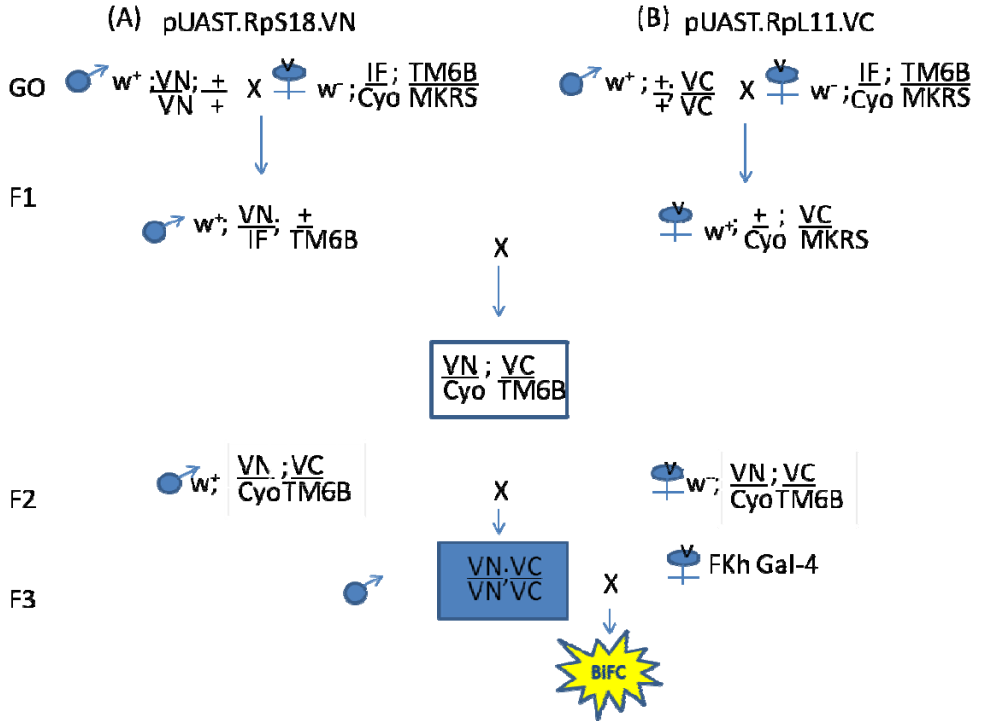

Figure 2.3. Schematic of the genetic protocol used to generate double-insert homozygous flies carrying the BiFC RPs pair. In the first cross (Go), homozygous red eyed males with pUAST-RpS18-VN on the 2nd chromosome (A) and pUAST-RpL11-VC on the 3rd chromosome (B) were crossed with double-balancer virgin females. In the F1 progeny, red eyed males with *IF* and *TM6B* markers (A) were crossed with red-eye virgin females with *Cyo* and *MKRS* of the F1 (B) progeny. F2 flies that carry both the BiFC inserts with the indicated genotypes were crossed to produce F3 flies homozygous for the two inserts, which were identified by the absence of both *Cyo and TM6B* dominant markers. The recombinant flies can be crossed with a desired gal4 lines to express the BiFC as shown above with *Fork*-head gal4 line that allows the expression of the tagged RPs in salivary glands.

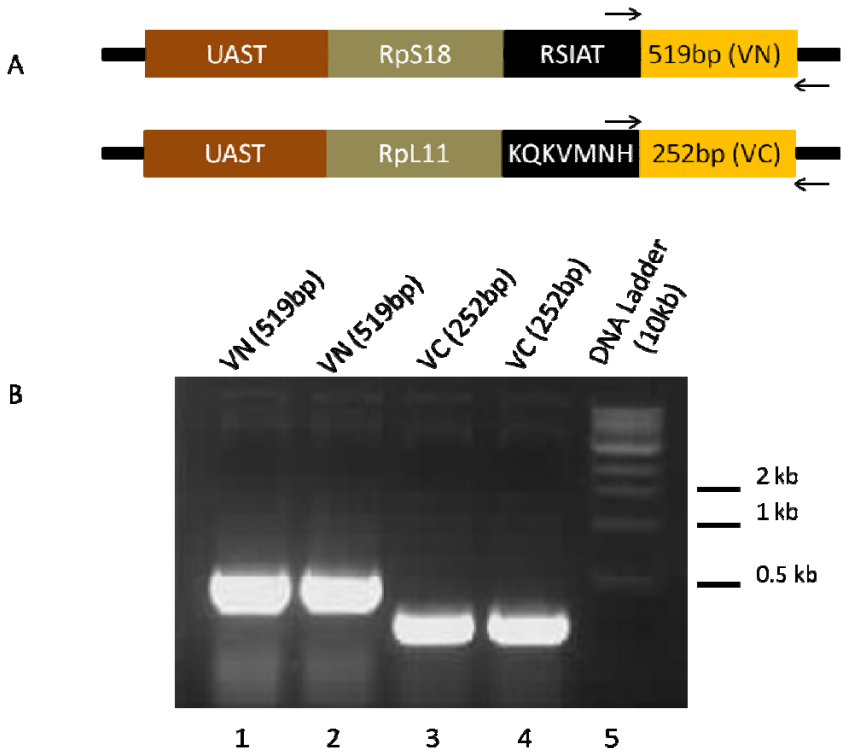

Figure 2.4. PCR validation of inserts in the recombinant flies. (A) Schematic of the BiFC reporter inserts in the recombinant flies indicating the position of the primers used to amplifying the VN or VC fragments. (B) DNA gel showing the amplified fragments from two recombinant flies as indicated with primers specific for VN and VC.

2.11.5 Setting up crosses

For Gal4/UAS expression system, the desired transgenic lines have to be crossed with the relevant gal4 line to allow expression of the fusion proteins to be expressed in the selected tissues/cells. *D. melanogaster* fly strains (homozygous flies for Venus BiFC inserts) were crossed with various gal4 lines that allow the expression of the BiFC fusion proteins in different tissues and cell types. Typically, six males BiFC fly strains were crossed with 10 virgin females of each of the various gal4 lines in a vial. Crosses were kept in 25^0C incubator for 3 nights and then moved to 18^0C incubator. The crosses were transferred to fresh food vials every 2 days. Third instar larvae (larvae that start crawling out of the food) were collected and the salivary glands, brain and gut were then dissected for the BiFC experiments. For the adult midgut cells analysis, 3 days old adult flies were collected and dissected to obtain the gut.

2.11.6 Salivary gland, brain and gut dissection and fixation for fluorescent Imaging

Third-instar larvae, i.e. larvae that start climbing out of food were selected for dissection. Larvae were then placed in a glass dissecting dish that contains tap water on ice to clean and put them to sleep. The larvae were then transferred to a fresh dissecting dish containing PBS and then dissected using fine forceps in a glass dissecting dish containing 20 µl of PBS. Dark fat bodies around the glands, gut and brain were removed as they interfere with the imaging. Following dissection, tissues were fixed by washing the glands in 4% formaldehyde solution diluted in PBS for 15 min, washed in PBS for 5 min, washed and permeabilised in cold PBS/ TWEEN 20 on ice for 10 min, washed again in PBS and the transferred in 0.1 µg/ mL DAPI/PBS solution for 10 min to stain the nuclei of the cells and finally washed in PBS

solution. After these steps the tissues were placed using forceps on a drop on mounting medium 20 µL (PromoFluor, Promokine) on a slide and a coverslip was placed on top.

2.11.7 Genetic cross for lethal mutation complementation

To investigate the functionality of the BiFC tagged ribosomal proteins, I carried out a lethal mutation complementation test to examine whether the expression of RpS18-VN and RpL11-VC can rescue lethal phenotype mutations of the corresponding endogenous genes. To achieve this, homozygous lethal mutants flies for RpS18 (RpS18 C02853/CyO; +) and RpL11 (RpL11K16914/CyO; +) both carrying mutation on the second chromosome were crossed with transgenic lines expressing RpS18-VN (line A05) and RpL11-VC (line A15) on third chromosomes respectively. The mutant flies RpS18C02853 was obtained from Exelixis and RpL11K16914 from Bloomington Stock Center. Evidence for the complementation was assessed by absence of the dominant markers in the balancer chromosomes in the F3 progeny. Flies carrying RpS18C02853 and RpL11K16914 on the second chromosome were identified by lack of balancer chromosomes markers (Figure 2.5 and 2.6).

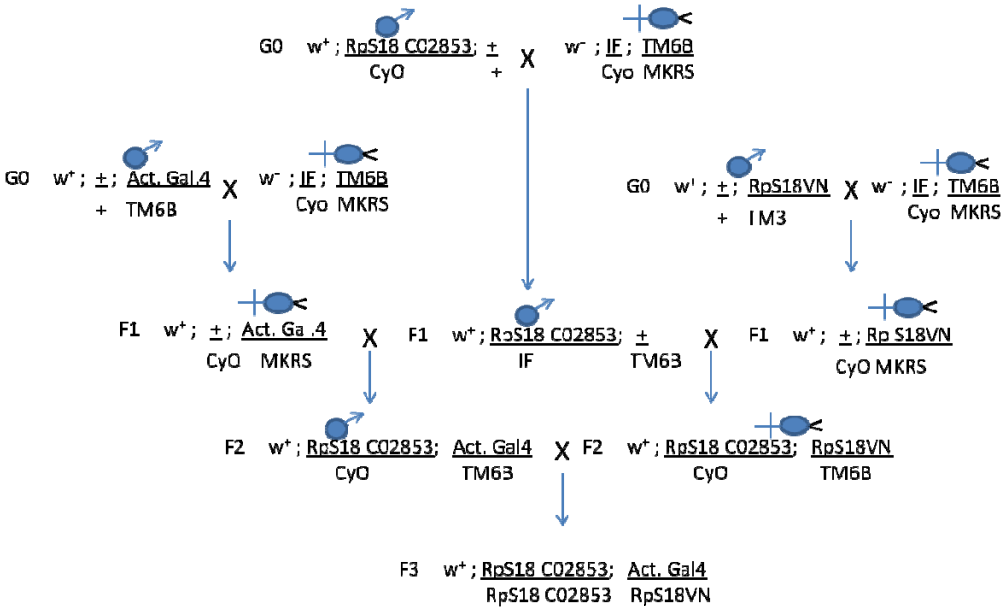

Figure 2.5. Schematic of the genetic cross for lethal mutation complementation by BiFC tagged ribosomal proteins. In the first crosses (GO), +;Actin Gal4, +;RpS18-VN, RpS18 C02853;+ were crossed with double balancer virgin females. Virgin females with Cyo and MKRS from Act. Gal4 and RpS18-VN F1 progeny were crossed with IF; TM6B male progeny from RpS18 C02853. In the final F2 cross, Cyo; TM6B were crossed with each other. F3 progeny were scored for flies lacking the dominant markers Cyo; TM6B.

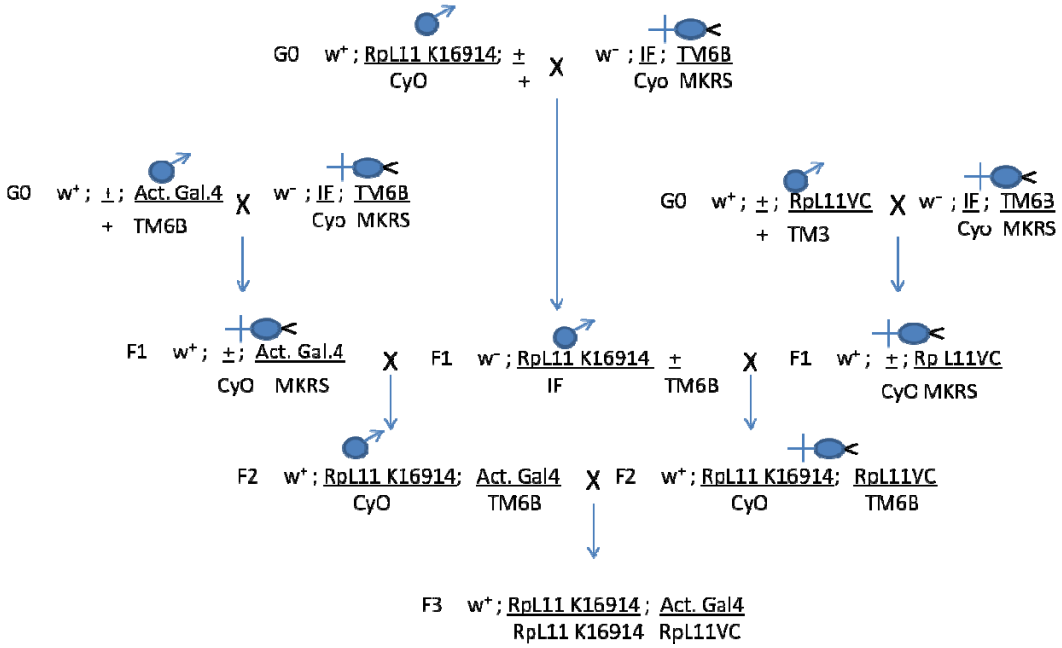

Figure 2.6: Schematic of the genetic cross for lethal mutation complementation by BiFC tagged ribosomal proteins. In the first crosses (GO), +;Actin Gal4, +;RpL11-VC, RpL11k16914;+ were crossed with double balancer virgin females. Virgin females with Cyo and MKRS from Act. Gal4 and RpL11-VC F1 progeny were crossed with IF; TM6B male progeny from RpL11 K16914. In the final F2 cross, Cyo; TM6B were crossed with each other. F3 progeny were scored for flies lacking the dominant markers Cyo; TM6B.

CHAPTER 3

3.0 BiFC 80S reporters detected translation-dependent subunits joining

3.1 Synopsis

Ribosomal subunits are synthesised and assembled in the nucleolus. The subunits are exported separately to the cytoplasm where the large subunit (60S) and small subunit (40S) join together to form 80S ribosome during translation initiation. As detailed in the Introduction, the consensus view is that 80S formation is exclusively a cytoplasmic event. However, there are observations which suggest that there are functional ribosomes within the nucleus. To further investigate whether ribosome subunits can join to form functional 80S ribosome in the nucleus and whether the resultant 80S is associated with translation, this laboratory has been developing a bimolecular fluorescence complementation (BiFC) 80S visualisation assay. In this 80S reporter assay, pairs of ribosomal proteins (RPs) that are located in the vicinity of the subunits interface are tagged with complementing halves of a fluorescent protein. Joining of the subunits to form the 80S ribosome, results in the folding of the two complementary fragments into a functional fluorescent protein that can be visualised by standard fluorescence microscopy (Figure 3.1). When I started working on this project, a previous PhD student in Brogna laboratory (Dr Khalid Al-Jubran) had already demonstrated the feasibility of such assay. The initial aim of my project was to validate these earlier observations, and test further its general validity by assessing other RP pairs that are in the vicinity of the subunit interface and, as negative controls, pairs that are not in close proximity on the 80S. Additionally, I characterised the effect that translation inhibitors have on the 80S BIFC signal. The results that I reported in this chapter are consistent with

the assay reporting translation-dependent ribosomal subunits joining. (Most of the data presented in this Chapter are part of my work published recently by our group (Al-Jubran et al., 2013) in which I am a shared first author).

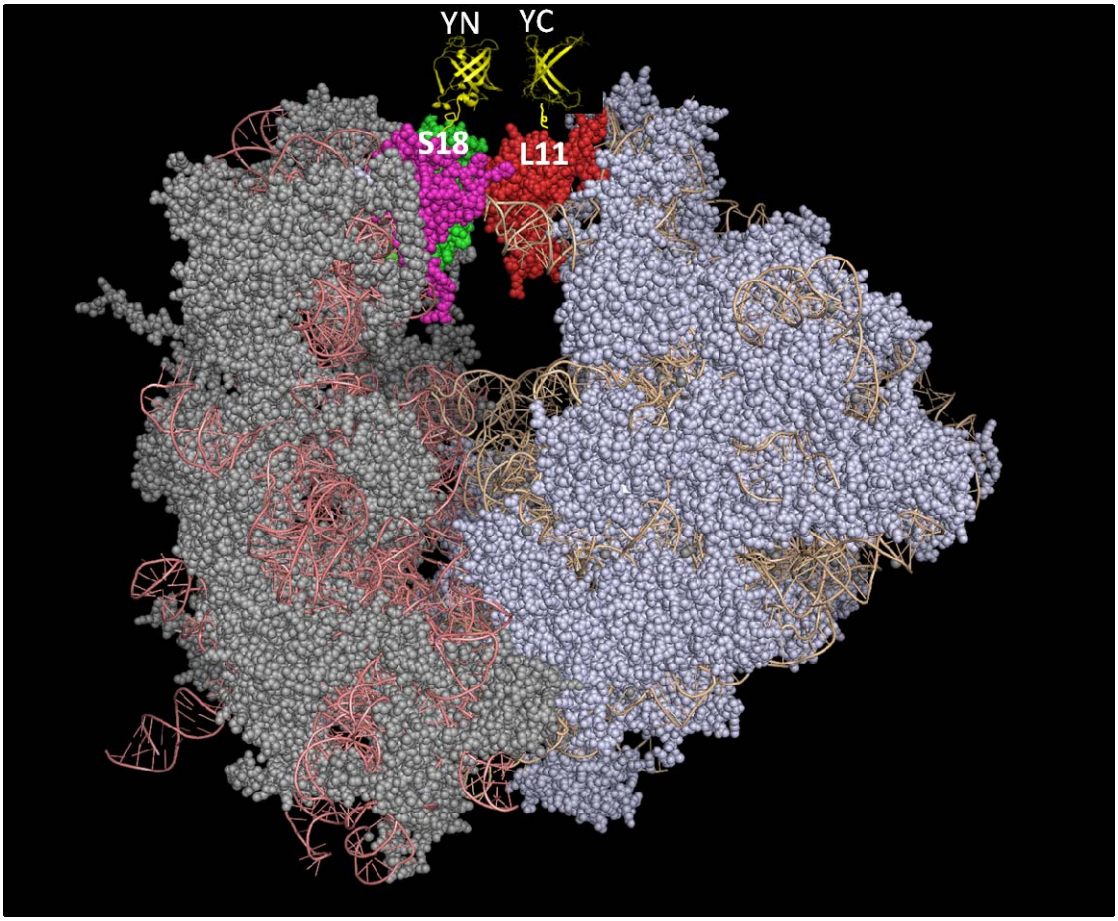

Figure 3.1. Schematic of the BiFC ribosomal subunits interaction technique. The diagram depicts the structures of yeast 80S: 40S subunit on the left and 60S subunit on the right as predicted by the EM structure of the yeast 80S ribosomes (Spahn et al., 2001a). Selected ribosomal proteins are shown with different colours: S15 in green, S18 in magenta and L11 in red. S15 and S18 are labelled with the YN and L11 with the YC BiFC interacting fragments shown above in yellow. This structure model was generated with PyMol by modifying a composite PDB file downloaded from www.mol.biol.ethz.ch/groups/Ribosomes, based on the PDB files 2XZM (40S) and 4A17, 4A19 (60S).

3.2 Results

3.2.1 Generation of BiFC reporter constructs

To visualise the joining of ribosomal subunits to form 80S ribosomes, pairs of RPs that form inter-subunit bridges on the 80S were identified based on the structures of yeast 80S, mammalian 80S and bacterial 70S ribosomes that were initially available at the start of the project (Chandramouli et al., 2008; Spahn et al., 2001b; Yusupov et al., 2001; Spahn et al., 2001a). My first experimental task was to verify a set of BiFC reporters developed previously in the Laboratory; these express RpS18-YN and RpL11-YC - RpS18 was fused to N-terminal fragment of YFP (YN) and RpL11 was fused to C-terminal fragment of the YFP (YC) (Figure 3.2 A and B). The BiFC fragments were attached to the RPs via short peptide linkers to enhance their mobility. These BiFC tagged RPs and those described below are regulated by the UAS promoter, which is activated by co-expression of the plasmids along with the transcription activator gal4, allowing the expression of BiFC tagged RPs in cells (Material and Methods). In addition to these two constructs, I tagged in a similar manner others RPs that are adjacent on the 80S structure, and as controls, others that are further apart (Figure 3.2 C-H). I reasoned that the RPs that are adjacent to one another should produce BiFC signal, whereas those that are further apart should not. This will maximize our chances of detecting a genuine BiFC signal stemming from the subunits joining (maps and additional information on these constructs are given in Appendix X). In parallel, I also constructed other versions of the BiFC reporters using a similar strategy but with longer peptide linker sequence; in these constructs, 25 amino acids helical linker was used to fuse the BiFC fragments to the RPs (Figure 3.14A). This is to avoid restricting the inter-subunit rotation that occurs during

translocation of the ribosome on the mRNA, which might be hindered by the short peptide linkers used in the earlier constructs.

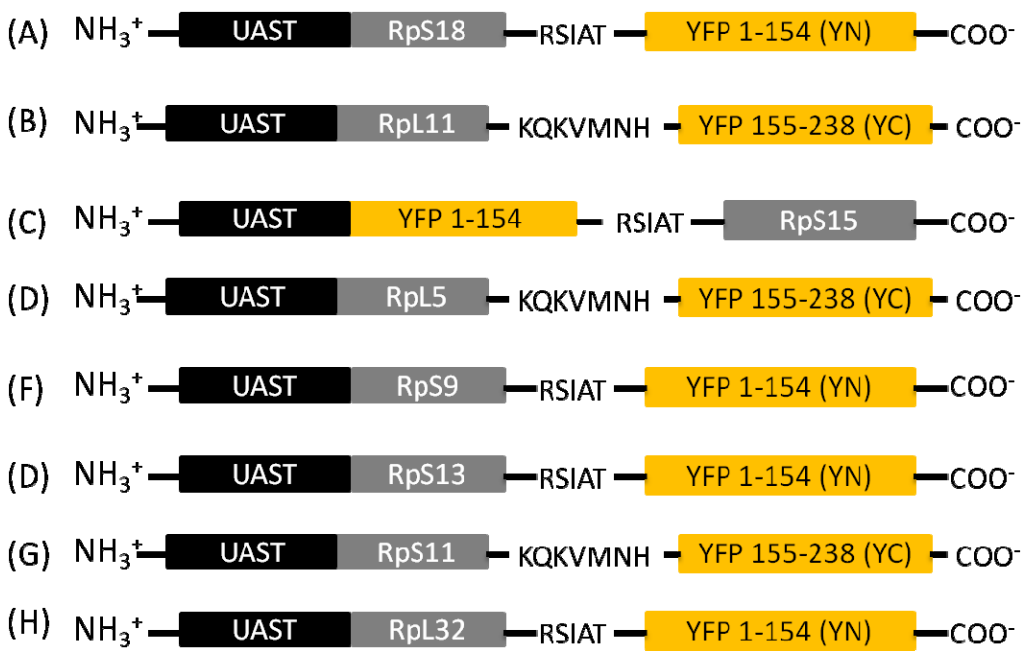

Figure 3.2 Schematic of the BiFC reporter constructs expressing RPs. (A) - (H) shows indicated RPs fused with YN or YC fragment of YFP, at either the C or N terminus. Vector backbone is pUAST. The RPs are separated from the BiFC fragments with either a seven amino acid linker, KQKVMNH or five amino acid RSIAT, as indicated above to enhance the mobility of the fused BiFC peptides.

3.2.2 BiFC reporter construct reports ribosomal subunits joining

After successful construction of the BiFC tagged reporter plasmids, these were transiently transfected along with the expressing plasmid gal4 into *Drosophila* S2 cells (details in Material and Methods). Fluorescence microscopy analysis of the transfected cells showed that the RpL11 and RpS18 pair produced the strongest fluorescence as previously observed. The BiFC signal was mostly localized in the cytoplasm in about 83-87% of the transfected cells (we call them Type I), while in about 15% of the cells (Type II); I also detected clear YFP fluorescence in the nucleus, particularly in the nucleolus (Figure 3.3A). The S18-YN and L11-YC BiFC reporters were well expressed, as can be seen from the Western blot analysis of the total cell extracts (Figure 3.3C). BiFC tagged RPs were abundant all over the cell as indicated by the immunostaining assay with antibodies against the BiFC peptides, but particularly accumulated in the nucleus (Figure 3.3B). These results clearly showed that there is no co-relation between the concentration of the tagged BiFC peptides and the BiFC signal observed, which is majorly cytoplasmic. This observation is in agreement with the initial results (Dr. Khalid Al-Jubran).

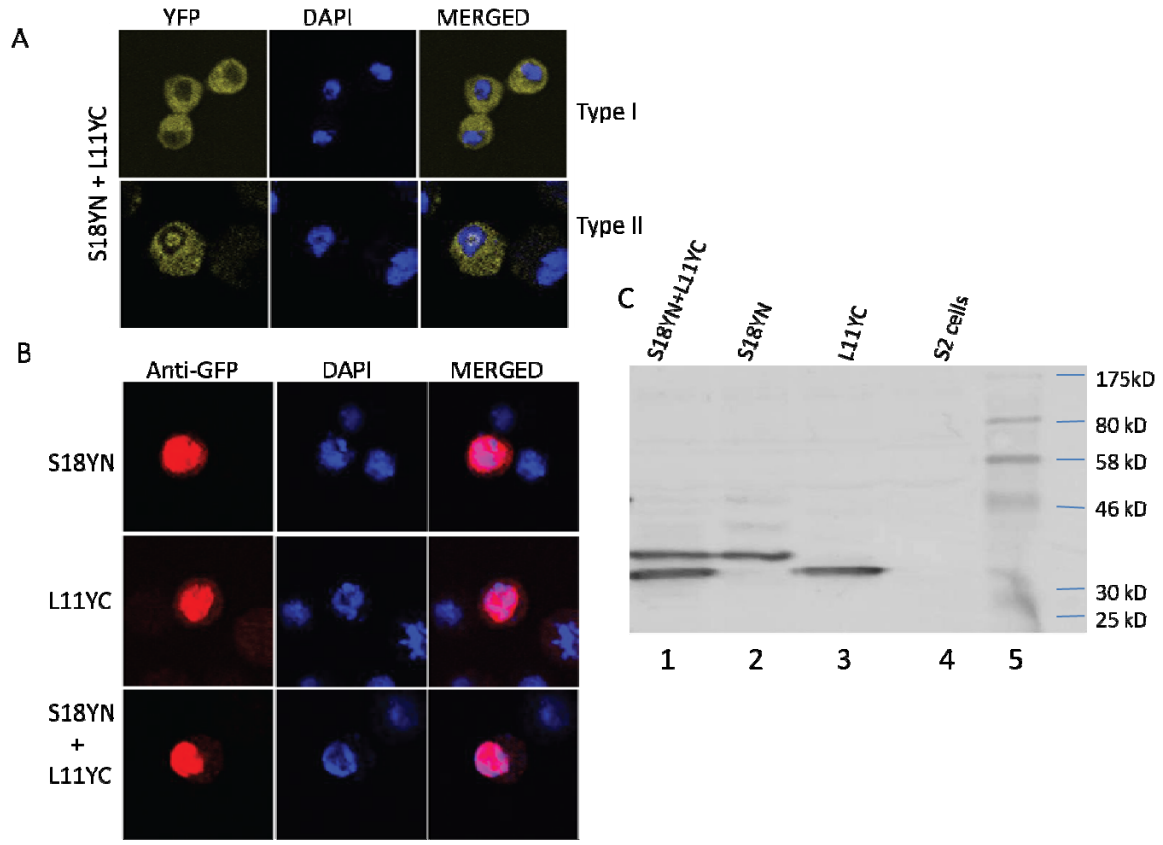

Figure 3.3. BiFC reporter constructs S18YN and L11YC detects 80S joining. (A) The top row shows cells with typical cytoplasmic YFP BiFC 80S signal pattern (Type I), and the bottom row, cells with both cytoplasmic and nucleolar signal (Type II). Left panel shows YFP signals, middle panel shows DAPI staining and the merged images are shown on the right. (B) Immunostaining of S2 cells transfected with the indicated BiFC tagged RPs with a polyclonal GFP antibody counter stained with DAPI, indicating sub-cellular distribution of the BiFC tagged peptides. All images were taken with laser confocal microscope using a 63X oil immersion objective. (C) Western blot of whole cell extracts from S2 cells transfected with the indicated BiFC constructs detected with a GFP polyclonal antibody (The molecular weights of the BiFC tagged ribosomal proteins are S18-YN, 35.8 kDa; RpL11-YC, 31.7 kDa).

3.2.3 BiFC signal is produced only when the tagged RPs are adjacent to one another on the 80S structure

To probe more directly the extent to which the BiFC signal relied on proximity of the interacting proteins, I assayed other RP pairs, including pairs that are far apart on the 80S structure, as such they are not expected to generate a signal (Figure 3.4): RpL5 (L5) is next to L11 and thus close to S15 and S18, and the other pairs (S11/L32, S13/L11, S13/L5 and S9/L11) are widely apart. When the BiFC-tagged pairs of these RP's were expressed in S2 cells, polypeptides of the expected size were produced (Figure 3.5A): they are abundant throughout the cell, but primarily concentrate in the nucleus (Figure 3.5B). The YN-S15/L11-YC and YN-S15/L5-YC pairs yielded a strong BiFC signal (Figure 3.6A) which was comparable to the signal observed in S18/L11 RP pairs (Figure 3.3), whereas the further separated RP pairs (S13-YN/ L5-YC, S11-YC/L32-YN and S13-YN/L11-YC) did not produce a signal or very weak fluorescence (Figure 3.6B). Interestingly, the distant RP pairs also did not generate any BiFC signal in the nucleus except for one pair, in the nucleolus, despite the fact that the proteins are mostly localised in the nucleus (Figure 3.5B and 3.6B). The exception was S9-YN/L11-YC, which produced fluorescence both in the nucleolus and a very dim cytoplasmic signal (Figure 3.6B). The result of these observations revealed that, strong BiFC signal was generated only when the RP pairs involved lie in close proximity at the inter-subunit boundary of the assembled 80S. The tagged BiFC constructs concentration is highest in the nucleus, same compartment where the ribosomal subunits are made, whereas the BiFC signal was mostly detected in the cytoplasm.

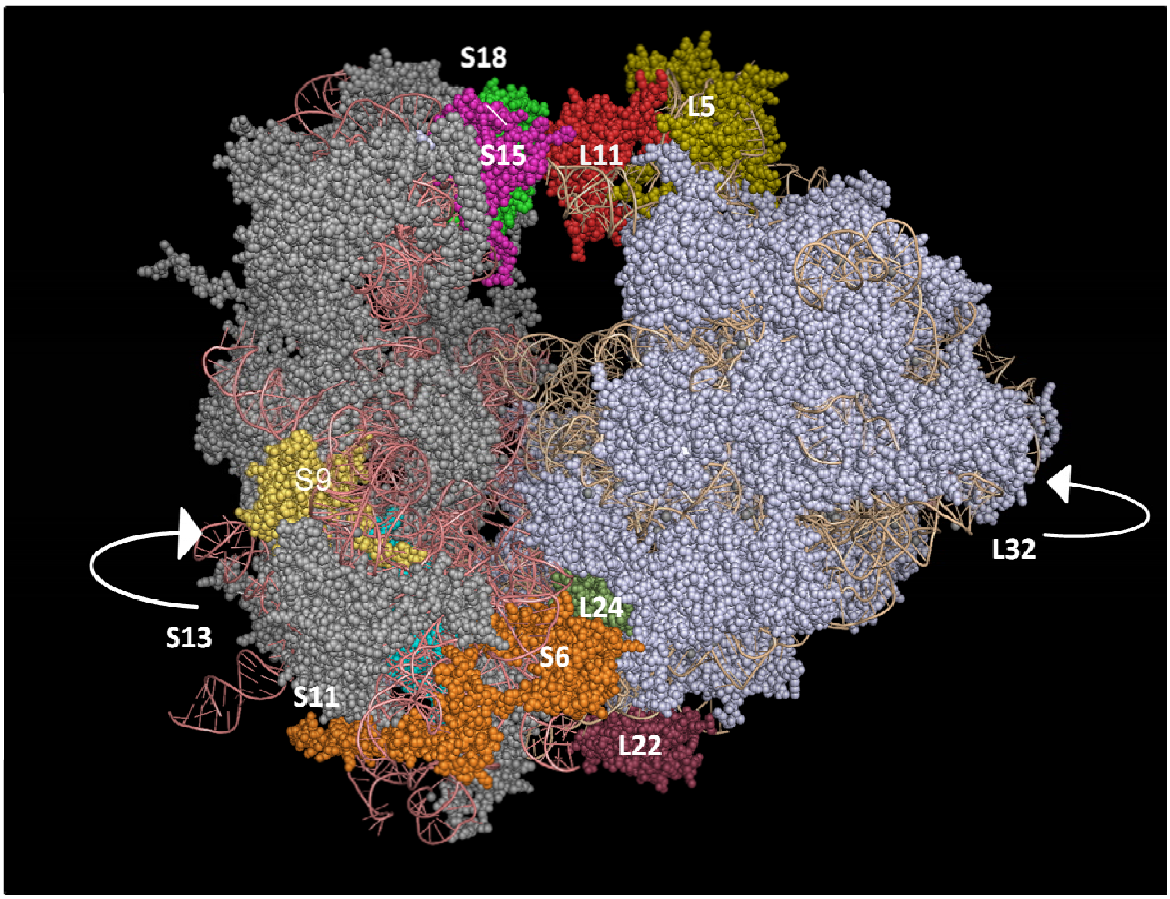

Figure 3.4. Schematic of the location of the tagged ribosomal subunits on the 80S structure. This model depicts the structures of the yeast 40S and 60S subunits, indicating the positions RPs tagged with the BiFC fragments highlighted in different colours. The structure model was generated with PyMol using composite PDB file downloaded and modified from www.mol.biol.ethz.ch/groups/Ribosomes, based on the PDB files 2XZM (40S) and 4A17, 4A19 (60S). Adapted from that published previously (Al-Jubran et al., 2013).

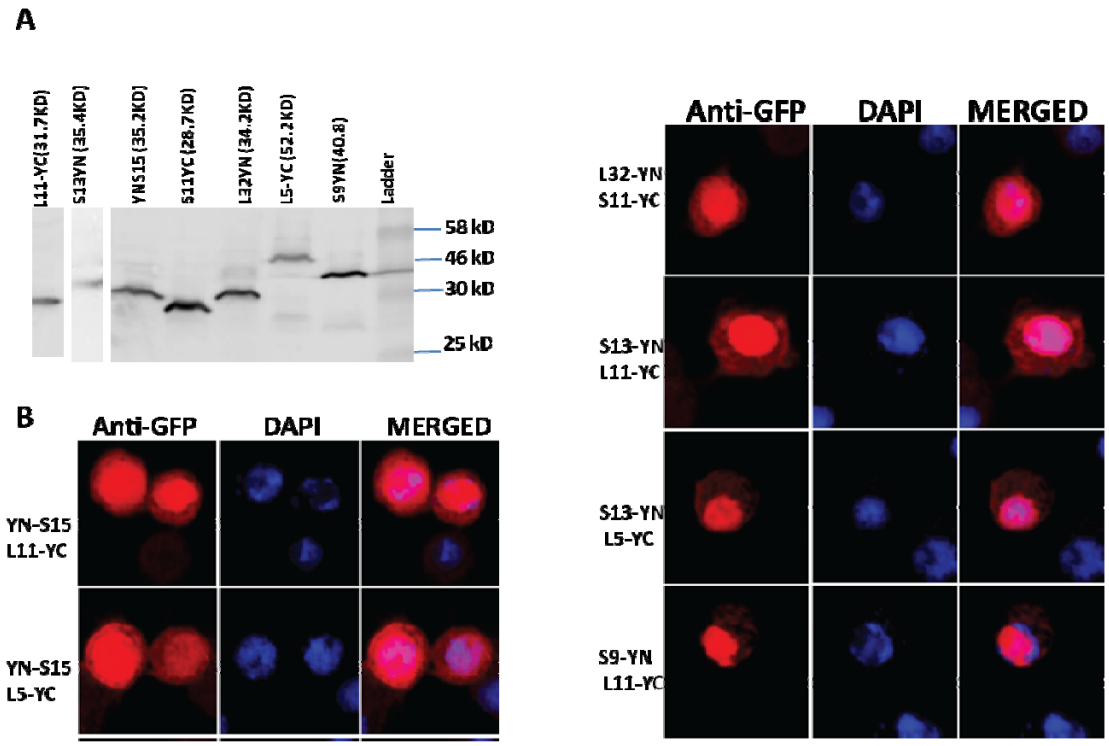

Figure 3.5. BiFC tagged reporter constructs are well expressed in S2 cells and localised primarily in the cytoplasm. (A) Western blot of whole cell extracts of S2 cells transfected with the indicated BiFC constructs recognised with anti-GFP antibody. The tagged RPs molecular weights are YN-S15, 35 kDa; L5-YC 52.2 kDa; S13-YN 35.2 kDa; L11-YC and YC-L11, 31.5 kDa; S9-YN, 40.8 kDa; L32-YN, 34.2 kDa S11-YC 28.5 kDa. (B) Indirect immunostaining of the indicated tagged BiFC reporters with polyclonal GFP antibody counterstained with DAPI. Images show the sub-cellular distribution of the BiFC tagged peptides. (Parts of this figure were published in Al-jubran et al, 2013).

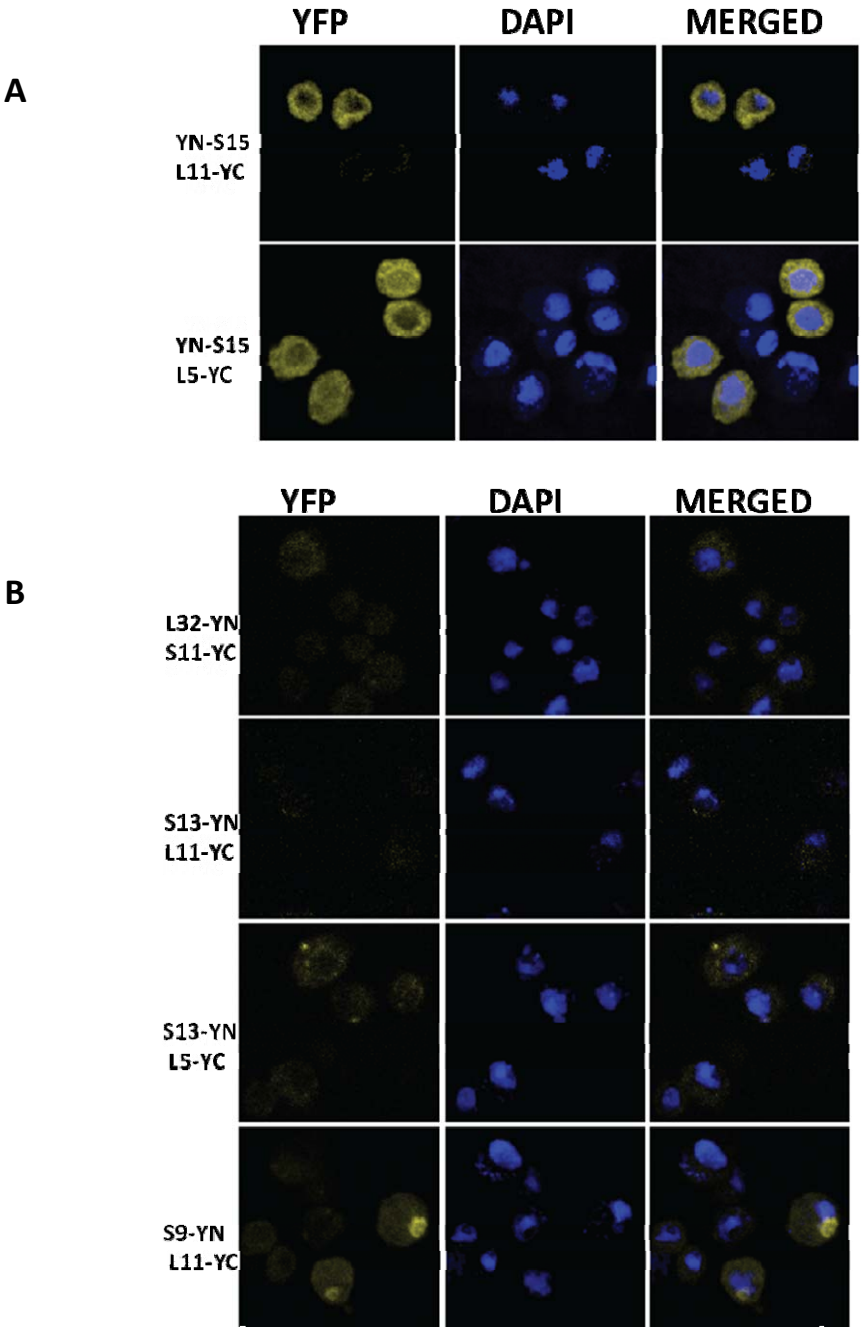

Figure 3.6. Tagged BiFC pairs produce signal only when they are adjacent to each other on the 80S ribosome. (A) Confocal images showing BiFC pairs that yielded BiFC signal in S2 cells transfected with the tagged RPs indicated. (B) Confocal images showing distant BiFC pairs that did not yield YFP signal in cells transfected with the constructs indicated. (Figure published in Al-jubran et al, 2013).

3.2.4 BiFC signal stems from 60S and 40S subunits association

A potential concern of using BiFC is that the signal observed might be driven by very high concentration of the BiFC fragments rather than a prior interaction between the two tagged proteins. Furthermore, in the nucleolus, the signal might be as a result of 5S RNP and 40S association rather than between the complete 60S and 40S subunits. In agreement with this interpretation, L11 and L5 that produced BiFC signal (Figure 3.6A) are both associated with the 5S RNP (Figure 3.4). To address these issues, I generated other BiFC reporter constructs located at "the foot" of the 80S ribosome. In particular, RPs of the 60S subunit that are not associated with the 5S sub-particle. RpS6 is in close proximity with RpL22 and RpL24 on the 80S and expected to generate BiFC signal (Figure 3.4). Both S6/L22 and S6/L24 pairs produce BIFC signal in a similar pattern as observed earlier with other positive pairs (Figure 3.7). The two protein constructs were present all over the cell, but concentrated in the nucleus (Figure 3.8A), and proteins of the correct size were produced and were stable (Figure 3.8B). As control, I paired some of the RP located at the "foot" of the ribosome with either S18 or L11 RPs located at the head of the ribosome subunits. As expected, no signal was observed from S18/L24 pair (Figure 3.9). The S6/L11 pair produced faint signal: I detected a few cells with a faint BiFC signal in the cytoplasm and an apparent signal in the nucleolus (Figure 3.9) (similar to our initial observation with S9/L11 (Figure 3.5B)). The results suggest that L11 might be interacting with other RPs even when not incorporated into 60S. However, it is unlikely that the nucleolar signal is an artefact of the high concentration of the tagged peptides. This is because the S18/L24 pair does not produce any signal despite the two protein constructs individually produced strong fluorescence when paired with tagged RPs located in close proximity on the 80S, as shown above for L11-S18 and S18/L24 (or L22).

Notably, all the BiFC reporter pairs that produced signal, show both the Type I and Type II cells; BiFC pattern with nucleolar and cytoplasmic signal (Figure 3.10).

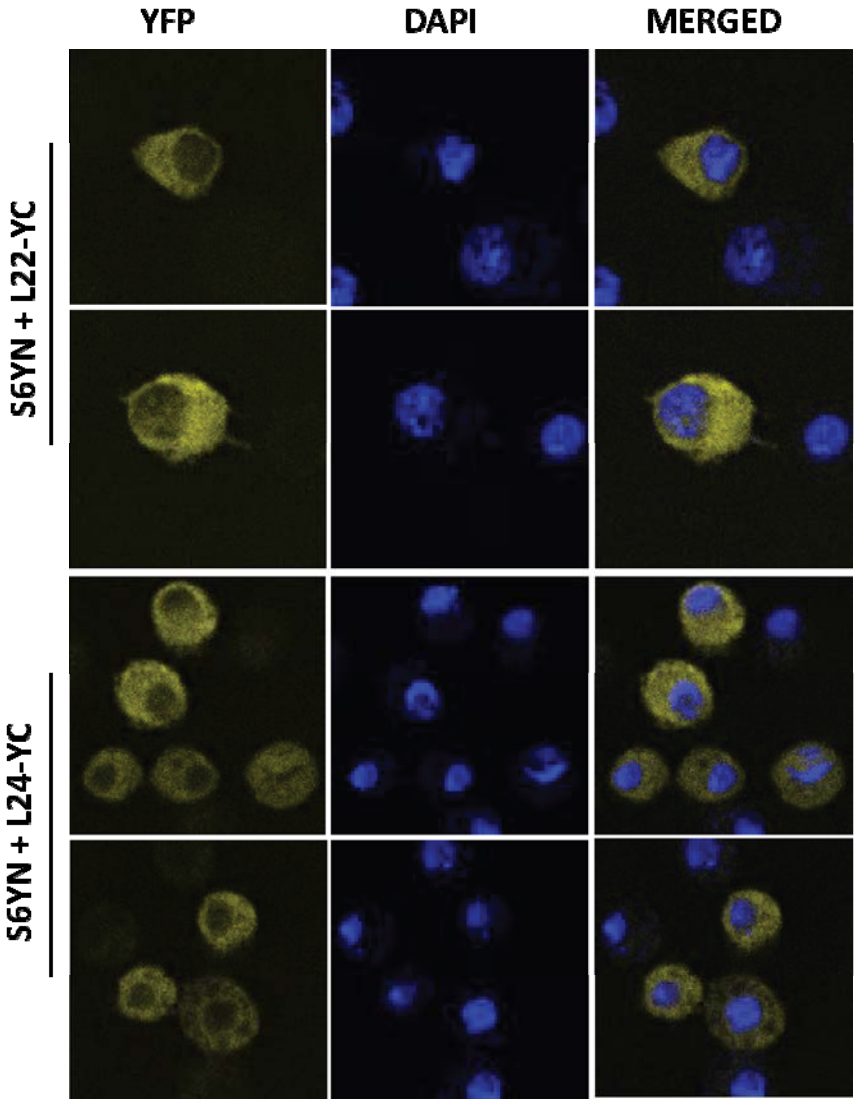

Figure 3.7. RP pairs at the "feet" of 80S also produced BiFC signal. Images of S2 cells transfected with the BiFC constructs indicated. Strong BiFC signal is observed with S6/L22 pairs (top two rows) and S6/24 pairs (bottom two rows). Left panel, YFP; middle panel, DAPI and right panel, merged. (Part of this figure was published in Al-jubran et al, 2013).

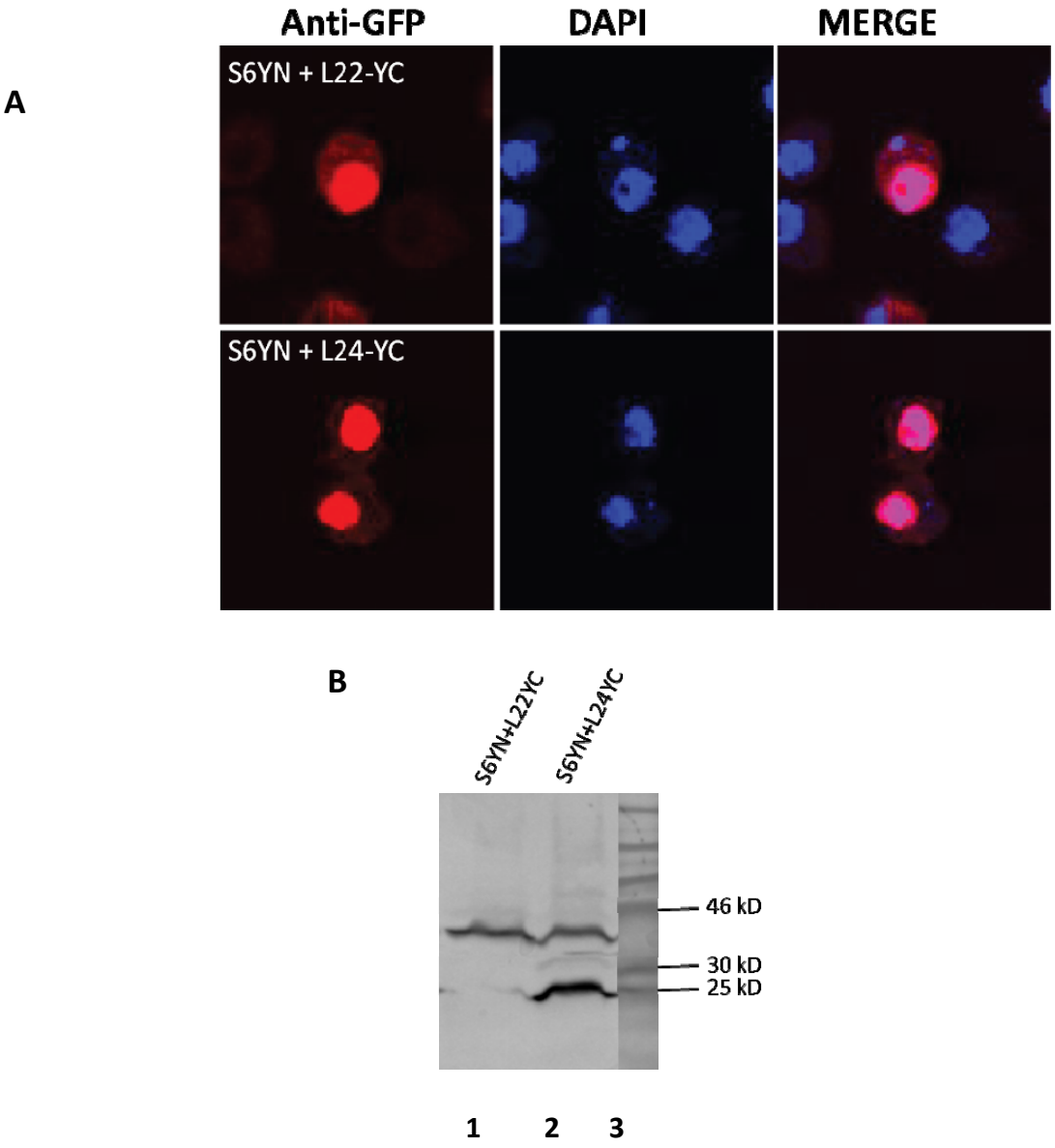

Figure 3.8. Non 5S RNP tagged RPs BiFC pairs localised primarily in the nucleus and are well expressed in S2 cells (A) Indirect immunostaining of tagged non-5SRNP RPs pairs with polyclonal GFP antibody indicating sub-cellular distribution of the BiFC tagged peptides. Top row; S6YN and L22YC and bottom row S6YN and L24YC. Left panel, anti-GFP; middle panel, DAPI and right panel, merged. (B) Western blot of whole cell extracts of cells transfected with the constructs indicated. The fusion proteins molecular weights are: From L-R: Lane 1: S6YN (39 kDa) and L22-YC (39 kDa), lane 2; S6YN (39 kDa) and L24YC (26 kDa). (Parts of this figure were published in Al-jubran et al, 2013).

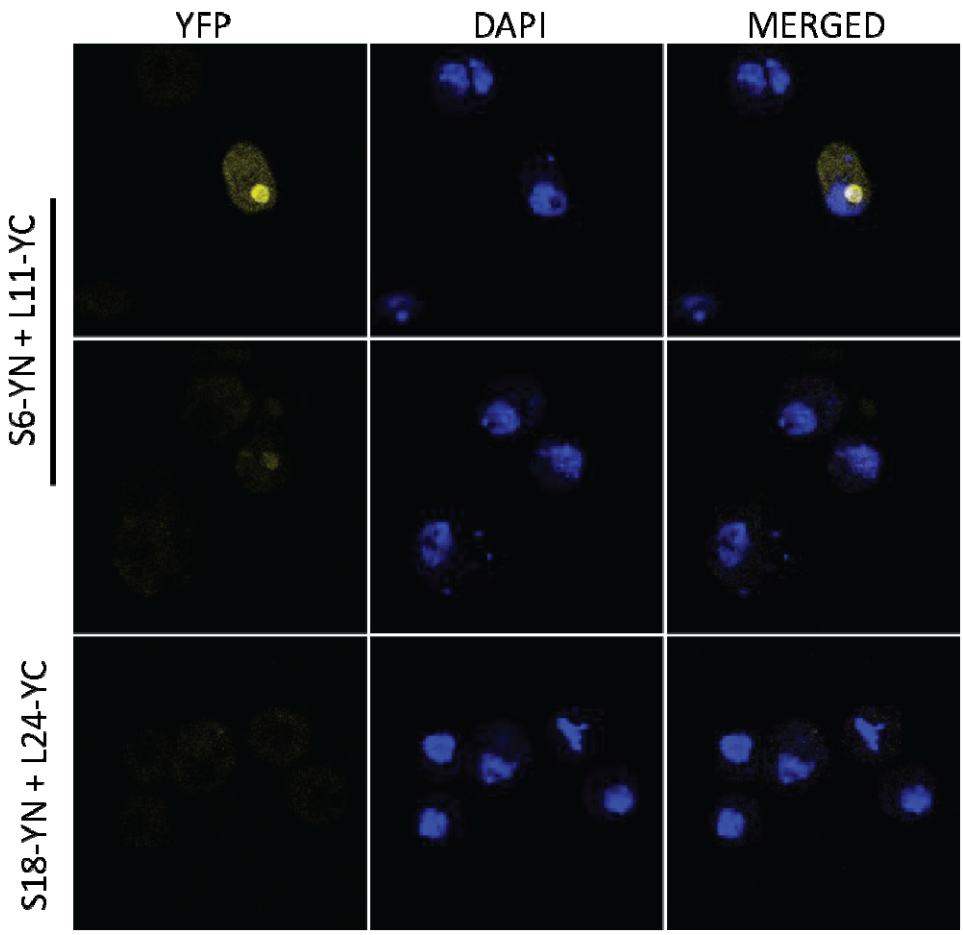

Figure 3.9. Distant RP pairs produced little or no BiFC signal. Confocal images of S2 cells transfected with the indicated constructs. Little or no BiFC signal is generated when the BiFC pairs expressed lie wide apart on the 80S. Top two rows; S6YN/L11YC pair, bottom row S18YN/L24YC. Left panel, YFP; middle panel, DAPI and right panel, merged.

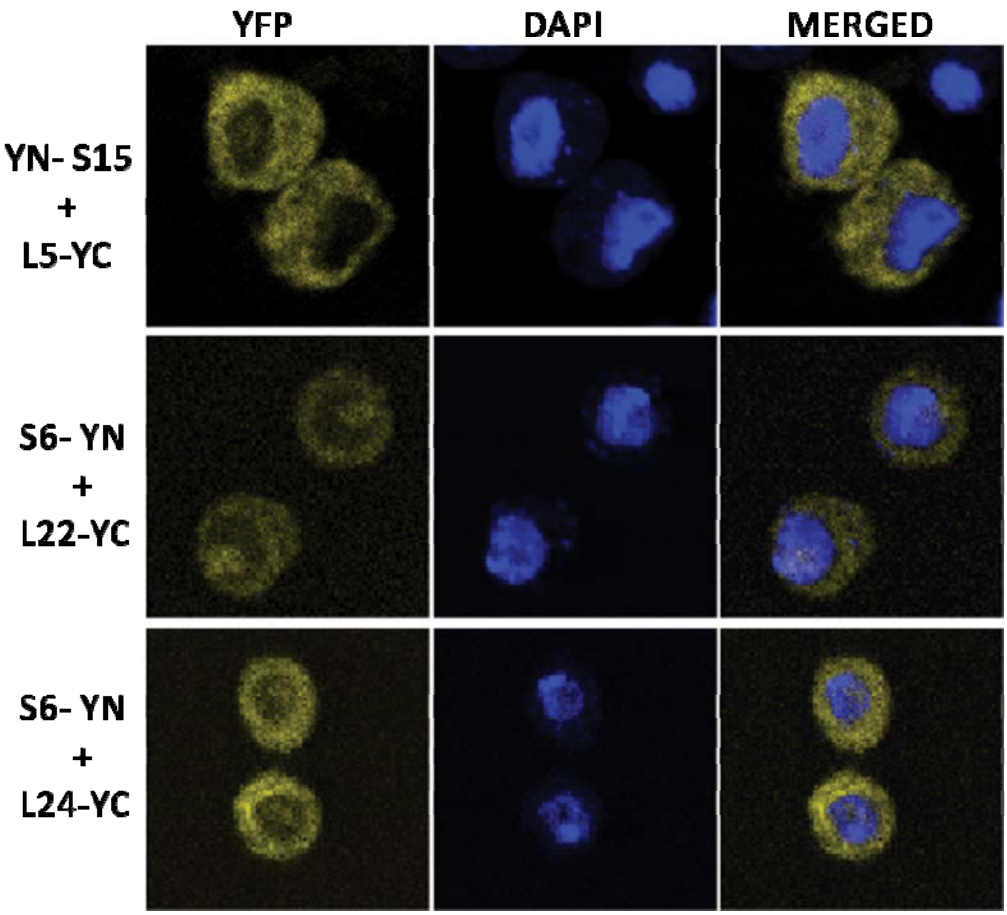

Figure 3.10. All RP BiFC pairs generated nuclear signal. Confocal images of S2 cells transfected with the indicated pairs of BiFC reporter constructs. Apparent cytoplasmic and nucleolar signal is observed (Type II cells signal pattern) in all the BiFC pairs studied. Left panel, YFP; middle panel, DAPI and right panel, merged. (This figure was published in Al-jubran et al, 2013).

3.2.5 The BiFC assay detects 80S ribosomes associated with translation

While the above results have established that the BiFC assay reports ribosomal subunits joining, it does not tell us whether the detected 80S ribosome is involved in translation. To verify whether the observed BiFC signal was genuinely due to the ribosomal subunit interaction during translation, I assessed whether the 80S BiFC signal is affected by translation inhibition drugs. Specifically, I characterised the translation elongation inhibitor emetine; treating the cells with this drug produced a clear change in the pattern of YFP signal, resulting in a stronger cytoplasmic and nucleolar signals (Figure 3.11). A brief incubation with this drug (30 min or 1 hr) revealed a significant increase in the Type II cells (Figure 3.12). Furthermore, in all experiments, treatment with emetine resulted in a visual apparent increase in the signal; quantification of a large sample of transfected cells showed a wide distribution in signal intensity but an apparent shift towards higher fluorescence in the emetine treated cells (Material and Methods) (Figure 3.13). Emetine binds to the 40S ribosome subunit, freezes the translation at elongation stage, increasing ribosome density on the mRNA yielding larger polysomes (Grollman, 1968a). Thus, the parallel increase in both cytoplasm and nucleolar signal suggest that the tagged ribosomal subunits engage in translation in both cytoplasm and the nucleolus.

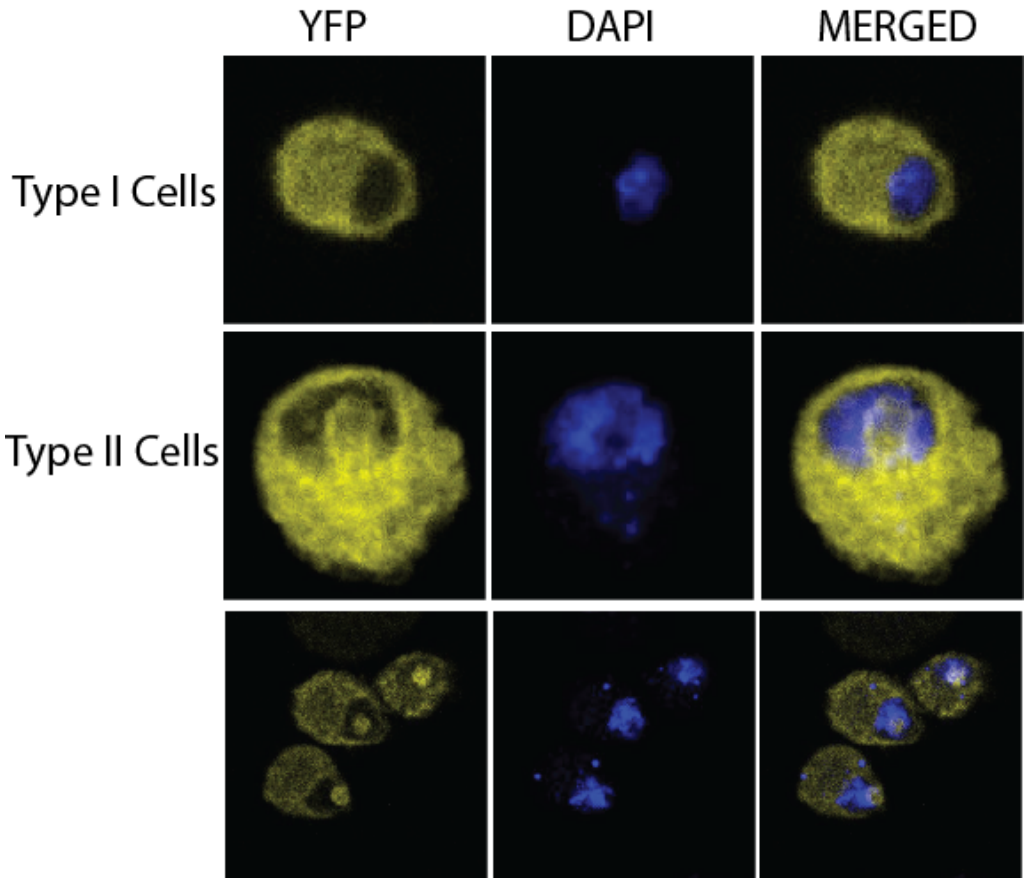

Figure 3.11. The translation elongation inhibitor emetine enhances the BiFC 80S signal. Confocal images of S2 cells pre-treated with 50 µg/mL emetine prior to fixation. Left panel, YFP; middle panel, DAPI and right panel, merged. Treating the cells with this drug for either 30 min or 1 hr produced a clear change in YFP signal pattern resulting to a stronger cytoplasmic and nucleolar signals and a significant increase in the Type II cells. (This figure was published in Al-jubran et al, 2013).

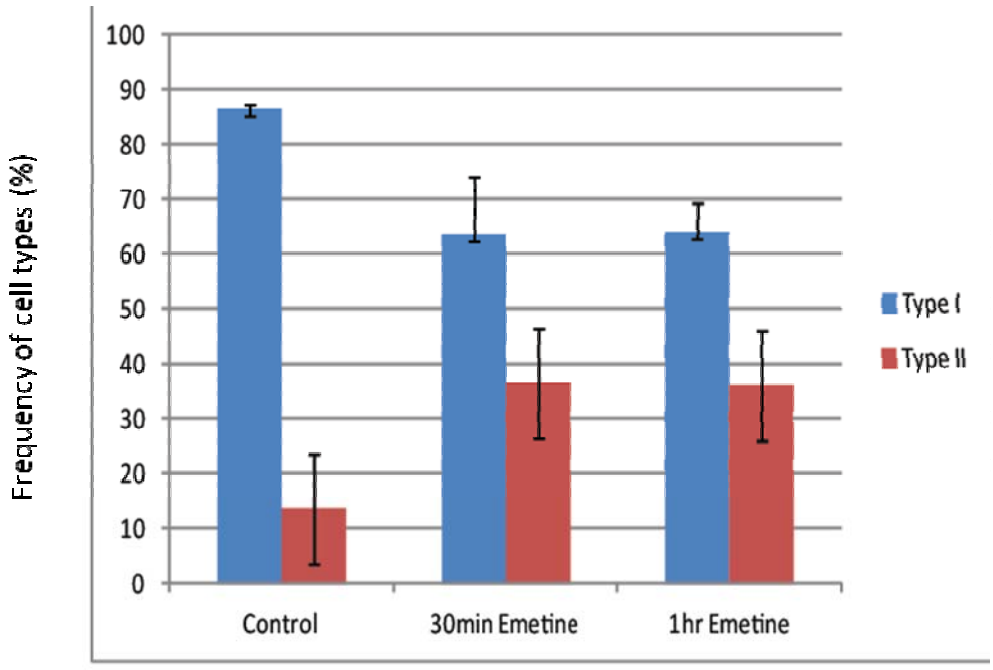

Figure 3.12. Emetine treatment increases the frequency of Type II cells. Relative frequencies of Type1 (blue bars) and Type II (red bars) cells treated with 50 µg/mL Emetine for the indicated times. One hundred cells were counted from two separate transfections. Bars indicate the standard deviations between the experiments. (This figure was published in Al-jubran et al, 2013).

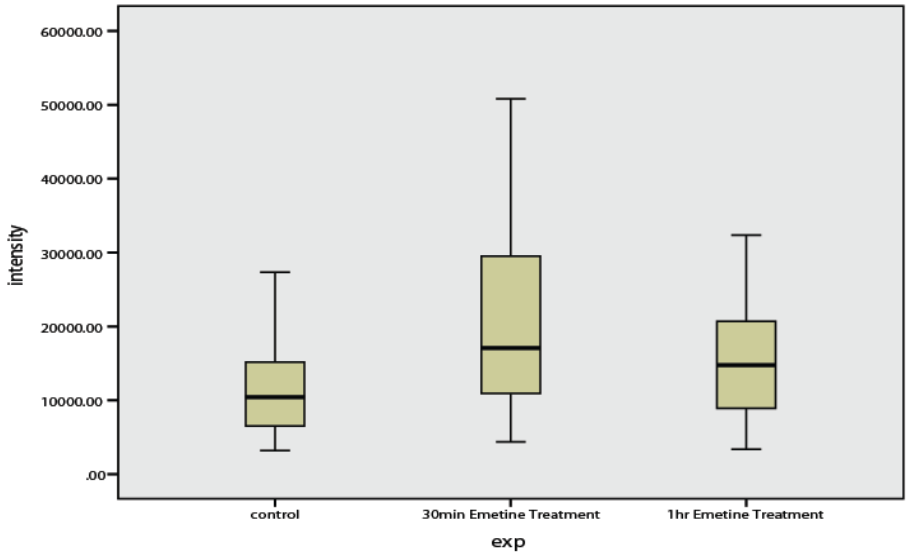

Figure 3.13. Emetine increases 80S signal. Boxplots showing whole cell mean fluorescence intensities of 100 transfected S2 cells treated with 50 µg/mL emetine for 30 min, 1 hr and control (without treatment). Cells were manually defined as regions of interest (ROI) and mean fluorescence values were obtained using the Automated Measurement function of NIS-BR Software (Nikon). Values were normalized by subtracting the intensities in identical ROIs defined in adjacent regions without cells. (This figure was published in Al-jubran et al, 2013).

3.2.6 Lengthening the spacers between RP and YFP fragments slightly increases the functionality of the BiFC-tagged 80S

Characterisation of the initial S18-YN/L11-YC proteins showed that, while the proteins are incorporated into ribosomal subunits, the BiFC interaction hinders translocation of the ribosomes during translation elongation (Al-Jubran et al., 2013). This conclusion was based on the observation that only 5% of YFP fluorescence could be detected in polysomal fractions. We reasoned that the relative short peptide linkers separating the BiFC fragments from the RPs that hinder inter-subunit translocation movement of the ribosome, once the BiFC complex is formed. To limit this effect, I generated S18/L11 and S15/L11 BiFC pairs with a longer 25 amino acids helical linker (HL4) to separate the RPs from the YFP peptides (Figure 3.14.4A). The HL4 linker was reported to effectively separate the domains of bi-functional fusion proteins (Arai et al., 2001). When transfected in S2 cells, these pairs produced a similar BiFC signal pattern as the previous BiFC reporters with the shorter linkers (Figure 3.14B). Pairing the short/long linker contructs; S18 HL4-YN/L11-YC and S18-YN/L11 HL4-YC also produced a clear signal (Figure 3.13B). These constructs were also well expressed (Figure 3.15), and similarly concentrate in the nucleus (Figure 3.16A). These protein constructs were incorporated into the polysomes (Figure 3.16B); fluorimetric analysis of the polysomal fractions revealed that about 85% of the signal detected corresponds to the 80S fractions, and about 7% in the polysomal fractions, which is slightly more than the 5% seen previously (data not included in this thesis because the experiment was done by a postdoc in our Lab, Dr. Jikai Wen). Other constructs will be discussed in the next chapter which produced higher polysomal signal.

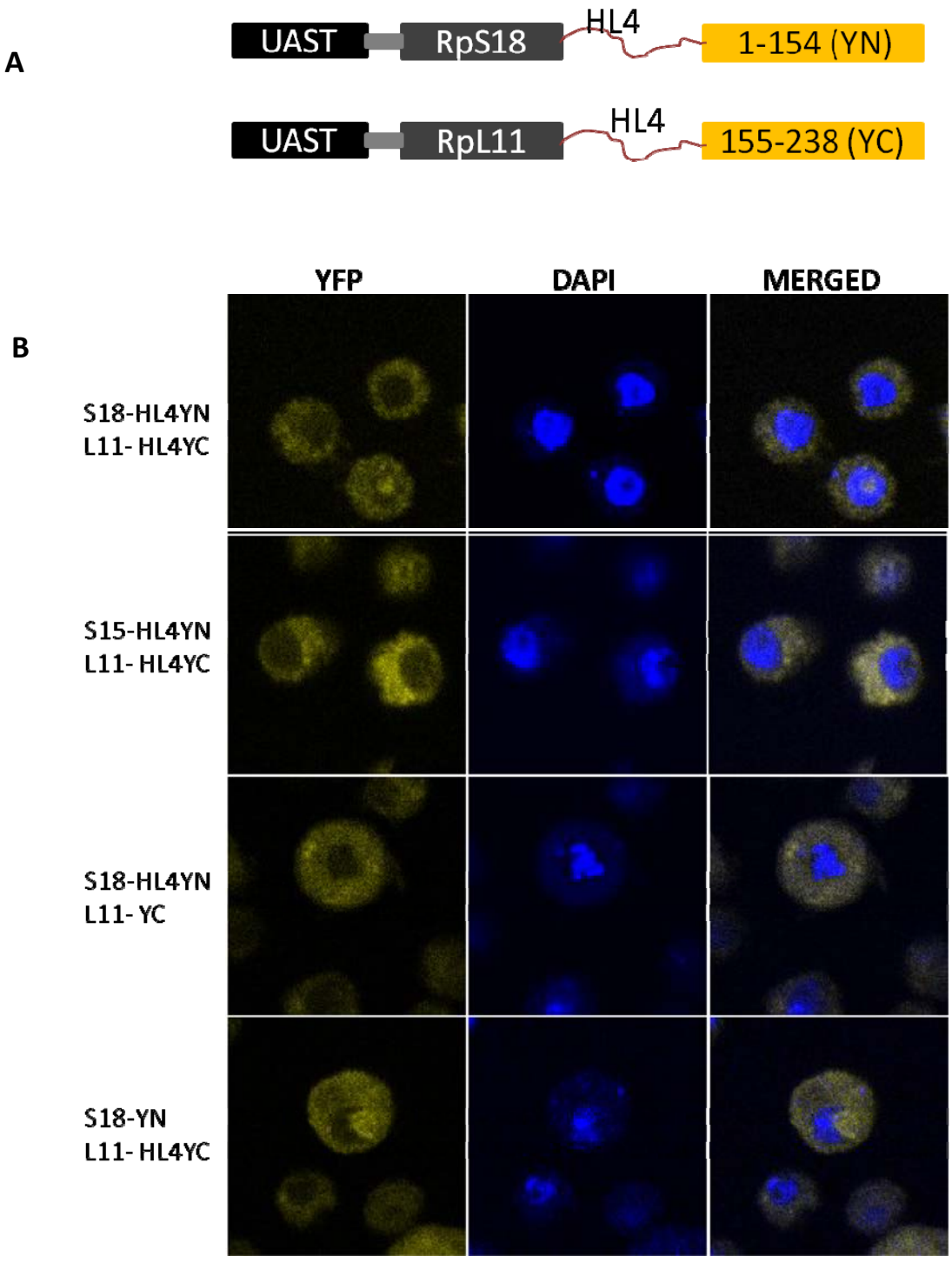

Figure 3.14. Visualisation of the ribosomal subunit interaction using the BiFC reporters with HL4 Linker. (A) Schematic of the BiFC constructs with the HL4 linker. (B) YFP signal was visualised in cells expressing the constructs indicated. Typical cytoplasmic signal (Type I) and cytoplasmic and nucleolar signal (Type II) were observed. Left panel, YFP; middle panel, DAPI and right panel, merged.

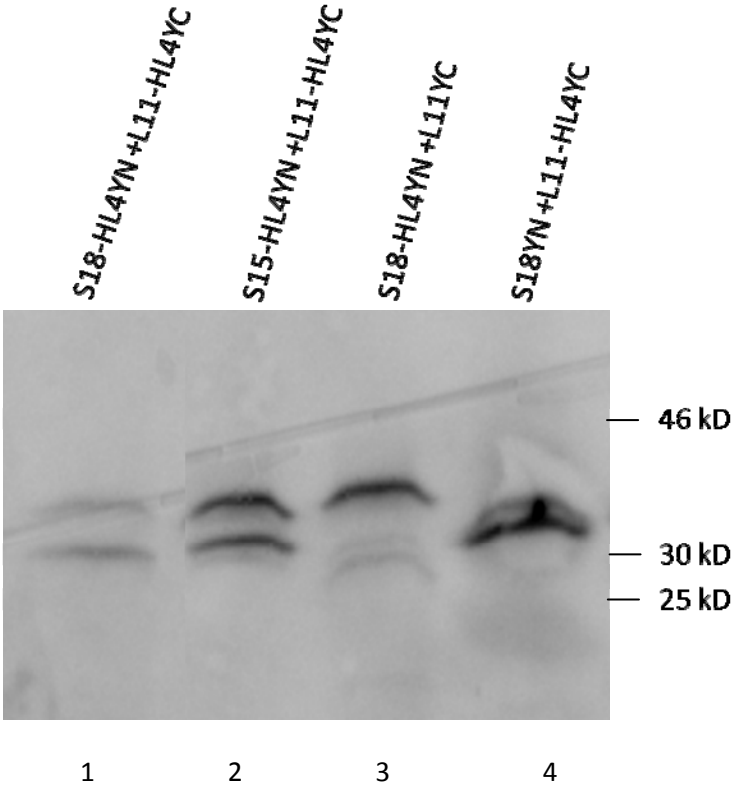

Figure 3.15. Western blots of cell extract transfected with BiFC HL4 reporters. Western blotting of S2 cells co-transfected with the BiFC HL4 tagged RPs indicated with a polyclonal GFP antibody. From L-R: Lane 1: S18-HL4YN (38 kDa) and L11-HL4YC (34 kDa), lane 2; S15-HL4YN (37 kDa) and L11-HL4YC (34 kDa), lane 3; S18-HL4YN (38 kDa) and L11-YC (31.7 kDa), lane 4 S18 YN (35.8 kDa) and L11-HL4YC (34 kDa).

A

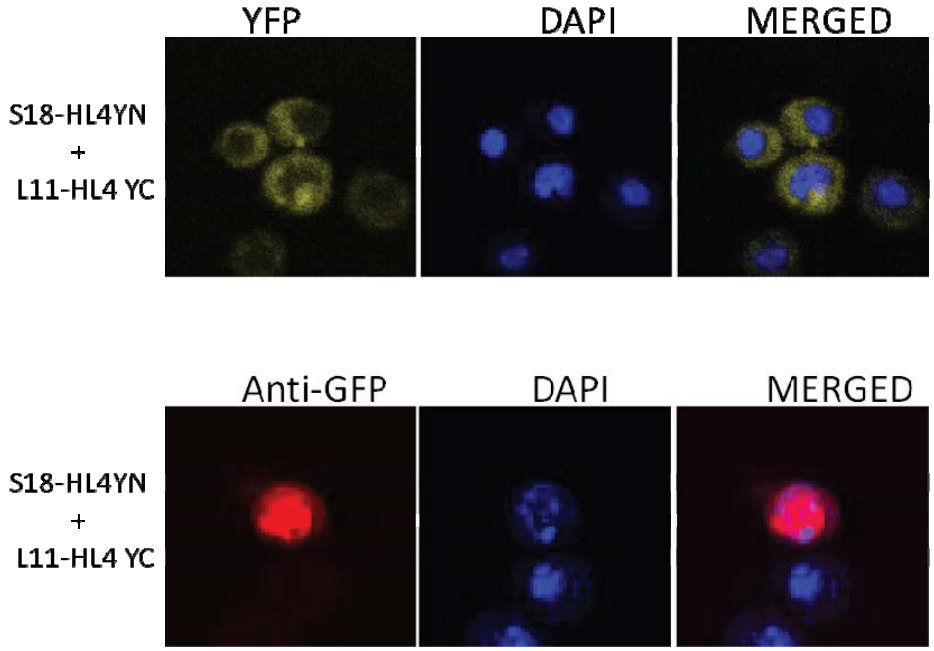
YFP
DAPI
MERGED
S18-HL4YN
+
L11-HL4 YC
Anti-GFP
DAPI
MERGED
S18-HL4YN
+
L11-HL4 YC

B

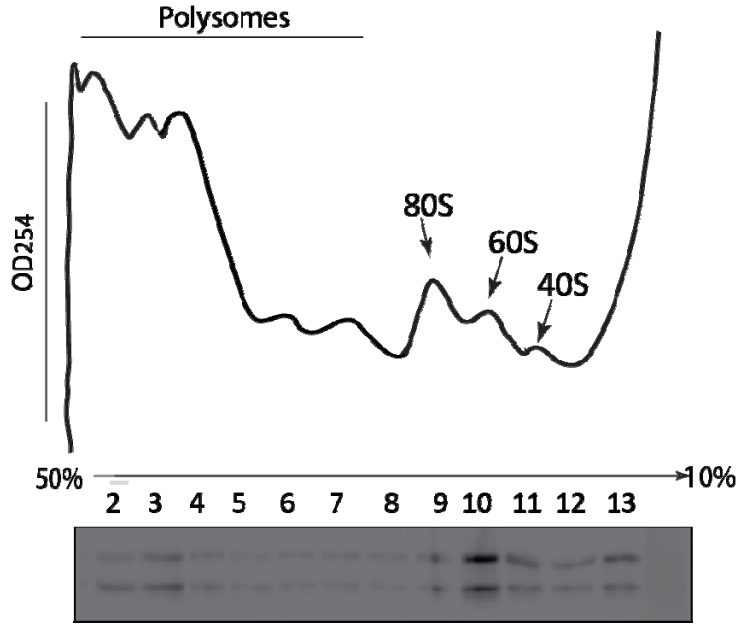
Polysomes
OD254
80S
60S
40S
50%
10%
2 3 4 5 6 7 8 9 10 11 12 13

Figure 3.16. The longer-linker BiFC reporters are functional. (A) Confocal images of S2 cells transfected with S18-HL4YN and L11-HL4YC**.** Top panel shows YFP BiFC 80S signal; bottom panel shows indirect Immunostaining with anti-GFP antibody that recognises YN and YC detected by a Cy5 conjugated secondary antibody, indicating their sub-cellular localisation. (B) Polysome analysis of S2 cells transfected with BiFC-tagged RpS18-HL4YN and RpL11-HL4-YC. The top portion of the panel shows the OD254 profile of the sucrose gradient (10-50%) fractionation of the total cell extract. Positions of the polysomes, monosomes (80S), and 60S, and 40S subunits are indicated with arrows. The bottom portion shows the result of Western blotting of the polysomes fractions recognised with polyclonal anti-GFP antibody.

3.3 Discussion

In this chapter, I have described data that showed the BiFC-based assay which was developed in the laboratory is reliably reporting 80S ribosome subunit joining in cultured *Drosophila* S2 cells. The observation that pairs of the tagged BiFC RPs produced signal only when they were in close proximity on the 80S ribosome strongly supports this view. Additionally, the observation that RP pairs "at the foot" of the ribosome produced signal similar to those pairs located on the head of the subunits excludes the possibility of the signal stemming from an association between 5S sub-particles and the 40S while it is not yet incorporated into the 60S. A notable observation in this study is the apparent 80S signal detected in the nucleus of a fraction of cells (Type II). The ratio of the Type I (signal mostly cytoplasmic) to the Type II cells is relatively the same with all the pairs. The observation that the signal was most apparent in the cytoplasm is in agreement with the accepted view that in eukaryotes, translation is restricted to the cytoplasm; however, the nucleus/nucleolar signal observed suggests the joining of the ribosome subunits also in the nuclear compartment. Only a fraction of the transfected S2 cells show the signal in the nucleolus, this may be due to the fact that the nucleolus is a dynamic structure that breaks down during cell division (Cmarko et al., 2008) or simply that the nuclear 80S is more active at particular stage/stages of cell cycle. The finding that the translation elongation inhibitor emetine enhanced both cytoplasmic and nucleolar signal suggest that the interaction is translation dependent in both locations. A visible increase in the BiFC signal intensity in the cytoplasm and at the periphery of the nuclear envelope demonstrates the effect of emetine freezing the ribosomes on the mRNA and increasing their mass. Notably, the most apparent effect of this drug is an obvious increase in the frequency of Type II cells. Emetine treatment increased BiFC fluorescence intensity also *in-vitro* in cell lysates, in a parallel experiments

conducted by Dr. Jikai Wen (Al-Jubran et al., 2013). In these in-vitro experiments, translation initiation inhibition drugs like puromycin and pectamycin, which are known to break down polysomes, led to a reduction in the fluorescence intensity *in-vitro* (Al-Jubran et al., 2013). The increase in the length of the linkers to 25 amino acids does not bring about a significant change in the translocation movement of the 80S ribosome during the elongation phase of translation when compared with the initial 7/5 amino acid linkers. As with the short linkers, bulk of the BiFC signal was also detected in the 80S fraction with only about 7% in the polysomes compared to initial 5% observed with the short linkers. This observation may imply that the YFP BiFC linkage is generally not strong enough to withstand the rotational movement of ribosome during the elongation phase. The inter-subunit rotation breaks the YFP BiFC interaction leading to a drastic decrease of the signal in the polysomes (more sensitive reporters are presented in the next chapter).

CHAPTER 4

4.0 Development of a more sensitive BiFC 80S reporters

4.1 Synopsis

As I have described in the previous chapter, the BiFC assay easily allows 80S visualisation in S2 cells. However, a limitation we encountered with YFP BiFC reporter constructs is that the YFP fluorescence intensity is relatively low. As such, very little signal could be detected in polysomes, possibly because the inter-subunits rotation of the ribosome impairs the formation of the YFP BiFC complex. In an attempt to increase the sensitivity of the assay, I generated additional pairs of BiFC reporter constructs based on the more sensitive Venus fluorescent protein (VFP). VFP fragments are reported to exhibit higher BiFC efficiency with about 13% more fluorescence intensity and fast chromophore maturation compared to YFP (Shyu et al., 2006). Employing a similar cloning strategy as with previous reporters, I tagged the RP pairs S18/L11 and S6/L24 with Venus BiFC fragments. The results of these experiments are that the Venus BiFC reporters produced signal both in the cytoplasm and nucleolus as before, but the signal is as expected, more intense with increase in frequency of cells that show nucleolar signal. Additionally, more of the BiFC signal was found in polysomal fractions compared to the YFP-based reporters. I have also generated transgenic flies expressing this new Venus constructs, which allowed me to visualise 80S ribosomes in different cell types, including photoreceptor neurons. Notably, in these neurons, 80S were unexpectedly also detected along axons. (Some of the data presented in this Chapter are part of my work published recently by our group (Al-Jubran et al., 2013) in which I am a shared first author).

4.2 Results

4.2.1 Development of an enhanced 80S reporter assay using Venus-based BiFC

Constructs expressing Venus-based BiFC fusion proteins were constructed similar to the YFP-based constructs described in the previous chapter (Figure 4.1A) (details are in Material and Methods). Subsequently, they were transiently transfected in S2 cells. The RpS18-VN and RpL11-VC constructs produced a strong VFP signal that mostly localised in the cytoplasm in about 35% of the cells (Type I), 38% of the cells (Type II) showed signal both in the cytoplasm and the nucleolus, while 10% (Type III) of the cells showed a strong signal throughout the nucleus as well as the cytoplasm (Figure 4.1C). About 17% (Type IV) of the cells also showed intense fluorescence all over the cell without any apparent pattern (Figure 4.1C); these had the appearance of damaged cells, possibly an artefact of over expression of the tagged BiFC peptides (see below). To assess whether both of the BiFC fusion proteins were well expressed in S2 cells, I analysed their expression by Western blotting of the total protein extracts, which showed bands of the right sizes corresponding to RpS18-VN and RpL11-VC (Figure 4.1A). As expected, no fluorescence was observed in cells transfected with individual tagged RPs and gal4 (Figure 4.2). Furthermore, cells were transfected with BiFC constructs that are not tethered to any RP: pUAST-VN and pUAST-VC, with which only a weak signal was observed throughout the cell (Figure 4.2). This observation further confirms that the signal observed in cells transfected with the BiFC tagged RPs could be primarily due to the ribosome subunit joining. Similar observations were made for the RpS6-VN/RpL24-VC pair (Figure 4.3 and 4.4).

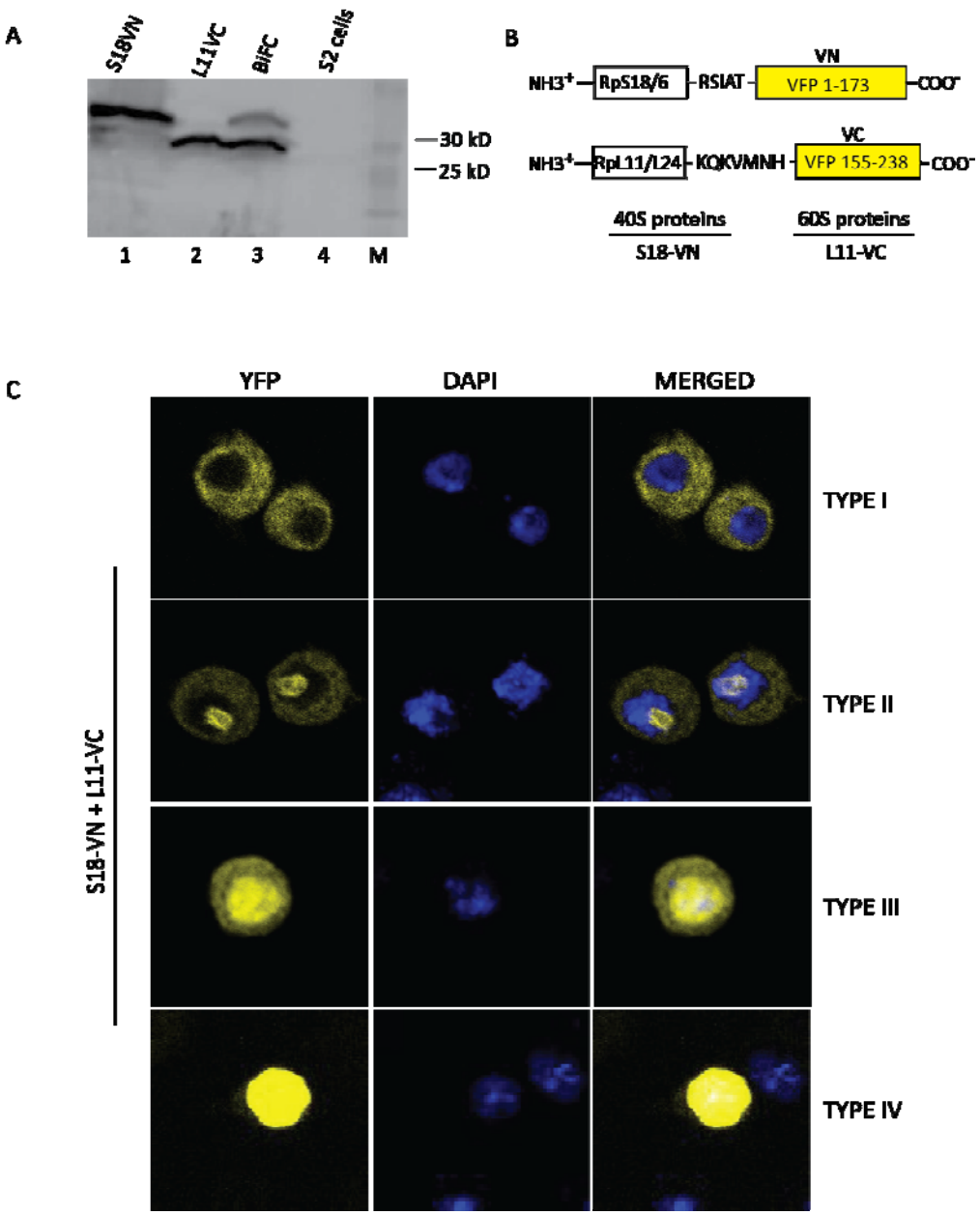

Figure 4.1. Visualisation of ribosomal subunit joining with Venus based BiFC reporter constructs. (A) Western blot analysis of cell extracts from cells transfected with the fused RPs and BiFC. Lane 1; RpS18-VN (35.8 kDa), lane 2; RpL11-VC (31.7 kDa); lane 3; BiFC (RpS18-VN + RpL11-VC), lane 4; S2 cells (Control) and lane 5; protein marker. (B) Schematics of the Venus BiFC reporter constructs. (C) Images of S2 cells co-transfected with pUAST-RpS18-VN and pUAST-RpL11-VC and gal4. From left panel to right: VFP, DAPI, and merge. Images were taken with a confocal microscope with 63X objective lens.

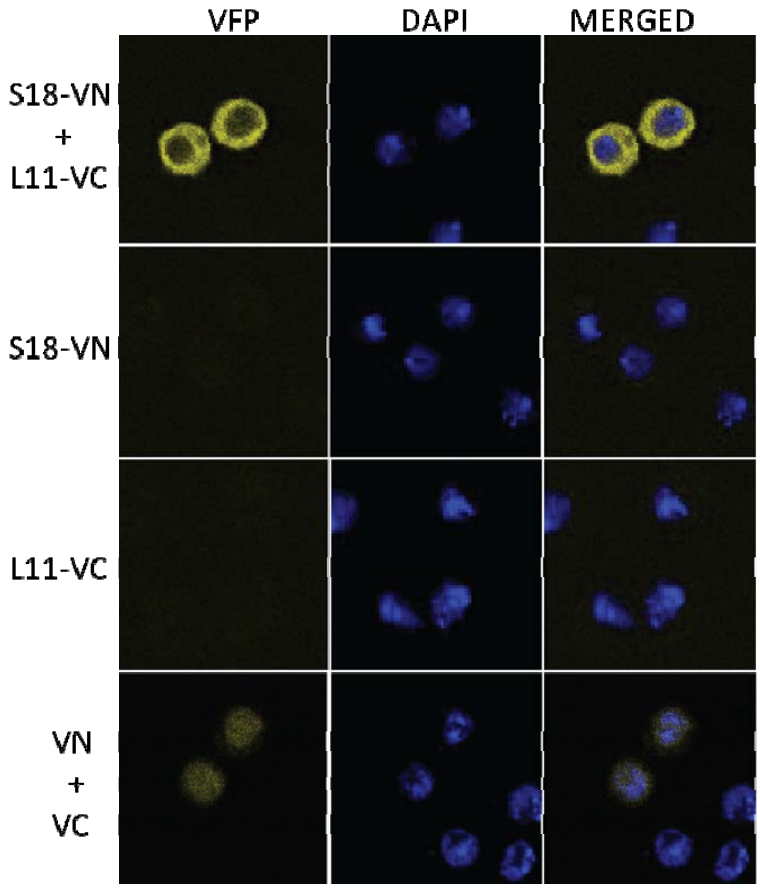

Figure 4.2. Fluorescence was observed only in cells co-transfected with the BiFC tagged RPs. Images of S2 cells transfected with the constructs indicated. BiFC signal is generated only when co-transfected with pUAST.RpS18-VN and pUAST.RpL11-VC along with gal4 driver. A dim fluorescence is observed when S2 cells are co-transfected with pUAST-VN and pUAST-VC.

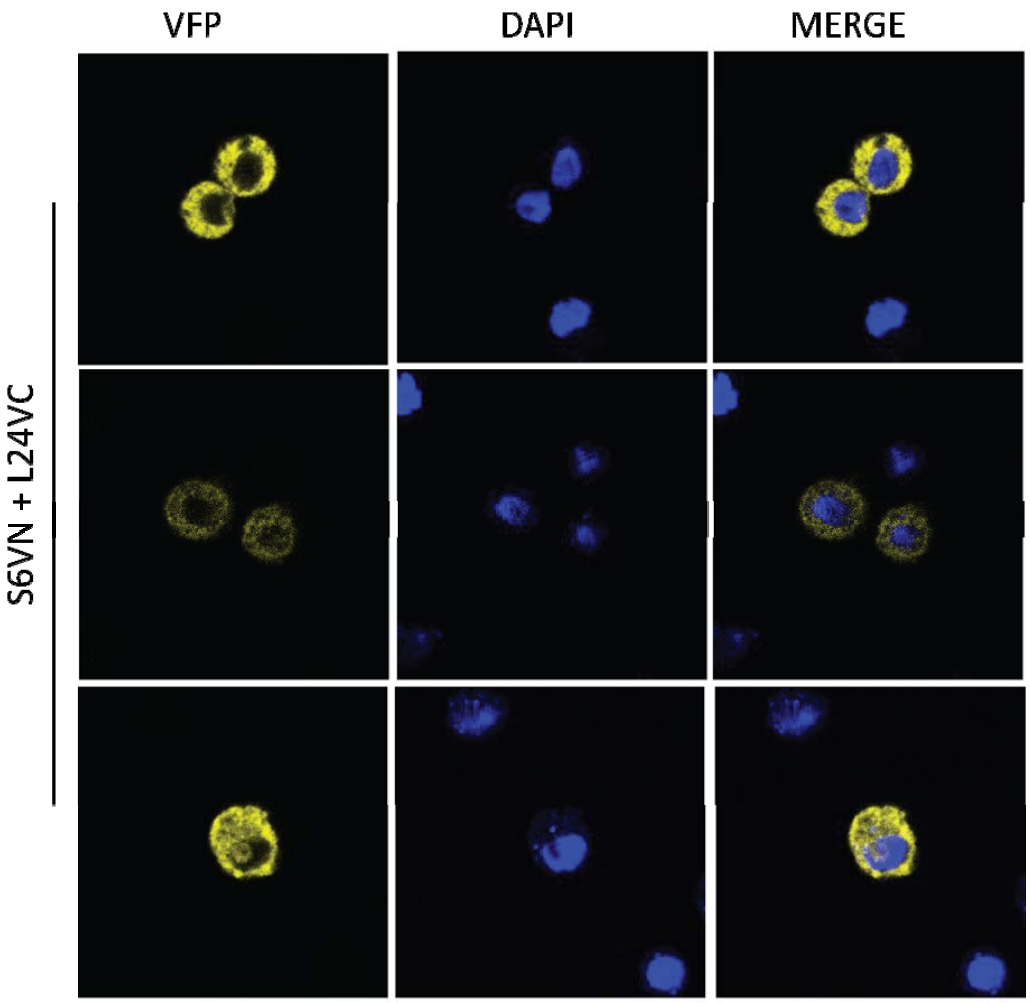

Figure 4.3. S6 and L24 tagged with Venus fragments also produce BiFC signal. Confocal images of S2 cells transfected with the indicated BiFC constructs. Typical cytoplasmic BiFC signal (Type I) is depicted in the top 2 rows and cytoplasmic and nucleolar signal (Type II) bottom row. Left panel, VFP; middle panel, DAPI and right panel, merged. The two top rows shows Type I cells and bottom row Type II.

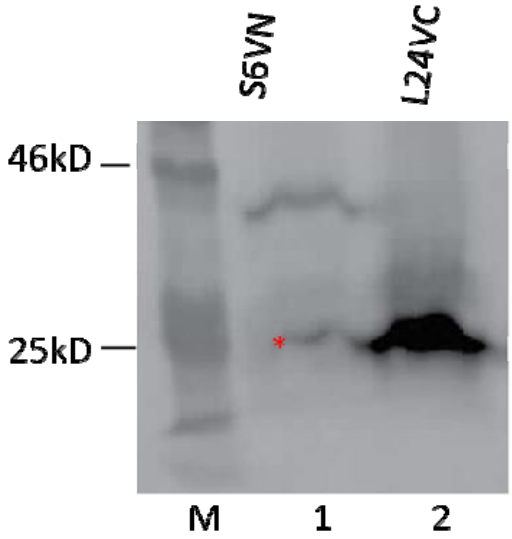

Figure 4.4: Western blot of whole cell extracts of cells transfected with fused RPs S6-VN and L24-VC. Western blotting of S2 cells transfected with the indicated constructs with a polyclonal GFP antibody recognising both VN and VC. From left to right: lane 1, S6-VN (39 kDa) and lane 2, L24-VC (26 kDa). The smaller band (indicated with an asterisk) visible in lane 1 is a spill over of the protein in lane 2.

The intense fluorescence seen in Type III and IV throughout the cell is possibly an artefact of over-expression of the tagged peptides. Types III and IV cells have very small nuclei, which could be a sign of dying or apoptotic cells. To verify that, I carried out an immunostaining assay to detect active caspase 3, with an anti-active caspase 3 primary antibody (see Materials and Methods). Caspase 3 is a member of cysteine proteases family whose activation is required for almost all forms of apoptosis (Salvesen and Dixit, 1997). The result of this assay showed that the Type III and Type IV cells were typically positive to anti-active caspase 3 (Figure 4.5). The anti- active caspase 3 was detected mainly in the DAPI stain region and the intensity of the stains is more intense in the Type IV cells (Figure 4.5E) compared to the Type III (Figure 4.5 panel C and D).

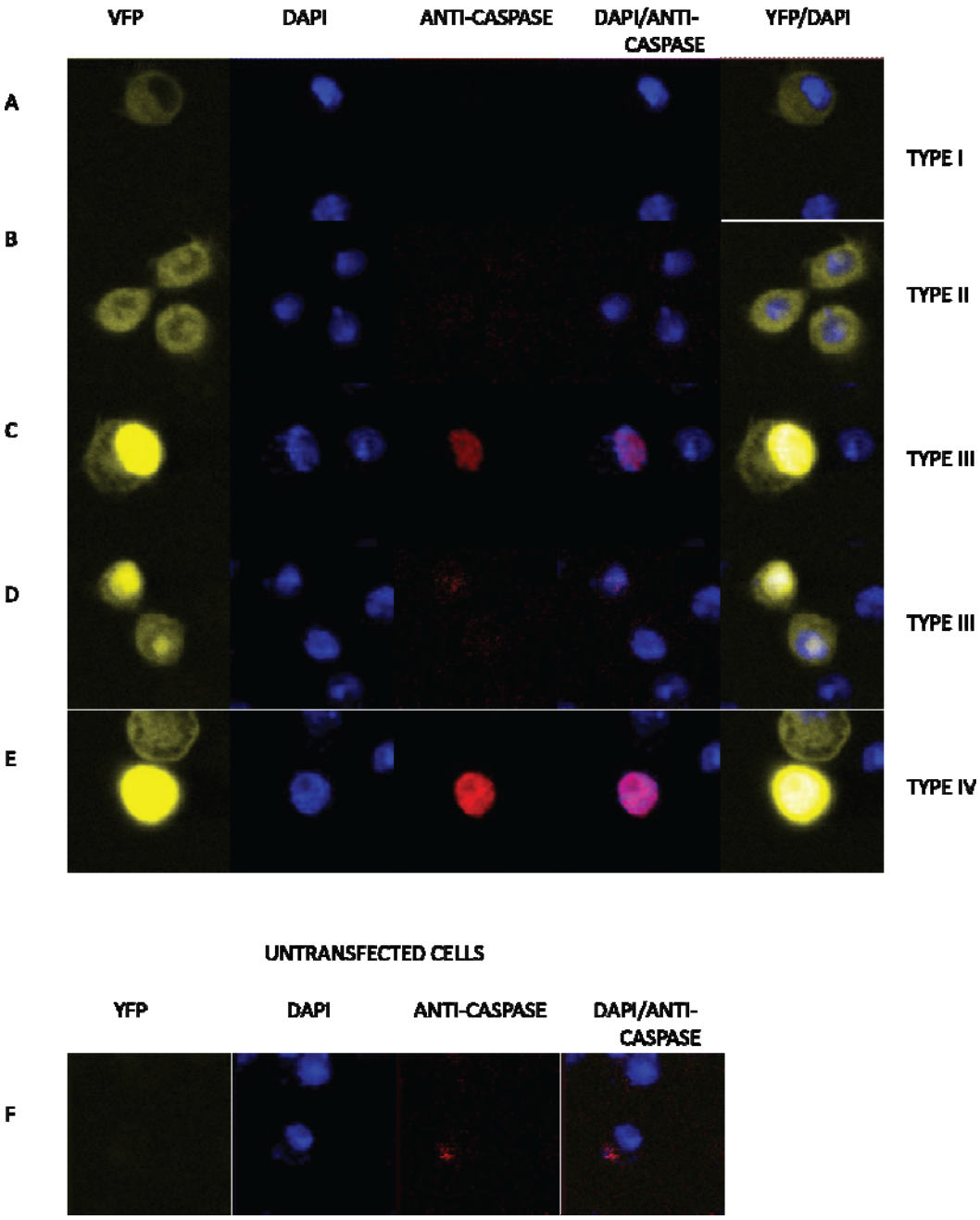

Figure 4.5. Type III and IV cells accumulate active caspase 3. (A-E) Immunostaining of BiFC transfected S2 cells with anti-active caspase 3 antibody. From left to right: panel 1, VFP, panel 2, DAPI, panel 3, anti-active caspase 3, panel 4, merge image of DAPI and anti-caspase and panel 5, merge image YFP and DAPI. The type III and IV (C, D and E) cells are mainly apoptotic cells as appear positive to anti- caspase stain (F) Untransfected cells showing anti-caspase stain (Control)**.**

I characterized the BiFC signal further by incubating the transfected cells with 50 µg/mL of emetine for 30 min. Apparent visual increase in the fluorescence was observed in treated cells (Figure 4.6A) with almost two fold increase in the Type II cells (Figure 4.6B). Comparing the level of significance in the increase of Type cells due to emetine treatment using the obtained mean values revealed a P- value of (0.00015); indicating that the increase in Type II cells was statistically significant and the effect of emetine on the BiFC signal could not have been due the chance.

A

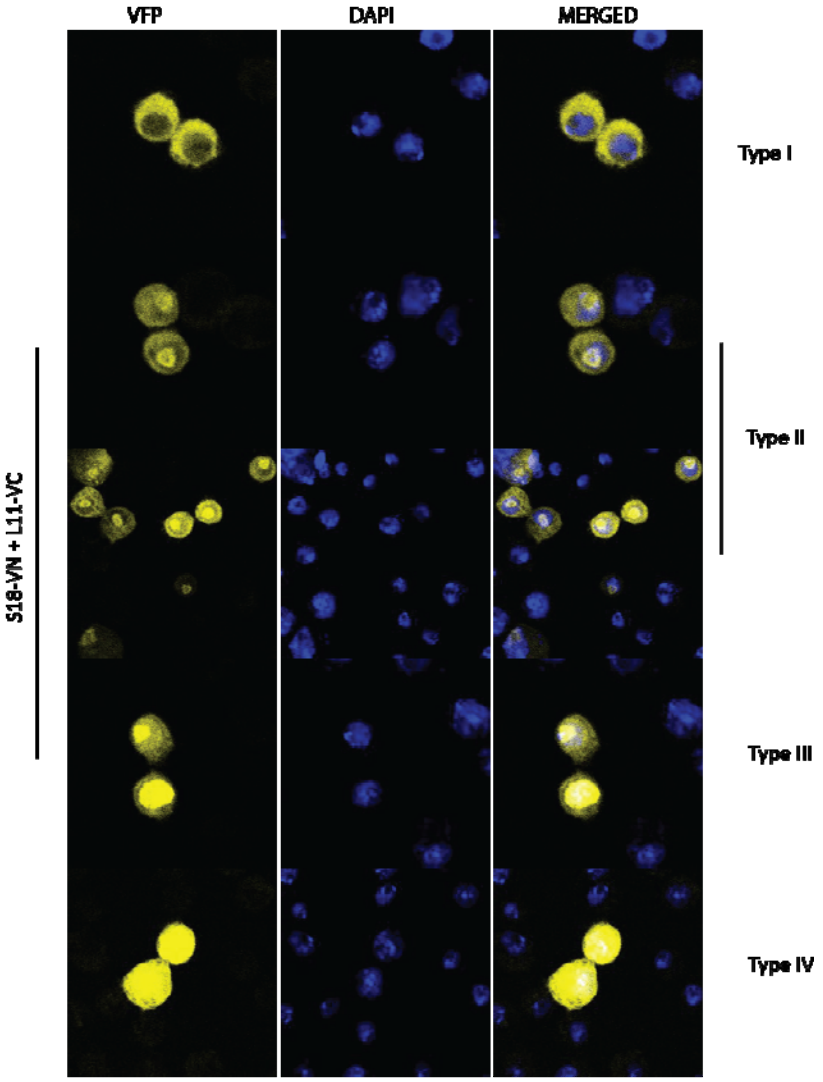
VFP
DAPI
MERGED
Type I
Type II
Type III
Type IV
S18-VN + L11-VC

B

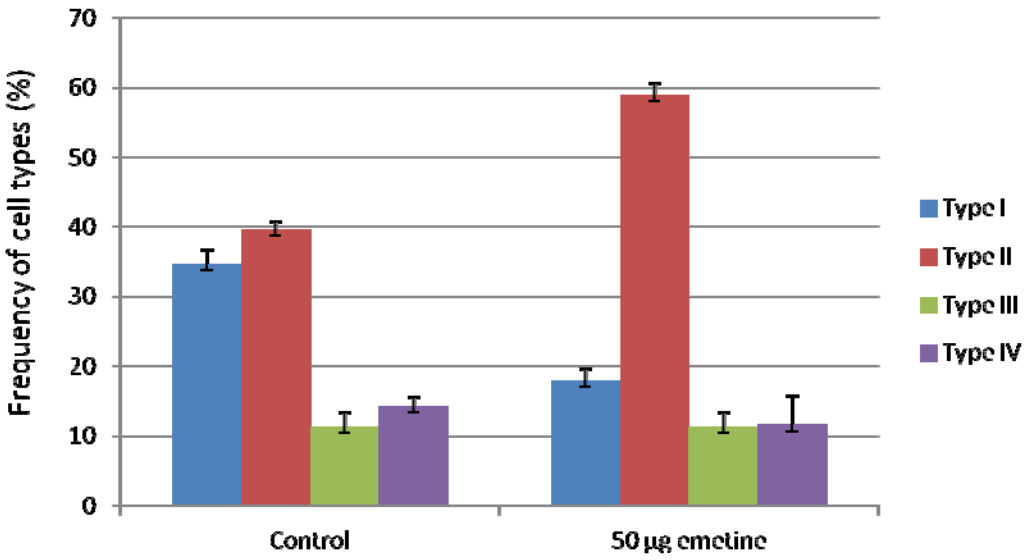
Frequency of cell types (%)
70
60
50
40
30
20
10
0
Control
50 µg emetine
Type I
Type II
Type III
Type IV

Figure 4.6. Emetine treatment increases the frequency of cells showing nuclear BiFC signal. (A) Confocal images of BiFC transfected cells treated with 50 µg emetine for 30 min prior to fixation indicating the cell types based on BiFC signal localisation pattern. High increase in the frequency of Type II cells was observed upon emetine treatment compared to the control (B) Effect of emetine treatment for 30 min prior to fixation on the frequency of cells type pattern. Values are mean of three replicates from two independent experiments where 100 cells were counted for each experiment. Error bars are indicative of standard deviation from the mean value.

Altogether, the observations that were made in this laboratory with the previous YFP-based BiFC constructs indicated that the BiFC signal is reporting association between proteins that are brought together by joined ribosomal subunits. As done with the YFP, I also tested whether the BiFC signal I have detected is not an artefact of over expression of the fusion proteins by analyzing the expression and sub-cellular distribution of the tagged RPs via immunostaining of transfected cells. The result of the assay revealed that both RpS18-VN and RpL11-VC are present all over the cells and are particularly more abundant in the nucleus (Figure 4.7); these results are similar to that obtained with the YFP-based constructs. The BiFC signal, however, was most apparent in the cytoplasm, as with the YFP reporter (Chapter 3). Therefore, this result indicates that the VFP fluorescence observed in the cytoplasm is unlikely to be an artefact of over expression of the tagged BiFC peptides, or the higher affinity of the Venus fragment, but the result of ribosomal subunit joining.

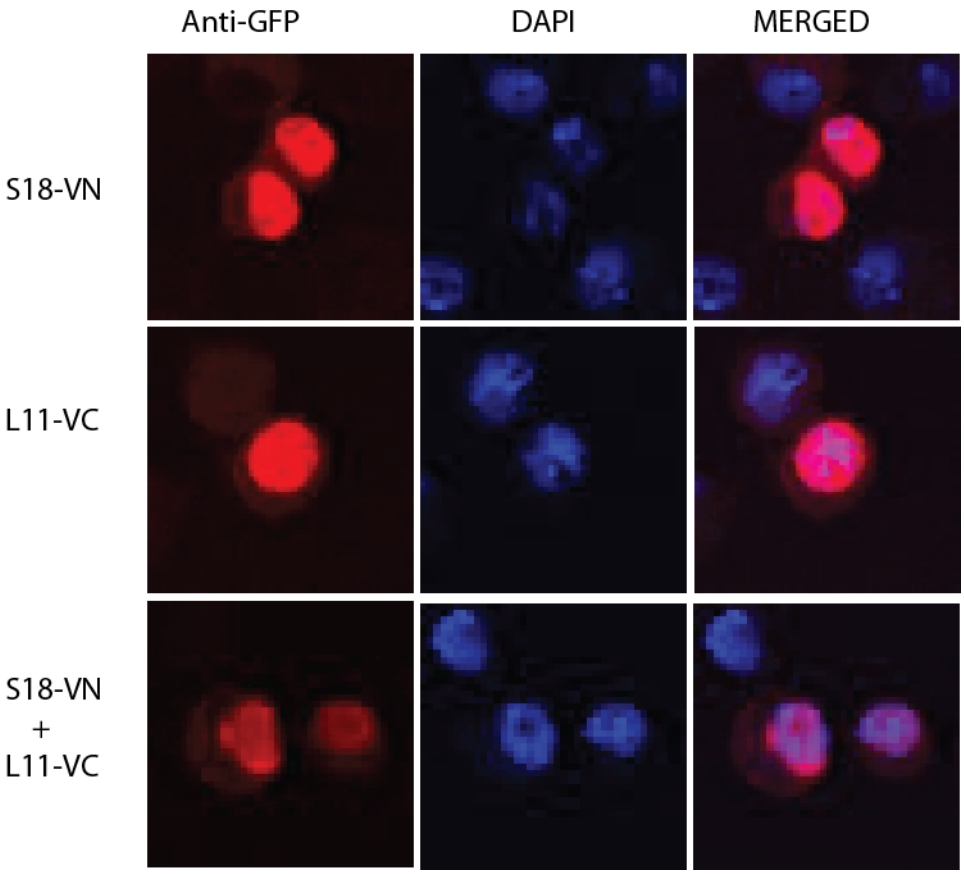

Figure 4.7. Sub-cellular localisation of the tagged BiFC RPs. Immunostaining of S2 cells transfected with the BiFC constructs indicated showing their sub-cellular localisation. VFP fragments were detected with polyclonal antibody against GFP (which also detect VFP). Cy3 conjugated secondary antibody was used to detect the anti-GFP primary antibody. From left to right, anti-GFP, middle panel, DAPI and right panel, merge image. Images were taken with Leica laser confocal microscope with 63X oil immersion lens.

4.2.2 RPs tagged with Venus BiFC fragments are found in polysomes

To investigate whether these new BiFC tagged RPs are incorporated into functional ribosomes, I purified polysomes and analysed by Western blotting the different fractions for the presence of S18-VN and L11-VC (Figure 4.8A). Additionally, the polysomal fractions were analysed with a fluorimeter. The results obtained showed that these tagged RPs are present in polysomes, as the flourimetric analysis revealed that about 23% of the BiFC signal is found in polysome fractions, about 41.2% came from the fractions that correspond to the 80S (Figure 4.8A and 4.8C), and the remaining co-migrates with lighter fractions. The signal detected in the lighter fractions might stem from the more long-lived degradation intermediates of BiFC-joined 80S. To further verify whether the tagged RPs are associated with functional ribosomes, the cells extract was treated with puromycin which breaks polysomes, dissociating the ribosomal subunits and should shift the ribosomal subunits to lighter fractions corresponding to the single subunits. This treatment shifted the signal and tagged proteins to the lighter fractions (Figure 4.8B); with only 5.4% of the BiFC signal remaining in heavier fractions, 14% in the monosome (80S) and about 55.3% detected lighter fractions (Figure 4.8B and 4.8D). This experiment was done together with Dr. Jikai Wen and published in (Al-Jubran et al., 2013).

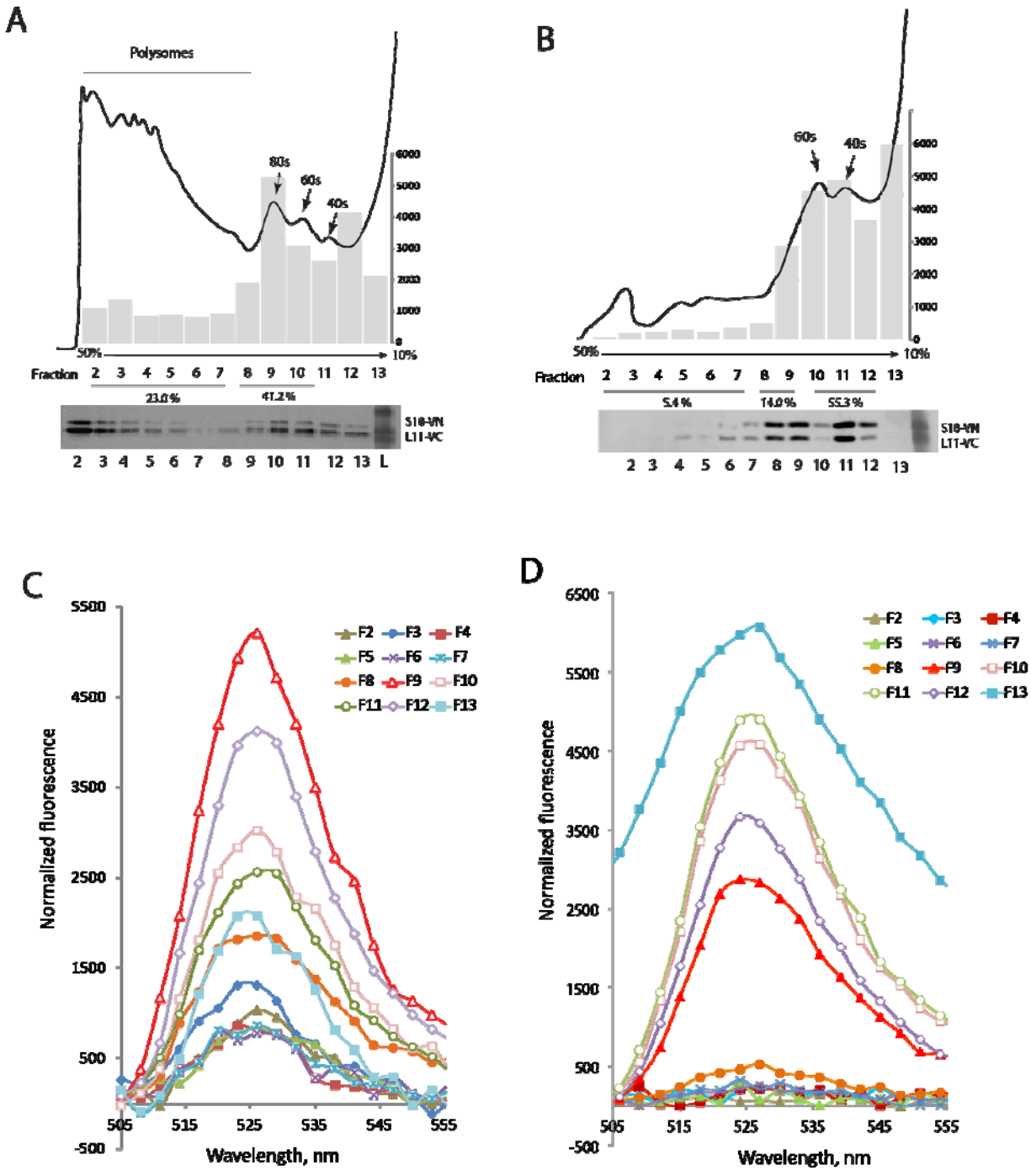
A
Polysomes
80s
60s
40s
50%
10%
Fraction 2 3 4 5 6 7 8 9 10 11 12 13
23.0%
41.2%
S18-VN
L11-VC
2 3 4 5 6 7 8 9 10 11 12 13 L
B
60s
40s
50%
10%
Fraction 2 3 4 5 6 7 8 9 10 11 12 13
5.4%
14.0%
55.3%
S18-VN
LTT-VC
2 3 4 5 6 7 8 9 10 11 12 13
C
Normalized fluorescence
Wavelength, nm
F2 F3 F4
F5 F6 F7
F8 F9 F10
F11 F12 F13
D
Normalized fluorescence
Wavelength, nm
F2 F3 F4
F5 F6 F7
F8 F9 F10
F11 F12 F13

Figure 4.8. BiFC 80S signal associated with the polysomes. Polysome analysis of S2 cells expressing S18 and L11 tagged with VN and VC fragments, respectively. (A) Polysome profile of cells transfected with pUAST-RpS18-VN and pUAST-RpL11-VC. Cells were treated with 20 µg/mL emetine for 30 min prior to lysis. Positions of polysomes, monosomes (80S) and 60S and 40S are indicated. Bar charts show normalized emission of Venus (528 nm) for the different polysomes fractions. Emission values were calculated from the emission spectra which were normalized by subtracting the background reading in parallel fractions from an untransfected cell lysate (Control). Bottom part of each panel shows Western blot of each fraction with a polyclonal GFP antibody recognising both both VN and VC fragments (see Materials and Methods). (B) Polysome profile as above of transfected cells treated with 100 µg/mL puromycin for 30 min before lysis. The lysate was treated with the same concentration of puromycin and 375 mM KCl for 30 min at room temperature prior to loading of the gradient (details in Materials and Methods). (C) and (D), Normalized emission spectra chart of the different fractions shown in A and B above respectively as measured with a fluorimeter. Parts of this figure were published in Al-jubran et al, 2013.

4.2.3 The nucleolar 80S signal is Pol II transcription dependent

The observation that emetine treatment enhances the nucleolar 80S BiFC signal as that in the cytoplasm indicates that the 80S in the nucleolus are translating nucleolar mRNAs. I therefore set out to investigate whether transcription inhibition affects signal in the nucleolus. To assess that, I incubated cells transfected with the Venus-based 80S reporters with different transcription inhibitors, including actinomycin D (act. D), triptolide and 5,6-dichloro-1-β-D-ribofuranosylbenzimidazole (DRB). The results of these experiments was that these three transcription inhibitors that are expected to block transcription by all three RNA polymerases, drastically reduced the BiFC signal in the nucleolus, resulting in a strong reduction in Type II cells from about 40% to less than 5% (Figure 4.9 and 4.10).

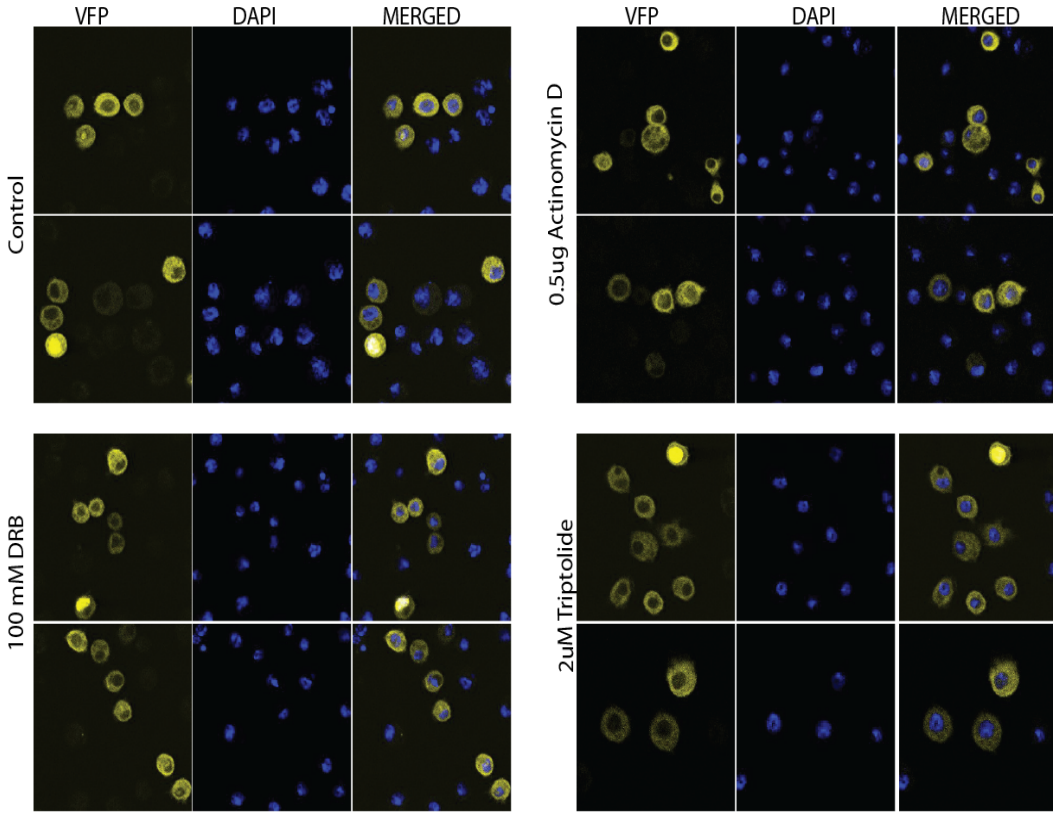

Figure 4.9. Blocking of transcription reduces nucleolar 80S signal. Confocal images of BiFC transfected S2 cells treated with the indicated transcription inhibitors for 4 hrs prior to fixation. The nucleolar BiFC signal is inhibited by these transcription inhibitors. Top left control, top right 0.5 µg act. D, bottom left 100 mM DRB and bottom right 2 µM triptolide. The VFP signals are shown in left column, DAPI staining in middle, and the merged image on right. All images were taken with confocal microscope with 63X oil immersion objective lens.

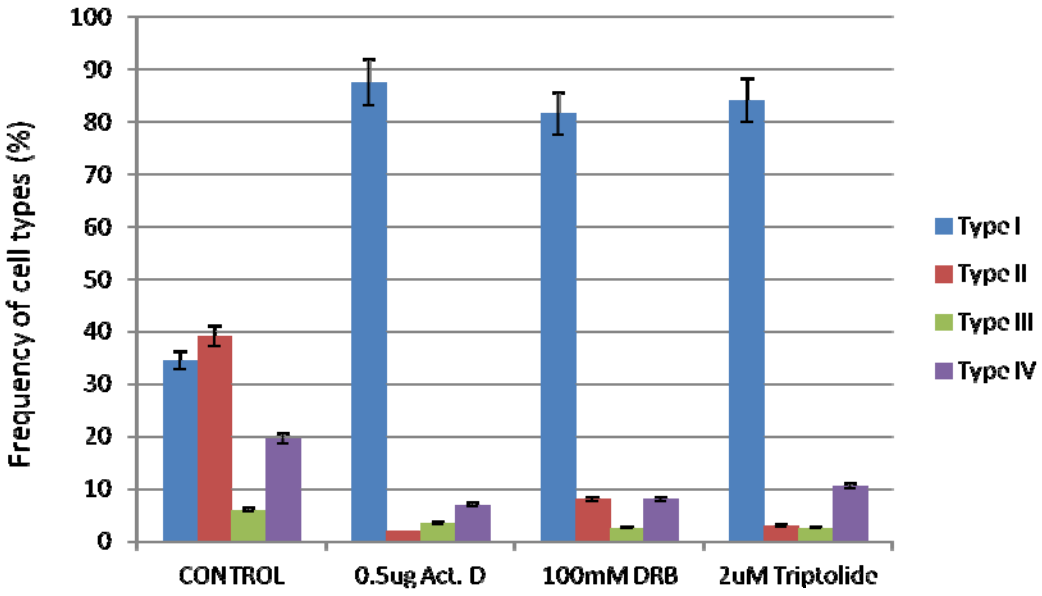

Figure 4.10. Transcription inhibition reduces Type II cells frequency. Bar chart shows frequency of different BiFC cell types pattern (Type I-IV) upon transcription inhibition with the indicated drugs. Transfected cells were incubated with these inhibitors 4 hrs prior to fixation**.** Bars indicate the mean of BiFC cell types in 100 randomly counted cells from two separate transfections. Error bars indicates variation between the 2 experiments.

To investigate what type of transcription is linked to the nucleolar signal, cells were treated with α-amanitin, a transcription inhibitor that has high affinity for Pol II but little or no affinity for Pol I or Pol III; this drug binds the catalytic active site of RNA polymerase II large subunit thereby changing its conformation (Kaplan et al., 2008; Brueckner and Cramer, 2008). I observed that 4 hrs incubation with α-amanitin resulted to a reduction in Type II cells, which became more apparent at 15 hrs treatment (Figure 4.11 and 4.12). Instead, a 4 hrs treatment with a low concentration of act.D (0.2 μg/mL), which is expected to block only RNA polymerase I does not affect the nucleolar signal (Figure 4.13). Transcription inhibition by act.D was validated by its ability to completely prevent fluorouridine (FU) incorporation (Figure 4.14). These data suggest that the BiFC signal in the nucleolus requires Pol II transcription and that the signal could probably be as a result of 80S ribosome translating nuclear mRNA.

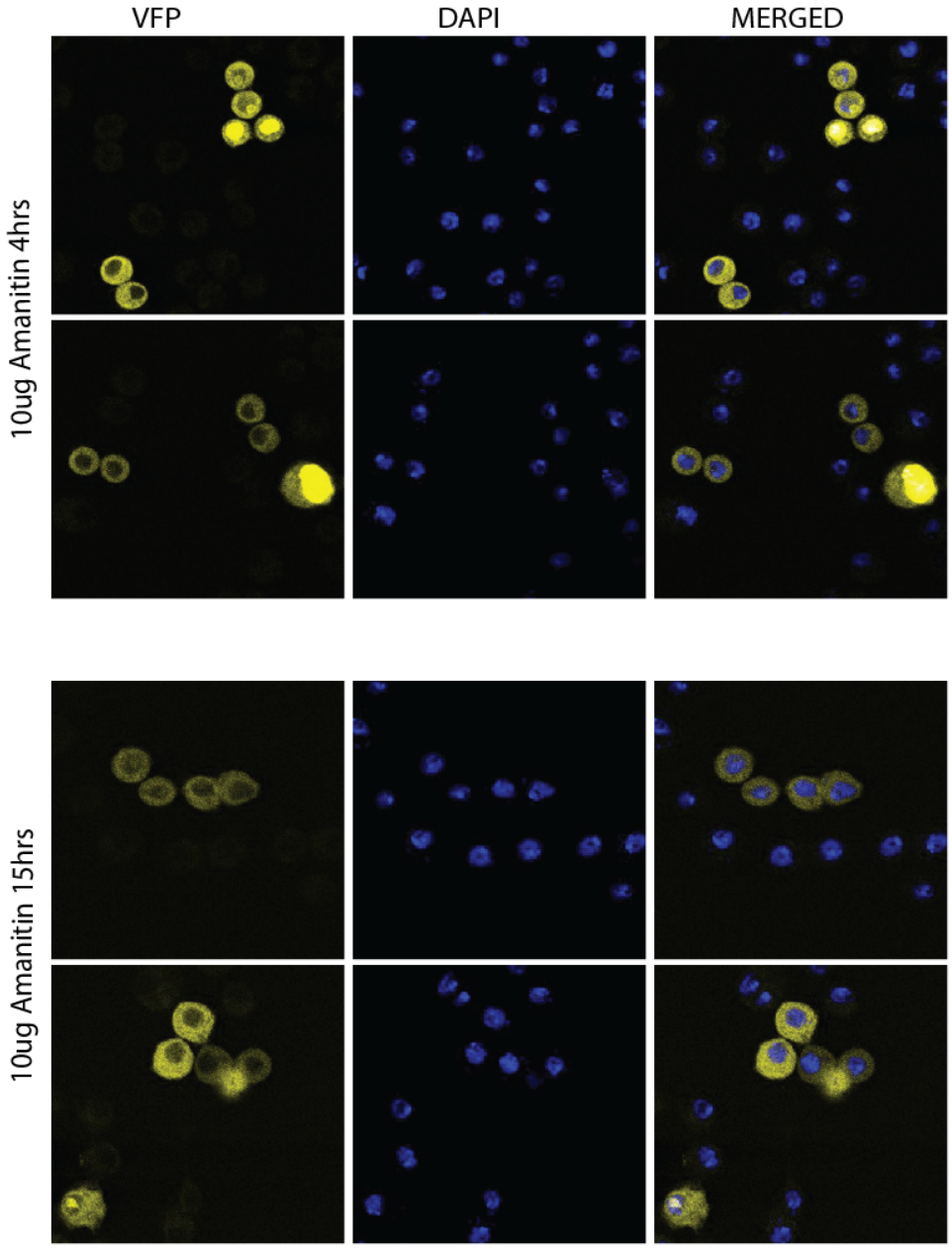

Figure 4.11. Transcription Inhibitor α-amanitin reduces the proportion of Type II cells. Treatment of transfected S2 cells with 10 µg α-amanitin prior to fixation depletes nucleolar signal. Panels show representative images of BiFC transfected S2 cells mostly depicting Type I BiFC signal pattern. Top two rows show 4 hrs treatment and bottom two rows show 15 hrs treatment. Left panel VFP, middle panel, DAPI and right panel merge.

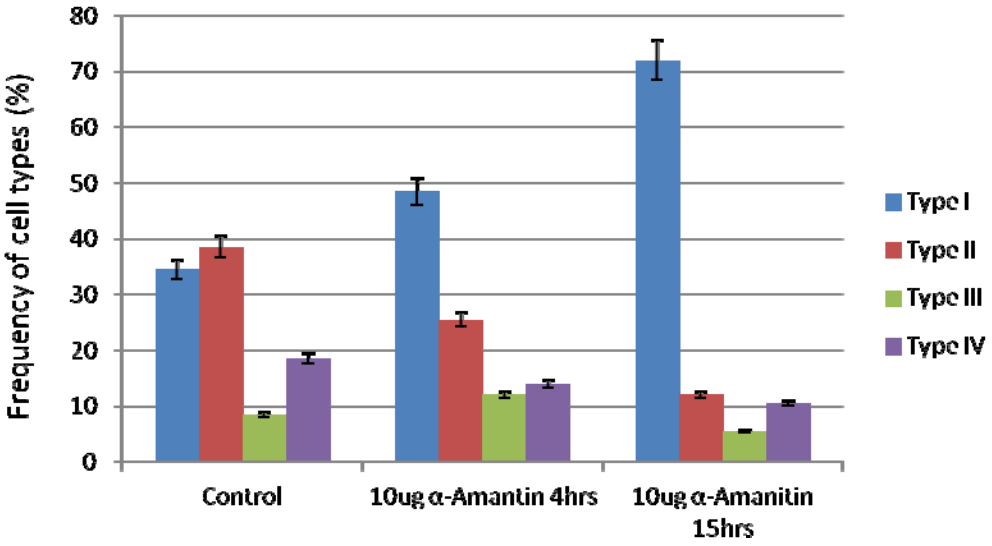

Figure 4.12. Incubation with α-amanitin reduces 80S nucleolar signal. Transcription inhibition of BiFC transfected S2 cells with 10 µg α-amanitin progressively decreases the proportion of Type II cells upon 4 hrs and 15 hrs treatment prior to fixation. Bars indicate the mean of BiFC cell types in 100 randomly counted cells from two separate experiments. Error bar indicates variation between the 2 experiments.

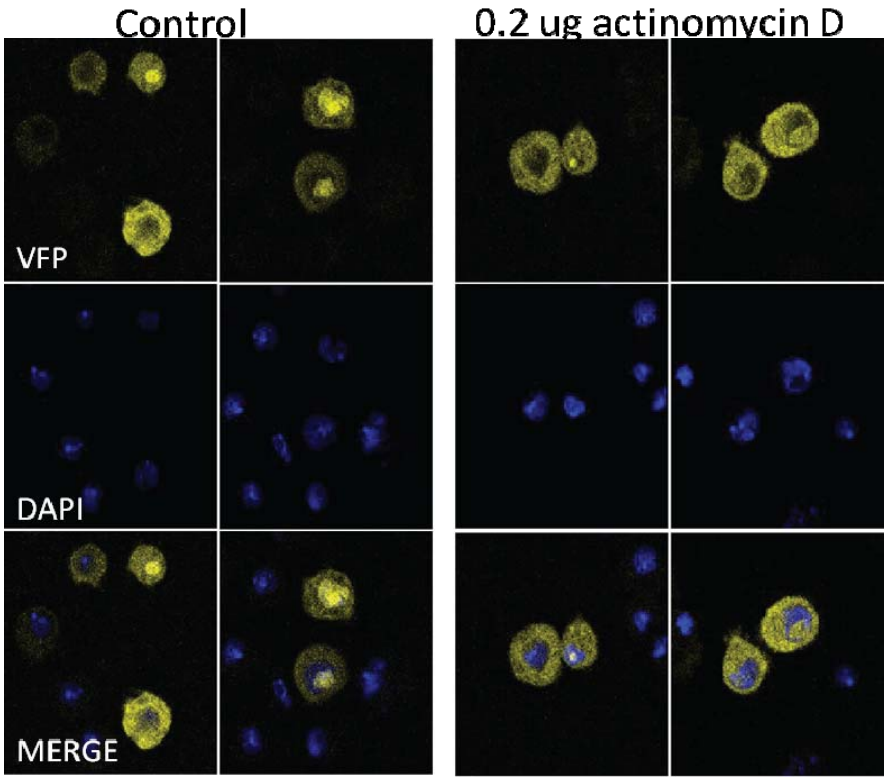

Figure 4.13. The 80S nucleolar signal does not require Pol I transcription. Representative images of BiFC transfected cells showing nucleolar signal persisted upon act.D treatment for 4 hrs at a concentration that is expected to selectively block RNA pol I. Panels in the left, shows control and panels in the right, shows treatment. Top rows VFP, middle rows DAPI and bottom rows, merge.

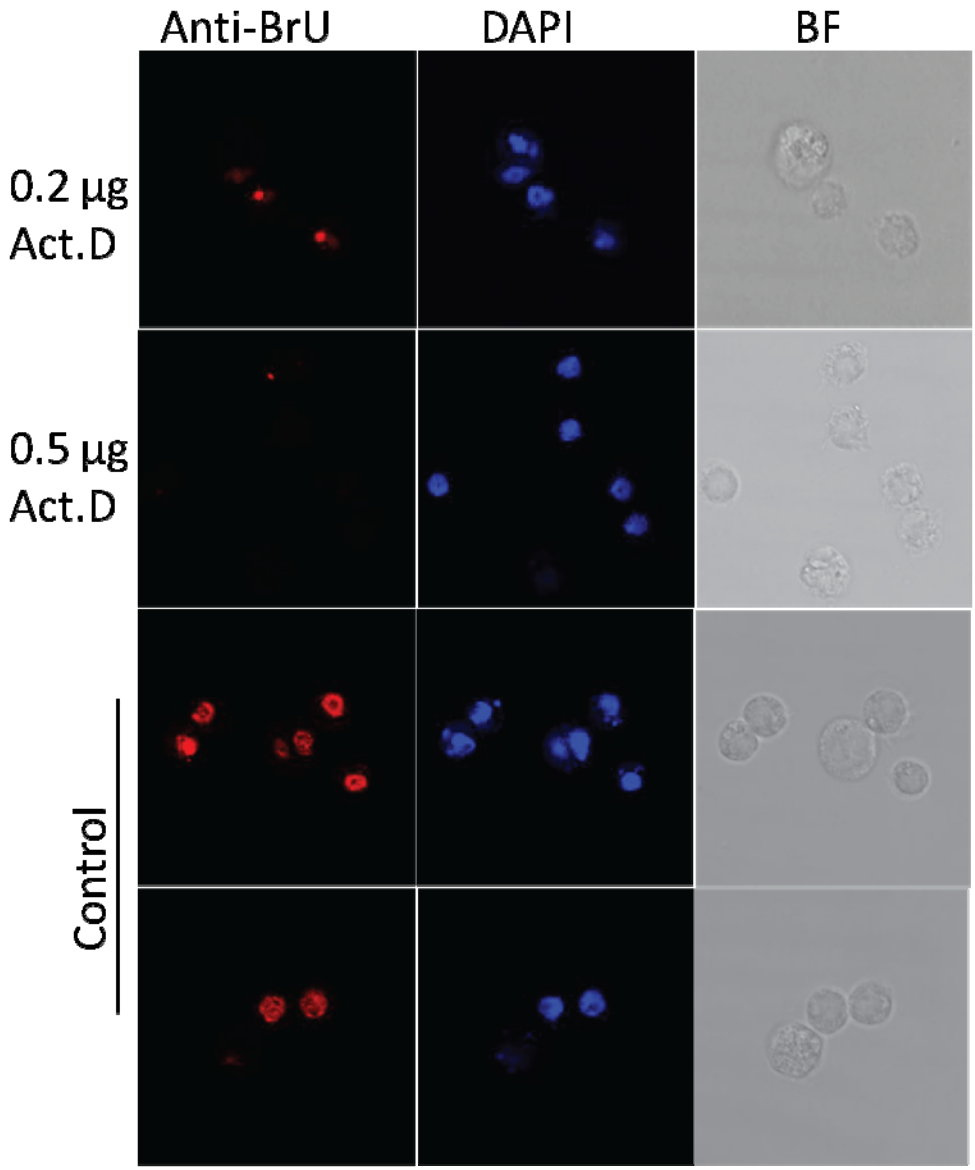

Figure 4.14. Transcription inhibition prevents incorporation of FlouroUridine (FU) into RNA. Left –right: Anti-BrU, middle panel; DAPI and right panel; Bright field. The first row indicates 0.2 µg/mL treatment, a concentration that blocks Pol I. Second row 0.5 µg/mL treatment, a concentration that blocks all the three polymerases indicating that the nucleolar signal requires Pol II transcription and bottom row, control. The cells were treated with the indicated concentrations of act.D for 4 hrs followed by 10 min FU labelling prior to fixation. The FU was detected by a Cy5 conjugated anti-BrU antibody.

4.2.4 Visualisation of ribosome subunit joining in transgenic flies

Having observed that Venus BiFC assay was successful in tracking ribosome subunit joining in S2 cells. I generated transgenic flies carrying the same constructs pUAST-RpS18-VN and pUAST-RpL11-VC. The BiFC transgenes were generated by P-element mediated germline insertion (See Materials and Methods). To visualise BiFC in transgenes, I crossed individual strains carrying the inserts p[W+=UAST.Rp18-VN] on 2^{nd} chromosome and p[W+=UAST.RpL11-VC] on 3^{rd} chromosome and generated a recombinant line expressing both inserts (details in Materials and Methods). The Presence of the two inserts in the established recombinant lines was verified by single fly PCR using primers specific for either VN or VC.

4.2.4.1 Visualisation of ribosomal subunit joining in salivary glands

Having generated homozygous flies carrying both BiFC inserts; next I examined whether co-expression of the two tagged ribosomal proteins can yield BiFC complementation as I observed in S2 cells. To achieve that, I crossed the BiFC transgenes with *forkhead*-gal4 driver flies. This driver is constitutively expressed in salivary glands (Henderson and Andrew, 2000). The salivary gland offers a suitable medium to visualise BiFC complementation due to its large size. The cross was initially kept at 25^0 C for 2 days and then moved to 18^0. This is because fluorophore maturation in BiFC is enhanced by lower temperature (Shyu et al., 2008). Third instar larvae (larvae that start crawling out of food) were collected and dissected to obtain the salivary glands.

The results of this study revealed BiFC signal both in the cytoplasm and nucleolus in fixed salivary glands. The signal was very intense and consistent in the nucleolus of majority of the cells in the tissue (Figure 4.15). The pattern of the signal is, therefore, similar to what

was previously observed with the YFP based transgenes (Al-Jubran et al., 2013) but with a higher fluorescence intensity. The signal was, at least visibly enhanced mainly in the cytoplasm by treatment with emetine for 30 min and 1 hr compared to the control (Figure 4.16). These observations were consistent with the results in S2 cells shown above and further indicated the presence of active 80S ribosome in the nucleolus.

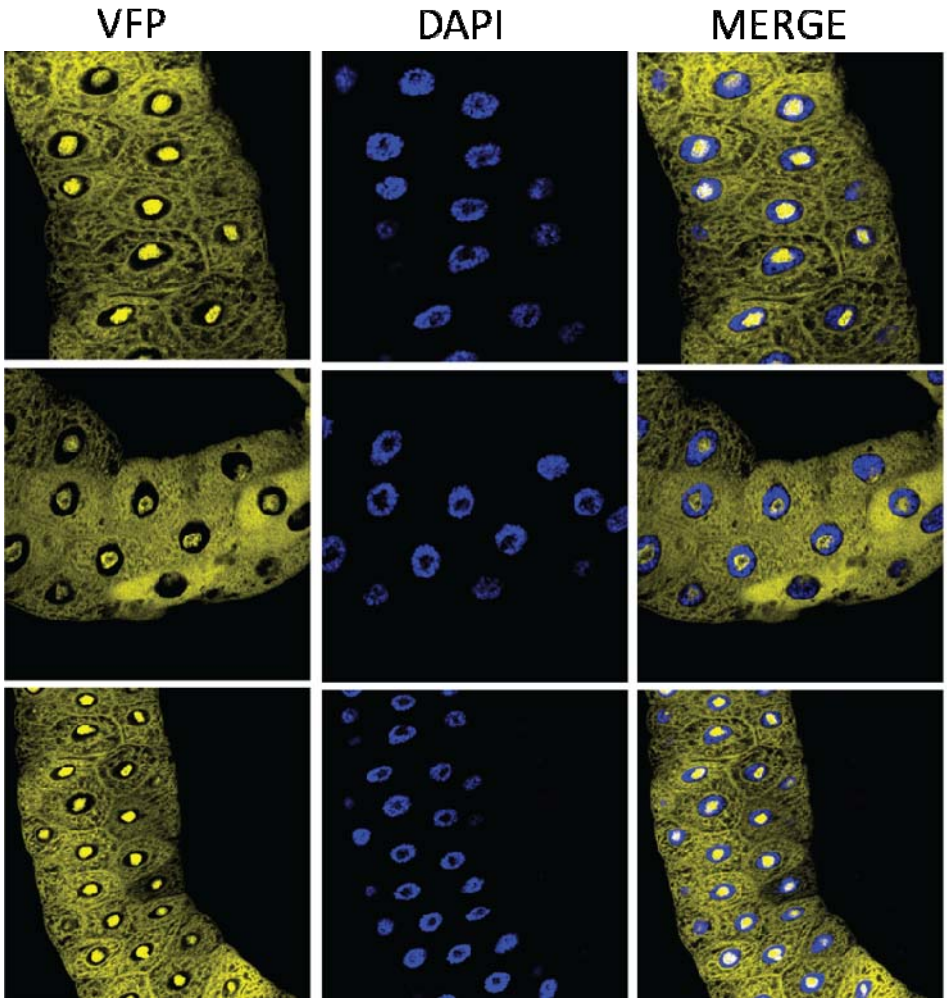

Figure 4.15. **BiFC tagging of S18 and L11 show ribosomal subunit joining in larval salivary gland**. Panels show BiFC signal detected in different sections of fixed and permeabilized third instar larval salivary glands. The BiFC expression was achieved by crossing the UAS transgenes with *forkhead*-gal4 driver that allows expression specifically in the salivary glands. Clear BiFC signal is observed in the cytoplasm and in the nucleolus. VFP signals are shown in the left column, DAPI in the middle and the merged image on the right. All images were taken with a confocal microscope.

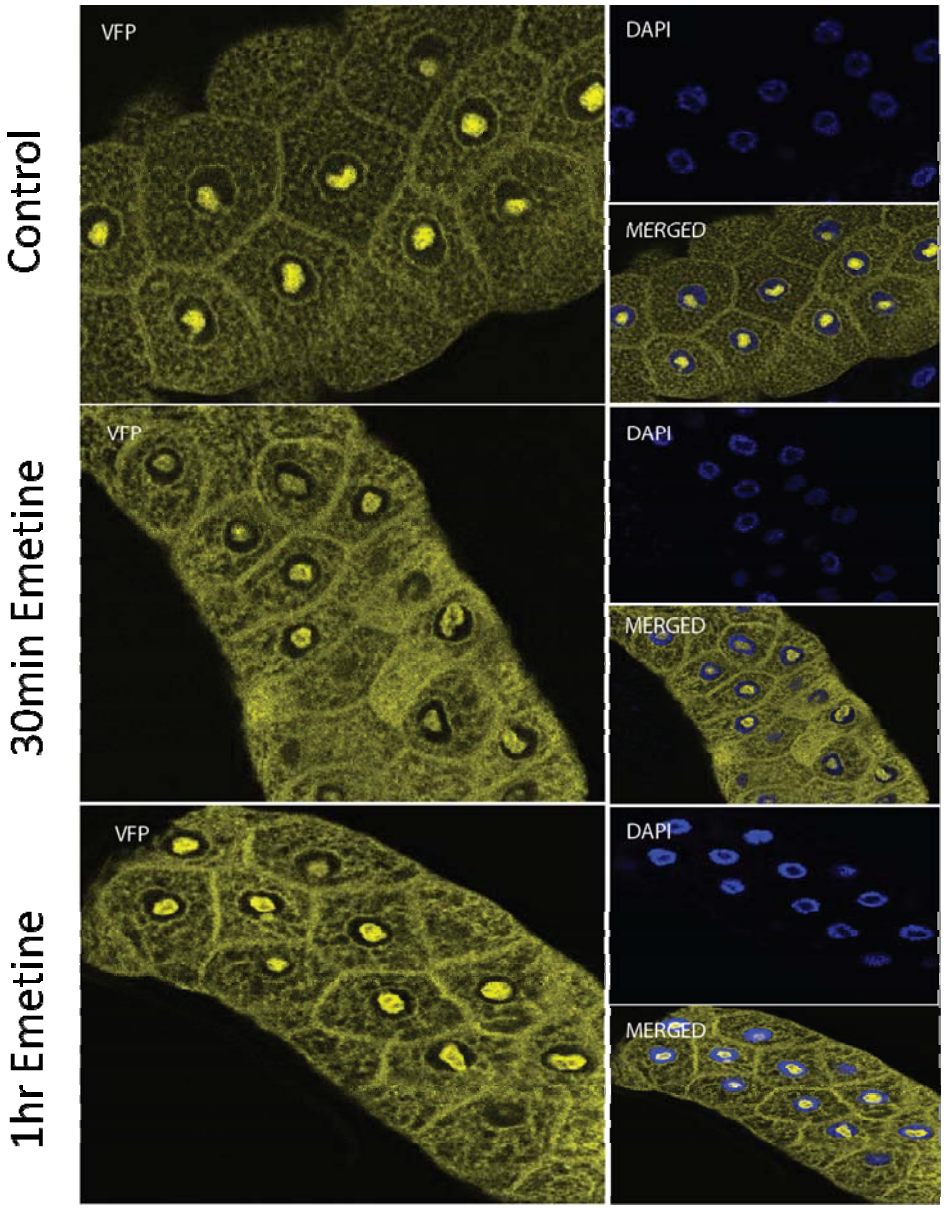

Figure 4.16. Emetine treatment increases fluorescence intensity in salivary glands. 50 µg/mL emetine treatments prior to fixation of the glands bring about visible increase in BiFC signal intensity mostly in the cytoplasm. Top row indicates no treatment (Control); middle row indicates 30 min treatment and bottom row show 1 hr treatment.

4.2.4.2 Visualisation of ribosome subunit joining in *Drosophila* midgut cells

The *Drosophila* adult midgut represented a useful system to study how ribosomal subunit joining changes during cell differentiation. This is because, it is characterized by rapid turnover of cells from continuous wear and tear, as a result of digestion (Ohlstein and Spradling, 2006). The midgut is maintained by intestinal stem cells (ISC), which divides rapidly to replenish the gut epithelium. The ISCs are localised at the basement membrane of the epithelia (Figure 4.17A). Each ISC continuously produces two daughter cells: one undergoes self-renewal as new ISC, and the other forms a transitional cell named enteroblast (EB) which rapidly differentiates to give rise to either enterocytes (EC) or enteroendoctrine (EE) (Figure 4.17B). The different cell types of the midgut provide an ideal system to investigate whether there are functionally important changes in the sub-cellular distribution of ribosomes between cell types. Little is known about this, but an emerging view is that there may be some variations in the ribosome composition or sub-cellular localisation that are important in regulating gene expression (Kondrashov et al., 2011). By employing the Venus-based 80S reporter, I have analysed the sub-cellular localisation of 80S ribosome in these cells using gal4 drivers that are specific to these cell types. In particular, I investigated whether 80S ribosomes are present in the nucleus of the *Drosophila* gut cells and assessed whether their sub-cellular distribution varies between ISCs and differentiated cells. When I expressed the 80S BiFC reporter with *escargot* (esg) gal4 which allows expression in ISC and EB cells of the midgut (Zeng et al., 2010), BiFC signal was observed almost exclusively in the cytoplasm of the adult midgut ISCs (Figure 4.18). Expressing the BIFC in differentiated cells with NP1-gal4, an enhancer trap in the gut-specific brush border

myosin IA gene (Morgan et al., 1994; Jiang et al., 2009), consistently showed a signal in both cytoplasm and nucleolus (Figure 4.19).

Additionally, I analysed the expression in larval adult midgut progenitor (AMP) cells with esg-gal4. Here also, the signal was largely cytoplasmic (Figure 4.20) similar to what I had observed earlier with the adult ISCs.

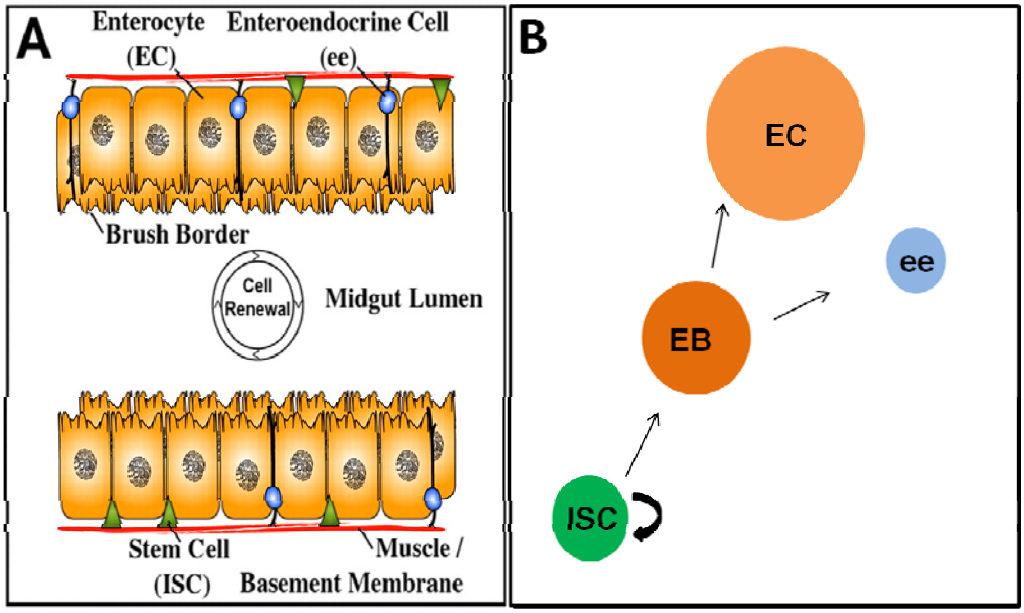

Figure 4.17. Adult *Drosophila* midgut cells are replenished by a population of multi-potent intestinal stem cells (ISCs). (**A**) Cross section of the adult midgut; ISCs indicated in green colour reside in the basal site in a niche close to the basement membrane and the visceral muscle (shown in red). (B) ISCs continuously gives rise to two cell types: one undergoes self-renewal as ISC and the other form enteroblast (EB); a transitional cell which immediately differentiates into 2 daughters, enteroendocrine (ee) cells (blue) and enterocytes (ECs; orange). Diagram adapted and modified from (Beebe et al., 2010).

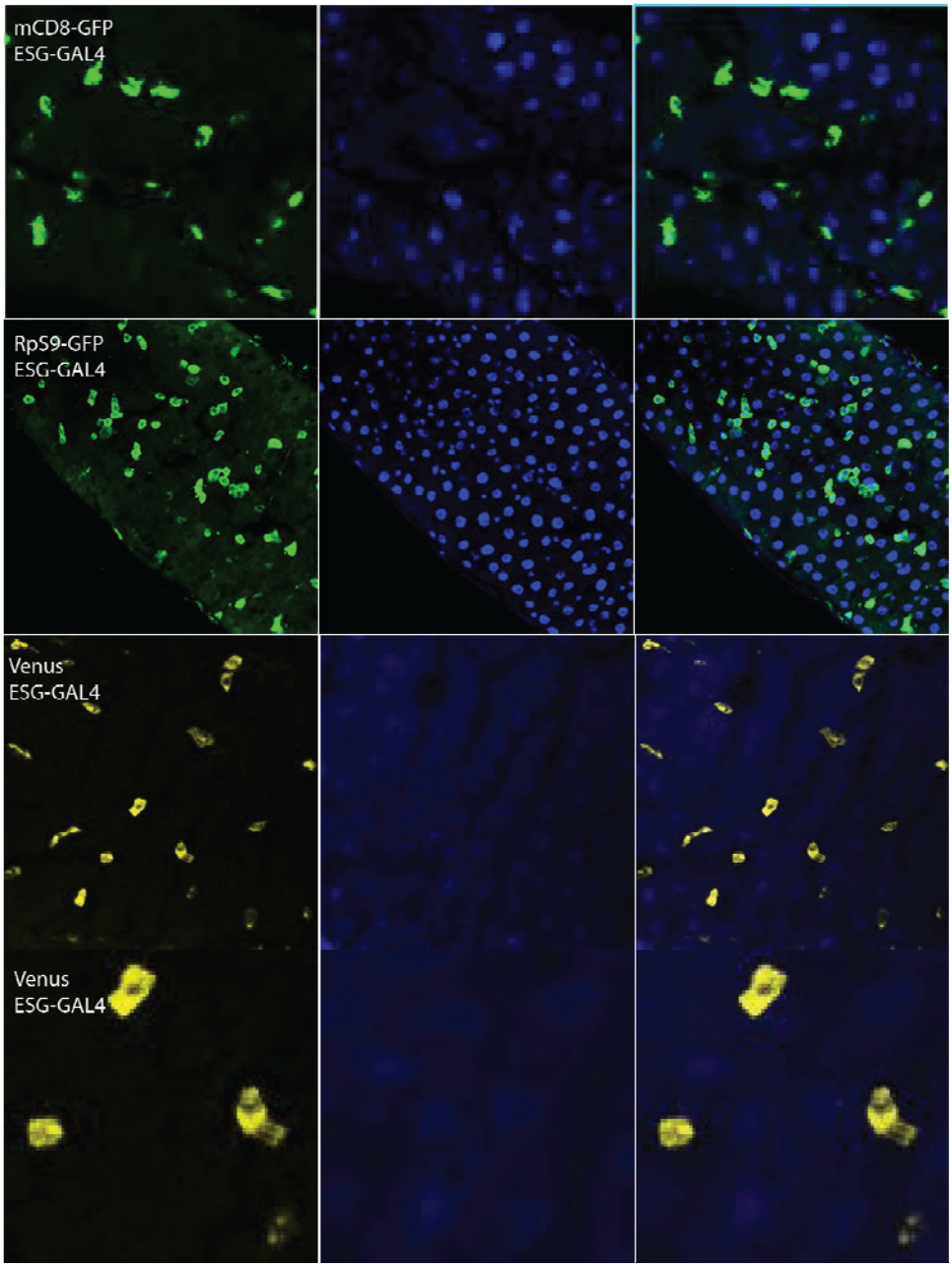

Figure 4.18. Visualisation of 80S ribosomes in adult midgut ISCs. Confocal images of midgut ISCs and EB cells. The BiFC expression was driven by esg-gal4 driver that is expressed specifically in the ISCs and EB cells. First row shows cd8-GFP/*esg*-gal4 as control, second row shows S9-GFP and bottom two rows shows Venus/*esg*-gal4. BiFC signal can be seen mainly in the cytoplasm of both the ISCs and EB cells. VFP signals are shown in the left column, DAPI in the middle and the merged image on the right.

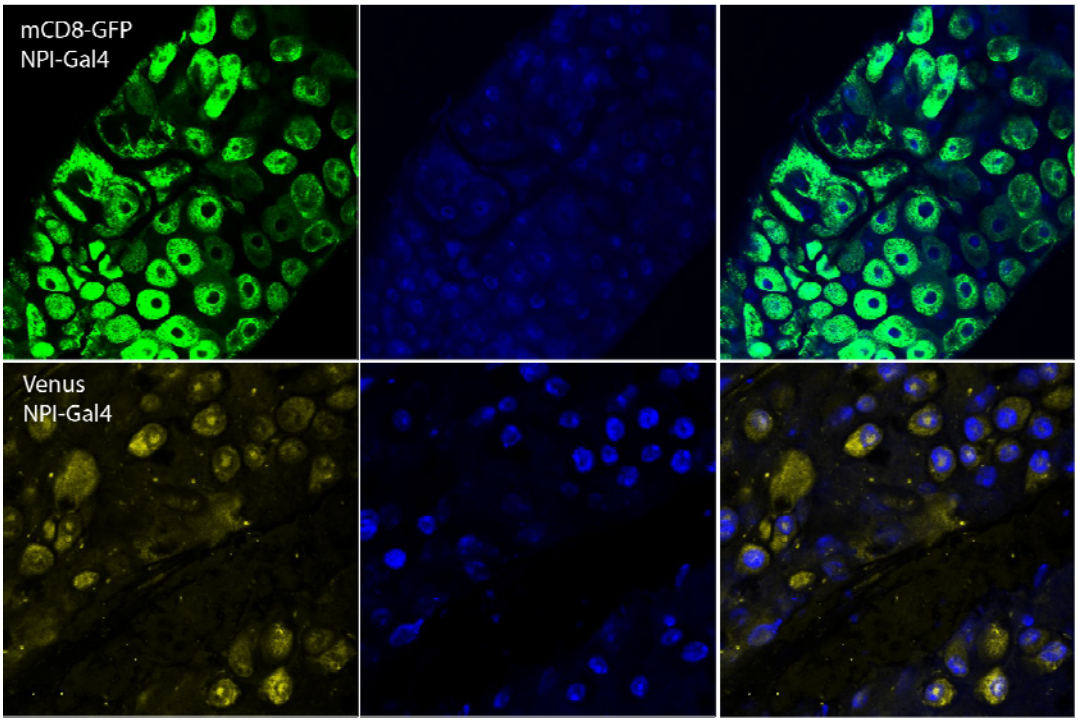

Figure 4.19. Visualisation of 80S ribosomes in differentiated adult midgut cells. BiFC expression was achieved by crossing the UAS transgenes with NP1-gal4 driver that is express specifically in the differentiated cells. Top row shows cd8-GFP/NP1-gal4 as control and bottom row shows Venus/NP1-gal4. Clear BiFC signal can be seen in both cytoplasm and nucleolus of the differentiated gut cells. VFP signals are shown in the left column, DAPI in the middle and the merged image on the right. All images were taken with a confocal microscope.

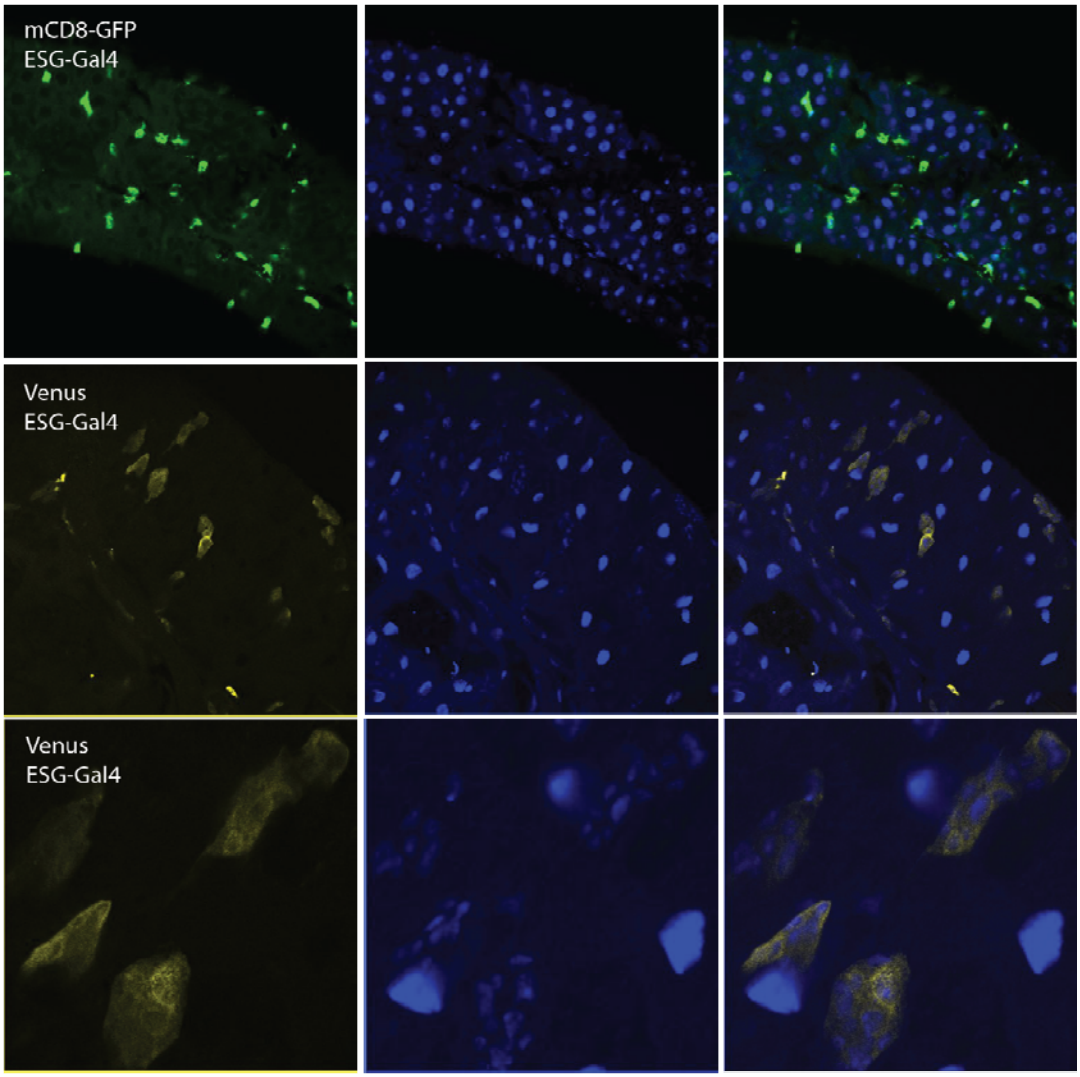

Figure 4.20. Visualisation of 80S ribosomes in midgut AMP cells of a third instar larvae. Confocal images of larval adult midgut progenitor cells**.** Visualisation of 80S was achieved by co-expressing Venus BiFC transgenic lines with the *esg*-gal4 driver, which is expressed specifically in the ISCs and EB cells. Top row shows cd8-GFP/*esg*-gal4 as control and bottom two rows shows Venus/*esg*-gal4. BiFC signal is mainly observed in the cytoplasm. VFP signals are shown in the left column, DAPI in the middle and the merge image in the right.

4.2.4.3 Visualisation of ribosome subunit joining in *Drosophila* photoreceptor neurons

To further determine how effective our BiFC assay is at reporting 80S ribosomes in different cell types, I applied this technique to visualise ribosomal subunit joining in highly polarised cells, such as neurons. The neuronal cells consist of a cell body, where the nucleus is located, dendrites and axons. The dendrites functions in receiving signals from other nerve cells, while axons transmit the signals. Protein synthesis in the dendrites has been established, but there is still a controversy whether there is local protein synthesis in the axons. However, there is growing body of evidence showing that protein synthesis can occur in the axons (Tennyson, 1970; Bunge, 1973; Perry and Fainzilber, 2014; Campbell and Holt, 2001). With Venus BiFC transgenic flies, I expressed the BiFC in photoreceptor neurons with GMR-gal4 which is expressed specifically in developing eye (Li et al., 2012). The results of this study indicate a clear BiFC signal along the axons and in the photoreceptor cells of the eye disc (Figure 4.21B).

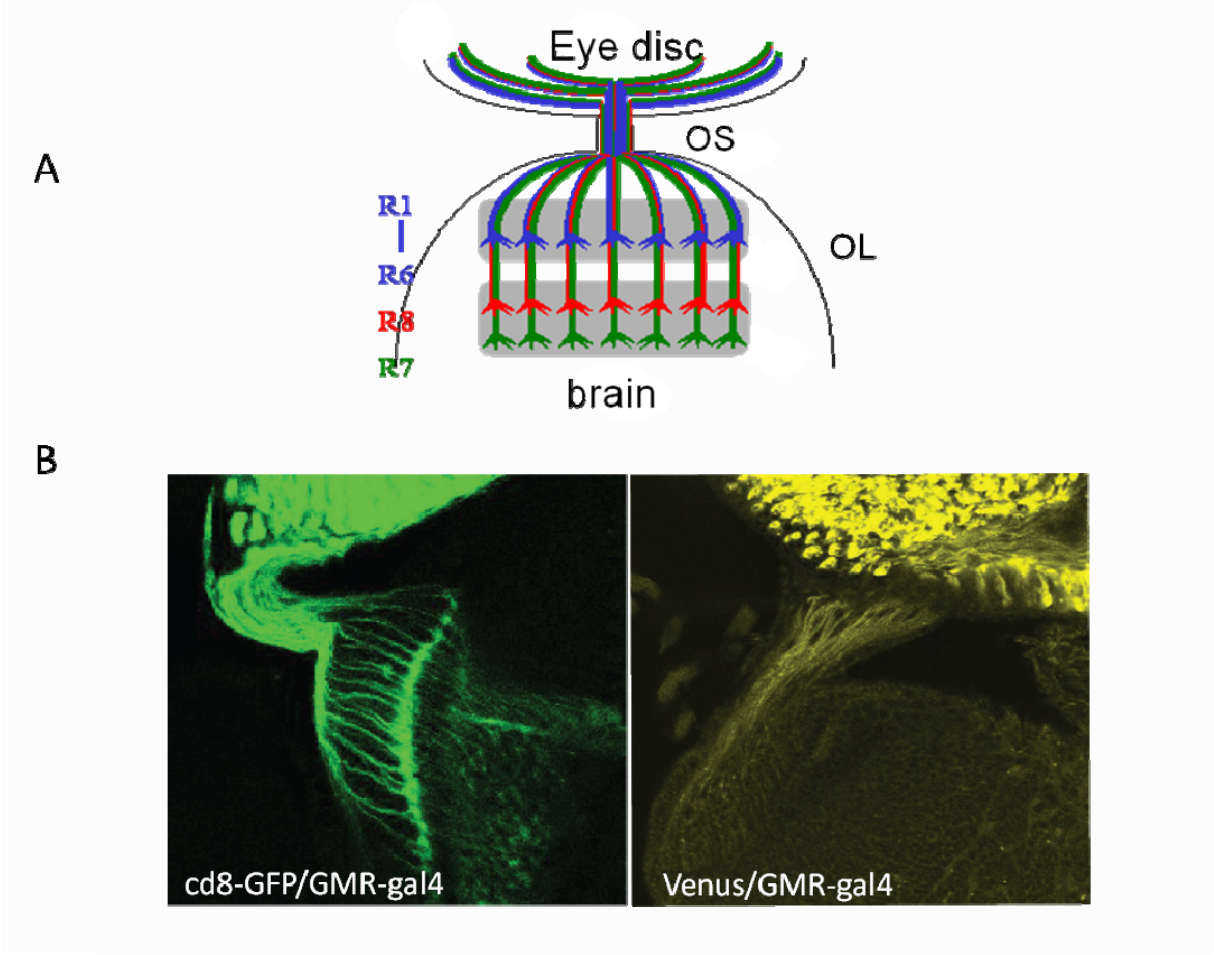

Figure 4.21. The Venus-based BiFC assay detected 80S ribosome along axons in photoreceptor cells. (A) Wild-type fly visual system, R-cell axons form a well organized projection pattern in the optic lobe. (Adopted with slight modifications from Rao Y (Y, 2005)). (B) Confocal images of fly visual system showing BiFC signal along axons. The BiFC expression was driven by GMR-gal4 driver that is expressed specifically in the developing eyes. Top row shows cd8-GFP/GMR-gal4 as control and bottom row shows Venus/GMR-gal4.

4.2.5 BiFC transgenes rescued lethal phenotype mutations of endogenous genes

To verify whether the BiFC tagged RPs are functional, I tested whether transgenes expressing the tagged RPs can rescue lethal phenotype mutations of the corresponding endogenous RP genes. To achieve this, homozygous lethal mutants flies for RpS18 and RpL11 both carrying mutation on the second chromosome were crossed with transgenic lines expressing RpS18-VN (A05) and RpL11-VC **(**A15**)** on third chromosomes respectively (see details in Materials and Methods). Complementation was apparent in F3 progeny, flies carrying RpS18C02853 on second chromosome were identified by the absence of dominant markers from the balancer chromosomes (Figure 2.5 and 2.6 in Materials and Methods and Appendix VIII for table of frequency). This serves as an evidence for the rescue of the homozygous mutation by the fused RPs on the third chromosome, under the constitutive induction of Actin-gal4 also on the third chromosome as driver.

Based on the score of the F3 progeny, the rescued flies of RpS18 was 22 out of 133. However, for RpL11, the score was 0 out of 72 flies. The percentage of the rescued flies in RpS18 mutants is 16.5% which was within the expected theoretical value of 14% (See appendix VIII). Another student Alex Sweet, who repeated this experiment found out that other RpL11-VC transgenic lines can rescue lethal mutation in the RpL11 mutants (but due to time constraint, I could not repeat the experiment). A similar previous complementation test showed that RpS18-YN and RpL11-YC can rescue the lethality of the mutations in the respective gene (Al-Jubran et al., 2013). Together, these genetic data along with observations that the BiFC tagged RPs are incorporated into polysomes in S2 cells indicates that the fusion proteins are, at least partially, functional components of the ribosome subunits.

4.3 Discussion

The results I have presented in this chapter show that the Venus-based 80S reporters are more sensitive than the previous YFP-based version (Al-jubran PhD thesis). With these reporters, I have observed more cells with both nucleolar and cytoplasmic signal (Type II). The fluorescence intensity and frequency of Type II cells was increased by emetine treatment, an indication that the signal is associated with translation as observed with the YFP reporters. The increase in the frequency of Type II cells was found to be statistically significant at 0.05 significance level. Notably, unlike the previous YFP-based version, BiFC signal was apparent also in polysomal fractions with the Venus reporters. Additionally, puromycin treatment led to an apparent shift of the BiFC signals and the BiFC tagged peptides towards lighter fractions, consistence with the BiFC signal reporting 80S translating ribosomes. It could be argued that a considerable fraction of the signal observed may come from non specific ribosome sub-units interaction that is not associated with translation. For example, there are many reports that indicated addition of puromycin or other inhibitors of translation initiation to cells results in running off of the polysomes and their accumulation as non translating 80S that can only be dissociated in a high salt concentration (Blobel and Sabatini, 1971; Ramirez M et al., 1991; Jackson, 2007). However, in this case, puromycin treatment resulted to a reduction in BiFC signal, further supporting our interpretation that the signal emanates from translating 80S. Although the Venus-based reporter gives a brighter fluorescence, it probably also raises the background at least in S2 cells, high fluorescence is often found in cells that appear to be damaged or dying cells as they seem to have shrunken nuclei and are positive to activated caspase. This was rarely detected with the YFP-based reporters (Chapter 3 and (Al-Jubran et al., 2013)).

By using the Venus-based reporter, I also found further evidence that the nucleolar signal required pol II transcription. In particular, act. D treatment at a concentration that blocks the three RNA polymerases abolished the nucleolar signal, but the signal persisted when cells were treated with the drug at a concentration that blocks only Pol I. A similar effect was observed in salivary glands upon incubation with act. D (Al-Jubran et al., 2013). The prevention of the BiFC signal mainly in the nucleolus by transcription inhibition may be explained by the presence of a small pool of mRNAs in the nucleolus which upon transcription inhibition, undergo a drastic reduction and hence the BiFC signal is lost within the 4 hrs incubation time. Less effect is seen in the cytoplasm because of the large pool of mRNAs in the compartment which does not show immediate effect upon transcription inhibition within the incubation time with the transcription inhibition agents.

Finally, I have reported that the Venus-based reporters allow 80S visualisation in different cell types. I have shown that it is very effective at detecting 80S in both ISCs and differentiated gut cells, and in neurons. Notably, I found that 80S ribosomes are also present along axons in larval photoreceptor.

CHAPTER 5

5.0 Nuclear 80S signal is found across all stages of the cell cycle and its level is increased by cellular stress

5.1 Synopsis

In view of the finding that 80S ribosomes were found in the nucleolus and other nuclear sites in *Drosophila* (Chapter 3 and 4), I set out to determine whether there is any link between the physiological state of the cell and the presence of ribosomes in the nucleus. First, I investigated whether the level of nuclear ribosomes changes during the cell cycle in S2 cells. Cells transfected with the described 80S reporter (Chapter 4) were synchronised with hydroxyurea (HU) and the sub-cellular pattern of the 80S signal was assessed by fluorescence microscopy at different time intervals for an entire cell cycle. HU arrests the cell cycle at S phase, so I monitored cell cycle progression at 2 hr intervals for 24 hrs, at which point the cells are expected to have reached S phase of a subsequent cycle. Results from this analysis revealed that nuclear 80S are found at all stages of the cell cycle. Although a more apparent increase was detected when the cells were initially blocked at S phase, the effect could perhaps be attributed to the stress induced by HU. Similarly, I investigated whether the level of nuclear 80S increases under cellular stresses such as serum starvation, puromycin, dithiothreitol (DTT), and thapsigargin treatments. The results obtained suggest that such cell stresses do increase the level of 80S ribosomes in the nucleolus.

5.2 Results

5.2.1 Determination of S2 cells doubling time

To monitor whether the level of 80S ribosomes changes during the cell cycle, I first calculated the doubling time of *Drosophila* S2 cells under the standard experimental conditions used in this laboratory (see Material and Methods). First, I monitored S2 cell growth rate by counting cell numbers at regular time intervals for 36 hrs (Figure 5.1). I found that the growth rate changes depending on cell density; the doubling time was about 20 hrs over the first 24 hrs period (Figure 5.1A), but 23 hrs if cell were grown continuously for 36 hrs (Figure 5.1B).

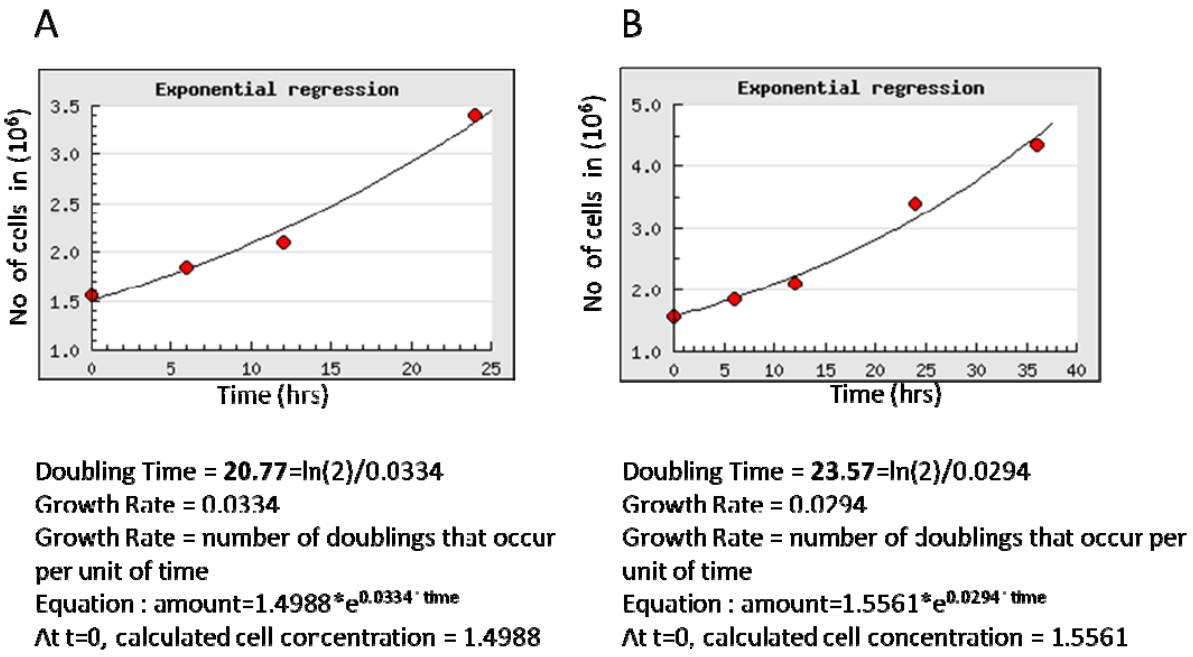

Figure 5.1. Doubling time of S2 cells. Exponential regression plot of S2 cells grown in complete media supplemented with 10% FBS and 1% antibiotics at 27^0C no CO_2 at different time points. Cells growth rate at time intervals of 0, 6, 12, 24 and 36 hrs was measured and the number of cells that were alive and viable was counted with the Countess Automated Cell Counter (Invitrogen). 3.5 x 10^6 and 4.4 x 10^6 cells were counted at 24 hrs and 36 hrs time points respectively. (A) Doubling time and growth rate over a 24 hr period. (B) Doubling time and growth rate over 36 hrs. Doubling time and growth rate indicated above were calculated from the exponential regression plot with Weisstein, Eric W. "Least Squares Fitting--Exponential" from *MathWorld*--A Wolfram Web Resource. http://mathworld.wolfram.com/LeastSquaresFittingExponential.html.

5.2.2 80S are present in the nucleus at all stages of cell cycle

S2 cells were synchronised by treatment with different concentrations of HU as previously reported (Lee et al., 2010). I firstly tested parental untransfected S2 cells using 1.5 mM, 2.0 mM or 2.5 mM HU treatment for 18 hrs (Figure 5.2) (details in Materials and Methods). Optimal synchronisation at the S phase stage was achieved using 2.0 mM HU treatment for 18 hrs. Following this observation, I synchronised S2 parental cells (unstransfected) with 2.0 mM HU for 18 hrs, so as to study cell cycle progression in these cells before studying the BiFC transfected cells. Following synchronisation, cells where washed to remove HU and aliquots of the culture were fixed and analysed by flow cytometry at 2 hr intervals up to 14 hrs time (Figure 5.3).

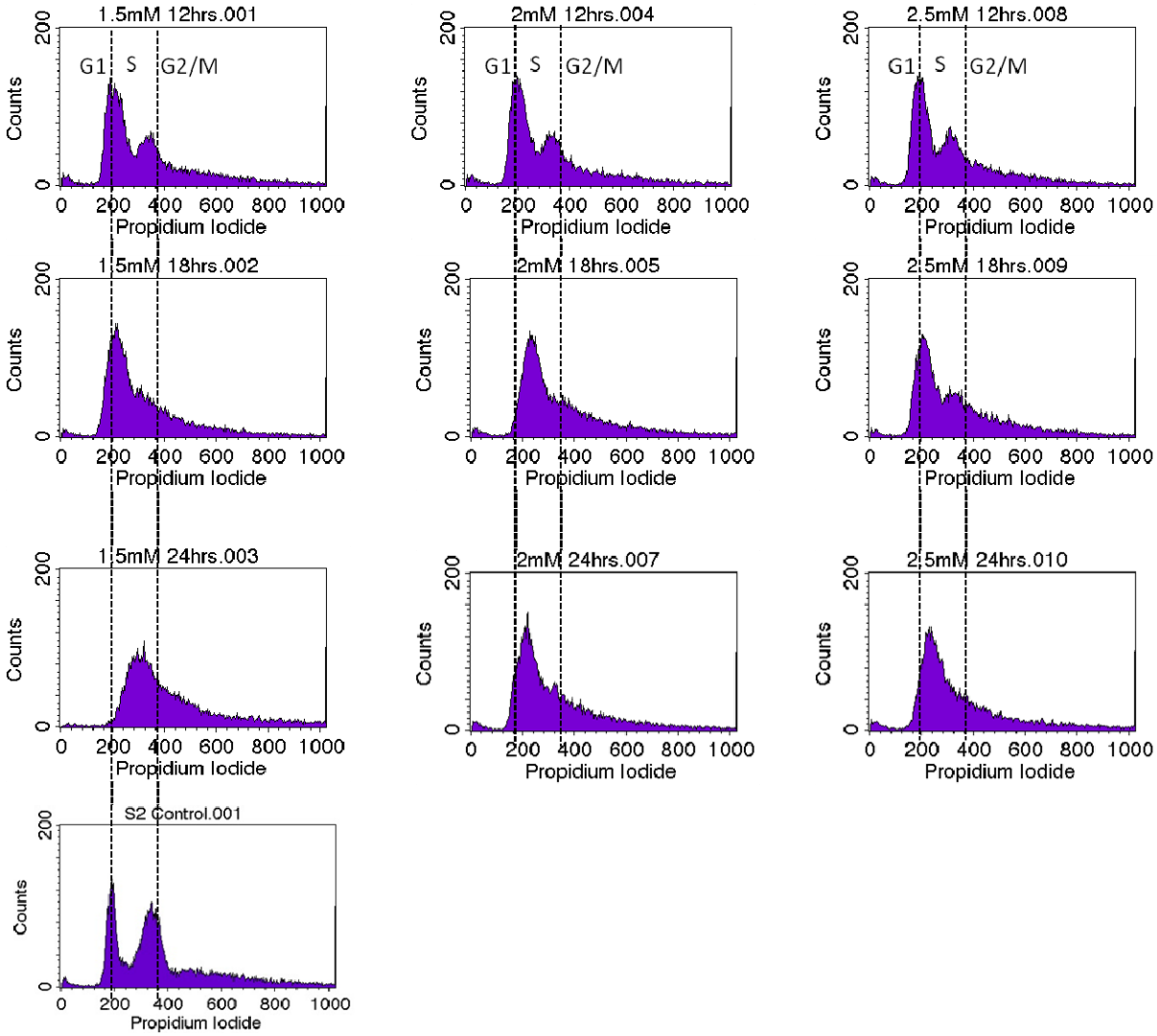

Figure 5.2. Optimisation of cell cycle synchronisation with HU. Exponentially growing S2 cells were treated with HU at the indicated concentrations and incubation times and the cell cycle was arrested at S phase. Peaks representing S phase are indicated in the panels which can be compared to the asynchronous cells (bottom row) were most of the cells are in G2/G1 phase. DNA content was measured by flow cytometry and the results of analysis were processed with CellQuestPro software (BD Biosciences).

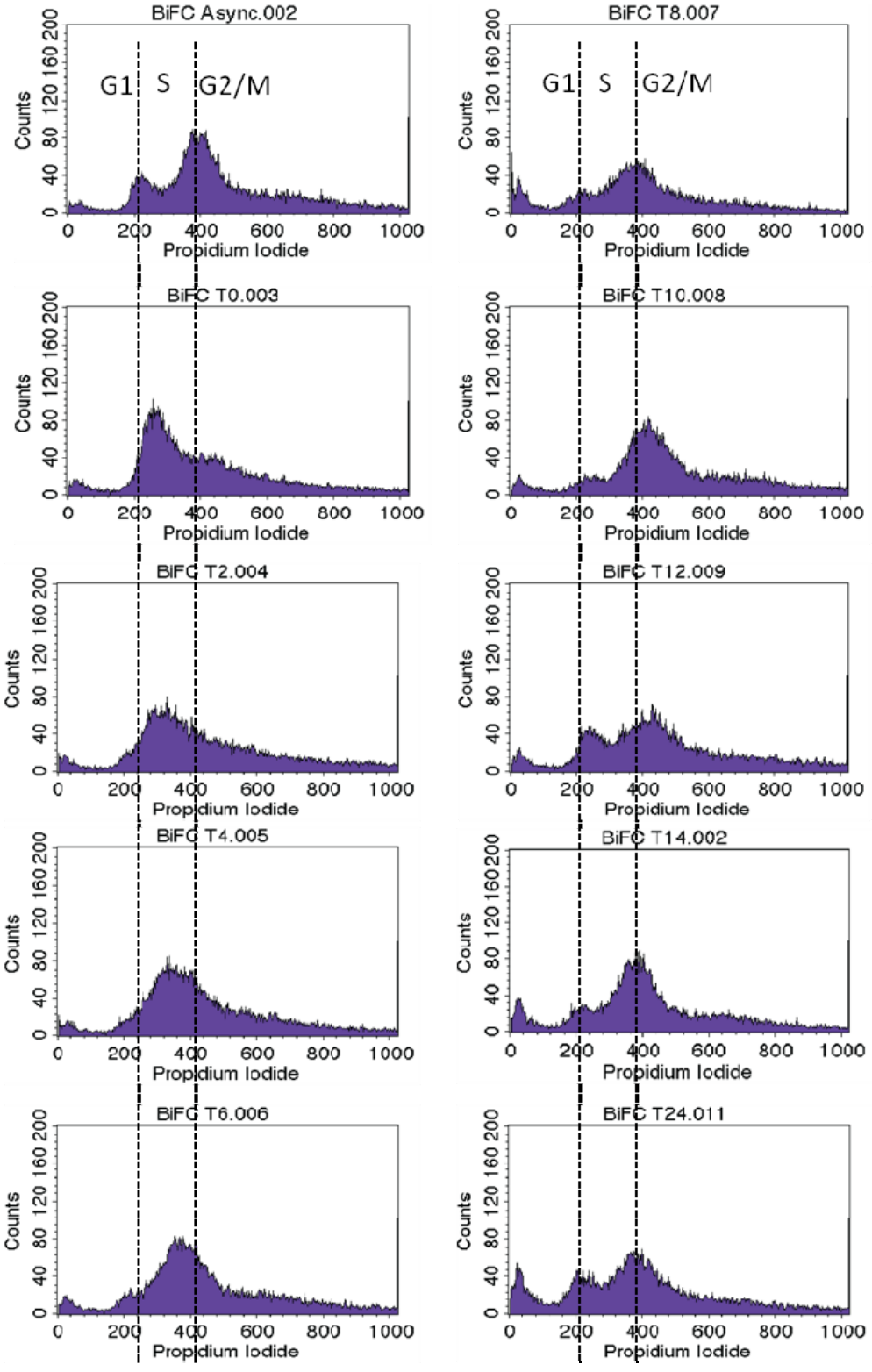
BiFC Async.002
G1
S
G2/M
Counts
Propidium Iodide
BiFC T8.007
BiFC T0.003
BiFC T10.008
BiFC T2.004
BiFC T12.009
BiFC T4.005
BiFC T14.002
BiFC T6.006
BiFC T24.011

Figure 5.3. Flow cytometric analysis of synchronised parental S2 cells with 2.0 mM HU for 18 hrs. Panels show the different stages of the cycle starting from initial time (T_0) followed by 2 hr interval analysis after HU release until T_{14} and at 24 hrs. Peaks as indicated, represents G1, S or G2 phase. From left, top panel shows asynchronous S2 cells, mostly at G2/G1 phase, followed by synchronised S2 cells at S phase. Cell cycle progression after HU release was monitored at 2 hrs interval as indicated in each panel. Results of the flow cytometric analysis were processed with CellQuestPro software (BD Biosciences).

Cells transfected with the Venus 80S BiFC reporters S18/L11, described in Chapter 4, were then synchronised as above and the sub-cellular pattern of the signal was visualised by fluorescence microscopy of individual cells at 2 hr time intervals after HU treatment for 24 hrs; this time duration is enough for the cells to complete one cell division and enter another S phase. A clear increase in the frequency of cells showing apparent nuclear/nucleolar signal (Type II) upon HU treatment was observed. Following HU treatment, the largest fractions of cells were in S phase ($T_{0,}$ Figure 5.4 and 5.5). Representative images of S2 cells for each time point showing patterns of BiFC signal localisation are presented in (Figure 5.6). The percentage of Type II cells progressively decreased following HU washout but recovered to a level close to the start point (T_0) after about 14 hrs. An attempt to further examine the cell cycle beyond 14 hrs was not possible because the cells appeared to have lost their synchronicity.

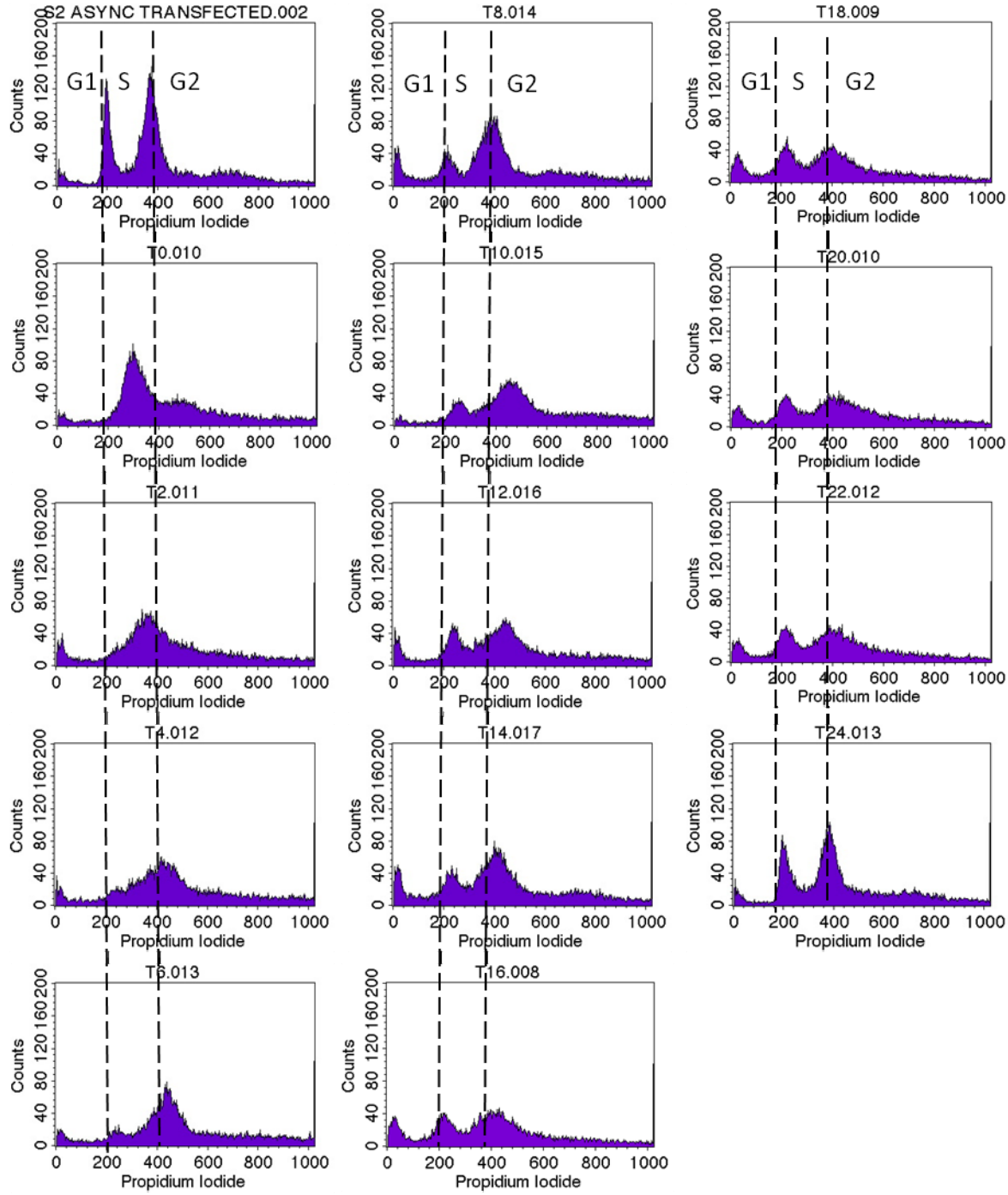

Figure 5.4. Flow cytometric analysis of synchronised BiFC transfected S2 cells with 2.0 mM HU for 18 hrs. First column, top left shows asynchronous BiFC transfected S2 cells followed by S phase synchronised BiFC transfected S2 cells at initial time T_0. Following HU release, cell were analysed at time points showing cell cycle progression through different stages of the cycle starting from T_2 (2 hrs after HU washout) followed by 2 hr interval analysis until 24 hrs as indicated in each panel. Peaks represent G1, G2 or S phase.

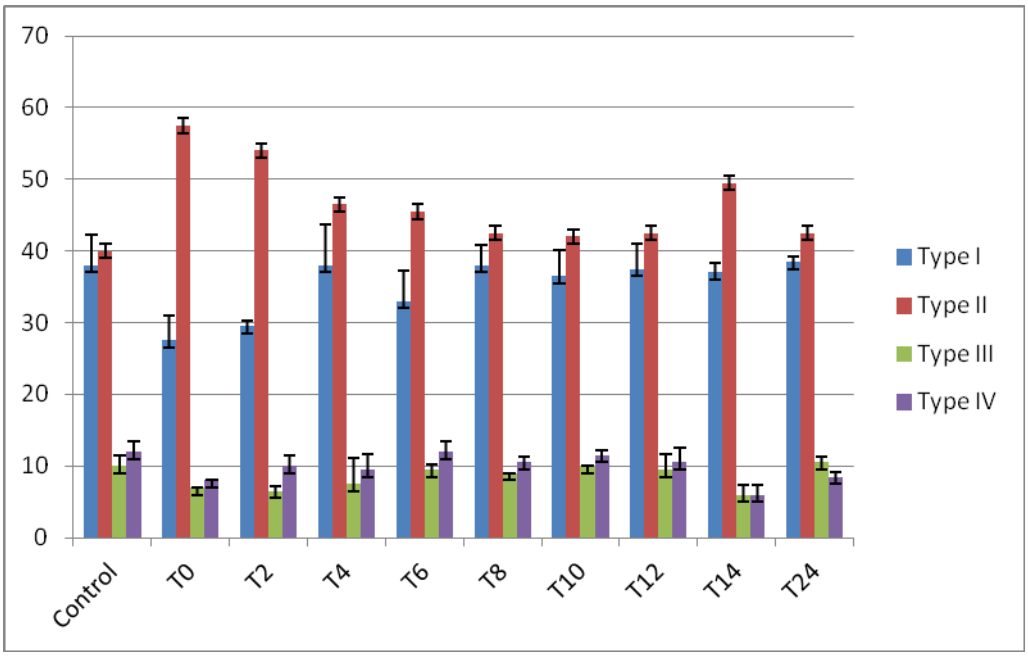

Figure 5.5: Quantification of BiFC cell type pattern in the different stages of the cell cycle upon synchronization with 2.0 mM HU for 18 hrs. Bars show mean frequency of BiFC cell types starting from T_0 followed by 2 hr interval analysis after HU release until 24 hrs. One hundred cells were counted in 2 separate experiments. Error bars represent the variation of 2 sets of experiments.

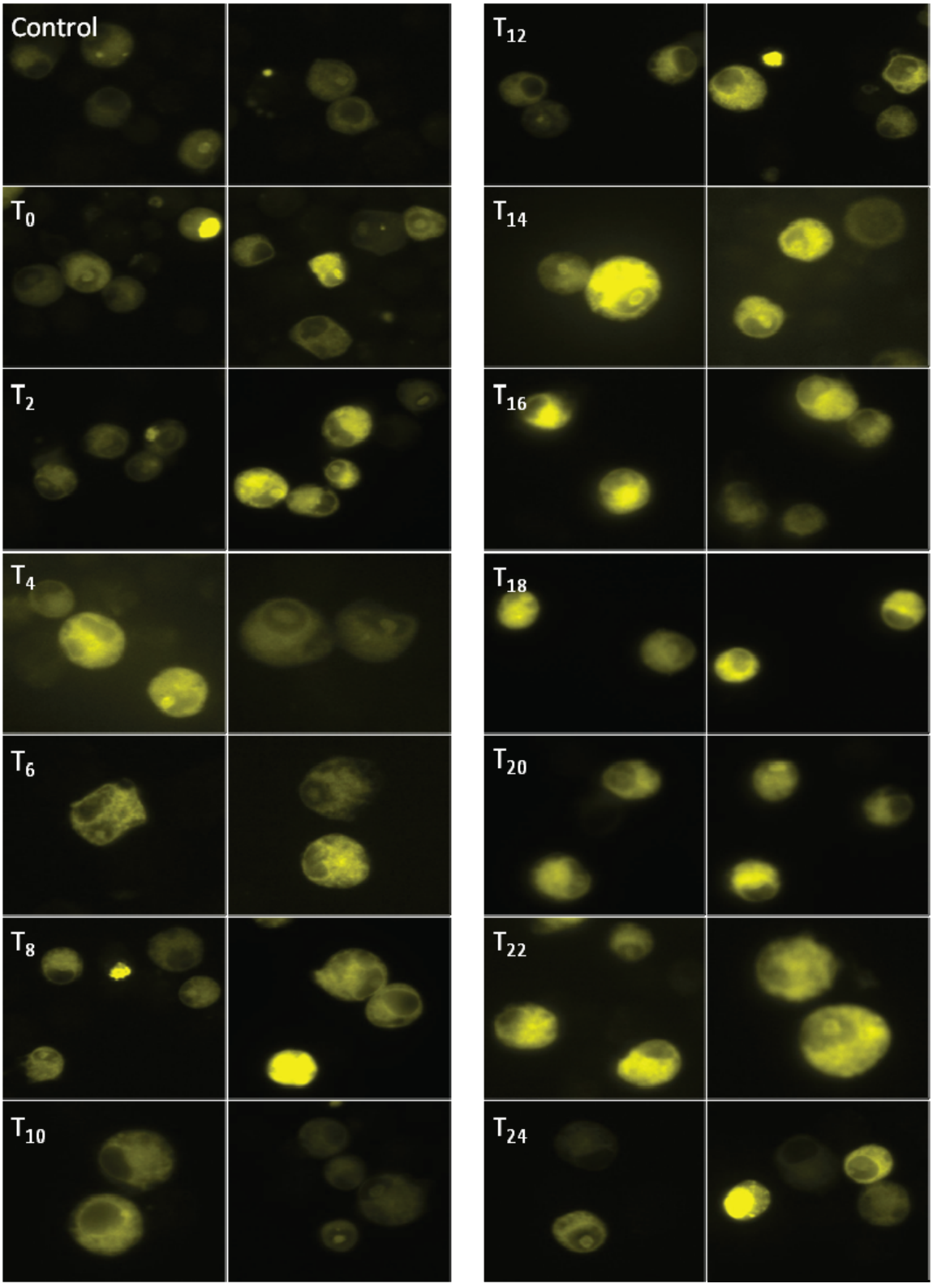
Control
T0
T2
T4
T6
T8
T10
T12
T14
T16
T18
T20
T22
T24

Figure 5.6 Visualisation of 80S S2 cells at the different stages of the cell cycle. Representative images of S2 cells transfected with Venus-based S18/L11 80S reporters. Images show sub-cellular pattern of signal localisation at each time point as analysed by fluorescence microscopy. Type II BiFC signal pattern was found in all the time points indicating that the nucleolar 80S signal is present at all the stages of the cell cycle. Panels as indicated show images at the start of the experiment, (control), after HU treatment (T_0) and at 2 hr time intervals until the end of 24 hrs.

5.2.3 Cellular stress enhances nuclear 80S

To investigate whether some pre-defined cellular stresses might increase 80S levels in the nucleus, I exposed S2 cells transfected with the YFP based 80S BiFC reporter to four different forms of stress; this included serum starvation, translation inhibition with puromycin, dithiothreitol (DTT) and thapsigargin treatments. Following incubation of BiFC transfected cells with these stress agents for different time lengths, I monitored the sub-cellular localisation of the BiFC signal and intensity over time. I chose to perform this analysis with the YFP based BiFC 80S reporter system as it produces less background when compared to the more sensitive Venus-based reporter used above. Additionally, the YFP-based reporter produces only two types of signal localisation pattern, Type I which shows only a cytoplasmic signal or Type II which gives a signal in both the cytoplasm and the nucleolus as reported in Chapter 3. This will minimise potential artefacts that may be associated with the stress conditions. The aim of this experiment was to investigate whether the nuclear/ nucleolar 80S is enhanced by certain stress conditions.

5.2.3.1 Serum starvation results in increased nuclear 80S activity

I was interested in testing whether the sub-cellular distribution of ribosomes changes upon serum starvation. S2 cells transfected with S18YN/L11YC BiFC reporter were serum starved for 6, 8 or 24 hrs. Microscopic inspection/imaging and quantification of these transfected cells revealed that the frequency of Type II cells increases from 13.5% in the control to 25%, 37.5% and 52% after 6, 8 and 24 hrs of starvation (Figure 5.7 and 5.8, and Chapter 3). Comparing the level of significance of the changes at 0.05 confidence level from the mean values obtained, the P-value at 6, 8 and 24 hrs was found to be statistically significant

(0.013183, 0.000395 and 1.39846E-05 respectively) and the effect of the serum starvation could not have been due to chance.

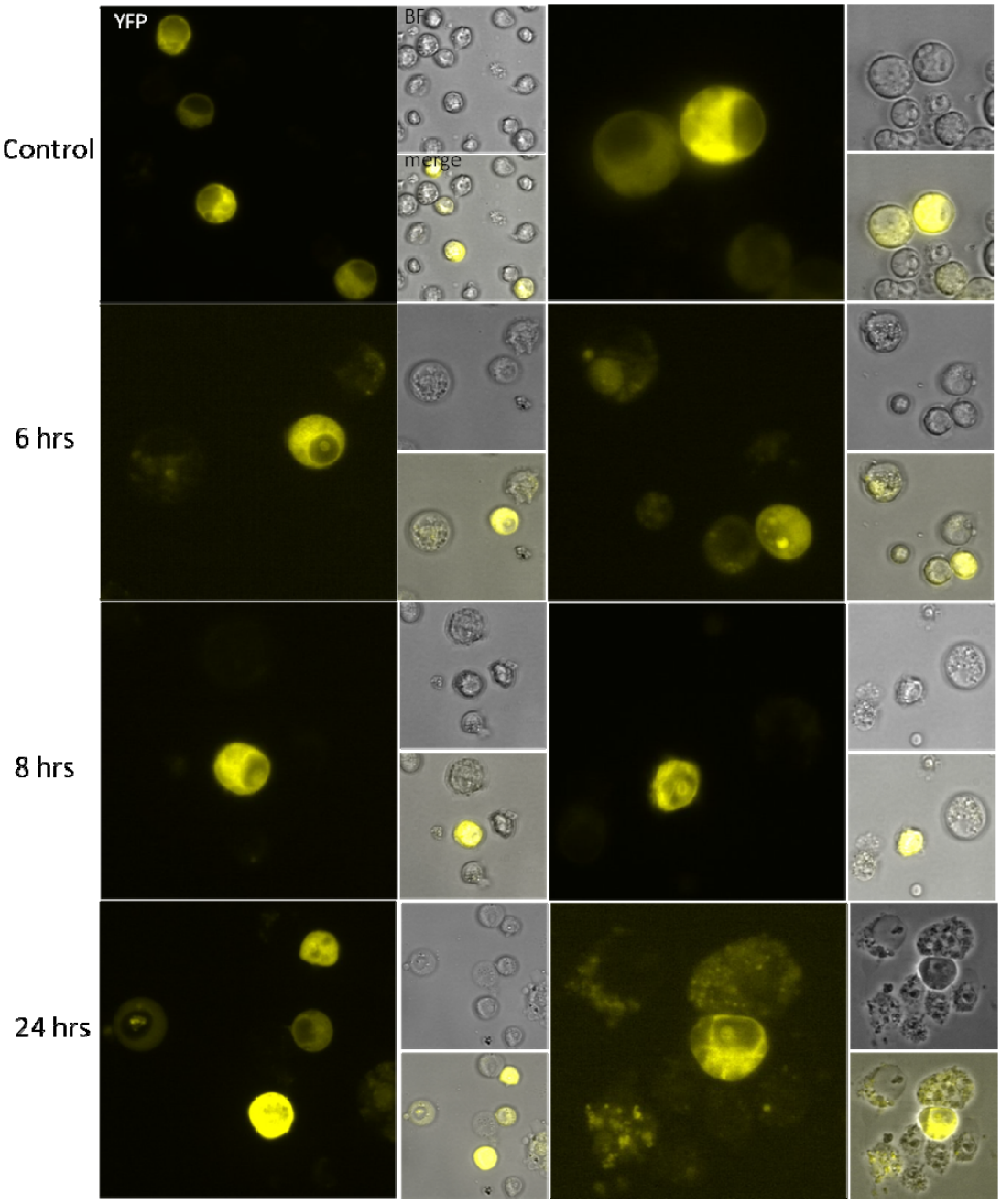

Figure 5.7. Serum starvation increases the frequency of S2 cells showing nuclear 80S. Images show live cells that have been subjected to serum starvation for the indicated time intervals in BiFC transfected S2 cells. More nucleolar BiFC signal is observed with increased starvation time. Images were taken with an epifluorescence microscope (Nikon Eclipse Ti).

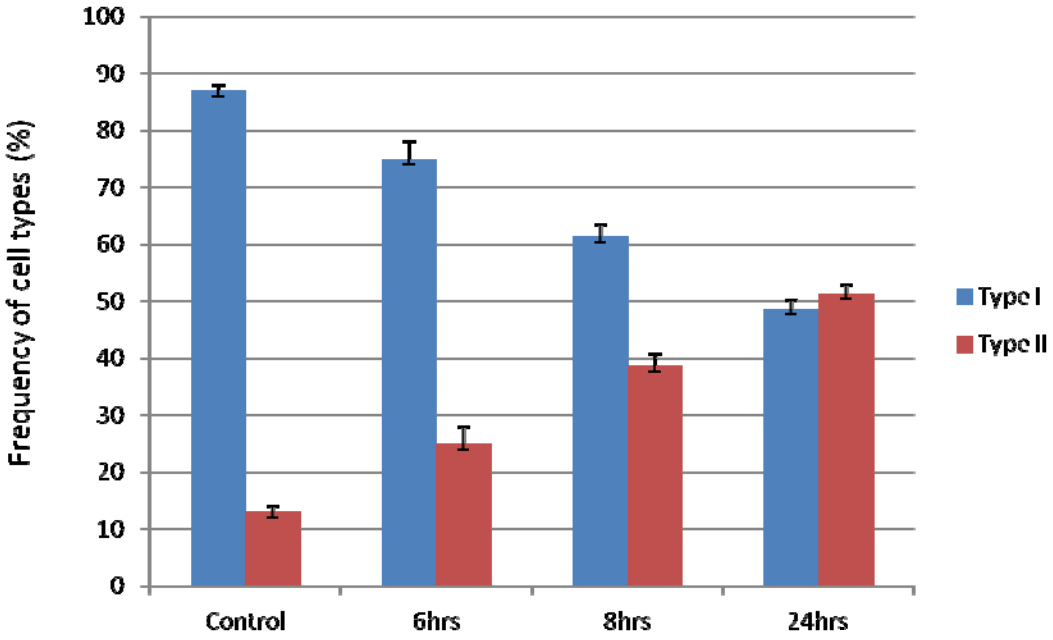

Figure 5.8. Effect of serum starvation on BiFC signal pattern in Type I and II cells. Bar chart indicates progressive increase in the frequency of Type II cells upon 6 hrs, 8 hrs and 24 hrs serum starvation prior to microscopic examination of live cells. Values are mean of three independent experiments where one hundred cells were counted for each separate transfection. Error bars show standard deviation from the mean value.

5.2.3.2 Puromycin stress increase the frequency of cells showing nuclear 80S

Puromycin is a translation inhibitor that structurally resembles a charged tRNA. It blocks translation by entering the ribosome's A site and gets covalently incorporated into the C-terminus of the growing nascent chain, leading to its release and subsequently disassembly of the 80S (Pestka, 1971; Nathans and Lipmann, 1961). Here, I used puromycin primarily to induce stress by blocking global translation; I then monitored changes in the sub-cellular localisation of 80S ribosomes compared to control cells. Transfected cells were treated with 100 µg/mL puromycin for different time intervals. The results of this experiment showed that puromycin treatment brings about a visual decrease in BiFC signal intensity when compared to the control (Figure 5.9). The decrease became more apparent when the fluorescence intensity of the treated cells and the control was quantified (Figure 5.10). This effect is similar to our observations *in vitro,* where puromycin treatment produced a significant decrease in the global 80S signal, possibly as a consequence of the disassociation of ribosomal subunits (Al-Jubran et al., 2013). However, puromycin treatment appeared to increase the proportion of Type II cells (Figure 5.11), indicative of a possible increase in nuclear 80S resulting from some undefined stress induced by puromycin, a reduced effect of puromycin on nuclear ribosomes or a reduced clearance of BiFC-joined subunits within the nucleus (discussed below).

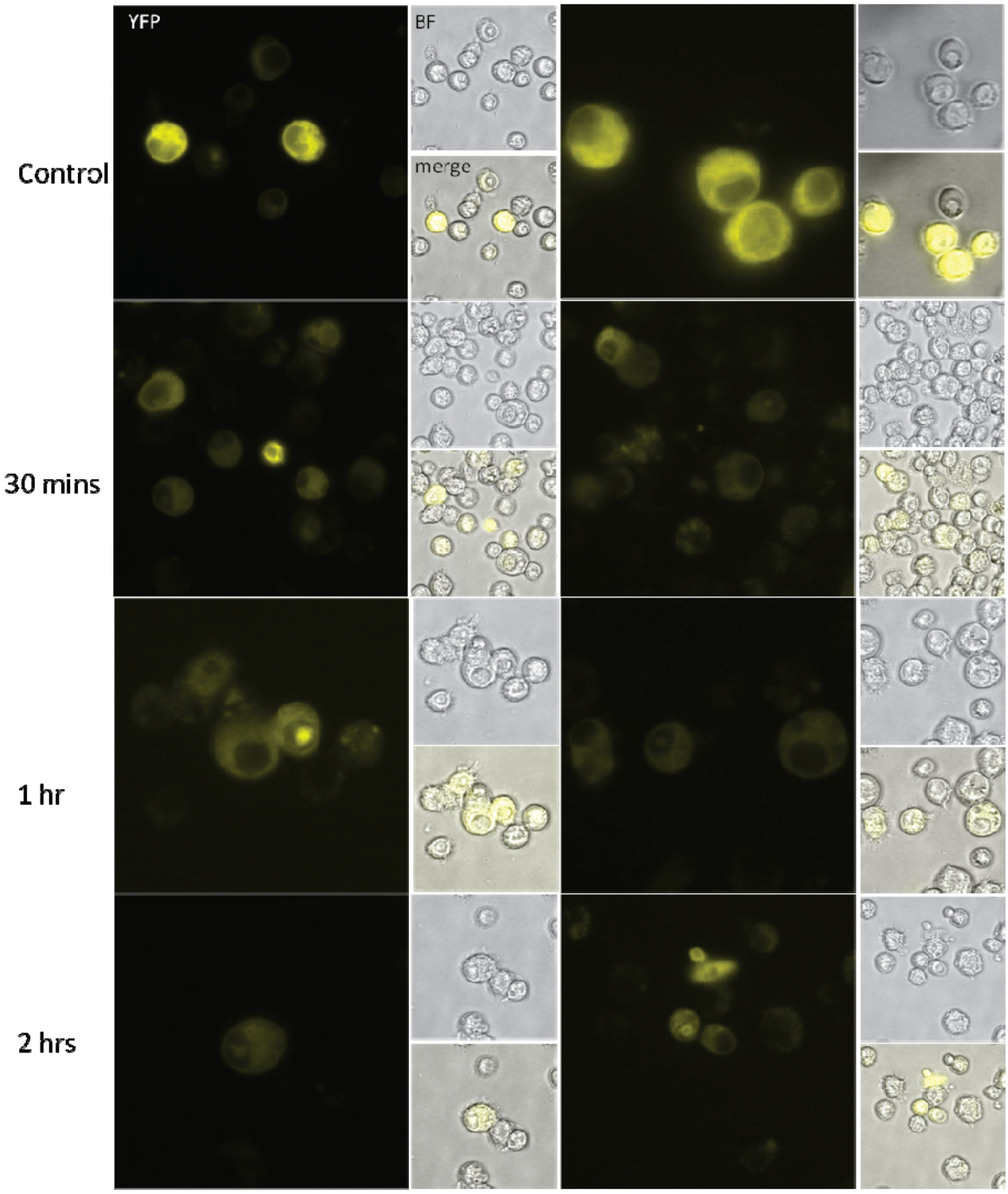

Figure 5.9. Puromycin treatment results to a global decrease in BiFC 80S signal. Images of live S2 cells transfected with 80S YFP BiFC-based reporters and incubated with or without puromycin (100 µg/mL) for the indicated time intervals prior to microscopic viewing. A visible decrease in the fluorescence intensity can be observed in experimental treatments compared to the control.

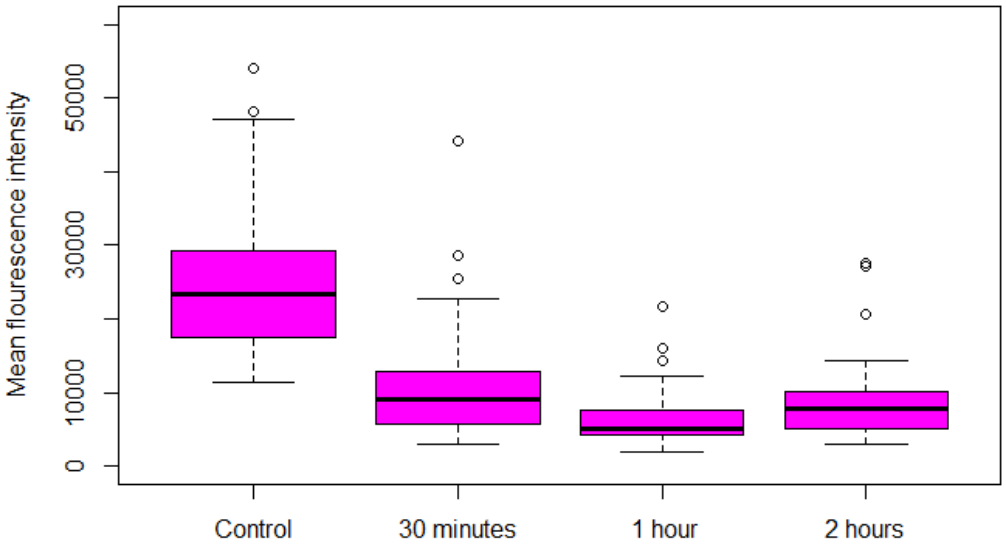

Figure 5.10. Puromycin treatment decreases the global BiFC 80S signal intensity in S2 cells. Boxplots showing whole cell mean fluorescence intensities of 100 transfected S2 cells treated with 100 µg/mL puromycin for the indicated times. Cells were manually defined as regions of interest (ROI) and mean fluorescence values were obtained using the Automated Measurement function of the NIS-BR Software (Nikon). Values were normalized by subtracting the intensities in identical ROIs defined in adjacent regions without cells.

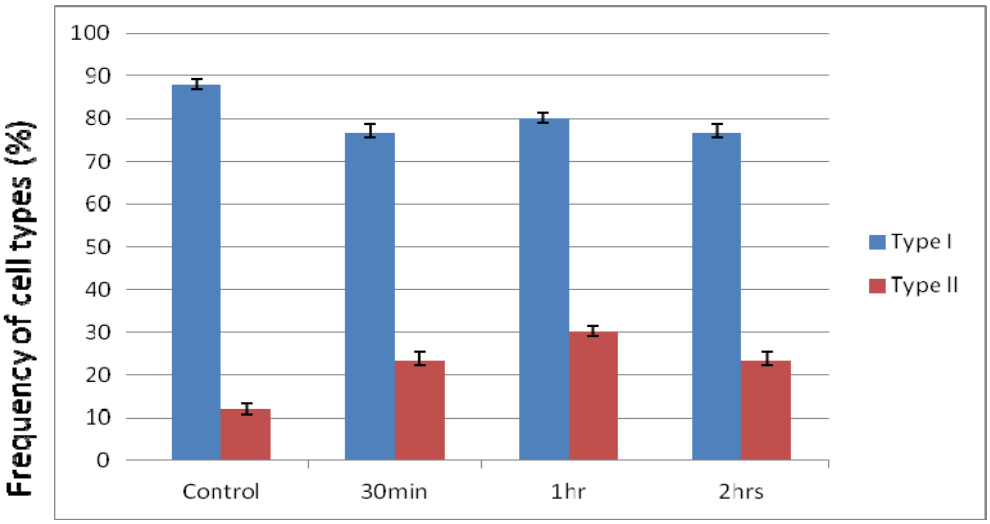

Figure 5.11. Puromycin might increase the fraction of cells showing nucleolar 80S signal. Bar chart shows frequency of cells with predominantly cytoplasmic signal (Type I) and those with an apparent nucleolar signal (Type II) in control and cells treated with 100 µg/mL puromycin for different time intervals (30 min, 1 hr and 2 hrs)**.** One hundred cells were counted in two independent experiments. Bar values indicate the mean frequencies of the cell types and error bars show variation between the 2 experiments.

5.2.3.3 Dithiothreitol (DTT) and thapsigargin treatments increase the level of nuclear and nucleolar 80S

DTT and thapsigargin are known to elicit cellular stress in different cell types and organisms (Liang et al., 2006). Particularly, it has been reported that both drugs elicit ER stress through the disruption of calcium homeostasis, leading to an unfolded protein response (UPR) in *Drosophila* (Kondylis et al., 2011; Yeromin et al., 2004) and mammalian cells (Liang et al., 2006; Urano et al., 2000). To examine whether these stress-inducing agents change the pattern of the 80S signal, BiFC transfected S2 cells were incubated with these chemicals for different lengths of time (30 min, 1 hr, 2 hrs and 4 hrs). Treatment with 10 mM DTT resulted in an increase in the level of nuclear 80S (Type II); the increase was most apparent after 2 hrs showing 42% Type II cells compared to 12% in the control (Figure 5.12 and 5.13). Thapsigargin treatment had less pronounced effect. The most apparent change was observed after 30 minutes treatment which increased Type II cells to 23% (Figure 5.14 and 5.15). The effect was lost upon longer incubation times, and after 4 hrs the proportion of Type II cells (13%) was similar to the control (Figure 5.14 and 5.15).

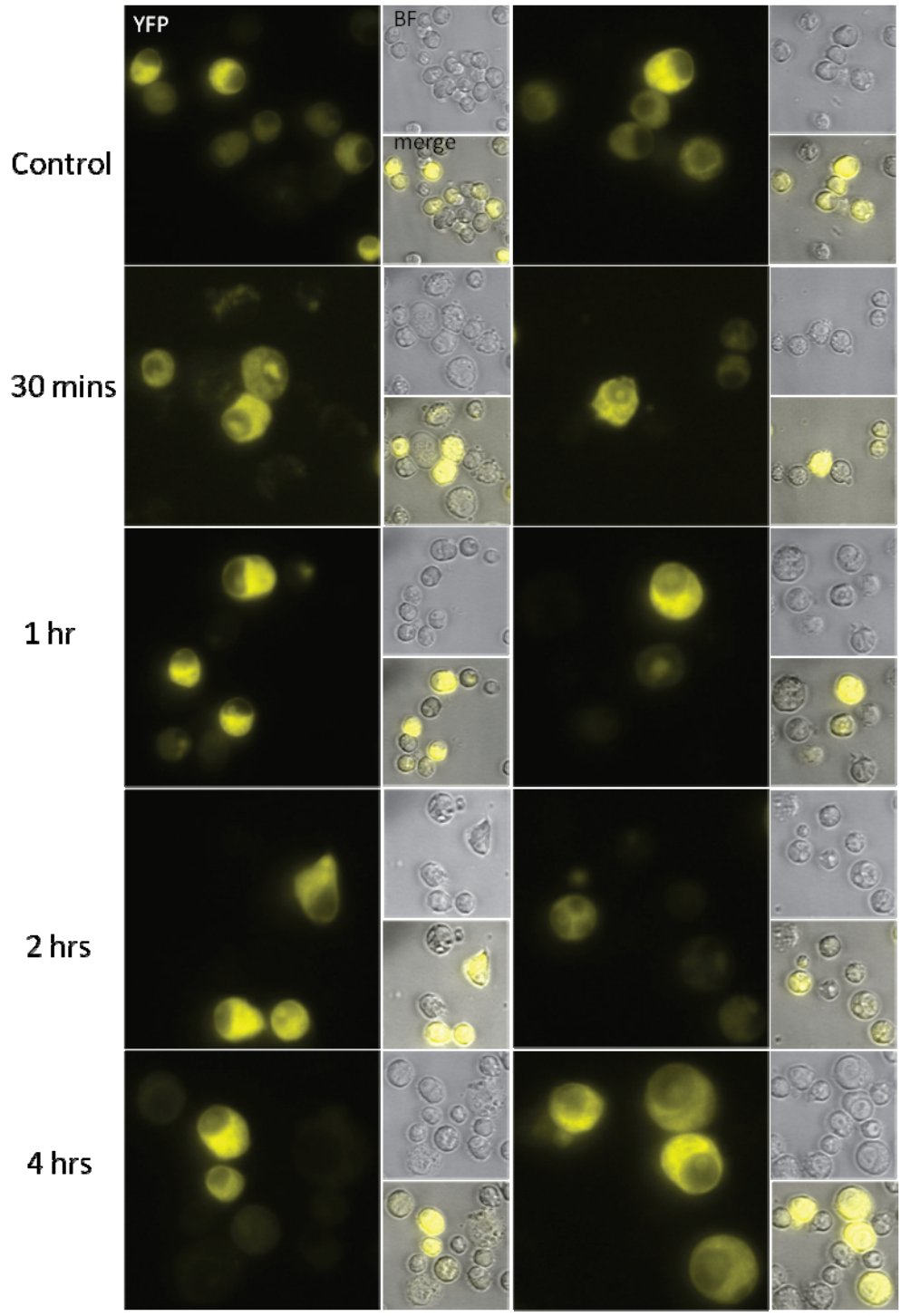

Figure 5.12. Visualisation of 80S BiFC in S2 cells treated with Dithiothreitol (DTT) revealed an increase in Type II cells. Images show the effect of 10 mM DTT stress for the indicated time intervals in BiFC transfected live S2 cells. Increased nucleolar signal is observed with increased incubation times. Images were taken with Nikon epifluorescence microscope (Nikon Eclipse Ti).

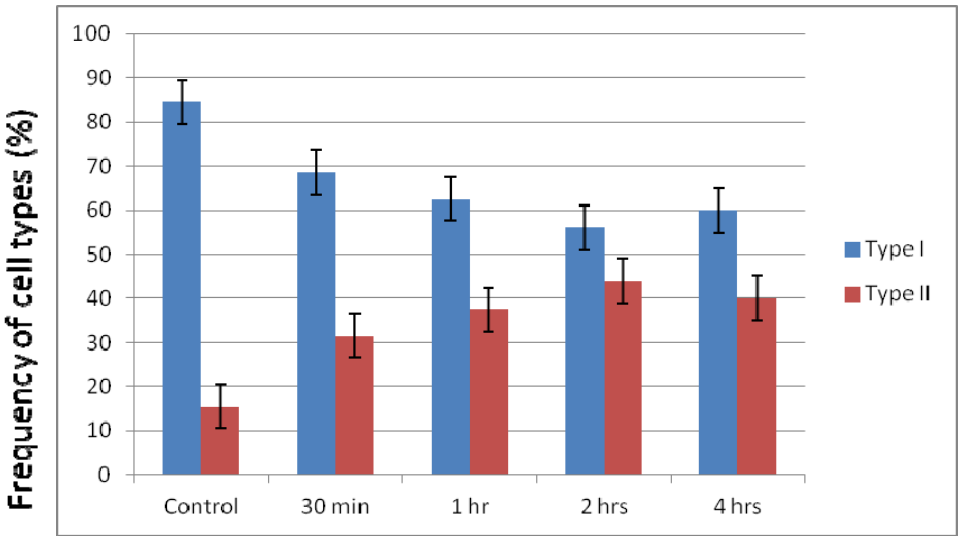

Figure 5.13. DTT treatment increases nucleolar 80S signal. Bar chart shows the mean frequencies of Type I and Type II cells upon 30 min, 1 hr, 2 hrs and 4 hrs treatment with 10 mM DTT and control cells (not treated with the drug). Quantification is based on visual inspection of one hundred cells from several micrographs of unfixed transfected cells. Error bars show variation of the 2 separate experiments.

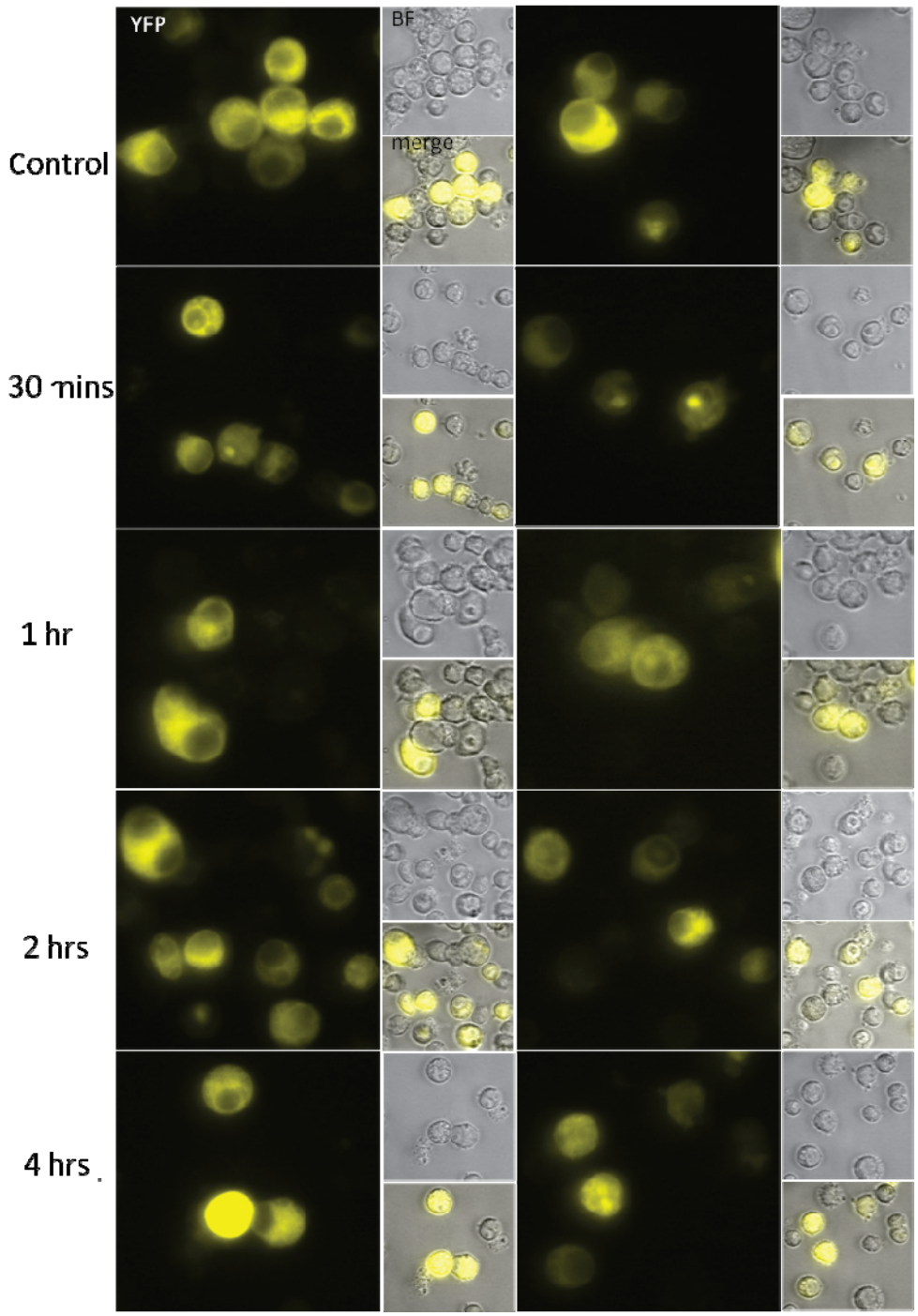

Figure 5.14.Thapsigargin treatment affects the 80S nucleolar signal. Images of transfected S2 cells expressing 80S BiFC reporters either untreated or treated with 1 µM thapsigargin for the indicated time intervals prior to microscopic inspection. Mild effect was observed in the frequency of Type II cells compared to the control. Images were taken with Nikon epifluorescence microscope (Nikon Eclipse Ti).

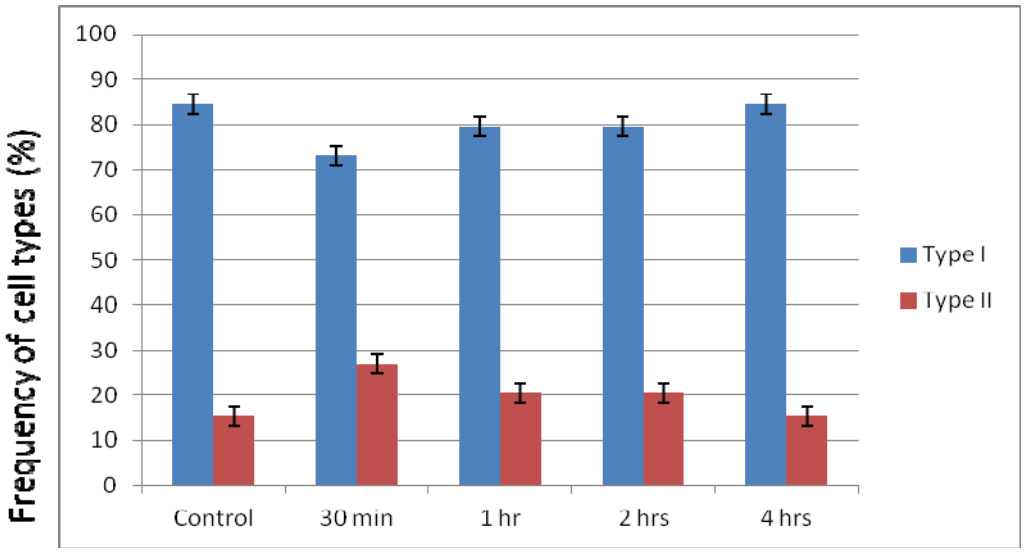

Figure 5.15. Quantification of BiFC cell types pattern upon Thapsigargin treatment. Bar chart shows mean frequencies of Type I and Type II BiFC signal pattern in untreated cells, and cells incubated with 1 µM thapsigargin for 30 min, 1 hr, 2 hrs and 4 hrs prior to microscopic viewing**.** Quantification is based on visual inspection of one hundred cells from several micrographs of unfixed transfected cells. Error bars show variation of 2 separate experiments.

5.3 Discussion

The data presented in this chapter show that cells with an apparent 80S signal in the nucleolus (Type II cells) are found across all the stages of the cell cycle but the frequency fluctuates at different stages of the cycle. The synchronisation achieved with HU is not optimal, as cells go out of synchrony within the first round of division; this behaviour is similar to that previously reported (Lee et al., 2010). My results indicate that although Type II cells (with a clear nucleolar signal) are found at all stages of the cell cycle, they are more frequent during the initial S phase before HU washout. The increase in the frequency of Type II cells at this stage could be linked to the stress of prolonged HU treatment. Yet, the alternative inference is that there may be more nuclear/nucleolar 80S during S phase. This latter interpretation could not be substantiated as the cells lost synchrony by the time they should re-enter S phase (20-23 hrs after HU washout). S2 cell doubling time was reported to be approximately 24 hrs (Yi et al., 2008) and most of the cells are in either G1 or G2 phase of the cell cycle, however, I found the doubling time in my experimental conditions to be between 20-23 hrs. The fact that more Type II cells were observed at S Phase following HU treatment compared to other stages of the cell cycle suggests a possible link between the physiological states of the cells, such as HU induced stress and nuclear translation. Probably, nuclear translation is required to overcome stress conditions such as those caused by a block in DNA replication.

Other forms of cellular stress might also enhance 80S assembly and translation in the nucleus/nucleolus. I observed that serum starvation steadily increases the frequency of Type II cells, which increased to about 5 fold after 24 hrs. The increase in the proportion of Type cells due to serum starvation was found to be statistically significant at 0.05 significance level. A more dramatic effect was observed when puromycin was used to

induce stress in the transfected cells. This translation inhibitor increased the frequency of Type II cells 30 minutes after treatment. Longer incubation with this drug for 1-2 hrs showed that most of the cells are either dead or showing signs of highly stressed/ dying cells. Notably, microscopic inspection and fluorescence intensity quantification of treated cells revealed that puromycin strongly decreases the BiFC signal. A similar effect was observed *in vitro* when BiFC transfected cells were treated with the same concentration of puromycin (Al-Jubran et al., 2013). Similarly DTT and thapsigargin treatments also increased the level of nucleolar 80S, with thapsigargin showing a milder effect. DTT and thapsigargin induced stress in mammalian cells was reported to activate JNK and p38 MAPK via the action PERK, which is an ER transmembrane kinase (Liang et al., 2006). The activation of these pathways by PERK leads to a global translational repression and a switch to the expression of many immediate-early genes such as c-*myc* and *egr-1* (Liang et al., 2006). Taken together, my results suggest that nuclear translation might be more active during cellular stress. Although cellular stress is known to inhibit global translation, instead, it may possibly trigger nuclear/ nucleolar translation, which perhaps translates transcripts that are required for stress response.

CHAPTER 6

6.0 Discussion and Conclusion

6.1 Discussion

6.1.1 BiFC is a powerful tool to detect ribosomal subunit interactions

Ribosomal subunits are synthesised and assembled in the nucleolus. The consensus at the start of this project was that the subunits are functionally inactive whilst in the nucleus. The view was that ribosomal subunits are exported as inactive precursors to the cytoplasm where they undergo final processing and maturation before they are engaged in translation (Panse and Johnson, 2010; Strunk et al., 2011). Yet, as detailed in the Introduction, there are observations suggesting the presence of functional ribosome within the nucleus. My project was aimed at further investigating whether ribosomal subunits can interact in the nucleus to form functional 80S ribosomes and whether the interaction is translation dependent. To address these questions, I have further characterised and improved a technique previously developed in our laboratory for the visualisation of the ribosomal subunit interaction *in vivo*. The method is based on the previously described BiFC protein-protein interaction assay (Hu et al., 2002a). Although the initial version of this technique, which made use of inter-subunit ribosomal proteins tagged with BiFC YFP fragments, could report 80S ribosome assembly in both cultured cells and tissues, the signal was weak. Therefore, as well as further characterising additional YFP-based 80S reporters (discussed in this section), I developed a similar technique using a more sensitive Venus fluorescent protein (discussed below).

Firstly, I further characterised the YFP-based BiFC assay. The tagged RPs of the large ribosomal subunit that were initially generated were all associated with the 5S sub-particle

of the 60S, thus raising a concern that any BiFC signal detected may not arise from interaction between fully assembled subunits, but rather from an interaction between a 5S sub-particle and the 40S subunit. Moreover, at the start of the project, we were not fully satisfied whether the interaction is translation dependent. To address the first issue on whether the interaction is between complete subunits, I generated tagged RP pairs located at ''the foot'' of the ribosome that are adjacent on the 80S, and are expected to generate a signal. As control, I generated other pairs located wide apart on the 80S structure, as such; they are not expected to produce a signal. My results indicated that the BiFC pairs at ''the foot'' of the ribosome did indeed produce a signal with similar localisation pattern and comparable intensity as the initial BiFC pairs that are located at the head of the ribosome (Al-jubran PhD thesis). Analysis of these additional pairs (Chapter 3) revealed that the BiFC signal is generated only when the tagged RPs are adjacent to each other on the 80S. Pairs of tagged RPs that are further apart on the 80S ribosome gave no BiFC signal even though their expression level and sub-cellular localisation are similar to the pairs that produced signal. Of the distant pairs, two, S9/L11 and S6/L11, gave a faint signal in the cytoplasm, but a more obvious signal in the nucleus/nucleolus was observed. These observations may indicate the existence of some complexes within the nucleolus whereby two RPs are closer to one other than they appear to be in the cytoplasmic 80S ribosome. The BiFC signal is strictly dependent on the interaction between the RPs as co-expression of the BiFC peptides alone, when not tethered to interacting proteins, produced only a weak signal that co-localised with DAPI stain. This region is where the two peptides are most abundant in transfected cells. Notably, the BiFC signal is sensitive to translation inhibitors. Emetine, an antibiotic known to block translation by freezing the ribosome at the elongation stage, (Grollman, 1968b) was found to greatly enhance BiFC fluorescence intensity *in vivo* as observed by

visual microscopic inspection of the BiFC transfected cells pre-incubated with this drug. This became more apparent when the fluorescence intensity of these cells was quantified. Similar translation-dependent changes in the BIFC signal were observed *in-vitro* with different translation inhibitors (experiments in collaboration with Dr Jikai Wen, a postdoc in the lab); inhibitors of translation elongation such as the above-described emetine were found to significantly increase the fluorescence intensity. Other inhibitors that block translation at the initiation stage, including puromycin, pectamycin and homoharringtonine, were found to decrease the signal (Al-Jubran et al., 2013). Collectively, these observations suggest that the BiFC signal generated is associated with translating 80S ribosomes. The BiFC 80S reporter assay we have developed is a powerful tool to study translation sites in living cells, via reporting the interaction between the small and large ribosome subunits to form translation competent 80S ribosome. The results of my characterisation established that the BiFC signal is produced only when the BiFC fusion proteins are in close proximity to one another at the interface between the subunits in the assembled 80S ribosome. The BiFC signal is observed predominantly in the cytoplasm, which is the acknowledged site for translation, but a fraction of the cells show a nuclear/nucleolar signal.

6.1.2 Venus-based BiFC 80S reporter yielded a more sensitive 80S reporter assay

A limitation with YPF-based 80S reporters is that the signal was not observed in the polysomal fractions of cell lysates of transfected S2 cells. The signal was predominantly detected in the 80S fractions. As such, I envisaged that the YFP BiFC linkage is not strong enough to withstand rotational movement of the ribosome during the translocation step. To enhance the efficiency of this assay, I utilised Venus, a more sensitive fluorescent protein that was reported to exhibit stronger fluorescence intensity (Shyu et al., 2006) and was

shown to give a brighter and a more specific BiFC signal in *Drosophila* (Hudry et al., 2011). As previously carried out with the YFP-based constructs, I tagged RpS18/L11 pairs that are located at the head of the subunits and RpS6/L24 pairs located at the ''foot'' of the ribosome with Venus fluorescent proteins. As was observed with the YFP reporters, the Venus tagged BiFC RPs, S18/L11, were found to be functional since they were detected in polysomes in S2 cells, and could partially complement lethal mutation of the corresponding endogenous ribosomal protein genes in flies. Although flies carrying only the tagged RPs were viable, they were sterile as we could not be bred them. These observations indicate that the 80S ribosome, in which one of its subunits contains the tagged RP (either S18 or L11), is functional and operates at near normal levels. Employing these more sensitive BiFC reporter constructs, I was able to study ribosome subunit joining in *Drosophila* S2 cells, salivary glands, midgut cells and the highly polarised cells of neurons. As with the YFP-based reporters, the BiFC signal was observed primarily in the cytoplasm in S2 cells, salivary gland and other investigated tissues, but a fraction of the cells showed nucleolar and nuclear signals. The intensity of the BiFC fluorescence was visibly higher compared to the YFP reporters in both *Drosophila* S2 cells and all fly tissues I have investigated. With the Venus reporters, a larger fraction of the transfected S2 cells (about 40%) showed both a cytoplasmic and nucleolar signal (Type II cells). Transfection with the Venus-based constructs also revealed that about 10% of cells show a predominant nuclear signal with a faint signal in the cytoplasm (Type III cells). An additional fraction of cells (17%) gave a strong fluorescent signal all over the cells (Type IV cells). The Type III & IV cells appeared to have shrunken nuclei, indicating that they could be stressed or dying cells. Investigation of these cell types with apoptotic marker, active-caspase antibody, revealed that these cells were positive to anti active-caspase 3, confirming my initial hypothesis.

Notably, our additional biochemical characterisation of the Venus BiFC signal in polysome fractions revealed that the largest fraction of the signal is found in 80S and polysomal fractions. Puromycin treatment of the extracts resulted in an evident shift of both the BiFC signal and tagged proteins to lighter fractions. I interpreted this later observation as the Venus-based BiFC linkage partly withstanding the inter-subunit rotation associated with translation elongation which appeared to break the YFP BiFC linkage. These observations therefore indicate that the BiFC signal is associated with translating ribosomes. Furthermore, the more sensitive Venus-based 80S reporter system allowed visualisation of 80S ribosomes along the axons of photoreceptor neurons, suggesting the occurrence of local translation at these sites.

6.1.3 Translating ribosomes are particularly apparent in the nucleolus

A key finding in this project is that the 80S BiFC signal was reproducibly detected in the cytoplasm as well as in the nucleus, particularly in the nucleolus. The nucleolar signal appear to also correspond to translating ribosomes, as short incubation with emetine results to a rapid increase in the intensity of the nuclear signal and a drastic increase in the frequency of cells displaying apparent nucleolar signals (Type II cells). It could be argued that the nucleolar signal can be attributed to the association of the BiFC RP pairs in a transient 90S pre-ribosomal intermediate similar to that detected in budding yeast (Grandi et al., 2002); however, my data argue against this interpretation because RP pairs that are not adjacent on the 80S structure did not produce BiFC fluorescence despite the fact that the fusion proteins concentrate in the nucleolus at levels similar to those that were found to produce a signal. The exceptions were, as discussed above, S9/L11 and S6/L11. Another observation that indicated the nucleolar signal is reporting translation was its dependence on Pol II

transcription but not Pol I. For example, α-amanitin which is a specific inhibitor of Pol II, and act.D at a level that blocks Pol II, both abolished the nucleolar signal, whereas act.D treatment at lower concentration that blocks only Pol I could not inhibit the signal. This observation suggests a steady state accumulation of mRNAs within the nucleolus and that the nucleolar signal originates from ribosomes that are translating mRNAs within the compartment. A previous study in *Arabidopsis thaliana* also demonstrated the accumulation of mRNAs in the nucleolus, particularly aberrant transcripts generated from incorrect splicing, suggesting the occurrence of NMD at this sites (Kim et al., 2009). As reviewed in the introduction, criticisms against nuclear translation are largely based on the functionality of translation machinery in the nucleus, as it was reported that complete processing of the ribosomal subunit occurs in the cytoplasm. This raises the possibility that the subunits are inactive whilst in the nucleus (Udem and Warner, 1973; Lebaron et al., 2012; Strunk et al., 2011). Yet, other studies reported that the immature pre-40S ribosome can associate with 60S and engage translation (Rouquette et al., 2005; Soudet et al., 2009). It was also argued that key translation factors are actively exported from the nucleus (Bohnsack et al., 2002). However, our results suggest that there must be some significant trace translation factors within the nucleus at a level that can initiate translation.

Collectively, mine and my laboratory collaborators' data suggest that the signal corresponds to ribosomes translating mRNA in the nucleus and particularly in the nucleolus (Al-Jubran et al., 2013). These observations are in agreement with an earlier study that reported the presence of several ribosome components and amino acids incorporation at polytene chromosomes and in the nucleolus of *Drosophila* cells (Brogna et al., 2002). A recent independent study also reported that translating ribosomes are present in the nucleus and particularly more abundant within the nucleolus of mammalian cells (David et al., 2012).

Furthermore, by utilising the ribopuromycylation method (RPM) described in this paper, we observed puromycin incorporation in the nucleolus and at transcription sites in *Drosophila* polytene chromosome (Al-Jubran et al., 2013). A pertinent question arising from these observations is what is the biological relevance of nuclear 80S? It was earlier postulated that most newly synthesised nuclear proteins are degraded (Iborra et al., 2001). It was reported in this study that translation sites within the nucleus overlapped with β- subunit of proteasome and the inhibition of proteasome increased the level of the observed nuclear fluorescence suggesting the accumulation of newly synthesised proteins. Other studies suggested that nuclear translation may serve as a quality control mechanism to assess either the fidelity of the newly made ribosomes or the integrity of the mRNAs before they exit the nucleus to the cytoplasm for translation (Reid and Nicchitta, 2012; Hentze, 2001; Iborra et al., 2001). Nuclear scanning of mRNA OFR will enable early detection of faulty mRNAs which may be either alternatively spliced or subjected to degradation. The quality control function on the newly synthesized mRNAs were further supported from the observation that translation factors, components of the NMD machinery associates with the transcriptional complex (Iborra et al., 2004) and that live-cell imaging of PTC containing mRNAs revealed that nonsense mutations are identified co-transcriptionally (de Turris et al., 2011).

A recent study in human cells reported a non-canonical translation of pre-mRNAs that occurs within the nucleus (Apcher et al., 2013). This nuclear translation might produce antigenic peptides for immunosurveillance by presentation through the major histocompatibilty complex (MHC) class I pathway. This study concluded that translation of pre-mRNA occurs in the nucleoplasm. Contrary to the observation by Apcher and colleagues, mine and my collaborators data indicates that the 80S signal is more abundant

in the nucleolus, which is in agreement with earlier observations in *Drosophila* and mammalian cells (Brogna et al., 2002; David et al., 2012). Evidence that linked the nucleolus to a role in protein synthesis was described in the early 70s by a study in which protein synthesis was monitored in a heterokaryon cell developed from the insertion of a chick erythrocyte nucleus into a mouse cell (DEÁK et al., 1972). This work reported that synthesis of chick-specific proteins did not occur directly after RNAs are synthesised, but only after nucleoli are formed in the chick nucleus. This observation led to the idea that nucleolus may have an important function in mRNA export. A more recent study in *S. pombe* also suggested a role for the nucleolus in mRNA export to the cytoplasm (Ideue et al., 2004). Although, it cannot be dismissed that the nucleolus functions in nuclear mRNA export, our data, and a number of previous observations, suggest that translation occurs in the outer shell of the nucleolus (McLeod et al., 2014).

6.1.4 Nuclear translation might be enhanced by cellular stress

As detailed in the results (Chapter 3 and 4), in S2 cells, the 80S is apparent only in a fraction of nuclei. This observation raises the question of whether nuclear translation is active only at particular stage/stages of the cell cycle. My analysis of synchronised S2 cells (Chapter 5) indicate, however, that nuclear 80S are found at all stages of the cell cycle, but the frequency of cells with an apparent nuclear signal might vary from one stage of the cycle to another. Another possible explanation for why only a fraction of S2 cells show nuclear 80S is that nuclear translation may be triggered by cellular stress which can affect a fraction of the cells during transfection. The results of the experiments I have undertaken are consistent with cellular stress affecting the sub-cellular distribution of ribosomes and translation. My observations from subjecting BiFC transfected S2 cells to some pre-defined stresses

revealed that stress from serum starvation, puromycin stress, and the ER stress inducers DTT and thapsigargin, all increased nuclear 80S levels and most likely nuclear translation. A possible interpretation of this finding is that the exposure of BiFC transfected S2 cells to these stress agents might result to a switch in selective mRNA translation required for remediating the effect of these stressors, or alternatively preparation of cells for apoptosis, which partly occurs in the nuclear/nucleolar compartment. Another possible interpretation is that stress response may lead to sequestration of ribosomes in the nucleus as a mechanism that will enable the selective translation of specific mRNAs localised within the nuclear compartment.

6.2 Conclusion

My data demonstrate that the BiFC-based technique we have developed to visualise ribosomal subunit interactions is correctly reporting translation-dependent joining of 80S ribosomes in *Drosophila* cells. Our extensive characterisation of the technique indicates that the interaction is the result of 80S joining at translation initiation. A disadvantage of this technique is the delay between interaction of the BiFC-tagged proteins and the resulting maturation of the BiFC complex and its chromophore activation (Kerppola, 2009), thus the assay does not allow real time detection of the assembly and disassembly of the 80S complex: it can only report that 80S have assembled. A limitation associated with this study is that some of the experimental treatments were carried out twice. As such, not much statistical evidence is provided to show whether there is any significant difference observed across experimental treatments.

Finally, whether functional proteins are synthesised within the nucleus or nucleolus remains to be investigated further. An interesting question that needs to be answered is the biological relevance of nuclear translation; are the proteins made in the nucleus functional?

As mentioned above, nuclear translation might generate defective ribosomal products (DRiPs) which provide immunogenic peptides for the MHC class pathway in mammalian cells (Apcher et al., 2013). However, *Drosophila* and most other eukaryotic organisms have no adaptive immune system. Future studies will need to address this important issue of identifying the function or functions of nuclear translation. A key step to explaining the function of nuclear translation is identifying the proteins that are made within the nuclear compartment. A method of choice to identify the transcripts that are translated by the nuclear polyribosomes is the ribosomes profiling; a technique that is based on deep sequencing of ribosome-protected mRNA fragments. However, like other earlier studies that isolated purified nuclei, a critical concern is applying an effective and convincing biochemical method of isolating nuclear polysomes without any possibility of cytoplasmic contamination, especially from the nuclear envelope, which harbours a pool of ribosomes attached to the ER. If successful, this approach will resolve the long controversial issue of translation within the nuclear compartment and usher in a new perspective in our understanding of eukaryotic gene expression.

REFERENCES

AGRAWAL, R. K., PENCZEK, P., GRASSUCCI, R. A. & FRANK, J. 1998. Visualization of elongation factor G on the Escherichia coli 70S ribosome: The mechanism of translocation. *Proceedings of the National Academy of Sciences,* 95**,** 6134-6138.

AL-JUBRAN, K., WEN, J., ABDULLAHI, A., ROY CHAUDHURY, S., LI, M., RAMANATHAN, P., MATINA, A., DE, S., PIECHOCKI, K., RUGJEE, K. N. & BROGNA, S. 2013. Visualization of the joining of ribosomal subunits reveals the presence of 80S ribosomes in the nucleus. *RNA,* 19**,** 1669-83.

ALBERTS, B., JOHNSON, A., LEWIS, J., RAFF, M., ROBERTS, K. & WALTER, P. 2008. *Molecular Biology of the cell.,* New York, U.S., Garland Science.

ALLEN, W. 1978. Does protein synthesis occur within the nucleus? Unambigous evidence is still needed. *Trends Biol. Sci,* 3**,** N255.

AMRANI, N., SACHS, M. S. & JACOBSON, A. 2006. Early nonsense mRNA decay solves translational problem. *Nat. Rev. Mol. Cell. Biol,* 7**,** 415-425

ANGER, A. M., ARMACHE, J. P., BERNINGHAUSEN, O., HABECK, M., SUBKLEWE, M., WILSON, D. N. & BECKMANN, R. 2013. Structures of the human and Drosophila 80S ribosome. *Nature,* 497**,** 80-5.

AOUFOUCHI, S., YÉLAMOS, J. & MILSTEIN, C. 1996. Nonsense Mutations Inhibit RNA Splicing in a Cell-Free System: Recognition of Mutant Codon Is Independent of Protein Synthesis. *Cell,* 85**,** 415-422.

APCHER, S., MILLOT, G., DASKALOGIANNI, C., SCHERL, A., MANOURY, B. & FÅHRAEUS, R. 2013. Translation of pre-spliced RNAs in the nuclear compartment generates peptides for the MHC class I pathway. *Proceedings of the National Academy of Sciences,* 110**,** 17951-17956.

ARAI, R., UEDA, H., KITAYAMA, A., KAMIYA, N. & NAGAMUNE, T. 2001. Design of the linkers which effectively separate domains of a bifunctional fusion protein. *Protein Engineering,* 14**,** 529-532.

AVERY, P., VICENTE-CRESPO, M., FRANCIS, D., NASHCHEKINA, O., ALONSO, C. R. & PALACIOS, I. M. 2011. Drosophila Upf1 and Upf2 loss of function inhibits cell growth and causes animal death in a Upf3-independent manner. *RNA,* 17**,** 624-38.

BAN, N., NISSEN, P., HANSEN, J., MOORE, P. B. & STEITZ, T. A. 2000. The complete atomic structure of the large ribosomal subunit at 2.4 Á resolution. *Science,* 289**,** 905-920.

BARNA, M. 2013. Ribosomes take control. *Proc Natl Acad Sci U S A,* 110**,** 9-10.

BEEBE, K., LEE, W.-C. & MICCHELLI, C. A. 2010. JAK/STAT signaling coordinates stem cell proliferation and multilineage differentiation in the Drosophila intestinal stem cell lineage. *Developmental Biology,* 338**,** 28-37.

BELGRADER, P., CHENG, J. & MAQUAT, L. E. 1993. Evidence to implicate translation by ribosomes in the mechanism by which nonsense codons reduce the nuclear level of human triosephosphate isomerase mRNA. *Proc Natl Acad Sci U S A,* 90**,** 482-6.

BEN-SHEM, A., GARREAU DE LOUBRESSE, N., MELNIKOV, S., JENNER, L., YUSUPOVA, G. & YUSUPOV, M. 2011. The Structure of the Eukaryotic Ribosome at 3.0 Å Resolution. *Science,* 334**,** 1524-1529.

BEN-SHEM, A., JENNER, L., YUSUPOVA, G. & YUSUPOV, M. 2010. Crystal structure of the eukaryotic ribosome. *Science,* 330**,** 1203-9.

BERINGER, M. & RODNINA, M. 2007. The ribosomal peptidyl transferase. *Mol Cell* 26(3)**,** 311-321.

BISCHOF, J., MAEDA, R., HEDIGER, M., KARCH, F. & BASLER, K. 2007. An optimized transgenesis system for Drosophila using germ-line-specific phiC31 integrases. *Proc Natl Acad Sci USA,* 104**,** 3312 - 3317.

BLOBEL, G. & SABATINI, D. 1971. Dissociation of mammalian polyribosomes into subunits by puromycin. *Proc Natl Acad Sci,* 68**,** 390-394.

BOHNSACK, M. T., REGENER, K., SCHWAPPACH, B., SAFFRICH, R., PARASKEVA, E., HARTMANN, E. & GORLICH, D. 2002. Exp5 exports eEF1A via tRNA from nuclei and synergizes with other transport pathways to confine translation to the cytoplasm. *EMBO J,* 21**,** 6205-15.

BRODERSEN, D. E., CLEMONS, W. M., JR., CARTER, A. P., WIMBERLY, B. T. & RAMAKRISHMAN, V. 2002. Crytal structure of 30S ribosomal subunit fro Thermus thermophilus: structure of proteins and their interactions with 16 S RNA. *J. Mol. Biol,* 316**,** 725-768.

BRODSKY, A. S. & SILVER, P. A. 2000. Pre-mRNA processing factors are required for nuclear export. *RNA New York,* NY 6**,** 1737-1739.

BROGNA, S. 1999. Nonsense mutations in the alcohol dehydrogenase gene of Drosophila melanogaster correlate with an abnormal 3' end processing of the corresponding pre-mRNA. *RNA,* 5**,** 562-73.

BROGNA, S., SATO, T. A. & ROSBASH, M. 2002. Ribosome components are associated with sites of transcription. *Mol Cell,* 10**,** 93-104.

BROGNA, S. & WEN, J. 2009. Nonsense-mediated mRNA decay (NMD) mechanisms. *Nat Struct Mol Biol,* 16**,** 107-13.

BRUECKNER, F. & CRAMER, P. 2008. Structural basis of transcription inhibition by [alpha]-amanitin and implications for RNA polymerase II translocation. *Nat Struct Mol Biol,* 15 811-818.

BUNGE, M. B. 1973. Fine structure of nerve fibers and growth cones of isolated sympathetic neurons in culture. *J Cell Biol,* 56**,** 713-35.

CAMPBELL, D. S. & HOLT, C. E. 2001. Chemotropic responses of retinal growth cones mediated by rapid local protein synthesis and degradation. *Neuron,* 32**,** 1013-26.

CHANDRAMOULI, P., TOPF, M., MENETRET, J. F., ESWAR, N., CANNONE, J. J., GUTELL, R. R., SALI, A. & AKEY, C. W. 2008. Structure of the mammalian 80S ribosome at 8.7 A resolution. *Structure,* 16**,** 535-48.

CHENG, J. C. & KAN, Y. W. Year. Beta O thalassemia, a nonsense mutation in man. *In:* Proceeding of National Academy of Science of the United States of America 1979. 2886-2889.

CMARKO, D., SMIGOVA, J., MINICHOVA, L. & POPOV, A. 2008 Nucleolus: the ribosome factory. *Histology and histopatholog, 23* 1291-1298.

COLENO-COSTES, A., JANG, S. M., DE VANSSAY, A., ROUGEOT, J., BOUCEBA, T., RANDSHOLT, N. B., GIBERT, J. M., LE CROM, S., MOUCHEL-VIELH, E., BLOYER, S. & PERONNET, F. 2012. New partners in regulation of gene expression: the enhancer of Trithorax and Polycomb Corto interacts with methylated ribosomal protein l12 via its chromodomain. *PLoS Genet,* 8**,** e1003006.

COLGAN, D. F. & MANLEY, J. L. 1997. Mechanism and regulations of mRNA polyadenylation. *Genes and Development* 11**,** 2755-2766.

COLON-RAMOS, D. A., SHENVI, C. L., WEITZEL, D. H., GAN, E. C., MATTS, R., CATE, J. & KORNBLUTH, S. 2006. Direct ribosomal binding by a cellular inhibitor of translation. *Nat Struct Mol Biol,* 13**,** 103-111.

CONTI, E. & IZAURRALDE, E. 2005. Nonsense Mediated mRNA decay: Molecular insights and mechanistic variations across species. *Cur. Opin. Cell Biol.,* 17**,** 316-325.

CULBERTON, M. R., UNDERBRINK, K. M. & FINK, G. R. 1980. Frameshift suppression in saccharomyces cerevisiae II. Genetic properties of group II suppressors. *Genetics,* 95**,** 833-853.

CULBERTSON, M. R. 1999. RNA surveillance: unforeseen consequences for gene expression, inherited genetic disorders and cancer. *Trends in Genetics,* 15**,** 74-80.

DAHLBERG, J. E., LUND, E. & GOODWIN, E. B. 2003. Nuclear translation: what is the evidence? *RNA,* 9**,** 1-8.

DAI, M. S., ARNOLD, H., SUN, X. X., SEARS, R. & LU, H. 2007. Inhibition of c-Myc activity by ribosomal protein L11. *EMBO J,* 26**,** 3332-45.

DAVID, A., DOLAN, B. P., HICKMAN, H. D., KNOWLTON, J. J., CLAVARINO, G., PIERRE, P., BENNINK, J. R. & YEWDELL, J. W. 2012. Nuclear translation visualized by ribosome-bound nascent chain puromycylation. *J Cell Biol,* 197**,** 45-57.

DE, S., VARSALLY, W., FALCIANI, F. & BROGNA, S. 2011. Ribosomal proteins' association with transcription sites peaks at tRNA genes in Schizosaccharomyces pombe. *RNA,* 17**,** 1713-26.

DE TURRIS, V., NICHOLSON, P., OROZCO, R. Z., SINGER, R. H. & MUHLEMANN, O. 2011. Cotranscriptional effect of a premature termination codon revealed by live-cell imaging. *RNA,* 17**,** 2094-107.

DEÁK, I., SIDEBOTTOM, E. & HARRIS, H. 1972. Further Experiments on the Role of the Nucleolus in the Expression of Structural Genes. *Journal of Cell Science,* 11**,** 379-391.

DOUDNA, J. A. & RATH, V. L. 2002. Structure and function of the eukaryotic ribosome: the next frontier. *Cell* 109(2)**,** 153-156.

DUFFY, J. B. 2002. GAL4 system in Drosophila: a fly geneticist's Swiss army knife. *genesis,* 34(1-2)**,** 1--15.

DUNDR, M. & RAŠKA, I. 1993. Nonisotopic Ultrastructural Mapping of Transcription Sites within the Nucleolus. *Experimental Cell Research,* 208**,** 275-281.

FERREIRA-CERCA, S., PÖLL, G., GLEIZES, P.-E., TSCHOCHNER, H. & MILKEREIT, P. 2005. Roles of Eukaryotic Ribosomal Proteins in Maturation and Transport of Pre-18S rRNA and Ribosome Function. *Molecular Cell,* 20**,** 263-275.

FILIPOVSKA, A. & RACKHAM, O. 2013. Specialization from synthesis: How ribosome diversity can customize protein function. *FEBS letters,* 587**,** 1189-1197.

FROMONT-RACINE, M., SENGER, B., SAVEANU, C. & FASIOLO, F. 2003. Ribosome assembly in eukaryotes. *Gene,* 313**,** 17-42.

GEBAUER, F. & HENTZE, M. W. 2004. Molecular mechanisms of translational control. *Nat. Rev. Mol. Cell. Biol,* **5,** 182-186.

GILBERT, W. V. 2011. Functional specialization of ribosomes? *Trends Biochem Sci,* 36**,** 127-32.

GOIDL, J. 1978. Does protein synthesis occur within the nucleus: Good eveidence that it does. *Trends Biol. Sci,* 3**,** N228.

GOIDL, J. A., CANAANI, D., BOUBLIK, M., WEISSBACH, H. & DICKERMAN, H. 1975. Polyanion-induced release of polyribosomes from HeLa cell nuclei. *J Biol Chem,* 250**,** 9198-205.

GOLDSTEIN, D. J. 1970. Aspect of scanning microdensitometry I. Stray light (glare). *Journal of microscopy* 92**,** 1-16.

GRAIFER, D., MALYGIN, A., ZHARKOV, D. O. & KARPOVA, G. 2014. Eukaryotic ribosomal protein S3: A constituent of translational machinery and an extraribosomal player in various cellular processes. *Biochimie,* 99**,** 8-18.

GRANDI, P., V. RYBIN, J., BASSLER, E., PETFALSKI, D., STRAUSS, M., MARZIOCH, T., SCHAFER, B., KUSTER, H., TSCHOCHNER, D., TOLLERVEY, A. C. G. & HURT., E. 2002. 90S preribosomes include the 35S pre-rRNA, the U3 snoRNP, and 40S subunit processing factors but predominantly lack 60S synthesis factors. *Mol Cell,* 10.

GRILL, S., GUALERZI, C. O., LONDEI, P. & BLASI, U. 2000. Selective stimulation of translation of leaderless mRNA by initiation factor 2: evolutionary implications for translation. *EMBO J,* 19**,** 4101-10.

GRIMSON, A., O'CONNOR, S., NEWMAN, C. L. & ANDERSON, P. 2004. SMG-1 is a phosphatidylinositol kinase-related protein required for nonsense-mediated mRNA decay in *Caenorhabditis elegans*. *Mol Cell Bio***,** 7483-7490.

GROLLMAN, A. P. 1968a. Inhibitors of Protein Biosynthesis .V. Effect of Emetine on protein and nucleic acid biosynthesis imn Hela cells. *J. Biol Chem,* 243**,** 4089-4094.

GROLLMAN, A. P. 1968b. Inhibitors of Protein Biosynthesis: V. EFFECTS OF EMETINE ON PROTEIN AND NUCLEIC ACID BIOSYNTHESIS IN HeLa CELLS. *Journal of Biological Chemistry,* 243**,** 4089-4094.

HARDING, H. P., ZHANG, Y., BERTOLOTTI, A., ZENG, H. & RON, D. 2000. Regulated translation initiation controls stress-induced gene expression in mammalian cells. *Mol Cell,* 6**,** 1099-1108.

HENDERSON, K. D. & ANDREW, D. J. 2000. Regulation and Function of Scr, exd, and hth in the Drosophila Salivary Gland. *Developmental Biology,* 217**,** 362-374.

HENTZE, M. W. 2001. Believe It or Not--Translation in the Nucleus. *Science,* 293**,** 1058-1059.

HOLCIK, M. & SONENBERG, N. 2005. Translational control in stress and apoptosis. *Nat Rev Mol Cell Biol,* 6**,** 318-327.

HOSODA, N., KIM, Y. K., LEJEUNE, F. & MAQUAT, L. E. 2005. CBP80 promotesinteraction of Upf1 with Upf2 during nonsense-mediated mRNA decay in mammaliancells. *Nature structural & molecular biology* 12**,** 893-901.

HOZAK, P., COOK, P. R., SCHOFER, C., MOSGOLLER, W. & WACHTLER, F. 1994. Site of transcription of ribosomal RNA and intranucleolar structure in HeLa cells. *Journal of Cell Science,* 107**,** 639-648.

HU, C. D., CHINENOV, Y. & KERPEKOLLA, T. K. 2002a. Visualization of interactions among bZIP and Rel family proteins in living cells using bimolecular fluorescence complementation. *Molecular Cell,* 9**,** 789-798.

HU, C. D., CHINENOV, Y. & KERPPOLA, T. K. 2002b. Visualization of interactions among bZIP and Rel family proteins in living cells using bimolecular fluorescence complementation. *Mol Cell,* 9**,** 789-98.

HU, C. D. & KERPPOLA, T. K. 2003. Simultaneous visualization of multiple protein interactions in living cells using multicolor fluorescence complementation analysis. *Nature Biotechnology,* 21**,** 539-545.

HUDRY, B., VIALA, S., GRABA, Y. & MERABET, S. 2011. Visualization of protein interactions in living Drosophila embryos by the bimolecular fluorescence complementation assay. *BMC Biology,* 9**,** 5.

HUI, A. & DE BOER, H. A. 1987. Specialized ribosome system: preferential translation of a single mRNA species by a subpopulation of mutated ribosomes in Escherichia coli. *Proc Natl Acad Sci U S A,* 84**,** 4762-6.

IBORRA, F. J., ESCARGUEIL, A. E., KWEK, K. Y., AKOULITCHEV, A. & COOK, P. R. 2004. Molecular crosstalk between the transcription, translation, and nonsense decay mechineries. *Journal of cell science,* 177**,** 899-906.

IBORRA, F. J., JACKSON, D. A. & COOK, P. R. 2001. Coupled transcription and translation within nuclei of mammalian cells. *Science,* 293**,** 1139-42.

IDEUE, T., AZAD, A. K., YOSHIDA, J., MATSUSAKA, T., YANAGIDA, M., OHSHIMA, Y. & TANI, T. 2004. The nucleolus is involved in mRNA export from the nucleus in fission yeast. *J Cell Sci,* 117**,** 2887-95.

ISHIGAKI, Y., LI, X., SESIN, G. & MAQUAT, L. E. 2001. Evidence for pioneer round of mRNA translation: mRNA subjected to nonsense-mediated decay in mammalian cells are bound by CBP80 and CBP20. *Cell* 106**,** 607-617.

JACKSON, R. J. 2007. The missing link in the eukaryotic ribosome cycle. *Mol Cell* 28**,** 356-358.

JACOBSON, A. 1996. Poly (A) metabolism and translation: The closed-loop model. In: SonenbergN, Hershey JWB, Mathews MB (eds) Translational Control of gene expression. *Cold Spring Harbour, NY, Cold Spring Habour Laboratory Press***,** 451.

JAILLON, O. E. A. 2008. Translational control of intron splicing in eukaryotes. *Nature,* 451**,** 359-362.

JANSSEN, G. R. 1993. Eubacterial, archaebacterial, and eukaryotic genes that encode leaderless mRNA. *In Industrial Microorganisms: Basic and Applied Molecular Genetics (Baltz, R.H. et al., eds). American Society for Microbiology Press***,** pp. 59-67.

JIANG, H., PATEL, P. H., KOHLMAIER, A., GRENLEY, M. O., MCEWEN, D. G. & EDGAR, B. A. 2009. Cytokine/Jak/Stat signaling mediates regeneration and homeostasis in the Drosophila midgut. *Cell,* 137(7)**,** 1343–1355.

JOHNSON, J. M., CASTLE, J., GARRETT-ENGELE, P., KAN, Z., LOERCH, P. M., ARMOUR, C. D., SANTOS, R., SCHADT, E. E., STOUGHTON, R. & SHOEMAKER, D. D. 2003. Genome-Wide Survey of Human Alternative Pre-mRNA Splicing with Exon Junction Microarrays. *Science,* 302**,** 2141-2144.

JOSEPH, S. 2003. After the ribosome structure: How does translocation work? *RNA,* 9**,** 160–164.

KAHVEJIAN, A., ROY, G. & SONENBERG, N. 2001. The mRNA closed loop model: The function of PABP and PABP-interacting proteins in mRNA translation. *Cold Spring Harb Symp Quant Biol,* 66**,** 300.

KAPLAN, C. D., LARSSON, K.-M. & KORNBERG, R. D. 2008. The RNA Polymerase II Trigger Loop Functions in Substrate Selection and Is Directly Targeted by α-Amanitin. *Molecular Cell,* 30**,** 547-556.

KAPP, L. D. & LORSCH, J. R. 2004. The molecular mechanics of eukaryotic translation. *Annual review of biochemistry,* 73**,** 657-704.

KARBSTEIN, K. 2013. Quality control mechanisms during ribosome maturation. *Trends in Cell Biology,* 23**,** 242-250.

KEEGAN, L., GILL, G. & PTASHNE, M. 1986. Separation of DNA binding from the transcription-activating function of a eukaryotic regulatory protein. *Science,* 231**,** 699-704.

KERPPOLA, T. K. 2009. Visualization of molecular interactions using bimolecular fluorescence complementation analysis: characteristics of protein fragment complementation. *Chem Soc Rev,* 38**,** 2876-86.

KIM, J., CHUBATSU, L. S., ADMON, A., STAHL, J., FELLOUS, R. & LINN, S. 1995. Implication of mammalian ribosomal protein S3 in the processing of DNA damage. *J. Biol Chem,* **270,** 13620-13629.

KIM, S. H., KOROLEVA, O. A., LEWANDOWSKA, D., PENDLE, A. F., CLARK, G. P., SIMPSON, C. G., SHAW, P. J. & BROWN, J. W. S. 2009. Aberrant mRNA Transcripts and the Nonsense-Mediated Decay Proteins UPF2 and UPF3 Are Enriched in the Arabidopsis Nucleolus. *The Plant Cell Online,* 21**,** 2045-2057.

KISLINGER, T., COX, B., KANNAN, A., CHUNG, C., HU, P., IGNATCHENKO, A., SCOTT, M. S., GRAMOLINI, A. O., MORRIS, Q., HALLETT, M. T., ROSSANT, J., HUGHES, T. R., FREY, B. & EMILI, A. 2006. Global Survey of Organ and Organelle Protein Expression in Mouse: Combined Proteomic and Transcriptomic Profiling. *Cell,* 125**,** 173-186.

KLINGE, S., VOIGTS-HOFFMANN, F., LEIBUNDGUT, M. & BAN, N. 2012. Atomic structures of the eukaryotic ribosome. *Trends in Biochemical Sciences,* 37**,** 189-198.

KONDRASHOV, N., PUSIC, A., STUMPF, C. R., SHIMIZU, K., HSIEH, ANDREW C., XUE, S., ISHIJIMA, J., SHIROISHI, T. & BARNA, M. 2011. Ribosome-Mediated Specificity in Hox mRNA Translation and Vertebrate Tissue Patterning. *Cell,* 145**,** 383-397.

KONDYLIS, V., TANG, Y., FUCHS, F., BOUTROS, M. & RABOUILLE, C. 2011. Identification of ER proteins involved in the functional organisation of the early secretory pathway in Drosophila cells by a targeted RNAi screen. *PLoS One,* 6**,** e17173.

KRESSLER, D. & AL., E. 1999. Protein trans-acting factors involved in ribosome biogenesis in *Saccharomyces cerevisiae*. *Mol. Cell. Biol.,* 19**,** 7897–7912.

LAM, Y. W., LAMOND, A. I., MANN, M. & ANDERSEN, J. S. 2007. Analysis of nucleolar protein dynamics reveals the nuclear degradation of ribosomal proteins. *curr. Biol,* **17,** 749-760.

LAMBERTSON, A. 1998. The minute genes in Drosophila and their molecular functions. *Adv Genet,* 38**,** 69-134.

LAMBERTSSON, A. 1975. The ribosomal proteins of Drosophila melanogaster. *Molecular and General Genetics MGG,* 139**,** 133-144.

LEBARON, S., SCHNEIDER, C., VAN NUES, R. W., SWIATKOWSKA, A., WALSH, D., BOTTCHER, B., GRANNEMAN, S., WATKINS, N. J. & TOLLERVEY, D. 2012. Proofreading of pre-40S ribosome maturation by a translation initiation factor and 60S subunits. *Nat Struct Mol Biol,* 19**,** 744-53.

LEE, A. S., BURDEINICK-KERR, R. & WHELAN, S. P. 2013. A ribosome-specialized translation initiation pathway is required for cap-dependent translation of vesicular stomatitis virus mRNAs. *Proc Natl Acad Sci U S A,* 110**,** 324-9.

LEE, M.-C., TOH, L.-L., YAW, L.-P. & LUO, Y. 2010. Drosophila Octamer Elements and Pdm-1 Dictate the Coordinated Transcription of Core Histone Genes. *Journal of Biological Chemistry,* 285**,** 9041-9053.

LEJEUNE, F., ISHIGAKI, Y. & MAQUAT, L. E. 2002. The exon junction complex is detected on CBP80-bound but not eIF4E-bound mRNA in mammalian cells: dynamics of mRNP remodeling. *The EMBO Journal,* 21**,** 3536-3545.

LI, W.-Z., LI, S.-L., ZHENG, H. Y., ZHANG, S.-P. & XUE, L. 2012. A broad expression profile of the GMR-GAL4 driver in Drosophila melanogaster. *Genet. Mol. Res,* 11 (3)**,** 1997-2002.

LI, Z., LEE, I., MORADI, E., HUNG, N. J., JOHNSON, A. W. & MARCOTTE, E. M. 2009. Rational extension of the ribosome biogenesis pathway using network-guided genetics. *PloS Biol,* 7**,** e1000213.

LIANG, S.-H., A ZHANG, W., A MCGRATH, B. C., A ZHANG, P. & A CAVENER, D. R. 2006. PERK (eIF2α kinase) is required to activate the stress-activated MAPKs and induce the expression of immediate-early genes upon disruption of ER calcium homoeostasis *Biochem J,* 393 201-209.

LIN, T.-A., KONG, X., HAYSTEAD, T. A. J., PAUSE, A., BELSHAM, G., SONENBERG, N. & LAWRENCE, J. J. C. 1994. PHAS-I as a link between motogen-activated protein kinase and translation initiation. *Science,* **266,** 653-656.

LINDSROM, M. S. 2009. Emerging functions of ribosomal proteins in gene-specific transcription and translation. *Biochem. Biophy. Res. Commun.,* **379,** 167-170.

LOZANO, F., MAERTZDOR, B., PANNELL, R. & MILSTEIN, C. 1994. Low cytoplasmic mRNA levels of immunoglobulin kappa light chain genes containing nonsense codons correlate with inefficient splicing. *EMBO J,* 13**,** 4617-4622.

MAGUIRE, B. A. & ZIMMERMANN, R. A. 2001. The ribosome in focus. *Cell,* 104**,** 813-816.

MALYGIN, A. A., PARAKHNEVITCH, N. M., IVANOV, A. V., EPERON, I. C. & KARPOVA, G. G. 2007. Human ribosomal proteins S13 regulates expression of its own geneat the splicing step by a feed back mechanism. *Nucleic acids research,* 35**,** 6414-6423.

MANGIAROTTI, G. 1999. Coupling of Transcription and Translation in Disctyostelium discoideum nuclei. *Biochemistry,* 38**,** 3996-4000.

MAQUAT, L. E. 1995. When cells stop making sense: Effect of nonsense codons on RNA metabolism in vertebrates cell. *RNA* 1**,** 453-465.

MAQUAT, L. E. 2004. Nonsense-mediated mRNA decay: splicing, translation and mRNP dynamics. *Nat. Rev. Mol. Cell. Biol,* 5**,** 89-99.

MARYGOLD, S. J., ROOTE, J., REUTER, G., LAMBERTSSON, A., ASHBURNER, M., MILLIBURN, G. H., HARRISON, P. M., YU, Z., KENMOCHI, N. & KAUFMAN, T. C. 2007. The ribosomal prorein genes and Minute loci of Drosophila melanogaster. *Genome Biol,* 8**,** R216.

MATSUDA, D., HOSODA, N., KIM, Y. K. & MAQUAT, L. E. 2007. Failsafe nonsense-mediated mRNA decay does not detectably target eIF4E-bound mRNA. *Nat Struct Mol Biol,* 14**,** 974.

MAURO, V. P. & EDELMAN, G. M. 2002. The ribosome filter hypothesis. *Proc Natl Acad Sci U S A,* 99**,** 12031-6.

MAURO, V. P. & EDELMAN, G. M. 2007. The ribosome filter redux. *Cell Cycle,* 6**,** 2246-51.

MCCONKEY, E. H., BIELKA, H., GORDON, J., LASTICK, S. M., LIN, A., OGATA, K., REBOUD, J. P., TRAUGH, J. A., TRAUT, R. R., WARNER, J. R. & AL., E. 1979. Proposed uniform nomenclature for mammalian ribosomal proteins. *Mol Gen Genet,* 169**,** 1-6.

MCLEOD, T., ABDULLAHI, A., MIN, L. & BROGNA, S. 2014. Recent studies implicate the nucleolus as the major site of nuclear translation. *Biochem Soc Trans.,* 42**,** 1224-8.

MOLL, I. & ENGELBERG-KULKA, H. 2012. Selective translation during stress in Escherichia coli. *Trends Biochem Sci,* 37**,** 493-8.

MOORE, M. J. 2005. From Birth to Death: The Complex Lives of Eukaryotic mRNAs. *Science,* 309**,** 1514-1518.

MOORE, M. J. & PROUDFOOT, N. J. 2009. Pre-mRNA processing reaches back to transcription and ahead to translation. *Cell* 136**,** 688-700.

MORGAN, N. S., SKOVRONSKY DM, ARTAVANIS-TSAKONAS S & MS, M. 1994. The molecular cloning and characterization of Drosophila melanogaster myosin-IA and myosin-IB. *Mol Biol,* 239**,** 347–356.

MUHLEMANN, O., MOCK-CASAGRANDE, C. S., WANG, J., LI, S., CUSTODIO, N., CARMON-FONSECA, M., WILKINSON, M. F. & MOORE, M. J. 2001. Precursor RNAs harboring nonsense codonsaccumulate near the site of transcription. *Mol Cell* 8**,** 33-43.

MUHS, M., YAMAMOTO, H., ISMER, J., TAKAKU, H., NASHIMOTO, M., UCHIUMI, T., NAKASHIMA, N., MIELKE, T., HILDEBRAND, P. W., NIERHAUS, K. H. & SPAHN, C. M. 2011. Structural basis for the binding of IRES RNAs to the head of the ribosomal 40S subunit. *Nucleic Acids Res,* 39**,** 5264-75.

MYASNIKOV, A. G., SIMONETTI, A., MARZI, S. & KLAHOLZ, B. P. 2009. Structure–function insights into prokaryotic and eukaryotic translation initiation. *Current Opinion in Structural Biology,* 19**,** 300-309.

NAGAI, T., IBATA, K., PARK, E., KUBOTA, M., MIKOSHIBA, K. & A., M. 2001. A variant of yellow fluorescent protein with fast and efficient maturation for cell-biological applications. *Nat Biotechnol,* 1**,** 87-90.

NATHANS, D. & LIPMANN, F. 1961. AMINO ACID TRANSFER FROM AMINOACYL-RIBONUCLEIC ACIDS TO PROTEIN ON RIBOSOMES OF ESCHERICHIA COLI. *Proceedings of the National Academy of Sciences,* 47**,** 497-504.

NATHANSON, L., XIA, T. & DEUTSCHER, M. P. 2003. Nuclear protein synthesis: a re-evaluation. *RNA (New York, NY),* 9**,** 9-13.

NI, J., LIU, L. P., HESS, D., RIETDORF, J. & SUN, F. L. 2006. Drosophila ribosomal proteins are associated with linker histone H1 and suppress gene transcription. *Genes and Development,* 20**,** 1959-1973.

NISHIYAMA, T., YAMAMOTO, H., UCHIUMI, T. & NAKASHIMA, N. 2007. Eukaryotic ribosomal protein RPS25 interacts with the conserved loop region in a dicistroviral intergenic internal ribosome entry site. *Nucleic Acids Res,* 35**,** 1514-21.

NOMURA, M. 1999. Regulation of ribosome biosynthesis in *Escherichia coli* and *Saccharomyces cerevisiae*: diversity and common principles. *J. Bacteriol,* 181**,** 6857-6864.

OHLSTEIN, B. & SPRADLING, A. 2006. The adult Drosophila posterior midgut is maintained by pluripotent stem cells. *Nature,* 439**,** 470-474.

PALAZZO, A. F. & AKEF, A. 2012. Nuclear export as a key arbiter of “mRNA identity” in eukaryotes. *Biochimica et Biophysica Acta (BBA) - Gene Regulatory Mechanisms,* 1819**,** 566-577.

PANSE, V. G. & JOHNSON, A. W. 2010. Maturation of eukaryotic ribosomes: acquisition of functionality. *Trends Biochem Sci,* 35**,** 260-6.

PEARCE, A. & HUMPHREY, T. 2001. Integrating stress-response and cell-cycle checkpoint pathways. *Trends Cell Biol,* 11(10)**,** 426-33.

PENMAN, S., SMITH, I. & HOLTZMAN, E. 1966. Ribosomal RNA synthesis and processing in a particulate site in the HeLa cell nucleus. *Science,* 154**,** 786-9.

PEREZ-FERNANDEZ, J., ROMAN, A., DE LAS RIVAS, J., BUSTELO, X. R. & DOSIL, M. 2007. The 90S preribosome is a multimodular structure that is assembled through a hierarchical mechanism. *Molecular and cellular biology,* 27**,** 5414-5429.

PERRY, R. B. & FAINZILBER, M. 2014. Local translation in neuronal processes—in vivo tests of a “heretical hypothesis”. *Developmental Neurobiology,* 74**,** 210-217.

PESTKA, S. 1971. Inhibitors of Ribosome Functions. *Annual Review of Microbiology,* 25**,** 487-562.

PISAREVA, V. P., PISAREV, A. V., HELLEN, C. U., RODNINA, M. V. & PESTOVA, T. V. 2006. Kinetic analysis of interaction of eukaryotic release factor 3 with guanine nucleotides. *J Biol Chem,* 281(52)**,** 40224-40235.

POLACEK, N. & MANKIN, A. S. 2005. The Ribosomal Peptidyl Transferase Center: Structure, Function, Evolution, Inhibition. *Critical Reviews in Biochemistry and Molecular Biology,* 40**,** 285-311.

RAMAGOPAL, S. 1990. Induction of cell-specific ribosomal proteins in aggregation-competent nonmorphogenetic Dictyostelium discoideum. *Biochemistry and Cell Biology,* 68**,** 1281-1287.

RAMAGOPAL, S. 1992. Are eukaryotic ribosomes heterogeneous? Affirmations on the horizon. *Biochem Cell Biol,* 70**,** 269–72.

RAMAKRISHMAN, V. 2002. Ribosome structure and the mechanism of translation. *Cell,* 108**,** 557-572.

RAMANATHAN, P., GUO, J., WHITEHEAD, R. N. & BROGNA, S. 2008. The intergenic spacer of the Drosophila Adh-Adhr dicistronic mRNA stimulates internal translation initiation. *RNA Biol,* 5**,** 149-56.

RAMIREZ M, WEK RC & AG, H. 1991. Ribosome association of GCN2 protein kinase, a translational activator of the GCN4 gene of Saccharomyces cerevisiae. *Mol Cell Biol,* **11,** 3027-3036.

REID, D. W. & NICCHITTA, C. V. 2012. The enduring enigma of nuclear translation. *J Cell Biol,* 197**,** 7-9.

ROUQUETTE, J., CHOESMEL, V. & GLEIZES, P. E. 2005. Nuclear export and cytoplasmic processing of precursors to the 40S ribosomal subunits in mammalian cells. *EMBO J,* 24**,** 2862-72.

RUGJEE, K. N., ROY CHAUDHURY, S., AL-JUBRAN, K., RAMANATHAN, P., MATINA, T., WEN, J. & BROGNA, S. 2013. Fluorescent protein tagging confirms the presence of ribosomal proteins at Drosophila polytene chromosomes. *PeerJ,* 1**,** e15.

SALVESEN, G. S. & DIXIT, V. M. 1997. Caspases: intracellular signalling by proteolysis. *Cell* 91**,** 443–446.

SAMBROOK, J., FRITSCH, E. F. & MANIATIS, T. 1989. Molecular Cloning: A Laboratory Manual (Second Edition) (New York, Cold Spring Harbor Laboratory Press).

SAYANI, S., JANIS, M., LEE, C. Y., TOESCA, I. & CHANFREAU, G. F. 2008. Widespread impact of nonsense-mediated mRNA decay on the yeast intronome. *Mol Cell* 31**,** 360-370.

SCHLUENZEN, F., TOCILJ, A., ZARIVACH, R., HARMS, J., GLUEHMANN, M., JANELL, D., BASHAN, A., BARTELS, H., AGMON, I., FRANCESCHI, F. & YONATH, A. 2000. Structure of Functionally Activated Small Ribosomal Subunit at 3.3 Å Resolution. *Cell,* 102**,** 615-623.

SCHNEIDER, D. A., MICHEL, A., SIKES, M. L., VU, L., DODD, J. A., SALGIA, S., OSHEIM, Y. N., BEYER, A. L. & NOMURA, M. 2007. Transcription elongation by RNA polymerase I is linked to efficient rRNA processing and ribosome assembly. *Mol Cell,* 26.

SCHRODER, P. A. & MOORE, M. J. 2005. Association of ribosomal proteins with nascent transcripts in S. cerevisiae. *RNA (New York, NY),* NY 11**,** 1521-1529.

SHAW, P. & BROWN, J. 2012. Nucleoli: composition, function, and dynamics. *Plant Physiol,* 158**,** 44-51.

SHEIKH, M. S. & FORNACE, A. J., JR. 1999. Regulation of translation initiation following stress. *Oncogene,* 18**,** 6121-8.

SHUMAN, S. 2001. Structure, Mechanism and Evolution of the mRNA capping apparatus. *Progress in nucleic acid research and molecular biology,* 66**,** 1-40.

SHYU, Y., LIU, H., DENG, X. & HU, C. 2006. Identification of new fluorescent protein fragments for bimolecular fluorescence complementation analysis under physiological conditions. *Biotechniques,* 40**,** 61 - 66.

SHYU, Y. J., HIATT, S. M., DUREN, H. M., ELLIS, R. E., KERPEKOLLA, T. K. & HU, C. D. 2008. Visualization of protein interactions in living caenorhabditis elegans using bimolecular flourescence complemetation analysis. *Nature protocols,* 3**,** 588-596.

SONENBERG, N. & HINNEBUSCH, A. G. 2009. Regulation of Translation Initiation in Eukaryotes: Mechanisms and Biological Targets. *Cell,* 136**,** 731-745.

SOUDET, J., GELUGNE, J. P., BELHABICH-BAUMAS, K., CAIZERGUES-FERRER, M. & MOUGIN, A. 2009. Immature small ribosomal subunits can engage in translation initiation in Saccharomyces cerevisiae. *EMBO J.,* 29**,** 80-92.

SPAHN, C. M., BECKMANN, R., ESWAR, N., PENCZEK, P. A., SALI, A., BLOBEL, G. & FRANK, J. 2001a. Structure of the 80S ribosome from Saccharomyces cerevisiae--tRNA-ribosome and subunit-subunit interactions. *Cell,* 107**,** 373-86.

SPAHN, C. M., BECKMANN, R., ESWAR, N., PENCZEK, P. A., SALI, A., BLOBEL, G. & J, F. 2001b. Structure of 80S ribosome fro saccahromyces cerevisiae tRNA-ribosome and subunit-subunit interactions. *Cell,* 107**,** 373-386.

SPRIGGS, K. A., STONELEY, M., BUSHELL, M. & WILLIS, A. E. 2008. Re-programming of translation following cell stress allows IRES-mediated translation to predominate. *Biology of the Cell,* 100**,** 27-38.

STAMM, S., BON-ARI, S., RAFALSKA, I., TANG, Y., ZHANG, Z., TOIBER, D., THANARAJ, T. A. & SOREQ, H. 2005. Function of alternative splicing. *Gene* 344**,** 1-20.

STRUNK, B. S., LOUCKS, C. R., SU, M., VASHISTH, H., CHENG, S., SCHILLING, J., BROOKS, C. L., KARBSTEIN, K. & SKINIOTIS, G. 2011. Ribosome Assembly Factors Prevent Premature Translation Initiation by 40S Assembly Intermediates. *Science,* 333**,** 1449-1453.

STRUNK, BETHANY S., NOVAK, MEGAN N., YOUNG, CRYSTAL L. & KARBSTEIN, K. 2012. A Translation-Like Cycle Is a Quality Control Checkpoint for Maturing 40S Ribosome Subunits. *Cell,* 150**,** 111-121.

TENNYSON, V. M. 1970. The fine structure of the axon and growth cone of the dorsal root neuroblast of the rabbit embryo. *J Cell Biol,* 44**,** 62-79.

THERMANN, R., NEU-YILIK, G., DETERS, A., FREDE, U., WEHR, K., HAGEMEIER, C., HENTZE, M. W. & KULOZIK, A. E. 1998. Binary specification of nonsense codons by splicing and cytoplasmic translation. *EMBO J.,* 17**,** 3484-3494.

THOMSON, E., FERREIRA-CERCA, S. & HURT, E. 2013. Eukaryotic ribosome biogenesis at a glance. *Journal of Cell Science,* 126**,** 4815-4821.

TRCEK, T., SATO, H., SINGER, R. H. & MAQUAT, L. E. 2013. Temporal and spatial characterization of nonsense-mediated mRNA decay. *Genes Dev,* 27**,** 541-51.

TSCHOCHNER, H. & HURT, E. 2003. Pre-ribosomes on the road from the nucleolus to the cytoplasm. *Trends Cell Biol,* 13(5)**,** 255-63.

UDEM, S. A. & WARNER, J. R. 1972. Ribosomal RNA synthesis in Saccharomyces cerevisiae. *Journal of Molecular Biology,* 65**,** 227-242.

UDEM, S. A. & WARNER, J. R. 1973. The Cytoplasmic Maturation of a Ribosomal Precursor Ribonucleic Acid in Yeast. *Journal of Biological Chemistry,* 248**,** 1412-1416.

UNTERHOLZNER, L. & IZAURRALDE, E. 2004. SMG7 acts as a molecular linkbetween mRNA surveillance and mRNA decay. *Mol Cell,* 16**,** 587-596.

URANO, F., WANG, X., BERTOLOTTI, A., ZHANG, Y., CHUNG, P., HARDING, H. P. & RON, D. 2000. Coupling of Stress in the ER to Activation of JNK Protein Kinases by Transmembrane Protein Kinase IRE1. *Science,* 287**,** 664-666.

URLAUB, G., MITCHELL, P. J., CIUDAD, C. J. & CHASIN, L. A. 1989. Nonsense mutations in the dihydrofolate reductase gene affect RNA processing. *Molecular and cellular biology,* 9**,** 2868-2880.

VAN DYKE, N., BABY, J. & VAN DYKE, M. W. 2006. Stm1p, a Ribosome-associated Protein, is Important for Protein Synthesis in Saccharomyces cerevisiae under Nutritional Stress Conditions. *Journal of Molecular Biology,* 358**,** 1023-1031.

VAN DYKE, N., PICKERING, B. F. & VAN DYKE, M. W. 2009. Stm1p alters the ribosome association of eukaryotic elongation factor 3 and affects translation elongation. *Nucleic Acids Research,* 37**,** 6116-6125.

VENEMA, J. & TOLLERVEY, D. 1999. Ribosome synthesis in Saccharomyces cerevisiae. *Annual review of genetics,* 33**,** 261-311.

VESPER, O., AMITAI, S., BELITSKY, M., BYRGAZOV, K., KABERDINA, ANNA C., ENGELBERG-KULKA, H. & MOLL, I. 2011. Selective Translation of Leaderless mRNAs by Specialized Ribosomes Generated by MazF in Escherichia coli. *Cell,* 147**,** 147-157.

WANG, H., YU, J., ZHANG, L., XIONG, Y., CHEN, S., XING, H., TIAN, Z., TANG, K., WEI, H., RAO, Q., WANG, M. & WANG, J. 2014. RPS27a promotes proliferation, regulates cell cycle progression and inhibits apoptosis of leukemia cells. *Biochemical and Biophysical Research Communications,* 446**,** 1204-1210.

WARNER, J. R. & MCINTOSH, K. B. 2009. How Common Are Extraribosomal Functions of Ribosomal Proteins? *Molecular Cell,* 34**,** 3-11.

WASKIEWICZ, A. J., JOHNSON, J. C., PENN, B., MAHALINGAM, M., R, K. S. & COOPER, J. A. 1999. Phosphorylation of the cap-binding protein eukaryotic translation initiation factor 4E by protrin kinase MnK1 invivo. *Molecular and Cell Biology,* 19 (No. 3)**,** 1871-1880.

WEIJERS, D., FRANKE-VAN DIJK, M., VENCKEN, R. J., QUINT, A., HOOYKAAS, P. & OFFRINGA, R. 2001. An Arabidopsis minute-like phenotype caused by a semi-dominant mutation in a RIBOSOMAL PROTEIN S5 gene. *Development,* 128**,** 4289-4299.

WEK, R. C., JIANG, H. Y. & ANTHONY, T. G. 2006. Coping with stress: eIF2 kinases and translational control. *Biochem Soc Trans,* 34**,** 7-11.

WELLS, S. E., HILLNER, P. E., VALE, R. D. & SACHS, A. B. 1998. Circularization of mRNA by Eukaryotic Translation Initiation Factors. *Molecular Cell,* 2**,** 135-140.

WEN, J. & BROGNA, S. 2010. Splicing-dependent NMD does not require the EJC in Schizosaccharomyces pombe. *EMBO J* 29**,** 1537-1551.

WIMBERLY, B. T., BRODERSEN, D. E., CLEMONS, W. M., JR., MORGAN-WARREN, R. J., CARTER, A.P., VONRHEIM, C., HARTSCH, T. & RAMAKRISHNAN, V. 2000. Structure of 30s ribosomal subunit. *Nature,* 407**,** 327-339.

WOOL, I. G. 1996. Extraribosomal functions of ribosomal proteins. *Trends Biochem,* Sci. **21,** 164-165.

WOOL, I. G., CHAN, Y. L., GLÜCK, A. & SUZUKI, K. 1991. The primary structure of rat ribosomal proteins P0, P1, and P2 and a proposal for a uniform nomenclature for mammalian and yeast ribosomal proteins. *Biochimie,* 73**,** 861-870.

XUE, S. & BARNA, M. 2012. Specialized ribosomes: a new frontier in gene regulation and organismal biology. *Nat Rev Mol Cell Biol,* 13**,** 355-69.

Y, R. 2005. Dissecting Nck/Dock Signalling Pathways in Drosophila Visual System. *Int J Biol Sci,* 1**,** 80-86.

YEROMIN, A. V., ROOS, J., STAUDERMAN, K. A. & CAHALAN, M. D. 2004. A store-operated calcium channel in Drosophila S2 cells. *J. Gen. Physiol.,* 123**,** 167-182.

YI, X., LEMSTRA, W., VOS, M. J., SHANG, Y., KAMPINGA, H. H., SU, T. T. & SIBON, O. C. 2008. A long-term flow cytometry assay to analyze the role of specific genes of Drosophila melanogaster S2 cells in surviving genotoxic stress. *Cytometry A,* 73**,** 637-42.

YUSUPOV, M. M., YUSUPOVA, G. Z., BAUCOM , A., LIEBERMAN, K., EARNEST, T. N., CATE, J. H. & NOLLER, H. F. 2001. Crystal structure of the ribosome at 5.5Á resolution. *Science* 292**,** 883-896.

ZEMP, I. & KUTAY, U. 2007. Nuclear export and cytoplasmic maturation of ribosomal subunits. *FEBS letters,* 581**,** 2783-2793.

ZENG, X., CHAUHAN, C. & HOU, S. X. 2010. Characterization of midgut stem cell- and enteroblast-specific Gal4 lines in drosophila. *Genesis,* 48**,** 607-11.

ZHANG, J., SUN, X. L., QIAN, Y. M., LADUCA, J. P. & MAQUAT, L. E. 1998. At least one intron is required fro the nonsense mediated decay of triosphophate isomerase mRNA: a possible link between nuclear and splicing and cytoplasmic translation. *Mol. Cell. Biol,* 18**,** 5272-5283.

ZHOU, Z., LICKELIDER, L. J., GYGI, S. P. & REED, R. 2002. Comprehensive proteomic analysis of the human sliceosome. *Nature,* 419**,** 182-185.

ZIMMERMANN, K. C., RICCI, J.-E., DROIN, N. M. & GREEN, D. R. 2002. The role of ARK in stress-induced apoptosis in Drosophila cells. *The Journal of Cell Biology,* 156**,** 1077-1087.

ZORIO, D. A. R. & BENTLEY, D. L. 2004. The link between mRNA processing and transcription: communication works both ways. *Experimental Cell Research,* 296**,** 91-97.

Appendices

Appendix I

Growth media recipes for the bacteria *E. coli*

LB broth

Weigh and dissolve 10 g Bacto-tryptone, 5 g yeast extract, and 10 g NaCl in 800 mL dd H_2O. Adjust pH to 7.5 with NaOH, make up the volume to 1 L with dd H_2O. Transfer the solution to a sterilized bottle and autoclave at 121°C for 15 min. Allow the media to cool after sterilization and add antibiotics at the required concentration before use.

Agar-LB plates

Weigh and dissolve 10 g Bacto-Tryptone, 5 g Yeast Extract, 10 g NaCl and 10 g Agar in 800 mL of dd H_2O. Adjust pH to 7.5 with NaOH, and make up the volume to 1 L with dd H_2O. Transfer the solution to a sterilized bottle and autoclave at 121°C for 15 min. Allow the media cool until about 50- 60°C, the add the required antibiotic (100 ug/mL ampicillin final concentration) and pour 25-30 ml/plate (9 cm Petri dishes). Cover the plates with the lid and allow them to cool for about 30-60 min until solidified. Plates can be stored at 4 °C for up to 4 weeks.

NZY Broth media

Weigh and dissolve 2 g NZ amine (casein hydrolysate), 1 g Yeast Extract, 1 g NaCl in 200 mL of dd H_2O. Adjust the pH to 7.5 with NaOH and sterilize by autoclaving at 121°C for 15 minutes (before autoclaving, the media can be aliquoted into 20 ml glass bottles for convenience). Before use, add the following filter sterilized supplements (for 20 ml aliquot): 250 µL of 1 M MgCl2, 250 µL of 1 M MgSO4 and 400 µL of 20% glucose.

Appendix II

Protocol for boiling prep (mini prep)

1. 1.5 mL of the culture was transferred in a fresh 1.5 mL tube and spun at 13000 rpm for 1 min and the supernatant was discarded completely.
2. 100 µL of ice cold STETL (8% sucrose, 50mM Tris pH 8.0, 50 mM EDTA pH 8.0, 5% Triton X-100, 20 mg/mL lysozyme) was added to each of the samples and the pellet was resuspended by vortexing and pipetting up and down.
3. Samples were placed a beaker of boiling water for 20 sec and then spun at 13000 rpm for 15 min and the pellets were removed using sterile toothpicks.
4. 100 µL of the isopropanol was added to the supernatant, mixed by vortexing and spun at 13000 rpm for 15 min. The supernatant was discarded.
5. The pellet was washed with 500 µL of 70% ethanol, air dried and resuspended in 50 µL of TE buffer (10 mM Tris/Cl pH 8.0, 1 mM EDTA pH 8.0). 1 µL of 1 mg/mL RNase stock was added to the DNA and incubated at room temparature for 15 min. The samples were used immediately or stored at -20^{0} for use when the need arise.

Appendix III

List of Primers

Code	Name	Sequence
A1	EcoR1-BiFC-VN F	GGGgaattc**AGATCCATCGCCACC**ATGGTGAGCAAGGGCGAC
A2	XhoI-BiFC-VN R	GGGctcgagTTACTCGATGTTGTGGCGGAT
A3	EcoR1-BiFC-VC F	GGGgaattc**AAACAGAAAGTCATGAACCAC**GCCGACAAGCAGAAGAAC
A4	XhoI-BiFC-VC R	GGGctcgagTTAGTACAGCTCGTCCATGCC
A9	EcoRI -RpS18 F	GGGgaattcACCATGTCGCTCGTCATCCCAGA
A10	EcoRI-RpS18 R	GGGgaattcCTTCTTCTTGGACACACCCAC
A11	EcoRI-RpL11 F	GGGgaattcACCATGGCGGCGGTTACCAAG
A12	EcoRI-RpL11 R	GGGgaattcCTTCTTGGTGTTCAAGAT
A13	EcoRI-RpS6 F	GGGgaattcACCATGAAGCTCAACGTTTCC
A14	EcoRI-RpS6 R	GGGgaattcCTTCTTGTCGCTGGAGAC
A15	EcoRI-RpL22 F	GGGgaattcACCATGGCTCCTACCGCCAAG
A16	EcoRI-RpL22 R	GGGgaattcCTCGGCATCGTCGTCCTC

A17	EcoRI-RpL24 F	GGGgaattcACCATGAAAATTGGCTTGTGC
A18	EcoRI-RpL24 R	GGGgaattcCCGCTTGCCTCCGACGC
A19	EcoRI-BiFC-YN F	GGGgaattcAGATCCATCGCCACCAT
A20	XhoI-BiFC-YN-R	GGGctcgagCTAGGCCATGATATAGAC
A21	EcoRI-BiFC-YC F	GGGgaattcAAACAGAAAGTCATGAAC
A22	EcoRI-BiFC-YC R	GGGctcgagTTACTTGTACAGCTCGTC
A23	R1-BiFC–HL4-YN F	GGGGAATTCCTGGCCGAGGCCGCTGCAAAGGAGGCCGCGGCTAAGGAGGCCGCTGCGAAGGAGGCCGCAGCCAAGGCGGCTGCCATGGTGAGCAAGGGCGAC
A24	R1-BiFC-HL4-YC-F	GGGGAATTCCTGGCCGAGGCCGCCGCCAAGGAGGCCGCCGCCAAGGAGGCCGCCGCCAAGGAGGCCGCCGCCAAGGCCGCCGCCGACAAGCAGAAGAACGGCATC
A25	EcoRI-RpL5 F	GGGgaattcACCATGGGTTTCGTTAAGGTAGTC
A26	EcoRI-RpL5 R	GGGgaattcAGCCTCAGTTTCAGACTGCAG
A27	EcoRI-RpL32 F	GGGgaatccACCATGACCATCCGCCCAGCATA
A28	EcoRI-RpL32 R	GGGgaatccCTCGTTCTCTTGAGAACGCA
A29	EcoRI-RpS15 F	GGGgaatccACCATGGCCGATCAAGTCGATGAA
A30	EcoRI-RpS15 R	GGGgaatccCTTCAGAGGAATGAAACGGGA

Appendix IV

List of Constructs

Construct Code	Construct Name
S01	pUAST-RpS18-VN
S02	pUAST-RpL11-VC
S03	pUAST-RpS6-VN
S04	pUAST-RpL24-VC
B131	pUAST-RpS18-YN
B132	pUAST-RpL11-YC
B134	pUAST-YN-RpS15
B200	pUAST-RpS9-YN
B201	pUAST-RpS13-YN
B202	pUAST-RpS11-YC
L32	pUAST-RpL32-YN
L5	pUAST-RpL5-YC
S6	pUAST-RpS6-YN
L22	pUAST-RpL22-YC
L24	pUAST-RpL24-YC
S18-HL4-YN	pUAST-RpS18-HL4-YN
S15-HL4-YN	pUAST-RpS15-HL4-YN
L11-HL4-YC	pUAST-RpL11-HL4-YC
VN	pUAST-VN
VC	pUAST-VC

Appendix V

List of Fly stock

ID name	Line	Origin
ASA01 (BiFC line)	w^+; UAS.RpS18.VN; UAS.RpL11.VC	Akilu
Fkh gal4	*Folkhead* gal4	Brogna Lab
Esg gal4	Escargot gal4	Y. Fan Lab
A-252	NPI gal4	Y. Fan Lab
Cd8. GFP	mCD8-GFP/Cyo	Hidalgo Lab
Rp.S9-GFP	w^+; UAS.RpS9-GFP	Brogna Lab
Double Balancer stock	w^+; IF; MKRS Cyo; TM6B	Hidalgo Lab
A02	RpS18 (8950-1-2M-CH2)	Akilu (Bestgenes)
A04	RpS18 (8950-1-4M-CH2)	Akilu (Bestgenes)
A05	RpS18 (8950-1-5M-CH3)	Akilu (Bestgenes)
A06	RpS18 (8950-1-6M-CH3)	Akilu (Bestgenes)
A11	RpL11 (8950-2-1M-CH3)	Akilu (Bestgenes)
A12	RpL11 (8950-2-2M-CH2)	Akilu (Bestgenes)
A13	RpL11 (8950-2-3M-CH2)	Akilu (Bestgenes)
A16	RpL11 (8950-2-6M-CH3)	Akilu

		(Bestgenes)
GMR gal4	GMR gal4 MF815/ GMR gal4 MF815	Hidalgo Lab
RpL11 (11208)	RpL11 (k16914)/ Cyo	Bloomington
RpS18 (02853)	Dmel/RpS18 ^{c02853}	Exelixi
Act. 5C gal4	w^{+}; +/+; Act.gal4/TM6B	Bloomington

Appendix VI

Plasmid map

Plasmid Name: pUAST

Plasmid Type: Drosophila

Plasmid Size: 8904

Notes: Brand and Perimon (1993) Development 118 401-415 pUAST consists of five tandemly arrayed optimized GAL4 binding sites followed by the hsp70 TATA box and transcriptional start , a polylinker containing unique restriction sites for EcoRI, BglII, NotI, Xho, KpnI and XbaI and the SV40 small T intron and polyadenylation site. These features are included in a P-element vector (pCaSpeR3) containing the P element ends (P3' and P5') and the white gene which acts as a marker for successful incorporation into the Drosophila genome. More information: Brand and Perimon (1993) Development 118 401-415 Plasmid.

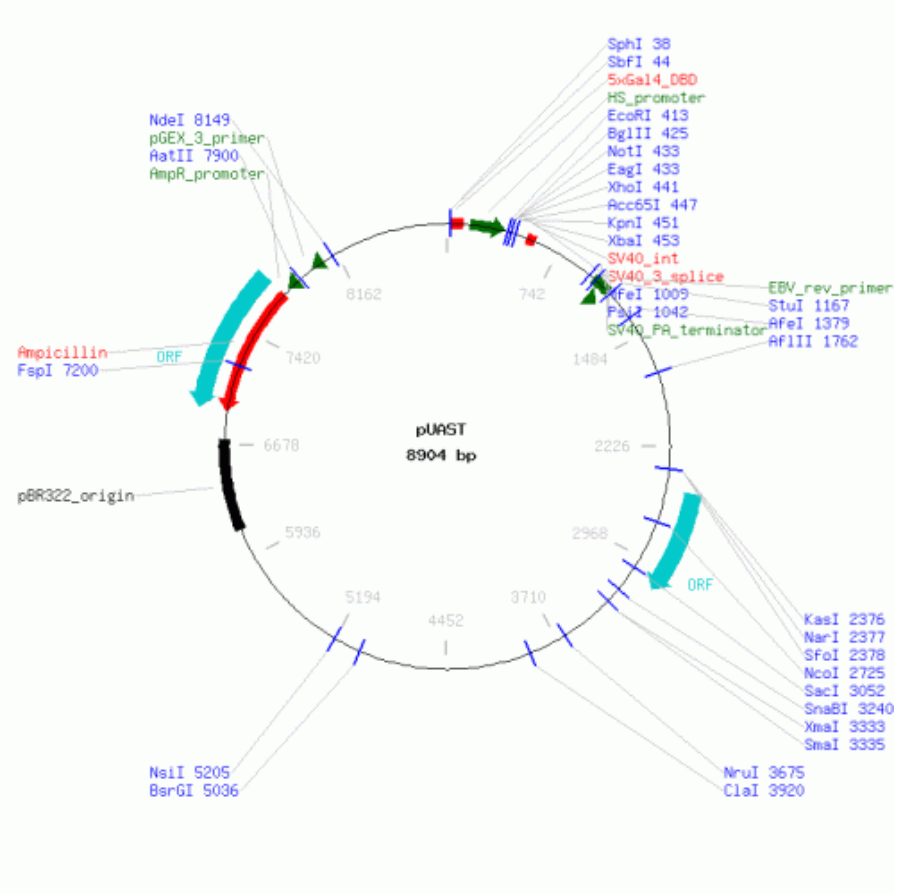

Source: This figure and the description text are from Addgene Vector Database

APPENDIX VII

Ribosomal Proteins (RPs), Venus and YFP cDNA nucleotide and amino acids sequences

RpS18
DEFINITION *Drosophila melanogaster* Ribosomal protein S18
ACCESSION NM_166383
Translation

"MSLVIPEKFQHILRIMNTNIDGKRKVGIAMTAIKGVGRRYSNIVLKKADVDLTKRAGECTEEEVDKVV
TIISNPLQYKVPNWFLNRQKDIIDGKYWQLTSSNLDSKLRDDLERLKKIRSHRGLRHYWGLRVRGQHTK
TTGRRGRTVGVSKKK"

cDNA sequence

ATGTCGCTCGTCATCCCAGAGAAGTTCCAGCACATCCTGCGTATCATGAATACGAACATCGACGGCA
AGCGCAAGGTTGGCATCGCCATGACCGCCATCAAGGGAGTGGGTCGCCGCTACTCCAACATTGTGC
TGAAGAAGGCCGATGTCGATCTTACCAAGCGCGCCGGTGAGTGCACCGAGGAGGAGGTCGACAAG
GTGGTGACCATCATCTCGAACCCTCTGCAGTACAAGGTGCCCAACTGGTTCCTCAACAGGCAGAAGG
ACATCATCGATGGCAAGTACTGGCAGCTGACCTCCTCCAACTTGGACTCGAAGCTGCGTGACGATCT
GGAGCGTCTGAAGAAGATCCGCTCCCACCGTGGTCTGCGTCACTACTGGGGCCTCCGTGTGCGTGG
CCAGCACACCAAGACCACCGGTCGTCGTGGTCGCACCGTGGGTGTGTCCAAGAAGAAGTAA

RpS9
DEFINITION *Drosophila melanogaster* Ribosomal protein S9
ACCESSION NM_168350
ORGANISM *Drosophila melanogaster* (fruit fly)

Translation="MVNGRIPSVFSKTYVTPRRPYEKARLDQELKIIGEYGLRNKREVWRVKYALAKIRK
AARELLTLDEKDEKRLFQGNALLRRLVRIGVLDESRMKLDYVLGLKIEDFLERRLQTQVFKLGLAKSIH
HARVLIRQRHIRVRKQVVNIPSFVVRLDSQKHIDFSLKSPFGGGRPGRVKRKNLKKNQGGGGGAAEEEE
D
cDNA sequence
ATGGTGAACGGCCGCATACCCTCGGTCTTCTCGAAGACCTACGTGACTCCCCGTCGCCCCTATGAGA
AGGCGCGTCTGGACCAGGAGTTGAAGATCATCGGCGAGTATGGTCTGCGCAACAAGCGCGAAGTG
TGGCGCGTCAAGTACGCCCTGGCTAAGATCCGTAAGGCCGCTCGTGAGCTGCTGACCCTCGACGAG
AAGGACGAGAAGCGTCTGTTCCAGGGTAATGCCCTGCTGCGCCGTCTGGTCCGTATCGGTGTCCTG
GACGAGTCCCGCATGAAGCTCGATTACGTGCTGGGTCTGAAGATTGAGGACTTCTTGGAGCGTCGT
CTGCAGACGCAGGTGTTCAAGCTGGGACTTGCCAAGTCCATCCATCATGCTCGCGTCCTGATCCGTC
AGCGTCACATTCGTGTCCGCAAGCAGGTGGTCAACATCCCGTCGTTCGTCGTGCGCCTGGACTCCCA
GAAGCACATCGACTTCTCCCTGAAGTCGCCCTTCGGCGGCGGCCGTCCCGGTCGCGTCAAGAGGAA
GAACCTGAAGAAGAACCAGGGCGGTGGCGGTGGAGCTGCTGAAGAGGAGGAGGACTAA

RpS15
DEFINITION *Drosophila melanogaster* Ribosomal protein S15
ACCESSION NM_137292
Translation"MADQVDENLKKKRTFKKFTYRGVDLDQLLDMPNNQLVELMHSRARRRFSRGLKRKPM
ALIKKLRKAKKEAPPNEKPEIVKTHLRNMIIVPEMTGSIIGVYNGKDFGQVEVKPEMIGHYLGEFALTY
KPVKHGRPGIGATHSSRFIPLK"

cDNA sequence
ATGGCCGATCAAGTCGATGAAAATCTGAAGAAGAAGCGTACCTTCAAGAAGTTCACCTACCGCGGT
GTCGACTTGGACCAGCTTCTGGACATGCCCAACAACCAGCTGGTGGAGCTGATGCACAGCCGTGCC
CGCAGGCGTTTCTCCCGCGGACTGAAGCGCAAGCCAATGGCTCTGATCAAGAAGCTGCGCAAGGCC
AAGAAGGAGGCACCGCCAAATGAGAAGCCCGAGATTGTCAAGACCCACCTGAGGAACATGATCATC
GTACCCGAGATGACCGGCTCCATCATTGGCGTCTACAACGGCAAGGACTTCGGACAGGTGGAGGTC
AAGCCCGAGATGATCGGTCACTACCTGGGCGAGTTCGCCCTGACCTACAAGCCCGTCAAGCACGGT
CGTCCTGGTATCGGTGCCACCCACAGCTCCCGTTTCATTCCTCTGAAGTGA

RpS13

DEFINITION *Drosophila melanogaster* Ribosomal protein S13.
ACCESSION AY058536

Translation="MGRMHAPGKGISQSALPYRRTVPSWLKLNADDVKEQIKKLGKKG
LTPSKIGIILRDSHGVAQVRFVNGNKILRIMKSVGLKPDIPEDLYHMIKKAVAIRKHL
ERNRKDKDGKFRLILVESRIHRLARYYKTKSVLPPNWKYESSTASALVA"

cDNA sequence
ATGGGTCGTATGCACGCTCCTGGCAAGGGTATTTCCCAATCAGCCCTCCCCTACAGACGCACTGTCC
CATCCTGGCTGAAACTGAACGCAGATGATGTCAAGGAGCAGATTAAGAAGCTGGGCAAGAAGGGT
CTGACTCCCTCCAAAATCGGCATCATCCTGCGTGACTCGCACGGAGTTGCCCAGGTGCGTTTCGTCA
ACGGAAACAAGATCCTGCGCATCATGAAGTCGGTGGGTCTGAAGCCCGACATTCCCGAGGATCTGT
ACCACATGATCAAGAAGGCCGTCGCCATCCGCAAGCACTTGGAGCGCAACCGCAAGGACAAGGAC
GGCAAGTTCCGTCTGATTCTGGTCGAGTCCAGGATCCACCGCCTGGCCCGCTACTACAAGACCAAGA
GCGTCCTGCCCCCCAACTGGAAATACGAGTCGAGCACTGCCTCCGCCCTGGTTGCCTAA

RpS11

DEFINITION ribosomal protein S11, isoform B (*Drosophila melanogaster*).
ACCESSION AAM71029

Translation=”MADQQTERSF RKQHAVVVVR RKSPNLKKRP RFYRQIGLGF RAPAEAIDGT
YIDKKCPWTGDVRIRGRILT GVVRKAKMQR TIVIRRDYLH FVRKYSRFEK RHRNMSVHCS
PVFRDVEHGDVTIGECRPL SKTVRFNVLK VSKGQGAKKSFKKY

cDNA sequence

ATGGCTGATCAGCAAACCGAACGCTCGTTCCGCAAGCAACACGCGGTGGTCGTTGTGCGTCGCAAG
AGCCCCAACTTGAAGAAAAGGCCCCGTTTCTATCGCCAAATTGGCCTGGGCTTCCGCGCTCCGGCGG
AGGCCATCGATGGTACCTACATCGACAAGAAGTGCCCCTGGACCGGTGATGTGAGGATCCGTGGTC
GCATTCTGACCGGCGTGGTCCGCAAGGCCAAGATGCAGCGCACCATTGTCATTCGGCGCGACTACCT
GCACTTTGTGCGCAAATACAGCCGTTTCGAGAAGCGTCACCGCAACATGAGCGTCCACTGCTCCCCT
GTGTTCAGAGATGTTGAGCATGGCGATATTGTCACCATTGGTGAGTGCCGTCCTCTGTCCAAGACTG
TGCGCTTCAACGTCCTGAAAGTCAGCAAGGGTCAGGGAGCCAAGAAGAGCTTCAAGAAGTACTAG

RpS6

Definition ribosomal protein S6, isoform B (*Drosophila* melanogaster).

ACCESSION NP_727213.

Translation=
MGQVVEADILGDEWKGYQLRIAGGNDKQGFPMKQGVLTHGRVRLLLKKGHSCYRPRRTGERKRKSVR
GCIVDANMSVLALVVLKKGEKDIPGLTDTTIPRRLGPKRASKIRKLYNLSKEDDVRRFVVRRPLPAKDNKK
ATSKAPKIQRLITPVVLQRKHRRIALKKKRQIASKEASADYAKLLVQRKKESKAKREEAKRRRSASIRESKSS
VSSDKK

cDNA sequence

ATGGGACAGGTTGTGGAGGCCGATATCCTCGGTGACGAGTGGAAGGGCTACCAGCTGCGCATCGC
CGGCGGCAACGACAAGCAGGGATTCCCCATGAAGCAGGGTGTCTTGACCCACGGCCGTGTGCGTCT
GCTCCTGAAGAAGGGACACTCCTGCTACCGTCCACGCCGCACTGGCGAGCGTAAGCGCAAGTCTGT
GCGTGGATGCATCGTGGACGCCAACATGTCTGTGCTGGCTCTGGTCGTCTTGAAGAAGGGTGAGAA
GGACATTCCCGGTCTCACCGACACCACCATCCCACGTCGCCTGGGACCCAAGCGTGCTAGCAAGATC
CGCAAGCTCTACAACTTGAGCAAGGAAGATGATGTGCGTCGCTTCGTTGTGCGTCGCCCTTTGCCCG
CCAAGGACAACAAGAAGGCCACCTCCAAGGCCCCCAAAATTCAGCGCCTGATCACCCCCGTTGTGCT
GCAGCGCAAGCACCGTCGCATTGCGCTGAAGAAGAAGCGCCAGATCGCTTCCAAGGAGGCTTCCGC
CGACTACGCCAAGCTGTTGGTGCAGCGCAAGAAGGAGTCCAAGGCCAAGCGCGAGGAGGCCAAGC
GCCGCCGTTCTGCCTCCATTCGCGAGTCCAAGAGCTCTGTCTCCAGCGACAAGAAGTAA

RpL11

DEFINITION *Drosophila melanogaster* Ribosomal protein L11

ACCESSION NM_057706

TRANSLATION="MAAVTKKIKRDPAKNPMRDLHIRKLCLNICVGESGDRLTRAAKVLEQLTGQQPVFSK
ARYTVRSFGIRRNEKIAVHCTVRGAKAEEILERGLKVREYELRRENFSSTGNFGFGIQEHIDLGIKYDPSIGIY
GLDFYVVLGRPGYNVNHRKRKSGTVGFQHRLTKEDAMKWFQQKYDGIILNTKK"

cDNA sequence
ATGGCGGCGGTTACCAAGAAGATTAAGCGCGATCCCGCGAAGAACCCGATGAGGGATCTGCACATC
CGCAAACTCTGCCTGAACATCTGCGTGGGCGAGTCCGGTGACAGGCTGACCCGTGCCGCCAAGGTG
CTGGAGCAGCTGACTGGTCAGCAGCCAGTGTTCTCCAAGGCCCGCTACACGGTCCGTTCGTTCGGTA
TTCGCCGTAACGAGAAGATCGCTGTCCACTGCACGGTGCGCGGCGCCAAGGCTGAGGAGATTCTGG
AGCGTGGCCTGAAGGTGCGCGAGTACGAGCTGCGTCGGGAGAACTTCTCCTCCACCGGCAACTTCG
GTTTCGGCATCCAGGAACACATCGATCTGGGCATCAAGTACGATCCCTCCATCGGTATCTATGGTCT
GGACTTCTACGTCGTCCTCGGCCGCCCTGGCTACAATGTGAACCACAGGAAGCGCAAGTCCGGCACT
GTCGGCTTCCAGCACCGCCTCACCAAGGAGGATGCCATGAAGTGGTTCCAGCAGAAATACGATGGT
ATCATCTTGAACACCAAGAAGTAG

RpL5

DEFINITION Ribosomal protein L5, isoform A (*Drosophila melanogaster*).
ACCESSION EAA46019

Translation=
“MGFVKVVKNKQYFKRYQVKFRRRREGKTDYYARKRLTFQDKNKYNTPKYRIVRLSNKDITVQIA
YARIEGDRVVCAAYSHELPKYGIQVGLTNYAAAYCTGLLVARRVLNKLGLDSLYAGCTEVTGEEFNVEPVD
DGPGAFRCFLDVGLARTTTGARVFGAMKGAVDGGLNIPHSVKRFPGYSAETKSFNADVHRAHIFGQHV
ADYMRSLEEEDEESFKRQFSRYIKLGIRADDLEDIYKKAHQAIRND PTHKVTAKKS SAVTKKRWNA
KKLTNEQRKT KIAAHKAAYVAKLQSETEA

cDNA Sequence

ATGGGTTTCGTTAAGGTAGTCAAGAACAAGCAGTACTTTAAGAGGTACCAAGTCAAGTTCCGAAGG
CGTCGCGAAGGAAAGACCGATTACTATGCCAGGAAACGCCTAACATTTCAGGACAAGAACAAGTAC
AACACTCCCAAGTACCGTTTGATCGTACGTTTGTCCAACAAGGACATCACAGTACAGATCGCCTATGC
TCGCATCGAGGGTGATCGCGTGGTGTGCGCTGCTTATTCCCATGAGCTTCCCAAATACGGGATCCAG
GTTGGATTGACCAACTACGCTGCTGCTTACTGCACAGGCCTGCTGGTCGCCCGTCGTGTCCTTAACA
AGTTGGGACTGGACTCCCTATATGCAGGATGCACTGAAGTGACTGGTGAGGAGTTCAACGTCGAGC
CTGTTGATGACGGCCCAGGGGCATTCCGTTGCTTCTTGGATGTTGGACTCGCTCGTACTACAACTGG
TGCCCGTGTGTTTGGCGCTATGAAGGGAGCAGTTGATGGTGGTCTAAACATACCTCACTCTGTGAAA
CGCTTTCCTGGATACTCTGCTGAAACCAAGAGCTTTAATGCCGATGTGCATCGCGCTCATATATTTGG
CCAGCACGTTGCAGACTATATGCGTTCTTTGGAGGAGGAGGATGAGGA
GAGCTTCAAAAGGCAGTTTAGCCGATACATCAAGTTGGGCATTCGTGCTGATGATCTTGAGGATATC
TATAAAAAAGCCCACCAGGCAATTCGTAACGACCCTACACACAAGGTCACCGCTAAGAAGTCTTCTG

CCGTTACGAAGAAAAGGTGGAATGCTAAGAAACTCACAAACGAGCAACGGAAGACTAAGATTGCA
GCTCATAAGGCAGCATATGTTGCCAAGCTGCAGTCTGAAACTGAGGCTTAA

RpL32

DEFINITION *Drosophila melanogaster* Ribosomal protein L32.
ACCESSION BT011442

Translation="MDTAQEASPTCFKMTIRPAYRPKIVKKRTKHFIRHQSDRYAKLSHKWRKPKGIDNRVRR
RFKGQYLMPNIGYGSNKRTRHMLPTGFKKFLVHNVRELEVLLMQNRVYCGEIAHGVSSKKRKEIVERAK
QLSVRLTNPNGRLRSQENE"

cDNA sequence
ATGACCATCCGCCCAGCATACAGGCCCAAGATCGTGAAGAAGCGCACCAAGCACTTCATCCGCCACC
AGTCGGATCGATATGCTAAGCTGTCGCACAAATGGCGCAAGCCCAAGGGTATCGACAACAGAGTGC
GTCGCCGCTTCAAGGGACAGTATCTGATGCCCAACATCGGTTACGGATCGAACAAGCGCACCCGCC
ACATGCTGCCCACCGGATTCAAGAAGTTCCTGGTGCACAACGTGCGCGAGCTGGAGGTCCTGCTCAT
GCAGAACCGCGTTTACTGCGGCGAGATCGCCCACGGCGTCTCCTCCAAGAAGCGCAAGGAGATTGT
CGAGCGCGCCAAGCAGCTGTCGGTCCGCCTCACCAACCCCAACGGTCGCCTGCGTTCTCAAGAGAAC
GAGTAA

RpL22

DEFINITION *Drosophila melanogaster* Ribosomal protein L22

ACCESSION AAB17433

Translation=
MAPTAKTNKGDTKTAAAKPAEKKAAPAAAAAKGKVEKPKAEAAKPAAAAAKNVKKASEAAKDVKAAA
AAAKPAAAKPAAAKPAAASKDAGKKAPAAAAPKKDAKAAAAPAPAKAAPAKKAASTPAAAPPAKKAAP
AKAAAPAAAAPAPAAAAPAVAKPAPKPKAKAAPAPSKVVKKNVLRGKGQKKKKVSLRFTIDCTNIAEDSI
MDVADFEKYIKARLKVNGKVNNLGNNVTFERSKLKLIVSSDVHFSKAYLKYLTKKYLKKNSLRDWIRVVAN
EKDSYELRYFRISSNDDEDDDAE

cDNA sequence

ATGGCTCCTACCGCCAAGACCAACAAGGGTGATACCAAGACCGCTGCCGCTAAGCCAGCGGAGAAG
AAGGCCGCTCCCGCAGCCGCCGCCGCCAAGGGCAAGGTGGAGAAGCCGAAGGCTGAGGCCGCCAA
GCCCGCCGCCGCCGCCGCGGCCAAGAACGTGAAGAAGGCGTCCGAGGCGGCCAAGGATGTAAAGGCA
GCCGCCGCTGCTGCCAAGCCCGCGGCAGCCAAGCCCGCAGCTGCCAAGCCCGCCGCCGCTTCCAAG
GATGCCGGAAAGAAGGCTCCCGCTGCCGCTGCTCCCAAGAAGGACGCCAAGGCTGCTGCTGCTCCG
GCTCCCGCCAAGGCTGCTCCGGCCAAGAAGGCTGCCTCCACGCCTGCTGCCGCTCCCCCAGCAAAGA
AGGCTGCTCCCGCCAAGGCCGCAGCCCCGGCTGCTGCTGCTCCCGCTCCGGCTGCAGCTGCTCCTGC
TGTCGCCAAGCCCGCGCCTAAGCCGAAGGCAAAGGCTGCCCCAGCTCCCAGCAAGGTGGTCAAGAA
GAACGTGCTGCGTGGCAAGGGACAGAAGAAGAAGAAGGTCTCGCTGCGCTTCACTATCGACTGCAC
CAACATT

GCTGAGGATAGCATCATGGATGTGGCCGACTTCGAGAAGTACATCAAGGCCCGCCTTAAGGTCAAC
GGCAAGGTGAACAACCTGGGCAACAACGTCACCTTCGAGCGCTCCAAGCTGAAGCTCATTGTCAGC
TCCGACGTTCACTTTTCCAAGGCATACCTCAAGTACTTGACCAAGAAGTACCTGAAGAAGAACAGTC
TGCGCGACTGGATCCGTGTGGTGGCCAACGAAAAGGACTCGTACGAGCTGCGCTACTTCAGAATCA
GCTCCAACGACGATGAGGACGACGATGCCGAGTAA

RpL24

DEFINITION *Drosophila melanogaster* Ribosomal protein L24 (isoform A)

ACCESSION NP_609649

Translation=MKIGLCAFSGYKIYPGHGKTMVKIDGKSFTFLDKKCERSYLMKRNPRKVTWTVLYRRKHR
KGIEEEASKKRTRRTQKFQRAIVGASLAEILAKRNMKPEVRKAQRDQAIKVAKEQKRAVKAAKKAAAPAP
AKKSAPKQKAAKVTQKAAPRVGGKR

cDNA sequence

ATGAAAATTGGCTTGTGCGCATTCAGCGGGTACAAAATCTACCCCGGTCATGGCAAGACCATGGTCA
AGATCGATGGCAAGTCGTTCACCTTCCTGGACAAGAAGTGCGAGCGCTCCTACCTGATGAAGCGCA
ATCCCCGCAAGGTTACGTGGACCGTGCTGTACCGCCGGAAGCACCGCAAGGGAATCGAGGAGGAG
GCCTCCAAGAAGCGCACCCGCCGCACCCAGAAGTTCCAGCGCGCCATCGTCGGTGCCTCGCTGGCC
GAGATTCTGGCCAAGCGTAACATGAAGCCCGAGGTGCGCAAGGCGCAGCGCGACCAGGCCATCAA
GGTGGCCAAGGAGCAGAAGCGTGCCGTCAAGGCCGCCAAGAAGGCTGCTGCCCCCGCTCCCGCTA
AGAAGTCGGCGCCCAAGCAGAAGGCCGCCAAGGTCACGCAGAAGGCTGCTCCCCGCGTCGGAGGC
AAGCGGTAA

Venus Fluorescent Proteins cDNA nucleotide and amino acids VFP

VFP
DEFINITION Yellow fluorescent protein Venus [cloning vector pHC04].
ACCESSION ACQ43942
TRANSLATION=“MVSKGEELFTGVVPILVELDGDVNGHKFSVSGEGEGDATYGKLTLKLICT
TGKLPVPWPTLVTTLGYGLQCFARYPDHMKQHDFFKSAMPEGYVQERTIFFKDDGNYKTRAEVKFEGD
TLVNRIELKGIDFKEDGNILGHKLEYNYNSHNVYITADKQKNGIKANFKIRHNIEDGGVQLADHYQQNTPI
GDGPVLLPDNHYLSYQSALSKDPNEKRDHMVLLEFVTAAGITLGMDELYK”

cDNA sequence
ATGGTGAGCAAGGGCGAGGAGCTGTTCACCGGGGTGGTGCCCATCCTGGTCGAGCTGGACGGCGA
CGTAAACGGCCACAAGTTCAGCGTGTCCGGCGAGGGCGAGGGCGATGCCACCTACGGCAAGCTGA
CCCTGAAGCTGATCTGCACCACCGGCAAGCTGCCCGTGCCCTGGCCCACCCTCGTGACCACCCTGGG
CTACGGCCTGCAGTGCTTCGCCCGCTACCCCGACCACATGAAGCAGCACGACTTCTTCAAGTCCGCC
ATGCCCGAAGGCTACGTCCAGGAGCGCACCATCTTCTTCAAGGACGACGGCAACTACAAGACCCGC
GCCGAGGTGAAGTTCGAGGGCGACACCCTGGTGAACCGCATCGAGCTGAAGGGCATCGACTTCAA
GGAGGACGGCAACATCCTGGGGCACAAGCTGGAGTACAACTACAACAGCCACAACGTCTATATCAC
CGCCGACAAGCAGAAGAACGGCATCAAGGCCAACTTCAAGATCCGCCACAACATCGAGGACGGCG
GCGTGCAGCTCGCCGACCACTACCAGCAGAACACCCCCATCGGCGACGGCCCCGTGCTGCTGCCCG
ACAACCACTACCTGAGCTACCAGTCCGCCCTGAGCAAAGACCCCAACGAGAAGCGCGATCACATGG
TCCTGCTGGAGTTCGTGACCGCCGCCGGGATCACTCTCGGCATGGACGAGCTGTACAAGTAA

Yellow Fluorescent Protein (YFP) cDNA nucleotide

(A) BiFC-YC (155-239)
AAACAGAAAGTCATGAACCACGACAAGCAGAAGAACGGCATCAAGGTGAACTTCAAGATCCGCCAC
AACATCGAGGACGGCAGCGTGCAGCTCGCCGACCACTACCAGCAGAACACCCCCATCGGCGACGGC
CCCGTGCTGCTGCCCGACAACCACTACCTGAGCTACCAGTCCGCCCTGAGCAAAGACCCCAACGAGA
AGCGCGATCACATGGTCCTGCTGGAGTTCGTGACCGCCGCCGGGATCACTCTCGGCATGGACGAGC
TGTACAAGTAA

(B) BiFC-YN (1-154)
AGATCCATCGCCACCATGGTGAGCAAGGGCGAGGAGCTGTTCACCGGGGTGGTGCCCATCCTGGTC
GAGCTGGACGGCGACGTAAACGGCCACAAGTTCAGCGTGTCCGGCGAGGGCGAGGGCGATGCCAC
CTACGGCAAGCTGACCCTGAAGTTCATCTGCACCACCGGCAAGCTGCCCGTGCCCTGGCCCACCCTC
GTGACCACCTTCGGCTACGGCCTGCAGTGCTTCGCCCGCTACCCCGACCACATGAAGCAGCACGACT
TCTTCAAGTCCGCCATGCCCGAAGGCTACGTCCAGGAGCGCACCATCTTCTTCAAGGACGACGGCAA
CTACAAGACCCGCGCCGAGGTGAAGTTCGAGGGCGACACCCTGGTGAACCGCATCGAGCTGAAGG
GCATCGACTTCAAGGAGGACGGCAACATCCTGGGGCACAAGCTGGAGTACAACTACAACAGCCACA
ACGTCTATATCATG

APPENDIX VIII

Lethal mutation complementation score

RpS18-VN rescues lethal mutation in the RpS18 locus (Mutation =RpS18c02853)				
	02853;S18VN	Cyo;TM6B	02853;TM6B	Cyo; Act. Gal4
02853; Act. Gal4	02853; Act. Gal4 02853;S18VN	02853; Act. Gal4 Cyo;TM6B	02853; Act. Gal4 02853;TM6B	
Cyo; TM6B	02853;S18VN Cyo; TM6B			
02853;TM6B				02853;TM6B Cyo; Act. Gal4
Cyo; Act. Gal4	02853;S18VN Cyo; TM6B		02853;TM6B Cyo; Act. Gal4	

Score

Rescued Flies (A) 02853; Act. Gal4
02853; S18VN — 22

Phenotype (B) 02853; Act. Gal4
CyO; TM6B — 41

Phenotype (C) 02853; Act. Gal4
02853;TM6B — 37

Phenotype(D) 02853;S18VN
Cyo; TM6B — 33